MONTHLY NOTICES

OF THE

ROYAL ASTRONOMICAL SOCIETY.

VOL. XCI. MARCH 13, 1931. No. 5

Dr. H. KNOX-SHAW, PRESIDENT, in the Chair.

---

The election by the Council of the following Fellows was duly confirmed :—

Hubert Slouka, Astronomical Institute of the University Charles IV., Prague-Smichov, Czechoslovakia ; and

George Kraal Thornhill, Acting Surveyor-General, Colombo, Ceylon.

---

The following candidates were proposed for election as Fellows of the Society, the names of the proposers from personal knowledge being appended :—

Clifford Chaffer, M.A., Rusland, Somerset Way, Iver, Bucks (proposed by E. A. Milne) ;

Donald Percy Dalzell, M.A., 28 Albany Park Road, Kingston-upon-Thames (proposed by H. Jeffreys) ;

Alan Fletcher, M.A., 66 Mount Street, Lincoln (proposed by W. M. Smart) ;

Alfred Henry Hockey, 86 Locket Road, Wealdstone, Harrow (proposed by A. G. Fellows) ;

Charles Theodore Jacob, Glemham, Harpenden Road, St. Albans, Herts (proposed by J. Evershed) ;

Abbé G. Lemaître, 40 rue de Namur, Louvain, Belgium (proposed by A. S. Eddington) ;

Wyndham Edward Buckley Lloyd, M.A., Bryn Cadwrfa, Montgomery (proposed by R. L. Waterfield) ; and

Richard Alexander Robb, M.A., B.Sc., M.Sc., F.R.S.E., Lecturer in Mathematics, University of Glasgow (proposed by L. Becker).

One hundred and twenty-seven presents were announced as having been received since the last ordinary meeting, including :—

Herschel (Miss F.), Portrait taken in 1916 by Sir W. J. Herschel, by the process of Lumière's colour photography;

King (E. F.), A biographical sketch of Sir Isaac Newton, 1858 (presented by Professor Stratton) ;

Knobel (the late E. B.), Drawings of Jupiter and Comets (presented by Miss M. Knobel) ;

Milne-Thomson (L. M.) and L. J. Comrie, Standard Four-Figure Mathematical Tables, Edition A ;

Minnesota University, Astronomical Observatory Publications. Vol. I. (F. Leavenworth Memorial Volume) ;

Payne (Miss C. H.), The Stars of High Luminosity (presented by Radcliffe College, Harvard University) ;

Pračka (L.), Untersuchungen über den Lichtwechsel älterer veränderlicher Sterne. Vol. II. 1916 (presented by the Astronomical Institute of Charles IV. University, Prague) ;

St. John (C. E.), Chemistry of the Sun. Periodic Table of the Elements grouped according to the number of outer (valence) electrons. (Chart.)

---

*Celestial Photographs.*

The following have been added to the list of Celestial Photographs reproduced by the Society for sale to the Fellows :—

R.A.S. Ref. No.

421. Solar Spectrum, Infra-red to $\lambda 9600$. Diffraction Grating. Abney.

422. Spectra of Carbon Monoxide and of Comet Morehouse (1908 III), Curtis. Fowler.

423. Coronal Line 5303. 1930 Aug. 10d. 10h. U.T. Exp. 6 min. Lyot, Pic du Midi.

424. Solar Prominence ($K_3$). 1929 Aug. 26, 27, 28, and 29. Meudon Observatory.

425. Chromospheric Spectra, H, K. $\alpha$ Boötis, Sun, $\alpha$ Aurigæ. Meudon Observatory.

---

*A Theorem concerning Incomplete Polytropes.*
By Sir Arthur S. Eddington.

It was proved by Emden that the negative potential energy of a distribution of matter of mass M and radius R arranged as a polytrope of index $n$ is

$$\Omega = \frac{3}{5-n}\frac{GM^2}{R}.$$

This result can be extended to a distribution in which the polytropic index $n$ is variable ; we shall prove that

$$\Omega = \frac{3}{5 - n_0} \frac{GM^2}{R} \quad . \quad . \quad . \quad . \quad (1)$$

where (so long as $n$ is positive) $n_0$ is an average value of $n$ taken in a particular way and is therefore intermediate between the minimum and maximum values, $n_1$ and $n_2$, for the distribution. It follows that

$$\Omega_1 < \Omega < \Omega_2 \quad . \quad . \quad . \quad . \quad (2)$$

where $\Omega_1$ and $\Omega_2$ are the negative potential energies of the complete polytropes $n_1$ and $n_2$. In particular the distribution is, on the whole, less condensed to the centre than the polytrope of index $n_2$.

Provided that the density curve does not cross that of the polytrope

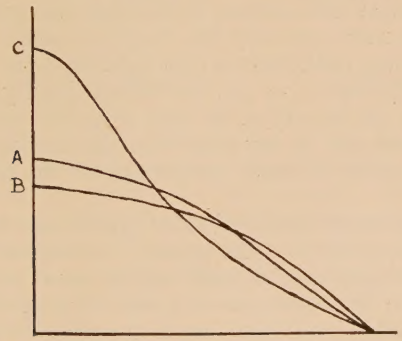


Ordinates $\rho$ ; Abscissæ $r$.

more than once, we can infer that the central density is less than the central density in the polytrope $n_2$. In the figure the density $\rho$ is plotted against the radius $r$. The curve A is that of the complete polytrope $n_2$, and the curves B and C represent the two alternative types of density curve which do not cross it more than once. Since C is derived from A by shifting matter towards the centre, its $\Omega$ is greater than $\Omega_2$ ; it is therefore excluded by (2). The distribution must therefore be of type B, giving a lower central density than the polytrope.

The physical importance of the theorem lies in the fact that in current investigations the failure of the gas-laws at high densities is found to correspond to a lowering of the polytropic index. Thus Milne, on the basis of physical theory, adopts $n = \frac{3}{2}$ (with possibly a central region where $n = 0$) in his non-gaseous cores. Moreover, an inward increase in the ratio of radiation-pressure to gas-pressure (which occurs when the source of energy is strongly concentrated to the centre of the star) causes the polytropic index to decrease inwards. Thus, unless the physical theory is greatly in error, the central density must be less than that calculated on the assumption that the polytropic

index for the outer gaseous portion (about 3) persists throughout. This is in accordance with the usual conclusion in all early investigations of dwarf stars and in the current theory of white dwarfs, that the greater resistance to compression of matter at high density lowers the density at the centre.

Professor Milne's new theory of stellar structure rests on the assumption that distributions of type C (" centrally condensed " distributions) are possible.* (The question as to the possibility of the density curves crossing more than once does not arise, since the modification of $n$ in the core does not begin until long after the maximum density of the polytrope has been passed.) But according to his own investigation of the state of the core, the polytropic index is reduced in the core, so that distributions of type C are impossible. Our result therefore disproves his theory as set forth in his detailed paper. To rehabilitate Milne's astronomical theory it would be necessary to suppose that the physics of the central core as given in his paper has gone widely astray.

We can define more narrowly the conditions under which an ordinary star, *e.g.* the sun, could have a core of white dwarf density. If the sun formed a polytrope $n = 4{\cdot}5$, its central density would be about 9000. Hence, for the density of the core to exceed 9000, we must have $n_0 > 4{\cdot}5$. It seems safe to say that $n$ in the core would have to be greater than 5 in order to make the average for the whole star greater than 4·5.

All possible spherical distributions of matter can be described by a varying polytropic index $n$. The phrase " incomplete polytropes " in my title has reference to the main astronomical application of the theorem, viz. when the outer part of a star is (with sufficient approximation) an incomplete polytropic region † resting on a central core of different structure.

## *Proof of the Theorem.*

For any distribution of matter with spherical symmetry the polytropic index $n$ is defined by ‡

$$1 + 1/n = d(\log \mathrm{P})/d(\log \rho) \quad . \quad . \quad . \quad (1)$$

For $n$ constant, this gives the usual expression $\mathrm{P} \propto \rho^{\gamma}$, $\gamma = 1 + 1/n$. By (1)

$$n\rho d\mathrm{P} = (n+1)\mathrm{P}d\rho.$$

* The comparison curve A in this case is the polytrope whose index corresponds to the outer part of the star.

† *Internal Constitution of the Stars,* p. 94.

‡ My adoption of this definition is due to a criticism privately communicated by Professor Milne. It is simpler physically and more in accordance with current practice than my original definition $n = d(\log \rho) / d(\log \phi)$. The theorem is true for either definition, but the method of averaging $n$ is different. Strictly speaking, the P used throughout this investigation is not the actual total pressure but its excess over the pressure (radiation-pressure) at the boundary (*cf.* equation (8)). This small correction to P, of the order 1 dyne per sq. cm., has no appreciable effect on $n$ in the interior, and it avoids a rapid variation of $n$ in the extreme outer layers.

We have $$d(\mathrm{P}/\rho) = \frac{\rho d\mathrm{P} - \mathrm{P}d\rho}{\rho^2} = \left(1 - \frac{n}{n+1}\right)\frac{\rho d\mathrm{P}}{\rho^2}$$

$$= \frac{1}{n+1}d\phi \quad . \quad . \quad . \quad . \quad . \quad . \quad (2)$$

since $d\mathrm{P} = \rho d\phi$. Hence, integrating from the boundary inwards,

$$\frac{\mathrm{P}}{\rho} = \int_0^\phi \frac{1}{n+1}d\phi = \frac{1}{\bar{n}+1}\phi \quad . \quad . \quad . \quad (3)$$

where $1/(\bar{n}+1)$ is the average value of $1/(n+1)$ outside the point considered for equal steps of $\phi$.

We shall introduce a further average value (for the whole star), viz. $n_0$, defined by

$$\frac{1}{n_0+1}\int \phi d\mathrm{M}_r = \int \frac{1}{\bar{n}+1}\phi d\mathrm{M}_r \quad . \quad . \quad . \quad (4)$$

so that

$$\frac{1}{n_0+1}\int_0^{\mathrm{M}}\int_0^\phi d\mathrm{M}_r d\phi = \int_0^{\mathrm{M}}\int_0^\phi \frac{1}{n+1}d\mathrm{M}_r d\phi \quad . \quad . \quad (4a)$$

If $n$ is positive, $n_0$ is an average value of $n$ intermediate between the maximum and minimum values. Negative values of $n$ might conceivably occur and are covered by our analysis; but in that case we must be content to say that $1/(n_0+1)$ is an average value of $1/(n+1)$. (It should be noticed that $n$ changes from positive to negative by passing through the value $\infty$, not by passing through zero; so that a physical condition intermediate between $n = +10$ and $n = -10$ corresponds to values of $n$ greater than $+10$ or less than $-10$.)

The calculation of $\Omega$ follows closely the method (due to Emden) given in *Internal Constitution of the Stars*, p. 87. We have *

$$\Omega = \mathrm{G}\int \frac{\mathrm{M}_r d\mathrm{M}_r}{r} = \tfrac{1}{2}\mathrm{G}\int \frac{d(\mathrm{M}_r^2)}{r} \quad . \quad . \quad . \quad (5)$$

$$= \tfrac{1}{2}\mathrm{G}\frac{\mathrm{M}^2}{\mathrm{R}} + \tfrac{1}{2}\mathrm{G}\int \frac{\mathrm{M}_r^2}{r^2}dr$$

by integration by parts. Or since $\mathrm{G}\mathrm{M}_r/r^2 = -d\phi/dr$,

$$\Omega = \tfrac{1}{2}\mathrm{G}\mathrm{M}^2/\mathrm{R} - \tfrac{1}{2}\int \mathrm{M}_r d\phi \quad . \quad . \quad . \quad (6)$$

Since $d\mathrm{M}_r = 4\pi\rho r^2 dr$ and $\mathrm{G}\mathrm{M}_r/r = -r d\phi/dr$, (5) can also be written

$$\Omega = -4\pi\int r^3\rho\frac{d\phi}{dr}dr$$

$$= -4\pi\int r^3 d\mathrm{P} \quad . \quad . \quad . \quad . \quad . \quad (7)$$

* When no limits are inserted in the integrals, integration from the centre to the surface is intended; $\phi$ is, as usual, measured from the boundary.

where

$$P = \int_0^\phi \rho d\phi = \rho\phi/(\bar{n}+1) \quad . \quad . \quad . \quad (8)$$

by (3). Integrating (7) by parts, the integrated part vanishes at both limits, so that

$$\Omega = 4\pi\int 3r^2dr \,.\, P$$

$$= 3\int \frac{\rho\phi}{\bar{n}+1} \cdot 4\pi r^2 dr$$

$$= 3\int \frac{\phi dM_r}{\bar{n}+1} = \frac{3}{n_0+1}\int \phi dM_r$$

by (4). By another integration by parts this becomes

$$\Omega = -\frac{3}{n_0+1}\int M_r d\phi \quad . \quad . \quad . \quad (9)$$

Combining (6) and (9) we eliminate the integral and obtain

$$\Omega = \frac{3}{5-n_0}\frac{GM^2}{R}$$

which is the theorem stated.

---

*Upper Limits to the Central Temperature and Density of a Star.*
By Sir A. S. Eddington, F.R.S.

1. *Stars degenerate at the Centre.*—We shall find upper limits to the central density and temperature of a star of given mass, assuming that

(*a*) The density does not decrease inwards;

(*b*) The equation of state of degenerate matter is correctly given by Milne's * equation

$$p = \kappa\rho^{\frac{5}{3}}, \qquad \text{where} \qquad \kappa = 3{\cdot}17.10^{12}.$$

Consider a star of mass M and central density $\rho$. The central pressure is always increased by transferring matter inwards; † hence the greatest possible central pressure is reached by transferring matter inwards until the distribution has uniform density $\rho$, further transfer being then forbidden by condition (*a*). Therefore, by the formula for a uniform sphere,

$$P_{max} = \frac{3}{8\pi}\frac{GM^2}{R^4} = \tfrac{1}{2}(\tfrac{4}{3}\pi)^{\frac{1}{3}}GM^{\frac{2}{3}}\rho^{\frac{4}{3}} = B\rho^{\frac{4}{3}} \quad . \quad . \quad (1)$$

where B depends only on the star's mass.

The gas-pressure being $\kappa\rho^{\frac{5}{3}}$ and the radiation-pressure $\frac{1}{3}aT^4$, we have

$$\kappa\rho^{\frac{5}{3}} + \tfrac{1}{3}aT^4 < B\rho^{\frac{4}{3}} \quad . \quad . \quad . \quad . \quad (2)$$

---

* *M.N.*, **91**, 30, 1930.

† *Internal Constitution of the Stars*, p. 91; German ed., p. 115.

Hence $\kappa\rho^{\frac{1}{3}} < B$, giving an upper limit

$$\rho_{max} = (B/\kappa)^3 \quad . \quad . \quad . \quad . \quad (3)$$

Again, for given $\rho$, the maximum value of T is given by

$$\tfrac{1}{3}aT^4 = B\rho^{\frac{4}{3}} - \kappa\rho^{\frac{5}{3}}$$

by (2). By differentiation, the maximum value of the right-hand side is obtained when

$$\tfrac{4}{3}B\rho^{\frac{1}{3}} - \tfrac{5}{3}\kappa\rho^{\frac{2}{3}} = 0$$

so that

$$\rho = (\tfrac{4}{5}B/\kappa)^3 \quad . \quad . \quad . \quad . \quad (4)$$

Hence

$$\tfrac{1}{3}aT^4_{max} = B(\tfrac{4}{5}B/\kappa)^4 - \kappa(\tfrac{4}{5}B/\kappa)^5 = \tfrac{1}{5}B(\tfrac{4}{5}B/\kappa)^4 \quad . \quad (5)$$

Since B varies as $M^{\frac{2}{3}}$, the upper limits given by (3) and (5) depend on the mass of the star as follows:

$$\rho_{max} \propto B^3 \propto M^2 \quad . \quad . \quad . \quad . \quad (6)$$

$$T_{max} \propto B^{\frac{4}{3}} \propto M^{\frac{2}{3}} \quad . \quad . \quad . \quad . \quad (7)$$

For mass equal to that of the sun the numerical results are

$$B = 8{\cdot}48.10^{14} \qquad \rho_{max} = 1{\cdot}91.10^7 \qquad T_{max} = 3{\cdot}44.10^9 \qquad (8)$$

By (4) the density which corresponds to $T_{max}$ is $9{\cdot}8.10^6$.

The temperature, however, will have to be very much lower than $T_{max}$ if the condition for degeneracy is to be fulfilled. Taking material of temperature $3{\cdot}4.10^9$ and the corresponding density, the pressure calculated according to

$$\begin{aligned} \text{degeneracy formula } (\kappa\rho^{\frac{5}{3}}) &= 1{\cdot}42.10^{24}, \\ \text{perfect gas formula } (R\rho T/\mu) &= 1{\cdot}26.10^{24} \end{aligned}$$

with $\mu = 2{\cdot}2$. If for given density we plot $p$ against T the degeneracy formula and the perfect gas formula give the two asymptotes to the actual pressure-curve. Thus the temperature $3{\cdot}4.10^9$ corresponds approximately to the intersection of the two asymptotes, or to a condition about midway between perfect gas and complete degeneracy.

2. *Non-degenerate Stars.*—An additional assumption is required—

(*c*) The pressure of non-degenerate matter is greater than the pressure of degenerate matter of the same density.

Consider matter of fixed density $\rho$ of the order $10^6$. At low temperatures it is completely degenerate; on increasing the temperature it becomes non-degenerate, until at sufficiently high temperatures it becomes a perfect gas and the pressure increases proportionately to the temperature. Presumably the change of $dp/dT$ from 0 to a limiting constant is continuous. At any rate it is scarcely conceivable that increase of temperature can cause decrease of pressure; thus assumption (*c*) appears inevitable.

Accordingly in non-degenerate matter we can set $p = \kappa'\rho^{\frac{5}{3}}$ where $\kappa' > \kappa$. It will be seen from (3) and (5) that the substitution of $\kappa'$ for

$\kappa$ decreases $\rho_{max}$ and $T_{max}$, the former being proportional to $1/\kappa'^3$ and the latter to $1/\kappa'$. From the result at the end of § 1 it seems likely that $\kappa'/\kappa$ is fairly large and that the reduction of the upper limits will be considerable; but we are scarcely in a position to guess the extent of the reduction.

We see that with assumptions (*a*), (*b*), and (*c*) the values of $\rho_{max}$ and $T_{max}$ calculated in § 1 remain as extreme upper limits in all circumstances.

3. *Remarks.*—The strict upper limits naturally correspond to rather extravagant conditions, and are not likely to be attained. Besides the reduction due to incomplete degeneracy, there is a further reduction due to the fact that the density of a star is not uniform, so that $P_{max}$ is not attained. To see the effect of this we calculate P for a polytrope with $\gamma = \frac{5}{3}$ instead of for a uniform sphere of the same central density. The result is

$$P = 0{\cdot}296(\tfrac{4}{3}\pi)^{\frac{1}{3}}GM^{\frac{2}{3}}\rho^{\frac{4}{3}}.$$

Comparing with (1), B is reduced approximately in the ratio 0·6, which leads to $\rho_{max}$ being divided by 5 and $T_{max}$ by 2. Thus for a distribution more or less of the character which might be expected in a white dwarf, the upper limits are only moderately reduced.

It is not supposed that the "reduced upper limits" (taking into account non-degeneracy and non-uniformity of density) give the actual temperature and density of a star. That depends on the radius, etc. But the star would probably attain these reduced limits at some stage during its collapse to the final state of extinction.

Upper limits to the temperature and density given by a universal formula must necessarily be rather high, since white dwarfs are included. Our result may, however, be of use in curbing riotous speculations which go beyond a temperature of $10^9$ degrees and a density of $10^6$.

---

## *The Dissociation Formula according to the Relativistic Statistics.*

By S. Chandrasekhar.

(*Communicated by R. H. Fowler and E. A. Milne.*)

1. The temperatures conceived by Professor Milne * for the interiors of stars quite transcend all previous expectations and are precisely those temperatures at which the relativistic effect becomes important in statistical theory—at least for the electron-assembly, if not for the atomic assembly. It was thought worth while therefore to work out the dissociation formulæ on the relativistic statistics. The method followed in this paper will be the very elegant method developed by Milne in his recent paper.† Indeed the following will have to be considered as merely supplementing his results.

* *The Observatory*, **53**, 238, 1930.
† *M.N.*, **90**, 769, 1930.

2. *The Enunciation of the Dissociation Formulæ for Particles obeying Different Statistics.*—If we consider the case of a neutral atom dissociating into an ion and an electron, we know for certain that the electrons obey the Fermi-Dirac statistics, but the neutral atoms in general obey only the Einstein-Bose statistics. We have in fact the empirical rule that particles carrying a charge of an even or an odd multiple of the electronic charge obey the Einstein-Bose or the Fermi-Dirac statistics respectively. Hence in considering the dissociative equilibrium of different types of particles "chemically" reacting with each other, in the light of the new statistics we must, in general, consider the case of the different particles obeying different statistics.*

Let us for simplicity consider the case of an equilibrium characterised by the chemical equation

$$aA + bB = A_aB_b + \chi \quad . \quad . \quad . \quad (1)$$

representing the reaction in which $a$ particles of type A react reversibly with $b$ particles of type B to produce one particle of type $A_aB_b$ with an evolution of energy $\chi$. Let the particles A and B obey the Fermi-Dirac statistics, and $A_aB_b$ the Einstein-Bose statistics,† which must happen when $a + b$ is even. Suppose that the total number of A's present in volume V be X, that of the B's Y. Let these occur in the assembly (in equilibrium) as L *free* particles of type A, and M *free* particles of type B. Then we have obviously

$$X = L + aN \quad . \quad . \quad . \quad . \quad (2)$$

$$Y = M + bN \quad . \quad . \quad . \quad . \quad (3)$$

If, further, $T_A$, $T_B$, and $T_{AB}$ are kinetic energies of the respective particles, the total energy U is given by

$$U = T_A + T_B + T_{AB} - N\chi \quad . \quad . \quad . \quad (4)$$

Let $x_s$, $y_s$, $z_s$ represent the numbers of cells associated with the energy-range $E_s$ to $E_s + dE_s$ for the particles A, B, and $A_aB_b$ respectively. The entropy of the whole assembly by the Boltzmann principle is

$$S = k \log \Pi_s \frac{x_s!}{(x_s - p_s')!\, p_s'!} \Pi_s \frac{y_s!}{(y_s - q_s')!\, q_s'!} \Pi_s \frac{(z_s + r_s')!}{z_s!\, r_s'!} \quad . \quad (5)$$

where each separate factor corresponds to the total number of "complexions" obtained by arranging $p_s'$ particles of type A into $x_s$ cells, $q_s'$ particles of type B into $y_s$ cells, and $r_s'$ particles of type $A_aB_b$ into $z_s$ cells with the conditions

$$\sum p_s' = L, \quad \sum q_s' = M, \quad \sum r_s' = M \quad . \quad . \quad (6)$$

and that the particles $A_aB_b$ obey the Einstein-Bose statistics, while the

* I am indebted to Mr. Fowler for a full appreciation of this point.

† If $a=b=1$, this would correspond to a neutral atom dissociating into an ion and an electron.

other two types of particles obey the Fermi-Dirac statistics. It is convenient to introduce

$$\left.\begin{aligned} p_s^0 &= x_s - p_s' \\ q_s^0 &= y_s - q_s' \\ r_s^0 &= z_s + r_s' \end{aligned}\right\} \quad . \quad . \quad . \quad . \quad (7)$$

The expression for the entropy (5) then reduces to

$$S = k \log \prod_s \frac{x_s!}{p_s^0!\, p_s'!} \prod_s \frac{y_s!}{q_s^0!\, q_s'!} \prod_s \frac{r_s^0!}{z_s!\, r_s'!} \quad . \quad . \quad (5')$$

Now the entropy will have to be a maximum subject to the conditions (2), (3), (6), (7), and the further condition

$$U = \sum_s p_s' E_s^A + \sum_s q_s' E_s^B + \sum_s r_s' (E_s^{AB} - \chi) \quad . \quad (8)$$

We apply, as usual in such problems, the Lagrange method.

Applying Stirling's theorem in the form

$$\log n! \sim n \log n - n,$$

and effecting the variation in the $p_s'$, etc. (with $x_s$, $y_s$, $z_s$ constant), we find

$$0 = -\sum \delta p_s^0 (1 + \log p_s^0) - \sum \delta p_s' (1 + \log p_s') - (\text{similar terms in } q)$$
$$+ \sum \delta r_s^0 (1 + \log r_s^0) - \sum \delta r_s' (1 + \log r_s') \quad . \quad . \quad . \quad (9)$$
$$0 = \delta p_s^0 + \delta p_s' \quad . \quad . \quad . \quad . \quad (10)$$
$$0 = \delta q_s^0 + \delta q_s' \quad . \quad . \quad . \quad . \quad (10')$$
$$0 = \delta r_s^0 - \delta r_s' \quad . \quad . \quad . \quad . \quad (10'')$$
$$0 = \sum \delta p_s' + a \sum \delta r_s' \quad . \quad . \quad . \quad (11)$$
$$0 = \sum \delta q_s' + b \sum \delta r_s' \quad . \quad . \quad . \quad (11')$$
$$0 = \sum_s E_s^A \delta p_s' + \sum_s E_s^B \delta q_s' + \sum_s (E_s^{AB} - \chi) \delta r_s' \quad . \quad (12)$$

In applying the Lagrange method multiply the equations (10), (10'), (10''), (11), (11'), and (12) by $F_s + 1$, $G_s + 1$, $H_s - 1$, $\alpha$, $\beta$, and $\gamma$ respectively. Adding the complete set of equations and equating to zero the coefficients of $\delta p_s^0 \ldots \delta r_s'$, we have easily

$$-\log p_s^0 + F_s = 0, \qquad -\log q_s^0 + G_s = 0, \qquad \log r_s^0 + H_s = 0.$$
$$-\log p_s' + F_s - \alpha - \gamma E_s^A = 0,$$
$$-\log q_s' + G_s - \beta - \gamma E_s^B = 0,$$
$$-\log r_s' - H_s - a\alpha - b\beta - \gamma(E_s^{AB} - \chi) = 0.$$

Altering the constants $F_s$, $G_s$, $H_s$ to new constants $C_s^{AB}$, etc., such that we have $r_s^0 = C_s^{AB}$, etc.,

$$r_s' = C_s^{AB} e^{-a\alpha - b\beta - \gamma(E_s^{AB} - \chi)},$$

or $$z_s = r_s^0 - r_s' = C_s^{AB}(1 - e^{-a\alpha - b\beta - \gamma(E_s^{AB} - \chi)}),$$

giving us $$r_s' = \frac{z_s}{e^{a\alpha+b\beta+\gamma(E_s^{AB}-\chi)} - 1}.$$

Similarly

$$p_s' = \frac{x_s}{e^{\alpha+\gamma E_s^A} + 1}, \qquad q_s' = \frac{y_s}{e^{\beta+\gamma E_s^B} + 1}.$$

$\gamma$ is easily identified to be $\frac{1}{kT}$. The values of L, M, and N follow from (6). Replacing the sums by integrals and writing $kT\theta$ for E, we have

$$L = kT\int_0^\infty \frac{x_s d\theta}{e^{\alpha+\theta} + 1},$$

$$M = kT\int_0^\infty \frac{y_s d\theta}{e^{\beta+\theta} + 1},$$

$$N = kT\int_0^\infty \frac{z_s d\theta}{e^{\left(a\alpha+b\beta-\frac{\chi}{kT}\right)+\theta} - 1}.$$

If we write in the integral for N

$$\alpha' = a\alpha + b\beta - \frac{\chi}{kT}$$

we have its equivalent

$$a\alpha + b\beta = \frac{\chi}{kT} + \alpha'. \qquad . \quad . \quad . \quad (13)$$

This is for the simple reaction (1). This result is easily generalised for more complicated reactions, and we can enunciate the following generalisation of the theorem proved by Milne (*loc. cit.*) :—

Let us consider a gaseous mixture in which the constituents $C_1$, $C_2$ . . . $C_r$ . . . react reversibly according to the chemical equation

$$\sum_r n_r C_r = \sum_{r'} n_{r'} C_{r'} + \chi$$

where $\chi$ is energy (expressed in ergs) evolved when $n_r$ molecules of $C_r$, etc. react to form $n_{r'}$ molecules of $C_{r'}$, etc. Let the gaseous mixture be contained in a volume V at temperature T and consist of $N_r$ molecules of $C_r$, etc., $N_{r'}$ molecules of $C_{r'}$, etc. The condition for dissociative equilibrium is obtained by eliminating $\alpha_1$, . . . $\alpha_r$ ; $\alpha_{1'}$ . . . $\alpha_{r'}$ from the set of equations

$$N_r = kT\int_0^\infty \frac{x_r d\theta}{e^{a_r+\theta+\epsilon_r}}; \text{ etc.} \qquad . \quad . \quad . \quad (14)$$

$$N_{r'} = kT\int_0^\infty \frac{x_{r'} d\theta}{e^{a_{r'}+\theta} + \epsilon_{r'}}; \text{ etc.} \qquad . \quad . \quad . \quad (15)$$

and

$$\sum_r n_r a_r = \sum_{r'} n_{r'} a_{r'} + \frac{\chi}{kT} \qquad . \quad . \quad . \quad (16)$$

where $x_r$, etc., $x_{r'}$, etc., are the numbers of cells in a given energy range E to E + $dE$ for the particles of the type $C_r$, etc., $C_{r'}$, etc., respectively, and $\epsilon_r$ equals + 1 or − 1 according as the particles "$C_r$" obey the Einstein-Bose or the Fermi-Dirac statistics.

3. *The Equations of Relativistic Statistics.*—When the relativistic effect is taken into account, the usual formula for the number of cells associated with a given energy range $E_s$ to $E_s + dE_s$ (*e.g.*)

$$Z_s dE_s = \frac{2\pi V q}{h^3}(2m)^{\frac{3}{2}}E_s^{\frac{1}{2}}dE_s \quad . \quad . \quad . \quad (17)$$

($q$ = the statistical weight) has to be replaced by

$$Z_s dE_s = \frac{2\pi V q}{h^3}(2m)^{\frac{3}{2}}E_s^{\frac{1}{2}}\left(1+\frac{E_s}{2mc^2}\right)^{\frac{1}{2}}\left(1+\frac{E_s}{mc^2}\right)dE_s \quad . \quad (17')$$

If the relativistic effect becomes predominant (we state the physical conditions for this later), we shall have to work with

$$Z_s dE_s = \frac{4\pi V q}{h^3 c^3}E_s^2 dE_s \quad . \quad . \quad . \quad (18)$$

To work out the dissociation formula when certain types of particles have a predominant relativistic effect while others have not, we have simply to use for the corresponding $x_r$ or $x_{r'}$ the expression (17) or (18) in equation (14) or (15). But we take this opportunity to write down the equations of the relativistic statistics for the *Fermi-Dirac* case in a form convenient for application. Working with (18), we can derive

$$\left.\begin{aligned} N &= 8\pi V q\left(\frac{kT}{hc}\right)^3 U_2 \\ E &= 24\pi V q k T\left(\frac{kT}{hc}\right)^3 U_3 \\ pV &= \tfrac{1}{3}E \\ S &= nk\left[4\frac{U_3}{U_2} - \log A\right] \end{aligned}\right\} \quad . \quad . \quad . \quad (18')$$

where

$$U_\rho = \frac{1}{\Gamma(\rho+1)}\int_0^\infty \frac{\theta^\rho d\theta}{\frac{1}{A}e^\theta + 1}.$$

In making the transition from the degenerate to the non-degenerate case we simply pass from one limiting value for $U_\rho$ characterised by large A to the other limiting value characterised by small A. It can easily be shown that the condition for degeneracy in this case is different from the Sommerfeld criterion for the non-relativistic case. If we should regard an assembly as degenerate when the relativistic effect is predominant, we must have the inequality

$$n >> \left(\frac{kT}{hc}\right)^3 \frac{4\pi q}{3} \left(= 2{\cdot}86T^3\right)$$

satisfied. The assembly must satisfy also another condition, namely, that which secures that the relativistic effect is predominant.

For convenience of reference we collect below the conditions which an assembly must satisfy in order that we can regard a system as degenerate or non-degenerate in the two distinct cases—where the relativistic effect is negligible and where it is highly predominant:

| Magnitude of Relativistic Effect. | State of the Assembly. | Conditions. (The Numerical Values are those for an *Electron*-Assembly.) |
|---|---|---|
| Second order effect | (i) Degenerate | $n << \frac{8\pi m^3c^3}{3h^3} = 5{\cdot}88 \times 10^{29}$ |
| | | $n >> \frac{q}{h^3}(2\pi mkT)^{\frac{3}{2}} = 4{\cdot}87 \times 10^{15} \times T^{\frac{3}{2}}$ |
| | (ii) Non-degenerate | $n << \frac{q}{h^3}(2\pi mkT)^{\frac{3}{2}} = 4{\cdot}87 \times 10^{15} \times T^{\frac{3}{2}}$ |
| | | $T << \frac{mc^2}{k} = 5{\cdot}9 \times 10^9$. |
| Predominant | (iii) Degenerate | $n >> \left(\frac{kT}{hc}\right)^3 \frac{4\pi q}{3} = 2{\cdot}86T^3$ |
| | | $n >> \frac{8\pi m^3c^3}{3h^3} = 5{\cdot}88 \times 10^{29}$ |
| | (iv) Non-degenerate | $n << \left(\frac{kT}{hc}\right)^3 \frac{4\pi q}{3} = 2{\cdot}86T^3$ |
| | | $T >> \frac{mc^2}{k} = 5{\cdot}9 \times 10^9$. |

The conditions (ii) and (iv) for the case of non-degeneracy hold good for the Einstein-Bose case also. This is clear when we note that the condition for the rapid convergence of the series expansion of (14) for large $\alpha_r$, when $\epsilon_r$ equals either $+1$ or $-1$, is just the same (and the non-degeneracy condition is merely the analytical expression of this). In the sequel we do *not* consider the case of degeneracy for the atomic assembly (some constituents of which will obey the Einstein-Bose statistics), for, first, such cases are of no practical value, and secondly, the question of degeneracy for the particles obeying the Einstein-Bose statistics is closely bound up with the difficulty pointed out by Uhlenbeck.* In fact, in the degenerate case the particles can *never* have a predominant relativistic effect because all the particles go down to the zero state. (In the Fermi-Dirac statistics this is prevented by Pauli's principle.)

4. *The Dissociation Formulæ for the Relativistic Case.*—(*a*) Let all the constituents be non-degenerate. We consider the case of the ionisation of an atom A capable of being in a state of lowest energy content $A^{(1)}$, its ionised form being $A_+^{(1)}$. Let $\chi$ be the energy of ionisation. If $C^{(1)}$ and $C_+^{(1)}$ are the atomic concentrations per unit

* G. E. Uhlenbeck, *Over Statistische Methoden in die Theorie der Quanta*, Thesis, Leiden (1927), p. 70.

volume we have equations corresponding to (14) and (15) reducing, on using for the number of cells, the value given by (18), to *

$$C^{(1)} = 8\pi q^{(1)}\left(\frac{kT}{hc}\right)^3 e^{-\alpha^{(1)}} \quad . \quad . \quad . \quad (19)$$

$$C_+^{(1)} = 8\pi q_+^{(1)}\left(\frac{kT}{hc}\right)^3 e^{-\alpha+^{(1)}} \quad . \quad . \quad . \quad (20)$$

$q^{(1)}$ and $q_+^{(1)}$ being the statistical weights. For $C_e$, the electron-concentration, we have

$$C_e = 8\pi q_e\left(\frac{kT}{hc}\right)^3 e^{-\alpha_e} \quad . \quad . \quad . \quad (21)$$

and as the chemical equation in this case is

$$A_+^{(1)} + e = A^{(1)} + \chi,$$

we have for our fourth equation, in addition to (19), (20), and (21), according to (16),

$$\alpha_+^{(1)} + \alpha^{(e)} = \alpha^{(1)} + \frac{\chi}{kT} \quad . \quad . \quad . \quad (22)$$

Hence our dissociation formula in this case is

$$\frac{C_+^{(1)} \cdot C_e}{C^{(1)}} = \frac{q_+^{(1)} q^{(e)}}{q^{(1)}} 8\pi\left(\frac{kT}{hc}\right)^3 e^{-\frac{\chi}{kT}} \quad . \quad . \quad (23)$$

The above equation is analogous to the Saha equation for the non-relativistic case.

(*b*) Let us now consider the case where the electrons are degenerate but the atoms and the ionised atoms are non-degenerate. Then we have in this case for the electron-concentration (because it obeys the Fermi-Dirac statistics)

$$C_e = \frac{4\pi}{3} q_e\left(\frac{kT}{hc}\right)^3 (-\alpha_e)^3 \text{ approximately} \quad . \quad . \quad (24)$$

giving

$$-\alpha_e = \left(\frac{3C_e}{4\pi q_e}\right)^{\frac{1}{3}} \frac{hc}{kT} \quad . \quad . \quad . \quad . \quad (24')$$

We have therefore for our eliminant

$$\log\left(\frac{C^{(1)}}{C_+^{(1)}} \frac{q_+^{(1)}}{q^{(1)}}\right) = \frac{\chi}{kT} + \frac{hc}{kT}\left(\frac{3C_e}{4\pi q_e}\right)^{\frac{1}{3}} \quad . \quad . \quad (25)$$

* (19) and (20) are true, independent of what statistics they obey, but (19) would in general correspond to the Einstein-Bose case, and (20) to the Fermi-Dirac case.

We give below the corresponding equation for the non-relativistic case for comparison : *

$$\log\left(\frac{C^{(1)}}{C_+^{(1)}}\frac{q_+^{(1)}}{q^{(1)}}\right) = \frac{\chi}{kT} + \frac{h^2}{2m_e kT}\left(\frac{3C_e}{4\pi q_e}\right)^{\frac{2}{3}} \quad . \quad . \quad (26)$$

5. *Other Possible Cases.*—We now pass on to the consideration of cases intermediate to the relativistic and the non-relativistic cases. As our table shows, it is quite possible for the electron-assembly to be governed by the relativistic equations, while the atomic assembly obeys reasonably well the non-relativistic equations. We assume that the atomic system is non-degenerate. We have then two cases corresponding to the two possible behaviours of the electron-assembly.

(i) *Non-degenerate Electrons.*—In the equations corresponding to (14) and (15) for $C^{(1)}$ and $C_+^{(1)}$ we have to use for the $x_r$'s the expression (17) and for $C_e$ the expression (18). We have then

$$C^{(1)} = \frac{q^{(1)}(2\pi m^{(1)}kT)^{\frac{3}{2}}}{h^3}e^{-\alpha^{(1)}} \quad . \quad . \quad . \quad (27)$$

$$C_+^{(1)} = \frac{q_+^{(1)}(2\pi m_+^{(1)}kT)^{\frac{3}{2}}}{h^3}e^{-\alpha+^{(1)}} . \quad . \quad . \quad (28)$$

But we have for the electron-concentration

$$C_e = \frac{8\pi q_e}{h^3c^3}(kT)^3e^{-\alpha_e} . \quad . \quad . \quad . \quad (29)$$

We have therefore for our dissociation formula, remembering (22),

$$\frac{C_+^{(1)}C_e}{C^{(1)}} = \frac{q_+^{(1)} \cdot q_e}{q^{(1)}}\left(\frac{m_+^{(1)}}{m^{(1)}}\right)^{\frac{3}{2}}8\pi\left(\frac{kT}{hc}\right)^3 e^{-\chi/kT} \quad . \quad . \quad (30)$$

which, neglecting the trivial factor $m_+^{(1)}/m^{(1)}$ is exactly the same as (23) derived for the case when the relativistic-non-degenerate equations were used for the atomic assembly.

(ii) *Degenerate Electrons.*—In this case, instead of (29) we have to use (24), and our dissociation formula is again

$$\log\left[\frac{C^{(1)}}{C_+^{(1)}}\frac{q_+^{(1)}}{q^{(1)}}\left(\frac{m_+^{(1)}}{m^{(1)}}\right)^{\frac{3}{2}}\right] = \frac{\chi}{kT} + \frac{hc}{kT}\left(\frac{3C_e}{4\pi q_e}\right)^{\frac{1}{3}} . \quad . \quad (31)$$

which is exactly the same as (25).

Thus we have the result that the dissociation formula is independent of whether the atomic assembly is governed by the relativistic or the non-relativistic equations in so far as it is postulated that it is in any case non-degenerate. It is the behaviour of the electron-assembly (*i.e.* whether it is degenerate or non-degenerate) that matters. Since this is so in the two extreme cases, we can reasonably generalise and assume that the equations (23) and (25) hold for all intermediate

* General formulæ for dissociative equilibrium were first given by R. H. Fowler, *Proc. Roy. Soc.*, A, **113**, 432, 1926. Explicit forms were given by S. Chandrasekhar, *Phil. Mag.*, **9**, 292, 1930, and also by E. A. Milne (*loc. cit.*).

behaviour of the atomic assembly. It is unlikely that the atomic assembly can be degenerate at those high temperatures (of the order of $10^{10}$) when the concentration would have to be greater than $5 \times 10^{38}$. (The electron-assembly is degenerate at very much higher temperatures and much lower concentration obviously because of its very small mass.) So far as the atomic assembly is concerned, therefore, the only question is whether the relativistic effect is large or small for the non-degenerate case. This question, as we have already seen, does not affect our dissociation formulæ. If we could be sure about the behaviour of the electron-assembly, we could immediately choose our dissociation formula independent of the behaviour of the atomic assembly.

What has been said regarding the dissociation formula with the relativistic equations is equally true for the electron-assembly with the non-relativistic equations, as can easily be verified. But a state of affairs where the electron-assembly is governed by non-relativistic equations while the atomic assembly obeys the relativistic equations is physically inconceivable. We have therefore to deal with four kinds of dissociation formulæ—namely, for the two possible behaviours of the electron-assembly for both the relativistic and the non-relativistic cases.

6. *Numerical Calculations.*—(i) According to Milne,* the central density, and the central and the effective temperatures of his highly collapsed configurations (which he identifies with the white dwarfs), are respectively for $M = \cdot 85\ \odot$:

$$\left.\begin{aligned} \rho_c &= 2{\cdot}87 \times 10^6 \beta^3 \\ T_c &= 2{\cdot}92 \times 10^9 \beta(1-\beta)^{\frac{1}{2}} \\ T_e &= 11{,}300\beta^{\frac{1}{2}} \end{aligned}\right\} \quad . \quad . \quad . \quad (32)$$

where

$$\beta = 1 - \frac{\kappa L}{4\pi c G M} \qquad (\kappa = \text{opacity}).$$

If the effective temperature should correspond to, say, 10000°, $\beta$ must be about 0·9. This gives us immediately

$$\left.\begin{aligned} C_e &= 7 \times 10^{29} \text{ per cm.}^3 \\ T_c &= 1{\cdot}4 \times 10^9 \text{ degrees} \end{aligned}\right\}.$$

The electron-assembly therefore just satisfies those conditions necessary for the system to be degenerate and at the same time have the relativistic effect predominant. Hence the dissociation formula we ought to use is (25), which reduces on using numerical values ($x$ = degree of dissociation) to

$$\log_e \frac{1-x}{x} = \frac{\chi}{kT} + \cdot 7045 \frac{C_e^{\frac{1}{3}}}{T}$$

$$= \frac{\chi}{kT} + 4{\cdot}483 \quad . \quad . \quad . \quad (33)$$

* E. A. Milne, *M.N.*, **91**, 4, 1930.

For temperatures of the order of $10^9$ the first term in (33) is negligible compared with the second, even when $\chi$ corresponds to the K-ionisation potentials for the heaviest elements. The degree of dissociation given by (34) is therefore practically zero, and independent of the ionisation potential. This at first sight would appear to contradict the common-sense view that at these extreme conditions of temperature and pressure matter must necessarily be ionised down to the bare nuclei. At the same time we have to recognise that at such high concentrations every electron must be under the influence of one atomic nucleus or another all the time. The whole system is, in fact, "a gigantic molecule in the lowest quantum state." * But "statistically" they must all be free in the sense that they travel the whole of the phase space. Our analysis giving 0 per cent. ionisation will have to be interpreted this way. Thus, whenever we get the calculated degree of dissociation as being practically zero and independent to a large extent of our choice of the ionisation potential, we can then safely conclude that matter has reached such extreme conditions that we must regard (statistically) all the atoms as being "ionised" down to their bare nuclei, and, further, the electron-assembly as being highly degenerate. We can use this result as a "degeneracy-condition." †

(ii) We now use the *non*-relativistic dissociation formula (26). At the interface of the "composite configurations," where we pass from a solution of Emden's equation "$n = 3$" to another of Emden's, "$n = \frac{3}{2}$," the pressure and temperature are (Milne, *loc. cit.*, equations (82) and (83))

$$\rho' = 3{\cdot}66 \times 10^7 \frac{1-\beta}{\beta}\,;\quad T' = {\cdot}843 \times 10^{10}\left(\frac{1-\beta}{\beta}\right)^{\frac{2}{3}}$$

or

$$\frac{C_e'^{\frac{2}{3}}}{T'} = \frac{(\rho'/2m_H)^{\frac{2}{3}}}{T'} = 5{\cdot}9 \times 10^{10} \quad . \quad . \quad . \quad (34)$$

Introducing (34) in (26) we have simply

$$\log_e \frac{1-x}{x} = \frac{\chi}{kT} + 2{\cdot}482 \quad . \quad . \quad . \quad (35)$$

Comparing (35) with (33) we can deduce that matter must from now onwards be treated as "degenerate"—justifying therefore the transition to the degenerate Fermi-Dirac equation of state for the electrons.

In conclusion I wish to express my thanks to Mr. R. H. Fowler and Professor E. A. Milne for their advice and encouragement during the course of the work.

* R. H. Fowler, "On Dense Matter," *M.N.*, **87**, 114, 1926.

† In this connection see W. Anderson, *Physik. Zeits.*, **30**, 360, 1929, also S. Chandrasekhar (*loc. cit.*), § 6.

## *The Highly Collapsed Configurations of a Stellar Mass.*

By S. Chandrasekhar.

(*Communicated by Professor E. A. Milne.*)

§ 1. Professor Milne in his recent paper * on "The Analysis of Stellar Structure" has put forward some essentially new considerations on the possible steady-state configurations of stellar aggregates of varying mass, luminosity, and opacity. One of the main consequences of the analysis is the explanation not only of the existence of white dwarfs—his collapsed configurations—but also of the principal physical characteristics of these configurations. The following is devoted to the development of Milne's theory of these collapsed configurations a stage further.

§ 2. Milne's estimates for the central density and temperature of these collapsed configurations indicate that in some cases we pass beyond the range of validity of the degenerate form of the Fermi-Dirac equation of state ($p = K\rho^{\frac{5}{3}}$). It can be shown that the pressure of an electron gas which is highly degenerate and which has a very highly predominant relativistic-mass variation effect, takes the limiting form †

$$p = \frac{n^{\frac{4}{3}}hc}{8}\left(\frac{3}{\pi}\right)^{\frac{1}{3}} \quad . \quad . \quad . \quad . \quad (1)$$

($c$ = velocity of light, $h$ = Planck's constant) if the following two conditions are satisfied :—

$$n > \left(\frac{kT}{hc}\right)^3 \frac{4\pi G}{3} \equiv 2{\cdot}86T^3 \qquad (G = 2) \quad . \quad (i)$$

$$n > \frac{8\pi m^3 c^3}{3h^3} \equiv 5{\cdot}88 \times 10^{29} \quad . \quad . \quad . \quad (ii)\ ‡$$

(i) replaces Sommerfeld's degeneracy criterion, and (ii) ensures the predominance of the relativistic effect. As the condition that configurations are highly collapsed is precisely equivalent to the condition that in the central regions the electron assembly is degenerate,§ it would be sufficient to consider whether (ii) is satisfied in order to count the relativistic effect as highly predominant. Further, as L for these configurations is very small, $T_c$ is normally of the order of $10^9$,‖ and (ii) then would automatically provide for (i). (See equation (19′)).

* *M.N.*, **91**, 4–55, 1930, referred to hereafter as *loc. cit.* For a general exposition of his main ideas see *Nature*, 1931 January 3, "Stellar Structure and the Origin of Stellar Energy."

† The corresponding expression for the energy E was obtained by E. C. Stoner, *Phil. Mag.*, **9**, 944, 1930. That $p = \frac{1}{3}E$ is generally true when the relativistic effect is highly predominant can easily be proved.

‡ (ii) is given in Stoner's paper; (i) now replaces Sommerfeld's criterion. These and other inequalities are briefly discussed in my paper on "The Dissociation Formula according to the Relativistic Statistics," *M.N.* (in course of publication).

§ Milne, *loc. cit.*, § 22.

‖ Milne, *loc. cit.*, p. 39.

Now the central density of a highly collapsed configuration considered as an Emden polytrope " $n = \frac{3}{2}$ " is given by *

$$\rho_c = \frac{32\pi G^3 M^2 \beta^3}{125 K_1^3 \times 7{\cdot}385} \quad . \quad . \quad . \quad . \quad (2)$$

where $K_1$ is the degenerate-gas constant and

$$\beta = 1 - \frac{\kappa L}{4\pi c G M} \quad . \quad . \quad . \quad . \quad (3)$$

It is clear then that the relativistic effect will be predominant in the central regions of those collapsed configurations whose masses satisfy the inequality

$$\frac{32\pi G^3 M^2 \beta^3}{125 K_1^3 \times 7{\cdot}385 \times \mu} > \frac{8\pi m_H^3 c^3}{3h^3}$$

or

$$M\beta^{\frac{3}{2}} > 5\left[\frac{5\mu \times 7{\cdot}385}{12}\right]^{\frac{1}{2}}\left(\frac{mcK_1}{Gh}\right)^{\frac{3}{2}} = 0{\cdot}434 \odot \quad (\text{if } \mu = 2{\cdot}5 m_H) \quad (4)$$

where $\mu$ is the mean molecular weight and $\odot$ denotes the mass of the Sun ( $= 1{\cdot}985 \times 10^{33}$ gms.).

The purpose of this paper is to find out the consequences of introducing the equation of state $p = K_2 \rho^{\frac{5}{3}}$. It will be shown that we can enumerate the complete linear sequence of steady-state configurations for an *assigned* small luminosity as the mass varies, the opacity and source-strength being constant and uniform (standard model).

§ 3. *The Equations of the Problem.*—We base our subsequent discussion exclusively on the standard model as it is considerably easier to work with.

We have the following set of equations for the standard model independent of the equation of state we may adopt. (The notation is identical with that used in Milne's paper.)

$$\frac{dp}{dr} + \frac{dp'}{dr} = -\frac{GM(r)}{r^2}\rho \quad . \quad . \quad . \quad (5)$$

$$\frac{dp'}{dr} = -\frac{\kappa L(r)}{4\pi c r^2}\rho \quad . \quad . \quad . \quad (6)$$

$$\frac{L(r)}{M(r)} = \epsilon = \frac{L}{M}.$$

We have also the following relation between the gas kinetic-pressure ($p$) and the radiation-pressure $p'$:

$$p = p'\frac{\beta}{1-\beta} \quad . \quad . \quad . \quad . \quad (7)$$

where $\beta$ is defined by (3).

*Case I.* (*The Relativistic-degenerate Case*).—We have for the gas

* Equation (55), *loc. cit.*

kinetic-pressure, taking into account only the electronic contribution, which is certainly by far the most important

$$p = \frac{n^{\frac{4}{3}}hc}{8}\left(\frac{3}{\pi}\right)^{\frac{1}{3}} \quad . \quad . \quad . \quad . \quad (1')$$

If we assume the molecular weight $\mu = 2{\cdot}5m_{\mathrm{H}}$, then

$$p = \mathrm{K}_2\rho^{\frac{4}{3}} \, . \quad . \quad . \quad . \quad . \quad (1'')$$

where

$$\mathrm{K}_2 = \frac{hc}{8(2{\cdot}5m_{\mathrm{H}})^{\frac{4}{3}}}\left(\frac{3}{\pi}\right)^{\frac{1}{3}} = 3{\cdot}619 \times 10^{14} \quad . \quad . \quad (1''')$$

With the equation of state given by (1''), the equation of mechanical equilibrium reduces to

$$\frac{4\mathrm{K}_2}{3\mathrm{G}\beta}r^2\rho^{-\frac{2}{3}}\frac{d\rho}{dr} = -\mathrm{M}(r) \quad . \quad . \quad . \quad (8)$$

Remembering that

$$\frac{d\mathrm{M}(r)}{dr} = 4\pi r^2\rho,$$

we have on differentiating (8)

$$\frac{4\mathrm{K}_2}{3\mathrm{G}\beta}\frac{d}{dr}\left(r^2\rho^{-\frac{2}{3}}\frac{d\rho}{dr}\right) = -4\pi r^2\rho \quad . \quad . \quad . \quad (9)$$

Putting

$$\rho = \lambda_3\chi^3 \, . \quad . \quad . \quad . \quad . \quad (10)$$

(9) reduces to

$$\frac{\mathrm{K}_2\lambda_3^{-\frac{2}{3}}}{\pi\mathrm{G}\beta} \cdot \frac{1}{r^2}\frac{d}{dr}\left(r^2\frac{d\chi}{dr}\right) = -\chi^3 \quad . \quad . \quad . \quad (11)$$

Changing $r$ to the variable $\zeta$ given by

$$r = \zeta\left[\frac{\mathrm{K}_2\lambda_3^{-\frac{2}{3}}}{\pi\mathrm{G}\beta}\right]^{\frac{1}{2}} \quad . \quad . \quad . \quad . \quad (12)$$

we have finally

$$\frac{1}{\zeta^2}\frac{d}{d\zeta}\left(\zeta^2\frac{d\chi}{d\zeta}\right) = -\chi^3 \, . \quad . \quad . \quad . \quad (13)$$

which is Emden's polytropic equation with index 3.

From (8), using the values of $\rho$ and $r$ given by (10) and (12), we have

$$\mathrm{M}(r) = -\frac{4}{\pi^{\frac{1}{2}}}\left(\frac{\mathrm{K}_2}{\mathrm{G}\beta}\right)^{\frac{3}{2}}\zeta^2\frac{d\chi}{d\zeta} \quad . \quad . \quad . \quad (14)$$

It may be noted that, unlike the degenerate non-relativistic case, $\lambda_3$ has disappeared from (14).

*Case II.* (*The Non-relativistic-degenerate Case*).—We can use the equations given by Milne, *loc. cit.*, equations (49), (48), (50), and (47) respectively:

$$\frac{1}{\eta^2}\frac{d}{d\eta}\left(\eta^2\frac{d\psi}{d\eta}\right) = -\psi^{\frac{3}{2}} \quad . \quad . \quad . \quad (15)$$

where
$$\rho = \lambda_2 \psi^{\frac{3}{2}} \quad . \quad . \quad . \quad . \quad . \quad (16)$$
$$r = \eta \left[ \frac{5K_1}{8\pi G\beta} \lambda_2^{-\frac{1}{3}} \right]^{\frac{1}{2}} . \quad . \quad . \quad . \quad (17)$$

We have also
$$M(r) = -\frac{1}{4(2\pi)^{\frac{1}{2}}} \left( \frac{5K_1}{G\beta} \right)^{\frac{3}{2}} \lambda_2^{\frac{1}{2}} \eta^2 \frac{d\psi}{d\eta} . \quad . \quad . \quad (18)$$

$K_1$ in (17) and (18) is the degenerate-gas constant.*

§ 4. *The Equations of Fit.*—Let $r = r'$ be the radius of the surface of demarcation, *i.e.* outside $r = r'$ the distribution of density is given by a solution of Emden's equation "$n = \frac{3}{2}$," and inside $r = r'$ by a solution of Emden's equation "$n = 3$."

Outside $r = r'$ the equation of state is $p = K_1 \rho^{\frac{5}{3}}$ and inside $r = r'$ we have $p = K_2 \rho^{\frac{4}{3}}$. Let $\rho'$ and T' be the values of $\rho$ and T at the interface, so that we have
$$K_1 \rho'^{\frac{5}{3}} = K_2 \rho'^{\frac{4}{3}} = \tfrac{1}{3} a T'^4 \frac{\beta}{1-\beta}$$

or
$$\rho' = \left( \frac{K_2}{K_1} \right)^3 ; \qquad T' = \frac{K_2}{K_1} \left[ \frac{K_2}{\frac{1}{3}a} \frac{1-\beta}{\beta} \right]^{\frac{1}{4}} . \quad . \quad (19)$$

or, using numerical values,†
$$\left.\begin{aligned} \rho' &= 4{\cdot}84 \times 10^6 \\ n' &= 1{\cdot}165 \times 10^{30} \end{aligned}\right\} ; \qquad T' = 3{\cdot}29 \times 10^9 \left( \frac{1-\beta}{\beta} \right)^{\frac{1}{4}} . \quad (19')$$

Let $\phi(\eta)$ be any solution of
$$\frac{1}{\eta^2} \frac{d}{d\eta} \left( \eta^2 \frac{d\psi}{d\eta} \right) = -\psi^{\frac{3}{2}} \quad . \quad . \quad . \quad (20)$$

and suppose that it vanishes at $\eta = \eta_0$. Then $B^4 \phi(B\eta)$ is also a solution of (20) and it vanishes at $\eta = \eta_1$, where $B\eta_1 = \eta_0$. Write $B\eta' = b_1$. By (19) and (16) we have
$$\rho' = \left( \frac{K_2}{K_1} \right)^3 = \lambda_2 \psi'^{\frac{3}{2}} = \lambda_2 B^6 [\phi(b_1)]^{\frac{3}{2}} \quad . \quad . \quad (21)$$

and
$$M(r') = -\frac{1}{4(2\pi)^{\frac{1}{2}}} \left( \frac{5K_1}{G\beta} \right)^{\frac{3}{2}} \lambda_2^{\frac{1}{2}} B^3 b_1^2 \phi'(b_1) \quad . \quad . \quad (22)$$

or, eliminating $\lambda_2^{\frac{1}{2}} B^3$ by (21), we have
$$M(r') = -\frac{1}{4(2\pi)^{\frac{1}{2}}} \left( \frac{5K_2}{G\beta} \right)^{\frac{3}{2}} \frac{b_1^2 \phi'(b_1)}{[\phi(b_1)]^{\frac{1}{4}}} \quad . \quad . \quad (23)$$

Also by (17)
$$r' = \frac{b_1}{B} \left[ \frac{5K_1}{8\pi G\beta} \right]^{\frac{1}{2}} \lambda_2^{-\frac{1}{6}} \quad . \quad . \quad . \quad (24)$$

---

* $K_1 = 2{\cdot}138 \times 10^{12}$ or $3{\cdot}17 \times 10^{12}$, according as $\mu = 2{\cdot}5 m_H$ or $2 m_H$. The former value will be used in the numerical work of this paper.

† Remembering that for collapsed configurations $\beta \sim 1$ we see that $n' = 1{\cdot}165 \times 10^{30}$ provides for the condition (i) (§ 2) also.

or, eliminating $B\lambda_2^{\frac{1}{3}}$ by (21), we have

$$r' = \left[\frac{5}{8\pi G\beta K_2}\right]^{\frac{1}{2}} K_1 b_1 [\phi(b_1)]^{\frac{1}{2}} \quad . \quad . \quad . \quad (25)$$

Now let $g(\zeta)$ be any solution of the equation

$$\frac{1}{\zeta^2}\frac{d}{d\zeta}\left(\zeta^2\frac{d\chi}{d\zeta}\right) = -\chi^3 \quad . \quad . \quad . \quad (26)$$

which has the first zero at $\zeta = \zeta_0$. Then $Ag(A\zeta)$ is also a solution of (26) which vanishes at $\zeta = \zeta_1$, where $A\zeta_1 = \zeta_0$. Write $c_1 = A\zeta'$. We have

$$\rho' = \left(\frac{K_2}{K_1}\right)^3 = \lambda_3 \chi'^3 = \lambda_3 A^3 g(c_1)^3 \quad . \quad . \quad (27)$$

By (12)
$$r' = \frac{c_1}{A}\left(\frac{K_2}{\pi G\beta}\right)^{\frac{1}{2}} \lambda_3^{-\frac{1}{3}}$$

or, eliminating $A\lambda_3^{\frac{1}{3}}$ by (27), we have

$$r' = \left[\frac{1}{\pi G\beta K_2}\right]^{\frac{1}{2}} K_1 c_1 g(c_1) \quad . \quad . \quad . \quad (28)$$

By (14) we have also

$$M(r') = -\frac{4}{\pi^{\frac{1}{2}}}\left(\frac{K_2}{G\beta}\right)^{\frac{3}{2}} c_1^2 g'(c_1) \quad . \quad . \quad . \quad (29)$$

Now our conditions of the fitting of our two configurations are that $r'$ given by (25) and (28) as also $M(r')$ given by (23) and (29) are identical. Equating the respective sides we find we are simply left with

$$\left(\frac{8}{5}\right)^{\frac{1}{2}} c_1 g(c_1) = b_1 [\phi(b_1)]^{\frac{1}{2}} \quad . \quad . \quad . \quad (30)$$

$$\left(\frac{8}{5}\right)^{\frac{3}{2}} c_1^2 g'(c_1) = \frac{b_1^2 \phi'(b_1)}{[\phi(b_1)]^{\frac{3}{2}}} \quad . \quad . \quad . \quad (31)$$

which are just Milne's equations of fit (100) and (101),* for the transition from a gaseous (Maxwellian) envelope to a degenerate core. We see therefore that when the conditions do not become so drastic as to necessitate the introduction of a homogeneous core, the analytical and the computational difficulties are reduced, as we have to solve the same set of equations for the two transitions—namely, that from a gaseous to a degenerate atmosphere, and then that from the degenerate to the relativistically degenerate atmosphere.

§ 5. *A Completely-relativistically Degenerate Configuration.* — We consider now a configuration built *entirely* on the relativistic-degenerate equation of state $p = K_2\rho^{\frac{4}{3}}$. This is therefore an Emden polytrope

* Professor Milne has since drawn my attention to the fact that this is just what we ought to expect, and that the $\left(\frac{8}{5}\right)$ occurring in (30) and (31) is just $\frac{n_1+1}{n_2+1}$, where $n_1$ and $n_2$ are the indices of the two Emden equations.

"$n = 3$" and is similar to the Emden-Eddington diffuse configurations. But since we assume the validity of the equation of state $p = K_2\rho^{\frac{4}{3}}$ right from the boundary it is clear that if this configuration is to approximate to anything practically realisable, the central density must be sufficiently high to make the correction due to the degenerate fringe negligible. We show later that this Emden polytrope has a $\rho_c = \rho_{\max}$ (the maximum density matter is capable of), in which case the correction due to the degenerate "fringe" does become negligible.

We choose $\lambda_3$ such that the value of $\zeta$ at which $\chi$ vanishes is unity, *i.e.* by (12) we choose $\lambda_3$ such that

$$r_1^2 = \frac{K_2\lambda_3^{-\frac{2}{3}}}{\pi G\beta} \quad . \quad . \quad . \quad . \quad (32)$$

where $r_1$ is the radius of the star. Hence

$$\lambda_3 = \left(\frac{K_2}{\pi G\beta}\right)^{\frac{3}{2}} \cdot \frac{1}{r_1^3} \quad . \quad . \quad . \quad . \quad (33)$$

The central density is given by

$$\rho_c = \lambda_3(\chi)_0^3 = \lambda_3\zeta_0^3 \quad . \quad . \quad . \quad (34')$$

or by (33)

$$\rho_c = \left(\frac{K_2}{\pi G\beta}\right)^{\frac{3}{2}}\frac{\zeta_0^3}{r_1^3} \quad . \quad . \quad . \quad . \quad (34'')$$

The central temperature would be given by

$$\tfrac{1}{3}aT_c^4\frac{\beta}{1-\beta} = K_2\rho_c^{\frac{4}{3}}$$

or

$$T_c = \left(\frac{K_2}{\frac{1}{3}a}\right)^{\frac{1}{4}}\left(\frac{1-\beta}{\beta}\right)^{\frac{1}{4}}\left(\frac{K_2}{\pi G\beta}\right)^{\frac{1}{2}} \cdot \frac{\zeta_0}{r_1} \quad . \quad . \quad . \quad (35)$$

As is well known, for the Emden polytrope "$n = 3$" the central density $\rho_c$ and the mean density $\rho_m$ are related by

$$\frac{\rho_c}{\rho_m} = -\frac{\zeta_0}{3\chi'(\zeta_0)} = 54{\cdot}36 \quad . \quad . \quad . \quad (35')$$

Finally we have a relation connecting the mass and luminosity, which is merely the condition that the whole mass shall be representable as a relativistic configuration of Emden type

$$M = -\frac{4}{\pi^{\frac{1}{2}}}\left(\frac{K_2}{G\beta}\right)^{\frac{3}{2}}\zeta_0^2\left(\frac{d\chi}{d\zeta}\right)_{\zeta=\zeta_0} \quad . \quad . \quad . \quad (36)$$

where, since for Emden's solution $\zeta_0^2\left(\frac{d\chi}{d\zeta}\right)_{\zeta=\zeta_0} = -2{\cdot}015$, we have, introducing numerical values in (36),

$$M = 0{\cdot}9177\,\odot\beta^{-\frac{3}{2}} \equiv M_3 \quad . \quad . \quad . \quad (36')$$

we have also the limiting relation

$$\underset{L\to 0}{M} \longrightarrow \frac{2{\cdot}015\times 4}{\pi^{\frac{1}{2}}}\left(\frac{K_2}{G}\right)^{\frac{3}{2}} = 0{\cdot}92\odot \quad . \quad . \quad (36'')$$

§ 6. If the white dwarf under consideration could legitimately be considered as obeying down to its central regions the Emden equation "$n=\frac{3}{2}$," it is clear that $\rho_c$ so calculated should not exceed $\rho'\left[=\left(\frac{K_2}{K_1}\right)^3\right]$. The central density of a highly collapsed configuration which is a complete Emden polytrope "$n=\frac{3}{2}$" is

$$\rho_c = \frac{32\pi G^3M^2\beta^3}{125K_1{}^3\times 7{\cdot}385} \quad . \quad . \quad . \quad (2)$$

We must have therefore

$$\frac{32\pi G^3M^2\beta^3}{125K_1{}^3\times 7{\cdot}385} \leqslant \left(\frac{K_2}{K_1}\right)^3.$$

Hence for considerations based on Emden's "$n=\frac{3}{2}$" alone to be valid we must have the inequality

$$M \leqslant 1{\cdot}214\times 10^{33}\beta^{-\frac{3}{2}}\text{ grams} = 0{\cdot}6115\odot\beta^{-\frac{3}{2}}\ (=M_{\frac{3}{2}}, \text{ say})$$

satisfied. Hence collapsed configurations of mass *less than* $M_{\frac{3}{2}}$ are Emden polytropes "$n=\frac{3}{2}$." For $M=M_{\frac{3}{2}}$, $\rho_c$ is just equal to our "interfacial density." If M becomes greater than $M_{\frac{3}{2}}$ the relativistic core spreads and the configurations become composite. We proceed now to the study of these composite-configurations.

§ 7. *The Composite Series I.*—In working out the composite series we again consider only Emden's solution for the relativistic core, *i.e.* we exclude for the present the possibility of the conditions becoming so drastic as to necessitate the changing over from $p=K_2\rho^{\frac{4}{3}}$ equation of state. (It will be seen that when $\rho_c$ becomes equal to $\rho_{\max}$—the maximum density matter is capable of—the degenerate fringe becomes negligible, and so we are not required to introduce the relativistic and the homogeneous core simultaneously.)

We have, since $\chi(0)=1$, if $\chi$ is Emden's solution for "$n=3$,"

$$\rho_c = \lambda_3 A^3 \quad . \quad . \quad . \quad . \quad (37)$$

or by (27)

$$\rho_c = \left(\frac{K_2}{K_1}\right)^3\frac{1}{[g(c_1)]^3} \quad . \quad . \quad . \quad . \quad (38)$$

For the central temperature we have, since

$$\tfrac{1}{3}aT_c{}^4 = K_2\rho_c{}^{\frac{4}{3}}\frac{1-\beta}{\beta},$$

$$T_c = \left(\frac{3K_2}{a}\right)^{\frac{1}{4}}\frac{K_2}{K_1}\left(\frac{1-\beta}{\beta}\right)^{\frac{1}{4}}\cdot\frac{1}{g(c_1)} \quad . \quad . \quad . \quad (39)$$

We have also

$$\frac{\rho'}{\rho_c} = [g(c_1)]^3; \qquad \frac{T'}{T_c} = g(c_1) \quad . \quad . \quad . \quad (40)$$

The radius $r_1$ of the whole configuration is given by

$$\frac{r'}{r_1} = \frac{\eta'}{\eta_1} = \frac{B\eta'}{B\eta_1} = \frac{b_1}{\eta_0} \quad . \quad . \quad . \quad (41)$$

or by (25)

$$r_1 = \left[\frac{5}{8\pi G\beta K_2}\right]^{\frac{1}{2}} K_1\eta_0[\phi(b_1)]^{\frac{1}{4}} \quad . \quad . \quad . \quad (42)$$

The effective temperature and the mean density are easily found to be

$$T_e = \left(\frac{L}{ac}\right)^{\frac{1}{4}}\left(\frac{8G\beta K_2}{5}\right)^{\frac{1}{4}} \cdot \frac{1}{K_1^{\frac{1}{2}}} \cdot \frac{1}{\eta_0^{\frac{1}{2}}[\phi(b_1)]^{\frac{1}{8}}} \quad . \quad . \quad (43)$$

$$\rho_m = \frac{3}{4}\left[\frac{8\pi G\beta K_2}{5}\right]^{\frac{3}{2}} \frac{M}{\pi K_1^3} \frac{1}{\eta_0^3[\phi(b_1)]^{\frac{3}{4}}} \quad . \quad . \quad . \quad (44)$$

It is not difficult to put the above equations in a form which makes it clear that as $b_1 \to \eta_0$ and $c_1 \to \zeta_0$ these composite configurations *continuously* pass over into the complete relativistic Emden polytrope "$n = 3$" with $M = \cdot 92 \odot \beta^{-\frac{3}{2}}$. In making the reduction we make free use of (30), (31), and (42):

$$\rho_c = \left(\frac{K_2}{\pi G\beta}\right)^{\frac{3}{2}} c_1^3 \cdot \frac{\eta_0^3}{b_1^3} \quad . \quad . \quad . \quad . \quad . \quad (45)$$

$$\frac{\rho_c}{\rho_m} = -\frac{1}{3}\frac{c_1}{g'(c_1)}\frac{M(r')}{M(r_1)} \cdot \frac{\eta_0^3}{b_1^3} \quad . \quad . \quad . \quad . \quad (45')$$

$$M(r') = -\frac{4}{\pi^{\frac{1}{2}}}\left(\frac{K_2}{G\beta}\right)^{\frac{3}{2}} \zeta_0^2 \left(\frac{d\chi}{d\zeta}\right)_{\zeta=\zeta_0} \left[\frac{c_1^2 g'(c_1)}{\zeta_0^2 g'(\zeta_0)}\right] \quad . \quad . \quad (46)$$

$$T_c = \left(\frac{K_2}{\frac{1}{3}a}\right)^{\frac{1}{4}}\left(\frac{1-\beta}{\beta}\right)^{\frac{1}{4}}\left(\frac{K_2}{\pi G\beta}\right)^{\frac{1}{2}} \frac{c_1}{r_1}\frac{\eta_0}{b_1} \quad . \quad . \quad (46')$$

But when $b_1 \to \eta_0$ and $c_1 \to \zeta_0$ it is clear from (42) and (38) that simultaneously $r_1 \to 0$ and $\rho_c \to \infty$.* Thus the completely relativistic model considered as the limit of the composite series is a point-mass with $\rho_c = \infty$! The theory gives this result because $p = K_2\rho^{\frac{4}{3}}$ allows any density provided the pressure be sufficiently high. We are bound to assume therefore that a stage must come beyond which the equation of state $p = K_2\rho^{\frac{4}{3}}$ is not valid, for otherwise we are led to the physically inconceivable result that for $M = 0{\cdot}92 \odot \beta^{-\frac{3}{2}}$, $r_1 = 0$, and $\rho = \infty$. As we do not know physically what the next equation of state is that we are to take, we assume for definiteness the equation for the homogeneous incompressible material $\rho = \rho_{\max}$, where $\rho_{\max}$ is the maximum density of which matter is capable. The preceding analysis would then break down when $\rho_c$ given by (38) exceeds $\rho_{\max}$. Now $\rho_{\max}$ must at the lowest estimate be of the order of $10^{12}$ grams cm.$^{-3}$, for if the "maximum density of matter is limited only by the sizes of the electrons and nuclei, densities of the order $10^{14}$ should not be impossible." † Our interfacial

* This suggests that when $g$ is Emden's solution, $\varphi$ is of the centrally condensed type.

† R. H. Fowler, *M.N.*, **87**, 114, 1926, "Dense Matter."

density is only $4{\cdot}84 \times 10^6$ and the ratio of this to the central density $\rho_c = \rho_{\max}$ is of the order of $10^{-6}$, and a reference to the Emden tables shows that if for the moment we assume the star as *completely* relativistically degenerate, before we have proceeded $\frac{1}{1000}$th of the radius of the star into the interior, our assumption becomes valid. Hence the correction due to the degenerate "fringe" is negligible. We can therefore to a high degree of approximation consider as the limit of these composite series, the Emden polytrope "$n = 3$" with $\rho_c = \rho_{\max}$ and $M = 0{\cdot}92 \odot \beta^{-\frac{3}{2}}$, it being understood that $\rho_{\max}$ is sufficiently high to make the correction due to the degenerate fringe negligible. (Hence for highly collapsed configurations of mass greater than $0{\cdot}92 \odot \beta^{-\frac{3}{2}}$ we can neglect the degenerate fringe.) Thus the highly collapsed configurations for which $0{\cdot}612 \odot \beta^{-\frac{3}{2}} < M < 0{\cdot}92 \odot \beta'^{-\frac{3}{2}}$ are composite, consisting of a degenerate envelope surrounding a relativistic core. These composite configurations are bordered on either side by two completely determinable configurations—on the one side by an Emden polytrope "$n = \frac{3}{2}$," and on the other by an Emden polytrope "$n = 3$" with $\rho_c = \rho_{\max}$.

§ 8. *Composite Series II.*—So far we have considered only the Emden solutions for the relativistic core, and we have been able to specify the steady-state configurations only for $M \leqslant M_3$. Further, $M = M_3$ corresponds to a high degree of approximation to an Emden-polytrope "$n = 3$" with $\rho_c = \rho_{\max}$. Hence for $M > M_3$ we should expect the homogeneous core to have spread out. We should therefore consider the fit of a relativistic envelope surrounding a homogeneous core with $\rho = \rho_{\max}$, the core and the envelope being continuous at the interface. If $r = r''$ (where $\zeta = \zeta''$ and $\chi = \chi''$) is the radius of the surface of demarcation, the equation of fit is found to reduce to

$$\tfrac{1}{3}\zeta''^3\chi''^3 = -\zeta''^2\left(\frac{d\chi}{d\zeta}\right)_{\zeta=\zeta''} . \quad . \quad . \quad (47)$$

It can easily be shown that if $\chi$ be an Emden or a centrally condensed type of solution, then (47) has no roots, except that in the former case we have the trivial solution $\zeta'' = 0$. Hence the introduction of the homogeneous core compels us to a consideration of only the collapsed-type solutions for $\chi$.

Now by (36)

$$-\zeta_0^2\left(\frac{d\chi}{d\zeta}\right)_{\zeta=\zeta_0} = \frac{M}{\frac{4}{\pi^{\frac{1}{2}}}\left(\frac{K_2}{G\beta}\right)^{\frac{3}{2}}} = \frac{1}{C_2^{\frac{1}{2}}} \quad . \quad . \quad (48)$$

where $C_2$ can now be called the "discriminant" of the relativistic standard model for $M > M_3$. It may be noted here that $C_2$ is primarily a function *only* of M, since the hypothesis that the configurations are highly collapsed provides us with $\beta \sim 1$ in any case. We can write (48) differently as

$$-\zeta_0^2\left(\frac{d\chi}{d\zeta}\right)_{\zeta=\zeta_0} = \frac{M}{M_3} \times 2{\cdot}015 \quad . \quad . \quad . \quad (49)$$

where 2·015 is the corresponding boundary value for the Emden solution. Hence for $M > M_3$ we clearly see from (49) that the solutions for $\chi$ now belong to the collapsed family. Thus the condition that $M > M_3$ is precisely equivalent to the condition that there is a homogeneous core. By methods similar to § 4 we easily obtain

$$M(r'') = \tfrac{4}{3}\pi r''^3\rho_{max} = -\frac{4}{\pi^{\frac{1}{2}}}\left(\frac{K_2}{G\beta}\right)^{\frac{3}{2}} c_1^2 g'(c_1) \quad . \quad . \quad (50)$$

$$r_1 = \frac{r''\zeta_0}{c_1} \quad . \quad . \quad . \quad . \quad (51)$$

where $c_1 = A\zeta''$ and $r_1$ is the radius of the whole configuration. Comparing (50) with (49) we see that as M increases beyond $M_3$ the collapse proceeds further and further till finally, when $M \to \infty$, $c_1 \to \zeta_0$, and $r_1 \to r''$, and the whole configuration has completely "collapsed" into one mass of incompressible matter at the highest density matter is capable of. We have in the limit, so to say, a "*solid star*."

Further, if $g(c_1)$ corresponds to the Emden solution there is only one "trivial" root for (47), namely, $c_1 = 0$, *i.e.* the central density of this completely relativistic Emden polytrope is just equal to $\rho_{max}$ and the radius of the star is then obviously given by

$$\frac{\frac{4}{3}\pi r_1^3\rho_{max}}{54{\cdot}36} = 0{\cdot}92 \odot \beta^{-\frac{3}{2}} \quad . \quad . \quad . \quad (52)$$

Thus this Composite Series II. joins continuously the Composite Series I. (§ 7) and the Emden polytrope "$n = 3$" with $\rho_c = \rho_{max}$, and $M = {\cdot}92 \odot \beta^{-\frac{3}{2}}$ is the *common limit* of both the series. We have therefore the following complete classification of the highly collapsed configurations ($L << L_0$, $\beta \sim 1$) for M *considered as a variable taking the whole range of values.*

| Mass. | Description. |
|---|---|
| Class I.—$M < 0{\cdot}61 \odot \beta^{-\frac{3}{2}}$ | Emden polytropes "$n = \frac{3}{2}$." |
| $M_{\frac{3}{2}} = M = {\cdot}61 \odot \beta^{-\frac{3}{2}}$ | An Emden polytrope $n = \frac{3}{2}$ with $\rho_c = \left(\frac{K_2}{K_1}\right)^3$. |
| Class II.—$0{\cdot}61 \odot \beta^{-\frac{3}{2}} < M < 0{\cdot}92 \odot \beta'^{-\frac{3}{2}}$ | Composite I.—Degenerate envelope surrounding a homogeneous core. |
| $M_3 = M = 0{\cdot}92 \odot \beta'^{-\frac{3}{2}}$ | Approximately an Emden polytrope "$n = 3$" with $\rho_c = \rho_{max}$. |
| Class III.—$M > {\cdot}92 \odot \beta'^{-\frac{3}{2}}$ | Composite II.—relativistic envelope and homogeneous core. |
| $M \to \infty$ | Completely homogeneous ($\rho = \rho_{max}$). |

That we are thus able to enumerate definitely the steady-state configurations for the whole range of M appears to be in complete conformity with the general scheme of Milne's ideas.

To apply the above classification to the known white dwarfs—$o_2$ Eridani B, Procyon B, and Van Maanen's star possibly belong to Class I. That the companion of Sirius is in Class II. is also likely.

But it appears that no white dwarf has yet been discovered which has a homogeneous core at the centre. This classification is made with caution, since, though they are certainly of the collapsed type, they are by no means "*highly*" collapsed, for then L and $T_e$ would be so small that we could not see the stars.

§ 9. *Summary.*—In this paper Milne's theory of collapsed configurations is developed a stage further, the essential refinement being in the introduction of a relativistically degenerate core with the equation of state $p = K_2\rho^{\frac{4}{3}}$. This enables an enumeration to be made of the steady-state configurations for the whole range of M considered as a variable with $L \sim 0$. The classification arrived at is shown in the table in § 8.

In conclusion, I wish to record my best thanks to Professor Milne for much valuable advice and criticism during the course of the work.

---

## *The Possible Solutions of the "Equations of Fit" on the Standard Model.*

By B. Strömgren, Ph.D.

(*Communicated by E. A. Milne.*)

1. In a recent paper * Professor E. A. Milne has reconsidered the problem of determining the structure of the stars. A full treatment is given of stars built on the standard model, $\kappa$ = constant, $\epsilon$ = constant. Professor Milne's treatment of this model is, however, not yet completed, as he himself states, so far as the actual fit of "$n = 3$"-polytropic solutions ($f$) on to "$n = \frac{3}{2}$"-polytropic solutions ($\phi$) is concerned. In fact, Professor Milne awaits the construction of a complete set of tables of the functions $f$ and $\phi$.

It is shown in the present note, however, that a discussion of the point mentioned is possible without these tables, certain general theorems on polytropic solutions established by Mr. R. H. Fowler † being sufficient.

2. The discussion is based on the equations of fit derived by Professor Milne and given in the paper quoted as equations (100) and (101). The line of thought leading to (100) and (101) may be briefly stated as follows. For a given mass M a solution is started from the boundary inwards; this solution is an "$n = 3$"-polytropic solution which is definite for definite values of the radius $r_1$ and the discriminant C depending on M, L, and $\kappa$ (the nature of the solution depends on C, solutions with the same C and different $r_1$ being homologous). At a certain definite point $\rho T^{-\frac{3}{2}}$ reaches a value where degeneracy sets in. The value of the radius $r_1$, the remaining mass $M(r)$, and the density $\rho$ at this point are definite functions of M, C, and $r_1$. These values, which may be denoted by $r'$, $M(r')$, and $\rho'$, now determine the "$n = \frac{3}{2}$"-polytropic solution that fits on to the selected "$n = 3$"-solution.

* *M.N.*, **91**, 4, 1930. † *M.N.*, **91**, 63, 1930.

Equations (100) and (101) express the relation between two solutions so obtained; in (100) and (101) the "$n = 3$"-polytropic solution is not, however, specified by a certain value of C, but by simultaneous values of $\xi\theta$ and $\xi^2\frac{d\theta}{d\xi}$ (simultaneous values of $\xi\theta$ and $\xi^2\frac{d\theta}{d\xi}$ determine C); similarly for the "$n = \frac{3}{2}$"-polytropic solution.

Before we pass on to the discussion of equations (100) and (101) it may be well to sketch the general line of thought of which this discussion is part, following Professor Milne.

Consider a model, of the type investigated, of mass M. We start from the boundary inwards with an $f$-solution of specified C and $r_1$, and fit it on to a $\phi$-solution as described. We then go on with the $\phi$-solution; if we reach the centre with the second equation of state, then the integration inwards is completed; if not, we have to fit the $\phi$-solution on to a solution corresponding to still another equation of state, and go on with this to the centre. In all cases our solution definitely reaches the centre, and we can now see whether our solution corresponds to an allowed configuration, or not; we have simply to examine whether the condition $\int_{\text{centre}}^{\text{boundary}} d\mathrm{M}_r = \mathrm{M}$ is fulfilled, or not. We see that, by the condition mentioned, given a mass M we are able to decide whether it is compatible with specified values of C and $r_1$; or, remembering the expression for C, whether mass M is compatible with certain specified values of $\kappa$L and $r_1$, or not.

Now Professor Milne showed that if the laws of a perfect gas hold for all densities and temperatures, then (again on a model of the type investigated) mass M and radius $r_1$ are compatible with all values of $\kappa$L between two definite limits.

In order to examine the condition $\int_{\text{centre}}^{\text{boundary}} d\mathrm{M}_r = \mathrm{M}$, assuming degeneracy setting in as described—to answer the question of the compatibility of specified values of M, $r$, and $\kappa$L, on the standard model—we have thus to complete the discussion of equations (100) and (101).

We now proceed to this discussion.

3. The equations are, in the notation of Professor Milne:

$$a_1^2 f'(a_1) = \left(\frac{5}{8}\right)^{\frac{3}{2}} \frac{b_1^2 \phi'(b_1)}{[\phi(b_1)]^{\frac{3}{4}}} \quad \text{Milne's equation (100)}$$

$$a_1 f(a_1) = \left(\frac{5}{8}\right)^{\frac{1}{2}} b_1 [\phi(b_1)]^{\frac{1}{4}} \quad \text{,,} \quad \text{,,} \quad (101).$$

We base the discussion on the theorems by R. H. Fowler already mentioned. With the aid of these theorems we can infer the general character of a polytropic solution (whether it is of the collapsed type or of the centrally condensed type) when we are given one set of simultaneous values of the polytropic variables and the polytropic slope of that solution; conversely, when the character of the solution is known, we can tell something of the slope when the variables are given.

Consider first the polytropic solutions with "$n = 3$." Suppose we are given a set of values as follows: $\left(\xi', \theta', \left(\frac{d\theta}{d\xi}\right)'\right)$. Following R. H. Fowler, we now determine the two Emden-solutions through $(\xi', \theta')$. Call the particular Emden-solution tabulated by Emden $\theta_E(\xi_E)$; the general Emden-solution is then $A\theta_E(A\xi_E)$. Thus we have

$$\xi' = \frac{\xi_E'}{A} \quad . \quad . \quad . \quad . \quad (1)$$

$$\theta' = A\theta_E' \quad . \quad . \quad . \quad . \quad (2)$$

$$S_E = \text{Emden slope} = A^2 \left| \left(\frac{d\theta_E}{d\xi_E}\right)' \right| \quad . \quad . \quad (3)$$

Given $(\xi', \theta')$, (1) and (2) determine A, Emden's table of $\theta_E(\xi_E)$ being used in numerical applications; $\left(\frac{d\theta_E}{d\xi_E}\right)'$ can be taken from Emden's table, and so the Emden slope $S_E$ is determined; there will be 2, 1, or 0 solutions according as $(\xi', \theta')$ is below, on, or above the critical curve $\xi\theta = 1{\cdot}171$.

We can now determine the type of the solution according to R. H. Fowler:

(1) If $\xi'\theta' > 1{\cdot}171$, then the solution is of the collapsed type.

(2) If $\xi'\theta' = 1{\cdot}171$ and $\left|\left(\frac{d\theta}{d\xi}\right)'\right| \neq S_{E_1} = S_{E_2}$, then the solution is of the collapsed type.

(3) If $\xi'\theta' < 1{\cdot}171$ and $S_{E_1} < \left|\left(\frac{d\theta}{d\xi}\right)'\right| < S_{E_2}$, then the solution is of the centrally condensed type.

(4) If $\xi'\theta' \leqq 1{\cdot}171$ and $S_{E_1} = \left|\left(\frac{d\theta}{d\xi}\right)'\right|$ or $S_{E_2} = \left|\left(\frac{d\theta}{d\xi}\right)'\right|$, then the solution is an Emden-solution.

(5) If $\xi'\theta' < 1{\cdot}171$ and either $\left|\left(\frac{d\theta}{d\xi}\right)'\right| < S_{E_1}$ or $S_{E_2} < \left|\left(\frac{d\theta}{d\xi}\right)'\right|$, then the solution is of the collapsed type.

Instead of computing $\xi_E'\theta_E' = \xi'\theta'$, $\xi_E'$ from $\xi_E'\theta_E'$ and $A = \frac{\xi_E'}{\xi'}$ $\left(\text{or} = \frac{\theta'}{\theta_E'}\right)$, $\left(\frac{d\theta_E}{d\xi_E}\right)'$ from $\xi_E'$ and $S_E = A^2\left|\left(\frac{d\theta_E}{d\xi_E}\right)'\right|$, and then comparing $S_{E1}$, $\left|\left(\frac{d\theta}{d\xi}\right)'\right|$ and $S_{E2}$, we can also proceed as follows: $\xi_E'\theta_E' = \xi'\theta'$ gives two values of $\xi_E'^2\left|\left(\frac{d\theta_E}{d\xi_E}\right)'\right|$, and these are compared with $\xi'^2\left|\left(\frac{d\theta}{d\xi}\right)'\right|$.

For we have

$$\xi_E'^2\left|\left(\frac{d\theta_E}{d\xi_E}\right)'\right| = \xi'^2A^2\left|\left(\frac{d\theta_E}{d\xi_E}\right)'\right| = \xi'^2S_E \quad . \quad . \quad (4)$$

More generally we can compare $\xi'^p\theta'^q\left(\frac{d\theta}{d\xi}\right)'$ with the corresponding Emden-value, provided $\xi^p\theta^q\left(\frac{d\theta}{d\xi}\right)$ is invariant under homology-transformations ($p - 1 = q + 1$ for "$n = 3$"-polytropes).

Quite similar formulations apply to the case "$n = \frac{3}{2}$."

Now let us first consider the fit of a centrally condensed "$n = 3$"-polytrope on to an "$n = \frac{3}{2}$"-polytrope according to equations (100) and (101).

From R. H. Fowler's theorems we know the following facts of the centrally condensed "$n = 3$"-polytrope:

(1) $\xi\theta < 1{\cdot}171$.

(2) $\xi_{E_1}^{\ 2}\left|\left(\frac{d\theta_{E_1}}{d\xi_{E_1}}\right)\right| < \xi^2\left|\frac{d\theta}{d\xi}\right| < \xi_{E_2}^{\ 2}\left|\frac{d\theta_{E_2}}{d\xi_{E_2}}\right|$.

In the following table Emden-values of $\xi\theta$ and of $\xi^2\left|\frac{d\theta}{d\xi}\right|$ are given; the values are computed from Emden's table for $n = 3$:—

TABLE I.

| $\xi$. | $\xi\theta$. | $\xi^2\left\|\frac{d\theta}{d\xi}\right\|$. | $\xi$. | $\xi\theta$. | $\xi^2\left\|\frac{d\theta}{d\xi}\right\|$. |
|---|---|---|---|---|---|
| 0·00 | 0·000 | 0·0000 | 2·1620 | 1·170 | 1·171 |
| 0·25 | 0·248 | 0·0051 | | | |
| 0·50 | 0·480 | 0·039 | 2·50 | 1·152 | 1·399 |
| 0·75 | 0·686 | 0·120 | 3·00 | 1·077 | 1·655 |
| 1·00 | 0·855 | 0·252 | 3·50 | 0·97 | 1·820 |
| 1·25 | 0·986 | 0·428 | 4·00 | 0·84 | 1·920 |
| 1·50 | 1·078 | 0·630 | 4·50 | 0·70 | 1·974 |
| 1·75 | 1·138 | 0·841 | 5·00 | 0·56 | 2·001 |
| 2·00 | 1·166 | 1·045 | 6·00 | 0·26 | 2·016 |
| | | | 6·80 | 0·03 | 2·016 |
| 2·1620 | 1·170 | 1·171 | 6·9011 | 0·00 | 2·016 |

An example may be given in illustration. Suppose $\xi\theta = 1{\cdot}078$ on a centrally condensed "$n = 3$"-polytrope; then from the table $0{\cdot}630 < \xi^2\left|\frac{d\theta}{d\xi}\right| < 1{\cdot}653$.

Returning now to equations (100) and (101) we see that, knowing the polytrope "$n = 3$" to be centrally condensed, we know that the left-hand side of (100) falls within certain limits, which are functions of the left-hand side of (101); the same is then, of course, true of the right-hand sides of the equations. We shall now show that this information is enough to establish the character of the fit-polytrope "$n = \frac{3}{2}$."

We now require a similar discussion, based on R. H. Fowler's

theorems, of the polytropes "$n = \frac{3}{2}$" as we have already given in detail for "$n = 3$"-polytropes. The general arguments are the same, and it will suffice to enumerate the differences due to the change of polytropic index. First, the critical curve is now $\eta^4\psi = 13{\cdot}4$ (or $\eta\psi^{\frac{1}{4}} = 1{\cdot}915$); the formulæ (1), (2), (3), and (4) are now

$$\eta' = \frac{\eta_E'}{A} \quad . \quad . \quad . \quad . \quad . \quad (1a)$$

$$\psi' = A^4\psi_E' \quad . \quad . \quad . \quad . \quad . \quad (2a)$$

$$S_E = \text{Emden slope} = A^5 \left| \left(\frac{d\psi_E}{d\eta_E}\right)' \right| \quad . \quad . \quad . \quad . \quad (3a)$$

$$\frac{\eta_E'^2}{\psi_E'^{\frac{3}{4}}} \left| \left(\frac{d\psi_E}{d\eta_E}\right)' \right| = \frac{\eta'^2}{\psi'^{\frac{3}{4}}} A^5 \left| \left(\frac{d\psi_E}{d\eta_E}\right)' \right| = \frac{\eta'^2}{\psi'^{\frac{3}{4}}} S_E. \quad . \quad (4a)$$

or more generally

$$\eta_E'^p \psi_E'^q \left| \left(\frac{d\psi_E}{d\eta_E}\right)' \right| = \eta'^p \psi'^q A^{p-4q} \left| \left(\frac{d\psi_E}{d\eta_E}\right)' \right| = \eta'^p \psi'^q S_E,$$

where

$$p - 1 = 4(q + 1) \quad \text{or} \quad p - 4q = 5 \text{ for } n = \tfrac{3}{2}.$$

We thus see that we can infer the character of the "$n = \frac{3}{2}$"-polytrope by comparing the quantities on the right-hand sides with the corresponding Emden-values.

In the following table Emden-values of $\left(\frac{5}{8}\right)^{\frac{1}{2}} \eta\psi^{\frac{1}{4}}$ and $\left(\frac{5}{8}\right)^{\frac{3}{2}} \frac{\eta^2}{\psi^{\frac{3}{4}}} \left| \frac{d\psi}{d\eta} \right|$ are given; the values are computed from Emden's table for $n = \frac{3}{2}$:—

TABLE II.

| $\eta$. | $\left(\frac{5}{8}\right)^{\frac{1}{2}} \eta\psi^{\frac{1}{4}}$. | $\left(\frac{5}{8}\right)^{\frac{3}{2}} \frac{\eta^2}{\psi^{\frac{3}{4}}} \left\lvert \frac{d\psi}{d\eta} \right\rvert$. | $\eta$. | $\left(\frac{5}{8}\right)^{\frac{1}{2}} \eta\psi^{\frac{1}{4}}$. | $\left(\frac{5}{8}\right)^{\frac{3}{2}} \frac{\eta^2}{\psi^{\frac{3}{4}}} \left\lvert \frac{d\psi}{d\eta} \right\rvert$. |
|---|---|---|---|---|---|
| 0·00 | 0·000 | 0·0000 | 2·8085 | 1·514 | 3·78 |
| 0·25 | 0·197 | 0·0026 | | | |
| 0·50 | 0·391 | 0·020 | 3·00 | 1·499 | 5·00 |
| 0·75 | 0·580 | 0·069 | 3·25 | 1·42 | 7·86 |
| 1·00 | 0·757 | 0·161 | 3·50 | 1·19 | 17·15 |
| 1·25 | 0·925 | 0·311 | 3·6571 | 0·00 | ∞ |
| 1·50 | 1·077 | 0·530 | | | |
| 1·75 | 1·212 | 0·836 | | | |
| 2·00 | 1·328 | 1·24 | | | |
| 2·25 | 1·420 | 1·78 | | | |
| 2·50 | 1·482 | 2·50 | | | |
| 2·75 | 1·513 | 3·48 | | | |
| 2·8085 | 1·514 | 3·78 | | | |

By inspection of Table I. and Table II. it is seen at once that for equal values of $\xi\eta$ and $\left(\frac{5}{8}\right)^{\frac{1}{2}}\eta\psi^{\frac{1}{2}}$ (*cf.* equation (101)) we have the following inequalities for the Emden-values :—

$$\left\{\left(\frac{5}{8}\right)^{\frac{3}{2}}\frac{\eta^2}{\psi^{\frac{3}{2}}}\left|\frac{d\psi}{d\eta}\right|\right\}_{E_1} < \left(\xi^2\left|\frac{d\theta}{d\xi}\right|\right)_{E_1} < \left(\xi^2\left|\frac{d\theta}{d\xi}\right|\right)_{E_2} < \left\{\left(\frac{5}{8}\right)^{\frac{3}{2}}\frac{\eta^2}{\psi^{\frac{3}{2}}}\left|\frac{d\psi}{d\eta}\right|\right\}_{E_2} \quad (5)$$

(Only for $\xi \to 0$, $\eta \to 0$ do the lower limits tend to each other, $\xi^2\frac{d\theta}{d\xi} \to \nu(\xi\theta)^3$ and $\left(\frac{5}{8}\right)^{\frac{3}{2}}\frac{\eta^2}{\psi^{\frac{3}{2}}}\frac{d\psi}{d\eta} \to \nu\left\{\left(\frac{5}{8}\right)^{\frac{1}{2}}\eta\psi^{\frac{1}{2}}\right\}^3$).

Below the result of comparison is given in detail :—

TABLE III.

| $\xi\theta$. | $\left\{\left(\frac{5}{8}\right)^{\frac{3}{2}}\frac{\eta^2}{\psi^{\frac{3}{2}}}\left\|\frac{d\psi}{d\eta}\right\|\right\}_{E_1}$. | $\left(\xi^2\left\|\frac{d\theta}{d\xi}\right\|\right)_{E_1}$. | $\left(\xi^2\left\|\frac{d\theta}{d\xi}\right\|\right)_{E_2}$. | $\left\{\left(\frac{5}{8}\right)^{\frac{3}{2}}\frac{\eta^2}{\psi^{\frac{3}{2}}}\left\|\frac{d\psi}{d\eta}\right\|\right\}_{E_2}$. |
|---|---|---|---|---|
| 0·000 | 0·00000 | 0·00000 | 2·016 | ∞ |
| 0·197 | 0·00257 | 0·00258 | | |
| 0·391 | 0·0204 | 0·0206 | | |
| 0·580 | 0·0686 | 0·0700 | <2·016 | >17 |
| 0·757 | 0·161 | 0·166 | | |
| 0·925 | 0·311 | 0·334 | | |
| 1·077 | 0·530 | 0·623 | | |
| 1·170 | 0·72 | 1·171 | 1·171 | >17 |

Using this result we can obtain the following information of the "$n = \frac{3}{2}$"-fit-polytrope. When the "$n = 3$"-polytrope is of the centrally condensed type, then the "$n = \frac{3}{2}$"-fit-polytrope is necessarily also centrally condensed. (The fit-solution at $\xi = 0$, $\eta = 0$ has been discussed by Professor Milne ; it corresponds to an "$n = 3$"-Emden-solution.)

4. Inspecting Table I. and Table II. we can easily confirm an expectation of Professor Milne. An "$n = 3$"-polytrope, fitting on to the Emden polytrope "$n = \frac{3}{2}$," is necessarily collapsed. We have three cases to consider. If on the Emden polytrope "$n = \frac{3}{2}$,"

(1) $0 \leqq \eta < 1{\cdot}6$, then $\left(\frac{5}{8}\right)^{\frac{3}{2}}\eta^2\left|\frac{d\psi}{d\eta}\right| < \left(\xi^2\left|\frac{d\theta}{d\xi}\right|\right)_{E_1} < \left(\xi^2\left|\frac{d\theta}{d\xi}\right|\right)_{E_2}$.

(2) $1{\cdot}6 < \eta < 3{\cdot}5$, then $\left(\frac{5}{8}\right)^{\frac{1}{2}}\eta\psi^{\frac{1}{2}} > 1{\cdot}171$.

(3) $3{\cdot}5 < \eta \leqq 3{\cdot}6571$, then

$$\left(\frac{5}{8}\right)^{\frac{3}{2}}\frac{\eta^2}{\psi^{\frac{3}{2}}}\left|\frac{d\psi}{d\eta}\right| > 2{\cdot}016 \geqq \left(\xi^2\left|\frac{d\theta}{d\xi}\right|\right)_{E_2} > \left(\xi^2\left|\frac{d\theta}{d\xi}\right|\right)_{E_1}.$$

In all three cases we see, with the aid of equations (100) and (101) and of R. H. Fowler's theorems, that the "$n = 3$"-polytrope is collapsed.

*Conclusion.*—With the aid of certain theorems established by R. H. Fowler it is possible to carry Professor Milne's discussion further, to show that centrally-condensed "$n = 3$" outer envelopes necessarily imply, for the standard model, "$n = \frac{3}{2}$"-solutions running in from the interface.

*University Observatory,*
*Copenhagen:*
1931 *February* 10.

---

## *Note on the Fitting of Polytropic Models in the Theory of Stellar Structure.* By T. G. Cowling, B.A.

(*Communicated by E. A. Milne.*)

1. In his recent paper entitled "The Analysis of Stellar Structure" * Professor Milne has made several interesting suggestions. One of these is the suggestion that ordinary giant and dwarf stars possess central densities and temperatures far in excess of those predicted by earlier theories. This suggestion arises out of a study of the standard model, for which the coefficients of opacity and generation of energy are constant throughout the star. It is found that the perfect gas model of this type possesses a series of configurations which are centrally condensed, *i.e.* which possess infinite central density and temperature. In a very dense region, perfect gas conditions will break down; and it is suggested that in consequence an actual infinity will be avoided, but that very large central densities and temperatures occur.

Milne suggests that the validity of this interpretation can be tested by a study of a composite model in which a perfect gas envelope is fitted to a core composed of degenerate gas. Through the whole model the coefficients of opacity and generation of energy are constant, and density, temperature, and radiation- and gas-pressures are continuous across the surface of fit. From these conditions of continuity he derives two equations. These can be put in the form

$$\left(\frac{8}{5}\right)^{\frac{3}{2}} x_1^2 \frac{dy_1}{dx_1} = \frac{x_2^2}{y_2^{\frac{3}{4}}} \frac{dy_2}{dx_2} \quad . \quad . \quad . \quad (1)$$

$$\left(\frac{8}{5}\right)^{\frac{1}{2}} x_1 y_1 = x_2 y_2^{\frac{1}{4}} \quad . \quad . \quad . \quad . \quad (2)$$

where $y_1$, $y_2$ are special solutions of the equations

$$\frac{1}{x_1^2} \frac{d}{dx_1}\left(x_1^2 \frac{dy_1}{dx_1}\right) = -y_1^3 \quad . \quad . \quad . \quad (3)$$

$$\frac{1}{x_2^2} \frac{d}{dx_2}\left(x_2^2 \frac{dy_2}{dx_2}\right) = -y_2^{\frac{3}{2}} \quad . \quad . \quad . \quad (4)$$

---

* *M.N.*, **91**, 4, 1930.

These are equivalent to equations M (100),* M (101), M (93), and M (93′). If $y_1$, $y_2$ are chosen to be such solutions of (3), (4) that positive values of $x_1$, $x_2$ can be found to satisfy (1), (2) and to give positive values of $y_1$, $y_2$, then there exists a corresponding composite model. It is the object of this paper to investigate for what pairs of solutions of (3) and (4) equations (1) and (2) are soluble.

We first derive some results as to the solutions of (3) and (4) by a method used by Emden. It may be remarked that this method is capable of giving R. H. Fowler's † results about Emden's equation.

2. Equations (3) and (4) are both special cases of Emden's equation

$$\frac{1}{x^2}\frac{d}{dx}\left(x^2\frac{dy}{dx}\right) = -y^n \quad . \quad . \quad . \quad (5)$$

where we set

$$n = 1 + 2/m \quad . \quad . \quad . \quad . \quad (6)$$

and $m \geqslant 1$. We limit our consideration to such solutions, or parts of solutions, as satisfy the conditions $x, y > 0$; these are equivalent to the conditions $\rho, r > 0$ (*cf.* M (24), M (27), M (47), M (48)).

The equation can be reduced to one of first order. We set

$$y = u/x^m \quad . \quad . \quad . \quad . \quad (7)$$

when we derive the equation

$$\frac{d}{dx}\left(x^{2-m}\frac{du}{dx} - mx^{1-m}u\right) = -u^n x^{-m}$$

or

$$x\frac{d}{dx}\left(x\frac{du}{dx} - mu\right) - (m-1)\left(x\frac{du}{dx} - mu\right) = -u^n.$$

Further, we set

$$v = -x\frac{du}{dx} \quad . \quad . \quad . \quad . \quad (8)$$

Then

$$v\left(\frac{dv}{du} + 2m - 1\right) = -(u^n + m(m-1)u) \quad . \quad . \quad (9)$$

which is the required equation. By equation (7) it follows that, when $x, y > 0$, $u > 0$. Hence we are only concerned with the behaviour of solutions of (9) when $u > 0$.

3. From equation (9) we derive the following facts :—

(i) If $v > 0$, $u > 0$, then $\frac{dv}{du} < -(2m-1)$.

(ii) If $0 > v > -[u^n + m(m-1)u]/(2m-1)$, and $u > 0$, then $\frac{dv}{du} > 0$.

(iii) If $-[u^n + m(m-1)u]/(2m-1) > v$, and $u > 0$, then $0 > \frac{dv}{du} > -(2m-1)$.

---

* Numbers preceded by a letter M refer to equations in Milne's paper.

† *M.N.*, **91**, 63, 1930.

(iv) If $u = 0$, and $v \neq 0$, then $\frac{dv}{du} = -(2m-1)$.

(v) If $v = -[u^n + m(m-1)u]/(2m-1)$, and $u > 0$, then $\frac{dv}{du} = 0$.

(vi) If $v = 0$, and $u > 0$, then $\frac{dv}{du}$ is infinite.

(vii) If $v = -mu$, and $u > 0$, then $\frac{dv}{du} > -m$.

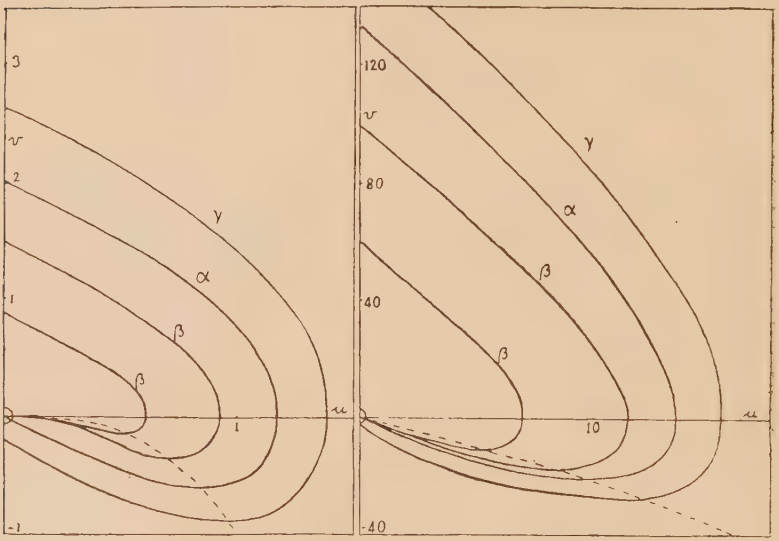


$n = 3$. $n = \frac{3}{2}$.

FIG. 1.—Showing the forms of solutions of equation (9) in the two cases $n = 3$, $n = \frac{3}{2}$.

(viii) The point $u = 0$, $v = 0$, is a singular point of the equation. There are two possible values of $\frac{dv}{du}$ at this point, namely, $-m$ and $-(m-1)$: the first of these corresponds to a unique solution, as can be shown by Fowler's * methods.

(ix) There exist no solutions for which either $u$ or $v$ becomes infinite when $u > 0$.

These facts enable us to trace the form of the $u$, $v$ curves when $u$ is positive. Any curve begins at a point $u = 0$, $v = v_0$, where $v_0 > 0$. At this point $\frac{dv}{du} = -(2m-1)$; and, if $u > 0$, $v > 0$, then $\frac{dv}{du} < -(2m-1)$. Hence $v$ decreases to zero on the curve as $u$ increases;

* *Loc. cit.*, § (6).

the curve cuts the line $v = 0$ at right angles, after which $\frac{dv}{du}$ becomes positive and $u$ begins to decrease. $v$ decreases till the curve meets the locus $v = -[u^n + m(m-1)u]/(2m-1)$, when $\frac{dv}{du}$ vanishes. The curve cannot recross this locus; as $\frac{dv}{du}$ now is negative, $u$ must decrease to zero. There is a unique solution for which $v \sim -mu$ as $u \to 0$. In this case, for small values of $u$,

$$v = -mu + u^n/3 + nu^{2n-1}/45 + \ldots \quad . \quad . \quad (10)$$

and hence, by (vii), $v > -mu$. This solution corresponds to a unique value $v_1$ of $v_0$. We call this solution the $\alpha$-solution: solutions for which $v_0$ is less or greater than $v_1$ are called $\beta$- and $\gamma$-solutions respectively. The $\alpha$-solution encloses the $\beta$-solutions, and is enclosed by the $\gamma$-solutions. Hence, as $u$ decreases to zero, $v$ being negative, $v$ tends to a finite negative limit along the $\gamma$-solutions, and to zero along the $\beta$-solutions (so that for $\beta$-solutions $\frac{dv}{du} \to -(m-1)$ as $u \to 0$). All solutions are included in these three types. The forms of solutions are illustrated in fig. 1. (*Cf.* Emden, *Gaskugeln*, pp. 51, 52, figs. 1, 4.)

4. It can be shown that the $\alpha$-, $\beta$-, and $\gamma$-solutions correspond respectively to Emden, centrally condensed, and collapsed models. For both perfect gas and degenerate gas models

$$r \propto x, \qquad \mathrm{M}(r) \propto -x^2\frac{dy}{dx}, \qquad \rho \propto y^n$$

by M (27), M (48), M (29), M (50), M (24), M (47).

Now, by equation (8),

$$\log(x/x_0) = -\int \frac{du}{v} \quad . \quad . \quad . \quad . \quad (11)$$

the integration being along the curve. But, when $v > 0$, $du > 0$; when $v < 0$, $du < 0$. Hence successive points on the curve correspond to decreasing values of $x$. The lower ends of $\alpha$- and $\beta$-curves correspond to zero values of $x$; the lower ends of $\gamma$-curves correspond to finite positive values of $x$.

By equations (7), (8)

$$x^2\frac{dy}{dx} = -x^{1-m}(v + mu).$$

Hence there is a point on every $\gamma$-curve for which $x^2\frac{dy}{dx} = 0$, so that the corresponding value of $\mathrm{M}(r)$ is zero. Hence the $\gamma$-curves correspond to collapsed models. For the $\alpha$- and $\beta$-curves $v + mu$ is always positive, and so $\mathrm{M}(r)$ is always positive for the corresponding models.

From equations (7) and (11) it follows that the lower end of the

$\alpha$-curve corresponds to a finite value of $y$; the lower ends of the $\beta$-curves correspond to values of $y$ such that

$$\text{if } n = 3, \quad y \sim 1/x(2\log(D/x))^{\frac{1}{2}}$$
$$\text{if } n = \tfrac{3}{2}, \quad y \sim D/x.$$

Hence $\alpha$-solutions correspond to Emden models and $\beta$-solutions to centrally condensed models.

5. We can now solve the problem of § (1). We set

$$w_1 = -\left(\frac{8}{5}\right)^{\frac{3}{2}} x_1^2 \frac{dy_1}{dx_1}, \qquad z_1 = \left(\frac{8}{5}\right)^{\frac{1}{2}} x_1 y_1$$
$$w_2 = -\frac{x_2^2}{y_2^{\frac{3}{4}}} \frac{dy_2}{dx_2}, \qquad z_2 = x_2 y_2^{\frac{1}{4}} \quad . \quad . \quad (12)$$

Then, if $(u_1, v_1)$ and $(u_2, v_2)$ are the values of $(u, v)$ corresponding to solutions of (3) and (4) respectively,

$$w_1 = \left(\frac{8}{5}\right)^{\frac{3}{2}} (u_1 + v_1), \qquad z_1 = \left(\frac{8}{5}\right)^{\frac{1}{2}} u_1$$
$$w_2 = \frac{v_2 + 4u_2}{u_2^{\frac{3}{4}}}, \qquad z_2 = u_2^{\frac{1}{4}} \quad . \quad . \quad . \quad (13)$$

To each $(u_1, v_1)$ curve corresponds a $(z_1, w_1)$ curve, etc.; the solution of equations (1) and (2) is equivalent to finding a point $(z, w)$ in which the $(z_1, w_1)$ curve cuts the $(z_2, w_2)$ curve. The shape of the two sets of $(z, w)$ curves can be inferred from that of the $(u, v)$ curves.

Consider first the $(z_1, w_1)$ curves. The new $\alpha$-curve is such that $w_1, z_1$ are always positive: $w_1$ decreases from a value $w'$ to zero on the curve: and at the two ends, $z_1 = 0$, $\dfrac{dw_1}{dz_1} = 0$. The $\beta$-curves are enclosed by the new $\alpha$-curve and the line $z_1 = 0$: on such a curve $w_1$ decreases from a value less than $w'$ to zero: at the upper end $z_1 = 0$, $\dfrac{dw_1}{dz_1} = 0$: at the lower end $z_1 = 0$, $\dfrac{dw_1}{dz_1} = \dfrac{8}{5}$. The $\gamma$-curves and the line $z_1 = 0$ enclose the $\alpha$-curve: on such a curve $w_1$ decreases from a value greater than $w'$ to a negative value; at the two ends, $z_1 = 0$, $\dfrac{dw_1}{dz_1} = 0$. On any of the curves, if $w_1 = 8z_1/5$, $\dfrac{dw_1}{dz_1}$ is infinite.

Next consider the $(z_2, w_2)$ curves. For any curve, at the upper end $w_2 \to +\infty$, $z_2 \to 0$ in such a way that $w_2 z_2^3$ remains finite. On the $\alpha$-curve $w_2$ is always positive; at the lower end $w_2 = 0$, $z_2 = 0$, $\dfrac{dw_2}{dz_2} = 0$. The $\beta$-curves are enclosed by the $\alpha$-curve and the line $z_2 = 0$; at the lower end $w_2 = 0$, $z_2 = 0$, $\dfrac{dw_2}{dz_2} = 1$. The $\gamma$-curves and the line $z_2 = 0$ enclose the $\alpha$-curve; at the lower end $w_2 \to -\infty$, $z_2 \to 0$, in such a way that $w_2 z_2^3$ remains finite. On any of the curves, if $w_2 = 4z_2$, $\dfrac{dw_2}{dz_2}$ is infinite.

The mutual relation of the two $\alpha$-curves can be determined by use of Emden's tables. It is found (see fig. 2) that the $\alpha_1$-curve lies inside

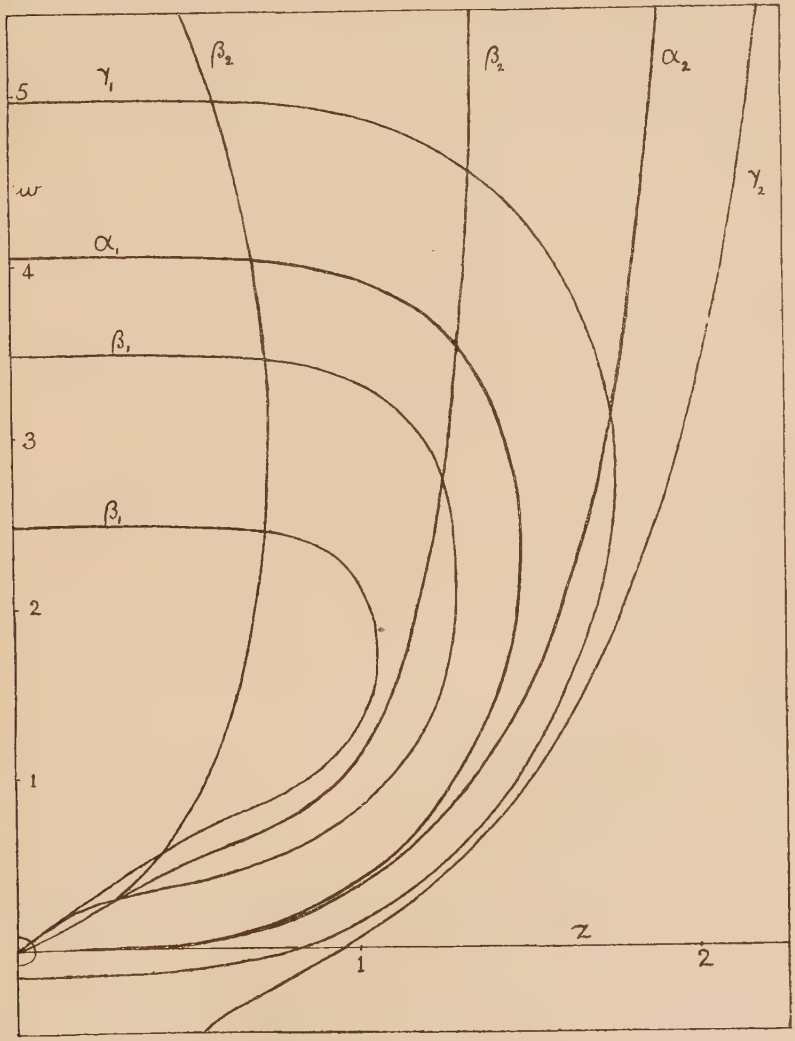


FIG. 2.—The $(z, w)$ curves. The two $\alpha$-curves are drawn accurately and the general relation of the $\beta$- and $\gamma$-curves to them is shown.

the $\alpha_2$-curve. Hence the family consisting of the $\alpha_1$-curve together with all the $\beta_1$-curves cannot have any intersections with the family consisting of the $\alpha_2$-curve together with the $\gamma_2$-curves. On the other hand, as the two ends of a $\gamma_1$-curve lie on opposite sides of the $\alpha_2$-curve,

a $\gamma_1$-curve always meets the $\alpha_2$-curve. It also always meets any $\beta_2$-curve and certain of the $\gamma_2$-curves.

[In fig. 2 the $\alpha_1$- and $\alpha_2$-curves are almost indistinguishable at their lower ends. As there may be some doubt as to whether these curves do not actually meet near the lower ends, we give a proof that if $z_1 = z_2 = z < 1$, then, for the parts of the curves for which $\frac{dw_1}{dz}, \frac{dw_2}{dz}$ are positive, $w_1 > w_2$. From equations (9) and (13) we have

$$\frac{dw_1}{dz_1} = \frac{8z_1^3}{8z_1 - 5w_1}$$

$$\frac{dw_2}{dz_2} = \frac{4z_2^4 + 3w_2^2}{z_2(4z_2 - w_2)}.$$

If $0 < z_1 = z_2 = z < 1$ and $\frac{dw_1}{dz}, \frac{dw_2}{dz}$ are positive, then $w_1 < 8z/5$, $w_2 < 4z$. Now

$$\frac{dw_2}{dz} - \frac{3z^2}{2} = \frac{3(w_2 - z^3/2)(w_2 + z^3) - 2z^4 + 3z^6/2}{z(4z - w_2)}$$

Hence, if $0 < z < 1$, and $w_2 < z^3/2$, $\frac{d}{dz}(w_2 - z^3/2) < 0$. But, by (10) and (13), if $z$ is small, $w_2 = z^3/3 + o(z^5) < z^3/2$. Hence, if $0 < z < 1$, $w_2 < z^3/2$.

Again

$$\frac{dw_1}{dz} - \frac{dw_2}{dz} = \frac{20(w_1 - w_2)z^4 + 12w_2z(z^3 - 2w_2) + 15w_1w_2^2}{z(4z - w_2)(8z - 5w_1)}$$

and so, if $0 < z < 1$ and $w_1 > w_2$, $\frac{dw_1}{dz} > \frac{dw_2}{dz}$.

But by (10) and (13), if $z$ is small, $w_1 - w_2 = z^5/120 + o(z^7) > 0$. Thus, if $0 < z < 1$, $w_1 > w_2$.]

6. The problem of § (1) is now solved. From the discussion of last section two facts at once emerge.

(i) Equations (1) and (2) can always be solved if $y_1$ corresponds to a collapsed perfect gas model and $y_2$ to a degenerate gas Emden model.

(ii) If $y_1$ corresponds to a centrally condensed perfect gas model, equations (1) and (2) are not soluble unless $y_2$ corresponds to a centrally condensed degenerate core.

Since a centrally condensed core possesses a central singularity, we infer from the second of these facts that a composite model of the type discussed above, of which the outer layers form part of a centrally condensed perfect gas model, cannot without modification represent the stars that exist in nature.

The above results were given in outline during the discussion at the Society's meeting in 1931 January.

*South Kensington :*
1931 *February 27.*

## *Note on "Equations of Fit" in the Theory of Stellar Structure.*

By E. A. Milne, F.R.S.

Mr. T. G. Cowling and Mr. B. Strömgren have simultaneously and independently established the result that in the steady-state configurations of a composite mass consisting of a gaseous envelope surrounding a degenerate core, the whole being of constant opacity and constant source-strength, if the solution for the envelope is of the centrally condensed type the solution for the degenerate core fitting on to the envelope at the surface of demarcation must necessarily also be of centrally condensed type. I propose to consider the physical interpretation of this result.

Configurations for which $L_0 < L < L_1$ must either settle down to a steady state or burst. If they could not exist, all configurations $L = L_0$ would be cataclysmically unstable to small increases of L, and the only possible stable configurations would be collapsed configurations of high mean density. This contradicts observation. Moreover, there is no reason why configurations for which $L_0 < L < L_1$ should burst, for outward radiation-pressure is less than inward gravity. Thus steady-state configurations for which $L_0 < L < L_1$ must be capable of existing. Such configurations are represented in their outer layers by centrally condensed solutions, and it is simply a question of ascertaining by the method of inward integration the physical state of their interiors.

My "equations of fit" for the standard model postulate nothing about the properties of the far interior of the core. They merely involve the nature of the solution which describes the state of affairs immediately interior to the surface of demarcation. Thus the result of Cowling and Strömgren implies that as we penetrate a standard model configuration from the outside inwards, having arrived at the surface of demarcation along a centrally condensed "$n = 3$" solution we must proceed inwards from the surface of demarcation with a centrally condensed "$n = \frac{3}{2}$" solution. Near the centre $\eta = 0$, and the solution $\phi$ has a singularity of the type $\phi \sim D/\eta$, where D is arbitrary. Further, $\rho \propto (D/\eta)^{\frac{3}{2}}$. It follows that as we go inwards the density increases indefinitely whatever centrally condensed $\phi$ we follow. Hence the physical conditions become more drastic, and the equation of state $p = K\rho^{\frac{5}{3}}$ must break down before we reach the centre.

After the equation of state $p = K\rho^{\frac{5}{3}}$ has broken down, the state of affairs depends on the next equation of state obeyed by the material.

Purely by way of illustration I consider first what happens when the next equation of state is $\rho = \rho_{\max}$, the equation of state of incompressible material. Proceed inwards until the mean density $\rho_m(r)$ of the remaining mass $M(r)$ is equal to $\rho_{\max}$. This occurs, for any arbitrarily selected $\phi$, for a determinate $r$, say $r = r''$, where $M(r'')/\frac{4}{3}\pi r''^3 = \rho_{\max}$. Replace the material inside $r = r''$ by a sphere of incompressible material of density $\rho_{\max}$. Since in the "$n = \frac{3}{2}$" distribution the density steadily increases inwards, it follows that at $r = r''$ there will now be a discontinuity of density, and so a discontinuity of phase. For

equilibrium across such a surface of discontinuity a thermodynamic condition must be satisfied, similar to that for the equilibrium contact of water with ice. The thermodynamic potentials of the degenerate-gas phase and the incompressible phase must be equal at the surface of discontinuity, as shown by Willard Gibbs. Now the function $\phi$ along which we have moved inwards is so far arbitrary (D arbitrary), and for an arbitrary $\phi$ the thermodynamic relation will not in general be satisfied at the determinate radius $r = r''$. Now adjust D, *i.e.* select $\phi$, in such a way that the thermodynamic condition is satisfied at $r = r''$. We then have a determinate configuration of equilibrium consisting of three phases—a perfect-gas phase, a degenerate-gas phase, and an incompressible phase; at the first surface of demarcation the densities are continuous; at the second surface of demarcation they are discontinuous.*

No surprise need be felt at the introduction of a discontinuity of phase. Discontinuities of phase are common in the configuration we know best, namely, the earth. This has discontinuities of phase at its air-earth, air-ocean, and ocean-earth interfaces, besides an important solid-liquid interface in the interior. I do not claim that actual stars necessarily possess such a discontinuity. I merely demonstrate its necessity in the configurations of a mass constructed on the standard model when the successive equations of state are of the type stated.

These considerations respecting the equation of state $\rho = \rho_{\max}$ illustrate the general procedure. It has been shown, however, by Stoner † and by Chandrasekhar ‡ that the next equation of state obeyed by a degenerate gas is the relativistic equation $p = K_2\rho^{\frac{4}{3}}$, corresponding to "$n = 3$." We have therefore to consider the fitting of an "$n = 3$" envelope round an "$n = \frac{3}{2}$" zone, and then the fitting of this "$n = \frac{3}{2}$" zone to an "$n = 3$" region inside it. If we are considering centrally condensed § configurations, we have first to join an "$n = 3$" centrally condensed $f$ to an "$n = \frac{3}{2}$" centrally condensed $\phi$; and then to join this to another "$n = 3$" $f$ of same type. Mr. Cowling informs me that his curves (his fig. 2) show that the new $f$ must also be centrally condensed on the standard model. (The necessary equations of fit have been found by Mr. Chandrasekhar in his paper.) Therefore once again, on the standard model, we are led to a still further change of equation of state, and so as before to an incompressible core with discontinuous change of density.

It will be apparent that progress with the analysis of centrally condensed configurations will be difficult until more is known of the thermodynamic properties of matter at very high densities and tempera-

* In "The Analysis of Stellar Structure," *M.N.*, **91**, 35, 1930, I showed that if $\varphi$ is centrally condensed, no fitting is possible if $\varrho$ is everywhere continuous. The above considerations show that it is necessary, in the case of the standard model, to allow for discontinuities in $\varrho$, and that the appropriate $\varphi$ then becomes determinate.

† Stoner, *Phil. Mag.*, **9**, 944, 1930.

‡ Chandrasekhar, *Phil. Mag.*, in press.

§ Collapsed configurations are considered separately by Mr. Chandrasekhar elsewhere in this number of *M.N.* (p. 456).

tures. One observational test is, however, possible. From equation (118) of "The Analysis of Stellar Structure"* it is possible to evaluate the core parameter $a$, for a star of observed M, L, and $T_e$, for any arbitrarily assigned opacity $\kappa$. From this the mean density of the core can be evaluated. The test is that this mean density must be less than the maximum possible density of matter. I have verified that this test is satisfied for the sun, but I postpone my numerical estimates of its core-radius, core-mass, etc., till a later occasion.

When we depart from the standard model, the result of Cowling and Strömgren no longer necessarily holds. The reader of their papers will see that their result depends to a certain extent on the numerical evaluation of relations in which the factor 8/5 plays a part. For the sake of greater generality I have recently worked out the form of the equations of fit when the core is not necessarily of the same opacity as the envelope, the source-strength remaining uniform. The following are the results :—

Let $\kappa_1$, $\kappa_2$ be the opacities in envelope and core respectively. Define two pure numbers $\beta_1$ and $\beta_2$ by the relations

$$\beta_1 = 1 - \frac{\kappa_1 L}{4\pi c G M}, \qquad \beta_2 = 1 - \frac{\kappa_2 L}{4\pi c G M}$$

in the usual notation. Then the equations of fit may be shown to be of the form

$$\left(\frac{8}{5}\frac{\beta_2}{\beta_1}\right)^{\frac{1}{2}} a f(a) = b[\phi(b)]^{\frac{1}{2}} \quad . \quad . \quad . \quad (1)$$

$$\left(\frac{8}{5}\frac{\beta_2}{\beta_1}\right)^{\frac{3}{2}} a^2 f'(a) = \frac{b^2\phi'(b)}{[\phi(b)]^{\frac{3}{2}}} \quad . \quad . \quad . \quad (2)$$

where $\phi$ is a solution of "$n = \frac{3}{2}$" and $f$ is that solution of "$n = 3$" which corresponds to a value of the discriminant equal to $C_1$, where $C_1$ is the value of the previously defined discriminant C when $\beta$ takes the value $\beta_1$.

Equations (1) and (2) may be simplified. Cubing (1) and dividing by (2) we have

$$\frac{a[f(a)]^3}{f'(a)} = \frac{b[\phi(b)]^{\frac{3}{2}}}{\phi'(b)} \quad . \quad . \quad . \quad . \quad (3)$$

Dividing (2) by (1) we have

$$\frac{af'(a)}{f(a)} = \frac{5}{8}\frac{\beta_1}{\beta_2}\frac{b\phi'(b)}{\phi(b)} \quad . \quad . \quad . \quad . \quad (4)$$

Equations (3) and (4), which are fully equivalent to (1) and (2), may be described as the "canonical form" of the equations of fit.†

It is now clear that the result of Cowling and Strömgren does not necessarily hold when the opacity of the core is not necessarily equal to the opacity in the envelope. For instead of the factor 5/8 we have the

* *Loc. cit.*

† For a variety of models for which I have now done the analysis, the equations of fit always permit a simplification of the above type.

factor $\frac{5}{8}(\beta_1/\beta_2)$, which may have any value. We can, in fact, show that we can always construct configurations in which the central core is occupied by a solution of Emden type devoid of singularity, by suitable choice of opacities. For let $\phi$ be of Emden type. Choose an arbitrary centrally condensed $f$, a solution of "$n = 3$." Choose an arbitrary value for $a$. Then a value of $b$ can always be found to satisfy (3), for the left-hand side is given and the right-hand side can take any value between 0 and $\infty$. Inserting these values of $a$ and $b$ in (4) we find a value for $\beta_1/\beta_2$. I have in this way, by graphical methods, constructed a number of solutions of this type. Thus it is quite possible to have a centrally condensed "$n = 3$" envelope and a core of Emden type "$n = \frac{3}{2}$" free from singularity.

I take this opportunity of mentioning that when the configuration is "highly collapsed," so that the discriminant $C_1$ (calculated from L, M, and $\kappa_1$) is very small, the equations of fit (3) and (4) (with $\phi$ of Emden type) possess solutions to which explicit approximations are

$$a = \xi_0\left[1 - \frac{5}{8}\frac{\beta_1}{\beta_2}C_1^{\frac{2}{3}}\omega_1^{\frac{1}{3}}\right], \quad . \quad . \quad . \quad (5)$$

$$b = \eta_0\left[1 - \left(\frac{5}{8}\frac{\beta_1}{\beta_2}\right)^2 C_1^{\frac{2}{3}}\omega_1^{\frac{1}{3}}\right] \quad . \quad . \quad . \quad (6)$$

In these formulæ $\xi_0$ and $\eta_0$ are the zeros of the functions $f(\xi)$ and $\phi(\eta)$ respectively, and $\omega_1$ is the invariant,

$$\omega_1 = -\eta_0^5\phi'(\eta_0) = 132{\cdot}39.*$$

The function $f$ satisfies

$$\xi_0^2 f'(\xi_0) = -C_1^{-\frac{1}{2}}.$$

The first of these formulæ, (5), evaluates the relative thickness $(\xi_0 - a)/\xi_0$ of the gaseous fringe of a highly collapsed configuration, as compared with the external radius of the configuration.

It is quite practicable to form equations of fit for a degenerate energy-generating core, of uniform source-strength and of opacity $\kappa_2$, surrounded by a gaseous envelope free from sources, of opacity $\kappa_1$ not necessarily equal to $\kappa_2$. The equations involve the "point-source" functions $f_1$, $f_2$, $f_3$ defined in Section A of "The Analysis of Stellar Structure."† The resulting formulæ for the radius, mean density, effective temperature, etc., are of the same form as those previously found for the standard model save for numerical factors which are functions of the pure numbers $\beta_1$, $\beta_2$, and the appropriate discriminant. This meets the criticism that my results are special to the standard model, so far as different source- and opacity-distributions affect the significant equations.

Practical application of the formulæ awaits the evaluation by theoretical physicists of the opacity of a degenerate gas.

* Fairclough's recalculation of Emden's "$n = \frac{3}{2}$" solution. † *Loc. cit.*

*Oxford:*
1931 *March* 7.

*A Homogeneous Universe of Constant Mass and Increasing Radius accounting for the Radial Velocity of Extra-galactic Nebulæ.* By Abbé G. Lemaître.

(*Translated by permission from "Annales de la Société scientifique de Bruxelles," Tome XLVII, série A, première partie.*)

## 1. *Introduction.*

According to the theory of relativity, a homogeneous universe may exist such that all positions in space are completely equivalent; there is no centre of gravity. The radius of space R is constant; space is elliptic, *i.e.* of uniform positive curvature $1/R^2$; straight lines starting from a point come back to their origin after having travelled a path of length $\pi R$; the volume of space has a finite value $\pi^2 R^3$; straight lines are closed lines going through the whole space without encountering any boundary.

Two solutions have been proposed. That of de Sitter ignores the existence of matter and supposes its density equal to zero. It leads to special difficulties of interpretation which will be referred to later, but it is of extreme interest as explaining quite naturally the observed receding velocities of extra-galactic nebulæ, as a simple consequence of the properties of the gravitational field without having to suppose that we are at a point of the universe distinguished by special properties.

The other solution is that of Einstein. It pays attention to the evident fact that the density of matter is not zero, and it leads to a relation between this density and the radius of the universe. This relation forecasted the existence of masses enormously greater than any known at the time. These have since been discovered, the distances and dimensions of extra-galactic nebulæ having become known. From Einstein's formulæ and recent observational data, the radius of the universe is found to be some hundred times greater than the most distant objects which can be photographed by our telescopes.

Each theory has its own advantages. One is in agreement with the observed radial velocities of nebulæ, the other with the existence of matter, giving a satisfactory relation between the radius and the mass of the universe. It seems desirable to find an intermediate solution which could combine the advantages of both.

At first sight, such an intermediate solution does not appear to exist. A static gravitational field for a uniform distribution of matter without internal stress has only two solutions, that of Einstein and that of de Sitter. De Sitter's universe is empty, that of Einstein has been described as "containing as much matter as it can contain." It is remarkable that the theory can provide no mean between these two extremes.

The solution of the paradox is that de Sitter's solution does not really meet all the requirements of the problem. Space is homogeneous with constant positive curvature; space-time is also homogeneous, for

all events are perfectly equivalent. But the partition of space-time into space and time disturbs the homogeneity. The co-ordinates used introduce a centre. A particle at rest at the centre of space describes a geodesic of the universe ; a particle at rest otherwhere than at the centre does not describe a geodesic. The co-ordinates chosen destroy the homogeneity and produce the paradoxical results which appear at the so-called " horizon " of the centre. When we use co-ordinates and a corresponding partition of space and time of such a kind as to preserve the homogeneity of the universe, the field is found to be no longer static ; the universe becomes of the same form as that of Einstein, with a radius no longer constant but varying with the time according to a particular law.

In order to find a solution combining the advantages of those of Einstein and de Sitter, we are led to consider an Einstein universe where the radius of space or of the universe is allowed to vary in an arbitrary way.

### 2. *Einstein Universe of Variable Radius. Field Equations. Conservation of Energy.*

As in Einstein's solution, we liken the universe to a rarefied gas whose molecules are the extra-galactic nebulæ. We suppose them so numerous that a volume small in comparison with the universe as a whole contains enough nebulæ to allow us to speak of the density of matter. We ignore the possible influence of local condensations. Furthermore, we suppose that the nebulæ are uniformly distributed so that the density does not depend on position. When the radius of the universe varies in an arbitrary way, the density, uniform in space, varies with time. Furthermore, there are generally interior stresses, which, in order to preserve the homogeneity, must reduce to a simple pressure, uniform in space and variable with time. The pressure, being two-thirds of the kinetic energy of the " molecules," is negligible with respect to the energy associated with matter ; the same can be said of interior stresses in nebulæ or in stars belonging to them. We are thus led to put $p = 0$.

Nevertheless it might be necessary to take into account the radiation-pressure of electromagnetic energy travelling through space ; this energy is weak but it is evenly distributed through the whole of space and might afford a notable contribution to the mean energy. We shall thus keep the pressure $p$ in the general equations as the mean radiation-pressure of light, but we shall write $p = 0$ when we discuss the application to astronomy.

We denote the density of total energy by $\rho$, the density of radiation energy by $3p$, and the density of the energy condensed in matter by $\delta = \rho - 3p$. We identify $\rho$ and $-p$ with the components $T_4{}^4$ and $T_1{}^1 = T_2{}^2 = T_3{}^3$ of the material energy tensor, and $\delta$ with T. Working out the contracted Riemann tensor for a universe with a line-element given by

$$ds^2 = -R^2 d\sigma^2 + dt^2, \qquad . \quad . \quad . \quad . \quad (1)$$

where $d\sigma$ is the elementary distance in a space of radius unity, and R is a function of the time $t$, we find that the field equations can be written

$$3\frac{R'^2}{R^2} + \frac{3}{R^2} = \lambda + \kappa\rho \quad . \quad . \quad . \quad (2)$$

and

$$2\frac{R''}{R} + \frac{R'^2}{R^2} + \frac{1}{R^2} = \lambda - \kappa p \quad . \quad . \quad . \quad (3)$$

Accents denote derivatives with respect to $t$. $\lambda$ is the unknown cosmological constant, and $\kappa$ is the Einstein constant whose value is $1{\cdot}87 \cdot 10^{-27}$ in C.G.S. units ($8\pi$ in natural units).

The four identities giving the expression of the conservation of momentum and of energy reduce to

$$\frac{d\rho}{dt} + \frac{3R'}{R}(\rho + p) = 0 \quad . \quad . \quad . \quad . \quad (4)$$

which is the energy equation. This equation can replace (3). As $V = \pi^2 R^3$ it can be written

$$d(V\rho) + p dV = 0, \quad . \quad . \quad . \quad . \quad (5)$$

showing that *the variation of total energy plus the work done by radiation-pressure in the dilatation of the universe is equal to zero.*

### 3. *Universe of Constant Mass.*

If $M = V\delta$ remains constant, we write, $\alpha$ being a constant,

$$\kappa\delta = \frac{\alpha}{R^3} \quad . \quad . \quad . \quad . \quad . \quad (6)$$

As

$$\rho = \delta + 3p$$

we have

$$3d(pR^3) + 3pR^2 dR = 0 \quad . \quad . \quad . \quad (7)$$

and, $\beta$ being a constant of integration,

$$\kappa p = \frac{\beta}{R^4} \quad . \quad . \quad . \quad . \quad . \quad (8)$$

and therefore

$$\kappa\rho = \frac{\alpha}{R^3} + \frac{3\beta}{R^4} \quad . \quad . \quad . \quad . \quad (9)$$

By substitution in (2) we have

$$\frac{R'^2}{R^2} = \frac{\lambda}{3} - \frac{1}{R^2} + \frac{\kappa\rho}{3} = \frac{\lambda}{3} - \frac{1}{R^2} + \frac{\alpha}{3R^3} + \frac{\beta}{R^4} \quad . \quad . \quad (10)$$

and

$$t = \int \frac{dR}{\sqrt{\frac{\lambda R^2}{3} - 1 + \frac{\alpha}{3R} + \frac{\beta}{R^2}}} \quad . \quad . \quad . \quad (11)$$

When $\alpha$ and $\beta$ vanish, we obtain the de Sitter solution in Lanczos's form—

$$R = \sqrt{\frac{3}{\lambda}} \cosh \sqrt{\frac{\lambda}{3}}(t - t_0) \quad . \quad . \quad . \quad (12)$$

The Einstein solution is found by making $\beta = 0$ and R constant. Writing $R' = R'' = 0$ in (2) and (3) we find

$$\frac{1}{R^2} = \lambda \qquad \frac{3}{R^2} = \lambda + \kappa\rho \qquad \rho = \delta$$

or

$$R = \frac{1}{\sqrt{\lambda}} \qquad \kappa\delta = \frac{2}{R^2} \quad . \quad . \quad . \quad (13)$$

and from (6)

$$\alpha = \kappa\delta R^3 = \frac{2}{\sqrt{\lambda}} \quad . \quad . \quad . \quad . \quad (14)$$

The Einstein solution does not result from (14) alone ; it also supposes that the initial value of R′ is zero. If we write

$$\lambda = \frac{1}{R_0^2} \quad . \quad . \quad . \quad . \quad . \quad (15)$$

we have for $\beta = 0$ and $\alpha = 2R_0$

$$t = R_0\sqrt{3}\int \frac{dR}{R - R_0}\sqrt{\frac{R}{R + 2R_0}} \quad . \quad . \quad . \quad (16)$$

For this solution the two equations (13) are of course no longer valid.

Writing

$$\kappa\delta = \frac{2}{R_E^2} \quad . \quad . \quad . \quad . \quad (17)$$

we have from (14) and (15)

$$R^3 = R_E^2 R_0 \quad . \quad . \quad . \quad . \quad (18)$$

The value of $R_E$, the radius of the universe computed from the mean density by Einstein's equation (17), has been found by Hubble to be

$$R_E = 8{\cdot}5 \times 10^{28} \text{ cm.} = 2{\cdot}7 \times 10^{10} \text{ parsec.} \quad . \quad . \quad (19)$$

We shall see later that the value of $R_0$ can be computed from the radial velocities of the nebulæ ; R can then be found from (18).

Finally, we shall show that a serious departure from (14) would lead to consequences not easily acceptable.

4. *Doppler Effect due to the Variation of the Radius of the Universe.*

From (1) we have for a ray of light

$$\sigma_2 - \sigma_1 = \int_{t_1}^{t_2} \frac{dt}{R} \quad . \quad . \quad . \quad . \quad (20)$$

where $\sigma_1$ and $\sigma_2$ relate to spatial co-ordinates. We suppose that the light is emitted at the point $\sigma_1$ and observed at $\sigma_2$. A ray of light

emitted slightly later starts from $\sigma_1$ at time $t_1 + \delta t_1$ and reaches $\sigma_2$ at time $t_2 + \delta t_2$. We have therefore

$$\frac{\delta t_2}{R_2} - \frac{\delta t_1}{R_1} = 0, \qquad \frac{\delta t_2}{\delta t_1} - 1 = \frac{R_2}{R_1} - 1 \quad . \quad . \quad (21)$$

where $R_1$ and $R_2$ are the values of the radius R at the time of emission $t_1$ and at the time of observation $t_2$. If $\delta t_1$ is the period of the emitted light, $\delta t_2$ is the period of the observed light. Now $\delta t_1$ is also the period of light emitted under the same conditions in the neighbourhood of the observer, because the period of light emitted under the same physical conditions has the same value everywhere when reckoned in proper time. Therefore

$$\frac{v}{c} = \frac{\delta t_2}{\delta t_1} - 1 = \frac{R_2}{R_1} - 1 \quad . \quad . \quad . \quad (22)$$

is the apparent Doppler effect due to the variation of the radius of the universe. *It equals the ratio of the radii of the universe at the instants of observation and emission, diminished by unity.*

$v$ is that velocity of the observer which would produce the same effect. When the light source is near enough, we have the approximate formulæ

$$\frac{v}{c} = \frac{R_2 - R_1}{R_1} = \frac{dR}{R} = \frac{R'}{R}dt = \frac{R'}{R}r$$

where $r$ is the distance of the source. We have therefore

$$\frac{R'}{R} = \frac{v}{cr} \quad . \quad . \quad . \quad . \quad . \quad (23)$$

From a discussion of available data, we adopt

$$\frac{R'}{R} = 0{\cdot}68 \times 10^{-27} \text{ cm.}^{-1} \quad . \quad . \quad . \quad (24)$$

and find from (16)

$$\frac{R'}{R} = \frac{1}{R_0\sqrt{3}}\sqrt{1 - 3y^2 + 2y^3} \quad . \quad . \quad . \quad (25)$$

where

$$y = \frac{R_0}{R} \quad . \quad . \quad . \quad . \quad . \quad (26)$$

Now from (18) and (26)

$$R_0^2 = R_E^2 y^3 \quad . \quad . \quad . \quad . \quad (27)$$

and therefore

$$3\left(\frac{R'}{R}\right)^2 R_E^2 = \frac{1 - 3y^2 + 2y^3}{y^3} \quad . \quad . \quad . \quad (28)$$

With the adopted numerical data (24) and (19), we have

$$y = 0{\cdot}0465$$

giving

$$R = R_E\sqrt{y} = 0{\cdot}215R_E = 1{\cdot}83 \times 10^{28} \text{ cm.} = 6 \times 10^9 \text{ parsecs.}$$
$$R_0 = Ry = R_E y^{\frac{3}{2}} = 8{\cdot}5 \times 10^{26} \text{ cm.} = 2{\cdot}7 \times 10^8 \text{ parsecs.}$$
$$= 9 \times 10^8 \text{ light-years.}$$

Integral (16) can easily be computed. Writing

$$x^2 = \frac{R}{R + 2R_0} \quad . \quad . \quad . \quad . \quad (29)$$

it can be written

$$t = R_0\sqrt{3}\int \frac{4x^2dx}{(1-x^2)(3x^2-1)}$$
$$= R_0\sqrt{3}\log\frac{1+x}{1-x} + R_0\log\frac{\sqrt{3}x-1}{\sqrt{3}x+1} + C \quad . \quad (30)$$

If $\sigma$ is the fraction of the radius of the universe travelled by light during time $t$, we have also

$$\sigma = \int\frac{dt}{R} = \sqrt{3}\int\frac{2dx}{3x^2-1} = \log\frac{\sqrt{3}x-1}{\sqrt{3}x+1} + C' \quad . \quad (31)$$

The following table gives values of $\sigma$ and $t$ for different values of $R/R_0$ :—

TABLE.—*Values of $\sigma$ and $t$.*

| $\frac{R}{R_0}$. | $\frac{t}{R_0}$. | $\sigma$ | | $\frac{v}{c}$. |
|---|---|---|---|---|
| | | Radians | Degrees. | |
| 1 | $-\infty$ | $-\infty$ | $-\infty$ | 19 |
| 2 | −4·31 | −0·889 | −51° | 9 |
| 3 | −3·42 | −0·521 | −30 | $5\frac{2}{3}$ |
| 4 | −2·86 | −0·359 | −21 | 4 |
| 5 | −2·45 | −0·266 | −15 | 3 |
| 10 | −1·21 | −0·087 | − 5 | 1 |
| 15 | −0·50 | −0·029 | − 1·7 | $\frac{1}{3}$ |
| 20 | 0·00 | 0·000 | 0·0 | 0 |
| 25 | 0·39 | 0·017 | 1 | .. |
| $\infty$ | $\infty$ | 0·087 | 5 | .. |

The constants of integration are adjusted to make $\sigma$ and $t$ vanish for $R/R_0 = 20$ in place of 21·5. The last column gives the Doppler effect computed from (22). The approximate formula (23) would make $v/c$ proportional to $r$ and thus to $\sigma$. The error is only 0·005 for $v/c = 1$. The approximate formula may therefore be used within the limits of the visible spectrum.

## 5. *The Meaning of Equation* (14).

The relation (14) between the two constants $\lambda$ and $\alpha$ has been adopted following Einstein's solution. It is the necessary condition that the quartic under the radical in (11) may have a double root $R_0$ giving on integration a logarithmic term. For simple roots, integration would give a square root, corresponding to a minimum of R as in de Sitter's solution (12). This minimum would generally occur at time of the order of $R_0$, say $10^9$ years—*i.e.* quite recently for stellar evolution.

If the positive roots were to become imaginary, the radius would vary from zero upwards, the variation slowing down in the neighbourhood of the modulus of the imaginary roots. In both cases the time of variation of R in the same sense would be of the order of $R_0$ if the relation between $\lambda$ and $\alpha$ were seriously different from (14).

### 6. *Conclusion.*

We have found a solution such that

(1°) The mass of the universe is a constant related to the cosmological constant by Einstein's relation

$$\sqrt{\lambda} = \frac{2\pi^2}{\kappa M} = \frac{1}{R_0}.$$

(2°) The radius of the universe increases without limit from an asymptotic value $R_0$ for $t = -\infty$.

(3°) The receding velocities of extragalactic nebulæ are a cosmical effect of the expansion of the universe. The initial radius $R_0$ can be computed by formulæ (24) and (25) or by the approximate formula

$$R_0 = \frac{rc}{v\sqrt{3}}.$$

This solution combines the advantages of the Einstein and de Sitter solutions.

Note that the largest part of the universe is for ever out of our reach. The range of the 100-inch Mount Wilson telescope is estimated by Hubble to be $5 \times 10^7$ parsecs, or about R/200. The corresponding Doppler effect is 3000 km./sec. For a distance of 0·087R it is equal to unity, and the whole visible spectrum is displaced into the infra-red. It is impossible to see ghost-images of nebulæ or suns, as even if there were no absorption these images would be displaced by several octaves into the infra-red and would not be observed.

It remains to find the cause of the expansion of the universe. We have seen that the pressure of radiation does work during the expansion. This seems to suggest that the expansion has been set up by the radiation itself. In a static universe light emitted by matter travels round space, comes back to its starting-point, and accumulates indefinitely. It seems that this may be the origin of the velocity of expansion R′/R which Einstein assumed to be zero and which in our interpretation is observed as the radial velocity of extra-galactic nebulæ.

### REFERENCES.

(1) For the different partitions of space and time in the de Sitter universe, see
K. Lanczos, *Phys. Zeits.*, **23**, 539, 1922.
H. Weyl, *Phys. Zeits*, **24**, 230, 1923.
P. du Val, *Phil. Mag.*, 6, **47**, 930, 1924.
G. Lemaître, *Journal of Math. and Phys.*, **4**, No. 3, May 1925.

(2) Equations of the universe of variable radius and constant mass have been fully discussed, without reference to the receding velocity of nebulæ, by
A. Friedmann, "Über die Krümmung des Raümes," *Z. f. Phys.*, **10**, 377, 1922; see also
A. Einstein, *Z. f. Phys.*, **11**, 326, 1922, and **16**, 228, 1923.
The universe of variable radius has been independently studied by
R. C. Tolman, *P.N.A.S.*, **16**, 320, 1930.
(3) Discussion of the theory, and recent developments are found in
A. S. Eddington, *M.N.*, **90**, 668, 1930.
W. de Sitter, *Proc. Nat. Acad. Sci.*, **16**, 474, 1930, and *B.A.N.*, **5**, No. 185, 193, and 200 (1930).
G. Lemaître, *B.A.N.*, **5**, No. 200, 1930.
(4) Popular expositions have been given by
G. Lemaître, "La grandeur de l'espace," *Revue des questions scientifiques*, March 1929.
W. de Sitter, "The Expanding Universe," *Scientia*, Jan. 1931.

---

## *The Expanding Universe.* By Abbé G. Lemaître.

(*Communicated by Sir A. S. Eddington.*)

### 1. *Introduction.*

Eddington has suggested that the expansion of a universe in equilibrium may be started by the formation of condensations. A preliminary investigation by W. H. McCrea and G. C. McVittie seems to point out an effect of opposite sense according to the nature of the condensations.* I find that the formation of condensations and the degree of concentration of these condensations have no effect whatever on the equilibrium of the universe. Nevertheless, the expansion of the universe is due to an effect very closely related to the formation of condensations, which may be named the "stagnation" of the universe. When there is no condensation, the energy, or at least a notable part of it, may be able to wander freely through the universe. When condensations are formed this free kinetic energy has a chance to be captured by the condensations and then to remain bound to them. That is what I mean by a "stagnation" of the world—a diminution of the exchanges of energy between distant parts of it.

In order to investigate the effect of condensations in a universe homogeneous in the mean, I consider a definite condensation of supposed spherical symmetry, and I average the outside condensations so that they also may be thought of as having spherical symmetry. The condensation under investigation is limited by a spherical shell which is the neutral zone between it and neighbouring condensations; a point on this neutral zone is not more within the gravitational influence of the interior condensation than of the condensations outside. The expansion of the neutral zone gives a measure of the expansion of the

* Sir A. S. Eddington, *M.N.*, **90**, 668, 1930; W. H. McCrea and G. C. McVittie, *M.N.*, **91**, 128, 1930; G. C. McVittie, *M.N.*, **91**, 274, 1931.

whole universe. I find by this method exactly the same equations as were deduced directly from the equations of a homogeneous universe of variable radius. The result does not depend on any variation in the degree of concentration of the matter, and it shows that the pressure $p$ of the homogeneous universe must be thought of in the case of condensations as the radial kinetic energy, the density of exchanges of energy between the condensation and the outside regions.

In order to study the effect of a variation of $p$ it is convenient to choose as an auxiliary variable the gravitational potential M/R, where M is the total proper mass. Then equations may be reduced to quadratures, and any law of variation can be easily discussed. Variations of $p$ in a universe in equilibrium are found to induce variations of R of the opposite sense.

In order to obtain quantitative formulæ for the expansion of a universe in equilibrium due to the stagnation process, I worked out the special case where the stagnation arose in an instant. The value of the actual radius of the universe depends on the observed receding velocity and mean density by formulæ practically independent of the degree of the initial stagnation. The epoch of the rupture of equilibrium is found for the capture of a millionth of the mass of the universe having velocity of 30 km./sec. to be of the order of $10^{11}$ years.

## 2. *Non-static Field of Spherical Symmetry: Birkhoff's Theorem.*

The problem of the condensations in a universe of variable radius can be considered as a problem of a non-static field with spherical symmetry. We shall therefore obtain the general equations of a spherical non-static field, and extend to the case where there is a cosmological constant a very important theorem due to Birkhoff; viz.—Schwarzschild's exterior solution is the general solution in empty space even if the field is not static.* Of course, this theorem makes abstraction of immaterial changes of co-ordinates; it supposes only that the spherical symmetry is conserved and that the exterior field remains empty. This is the relativistic transposition of Newton's theorem that the exterior field of a spherical body does not depend on its condensation or expansion; or, otherwise stated, that spherical pulsations do not induce gravitational waves.

Spherical symmetry is characterised by an interval

$$ds^2 = g_{11}dx_1^2 + g_{22}(d\theta^2 + \sin^2\theta d\phi^2) + 2g_{14}dx_1dx_4 + g_{44}dx_4^2$$

where $g_{11}$, $g_{22}$, $g_{14}$, and $g_{44}$ are functions of $x_1$ and $x_4$ only. This expression is invariant for the group of transformations which keeps $d\theta^2 + \sin^2\theta d\phi^2$ invariant and which represents the rotations of a sphere on itself.

We introduce standard co-ordinates $r$, T; first $r$ in place of $x_1$ by

$$r^2 = -g_{22},$$

* G. D. Birkhoff, *Relativity and Modern Physics*, p. 253 (1923).

and then with the new $g$—*i.e.* the $g$ after this first transformation has been performed

$$\epsilon dT = g_{14}dr + g_{44}dx_4,$$

where $1/\epsilon$ is an integrand factor of the expression on the right-hand side. Then we obtain expressions of the form

$$ds^2 = -e^{\lambda}dr^2 - r^2(d\theta^2 + \sin^2\theta d\phi^2) + e^{\nu}dT^2 \quad . \quad . \quad (1)$$

where $\lambda$ and $\nu$ are functions of $r$ and T.

For instance, if R is a function of $t$ and

$$ds^2 = -R^2(d\chi^2 + \sin^2\chi d\theta^2 + \sin^2\chi\sin^2\theta d\phi^2) + dt^2,$$

we write

$$r = R\sin\chi,$$

giving

$$ds^2 = -r^2(d\theta^2 + \sin^2\theta d\phi^2) - \frac{1}{R^2\cos^2\chi}(dr - R'\sin\chi dt)^2 + dt^2,$$

and by

$$T = \frac{1}{\cos\chi}e^{\int\frac{dt}{RR'}}$$

we obtain

$$ds^2 = -r^2(d\theta^2 + \sin^2\theta d\phi^2) + \frac{-dr^2 + R^2R'^2\cos^2\chi}{\cos^2\chi - R'^2\sin^2\chi}dT^2$$

where R and $\chi$ must be replaced by their expressions in terms of $r$ and T. Except in special cases as for the de Sitter universe, elimination of R and $\chi$ cannot be performed explicitly. Note that the transformation is only admissible when $\tan\chi < R'$. For $\tan\chi = R'$, we have apparent singularities as is well known in the de Sitter universe at the so-called "horizon" of the centre. Our process is thus to come back to such non-homogeneous co-ordinates as the original co-ordinates used by de Sitter.

Writing

$$p = -T_1^1, \qquad \tau = -T_2^2 = -T_3^3, \qquad \rho = T_4^4, \qquad q = T_{14}$$

the computation of the energy tensor for interval (1) gives

$$-\lambda + \kappa p = e^{-\lambda}\nu_1/r + (e^{-\lambda} - 1)/r^2 \quad . \quad . \quad . \quad . \quad (2)$$

$$\lambda + \kappa\rho = e^{-\lambda}\lambda_1/r - (e^{-\lambda} - 1)/r^2 \quad . \quad . \quad . \quad . \quad (3)$$

$$\kappa q = \lambda_4/r \quad . \quad . \quad . \quad . \quad . \quad . \quad . \quad (4)$$

$$-\lambda + \kappa\tau = e^{-\lambda}[\tfrac{1}{2}\nu_{11} - \tfrac{1}{4}\lambda_1\nu_1 + \tfrac{1}{4}\nu_1\nu_1 - (\lambda_1 - \nu_1)/2r] - e^{-\nu}[\tfrac{1}{2}\lambda_{44} - \tfrac{1}{4}\lambda_4\nu_4 + \tfrac{1}{4}\lambda_4\lambda_4] \quad . \quad . \quad . \quad (5)$$

The $\lambda$ on the left-hand side is the cosmological constant and not the function $\lambda$. Indices 1 and 4 mean partial derivatives with respect to $r$ and T.

These equations are very convenient for studying the transition between static solutions. If we allow parameters in these solutions to vary with time, the energy tensor has the same value as that computed with parameters constant, with the addition of the impulse term

$q$ and the second line in the expression of $\tau$. These two additional terms form a transversal elastic wave making the transfer of energy supposed by the variation of the parameters. When the function $\lambda$ does not vary, this additional wave vanishes. For instance, in Schwarzschild's interior solution

$$ds^2 = -R^2(d\chi^2 + \sin^2\chi d\theta^2 + \sin^2\chi \sin^2\theta d\phi^2) + (A - B\cos\chi)^2 dt^2$$

we can let A and B vary with time, the value of $p = \tau$ remains the same as for A and B constant. Note that Einstein and de Sitter universes are special cases of Schwarzschild's interior solution (B = 0, A = 0), but with different values of the cosmological constant.

For a vacuum, we have $\rho = 0$, thus from (3)

$$e^{-\lambda} = 1 - \frac{2m}{r} - \frac{\lambda r^2}{3},$$

where $m$ may be a function of T. But $q$ vanishes and therefore, from (4), $m$ is simply a constant.

Again, by (2) and (3)

$$\kappa(p + \rho) = \frac{e^{-\lambda}}{r}(\lambda_1 + \nu_1);$$

thus

$$\frac{\partial\lambda}{\partial r} + \frac{\partial\nu}{\partial r} = 0$$

and

$$\nu = -\lambda + f(T);$$

the function $f(T)$ may be absorbed in $dT$ by using $\int e^{\frac{1}{2}f(T)}dT$ as a new time. Therefore

$$ds^2 = \frac{-dr^2}{1 - \frac{2m}{r} - \frac{\lambda r^2}{3}} - r^2(d\theta^2 + \sin^2\theta d\phi^2) + \left(1 - \frac{2m}{r} - \frac{\lambda r^2}{3}\right)dT^2 \quad . \quad (6)$$

is the solution in vacuum even when the field is not supposed static. This is Birkhoff's theorem.

The second derivative $\lambda_{11} \equiv \frac{\partial^2\lambda}{\partial r^2}$ does not appear in the equations. We can therefore accept discontinuities of $\lambda_1$ and we obtain

$$e^{-\lambda} = 1 - \frac{2m}{r} - \frac{\lambda r^2}{3} - \frac{\kappa}{r}\int \rho r^2 dr \quad . \quad . \quad . \quad (7)$$

where there is no inconvenience in supposing that $\rho$ has points of discontinuity. Therefore the Schwarzschild interior and exterior field may be dealt with as a unique problem with a discontinuity of $\rho$ at the boundary of the fluid sphere.

On the other hand, $\nu_{11} \equiv \frac{\partial^2\nu}{\partial r^2}$ appears in the equations so that $\nu_1$ and $p$ must be continuous. This is the mathematical justification of the physically evident condition $p = 0$ at the boundary of the material

sphere. Otherwise, it would be necessary to suppose infinite values of $\tau$ at the boundary, which would be equivalent to supposing a rigid shell, a kind of vessel enclosing the fluid.

Therefore discontinuities of $\rho$ in infinitely small regions do not modify the field, but discontinuities of $p$ cannot be admitted. Also discontinuities of $\tau$ are of no consequence.

When $p + \rho = 0$ and $q = 0$, we have an immediate extension of Birkhoff's theorem, the field being defined by

$$e^{-\lambda} = e^{\nu} = 1 - \frac{2m}{r} - \frac{\lambda r^2}{3} + \frac{\kappa}{r}\int pr^2 dr; \quad . \quad . \quad (8)$$

but, when $p$ does vary with time, $m$ is a function of T such that $\lambda_4$ remains equal to zero.

Note that, for a fluid $p = \tau$, $p + \rho = 0$, $q = 0$ can be put in tensorial form as

$$T_{\mu}^{\nu} = -g_{\mu}^{\nu} p \quad . \quad . \quad . \quad . \quad (9)$$

where $p$ is an invariant.

### 3. *Expansion of the Universe deduced from the Motion of a Material Particle at the Neutral Zone between the Condensations.*

In order to study the motion of the neutral zone between a particular condensation and the rest of the universe we can consider a material particle placed at this neutral zone. It is clear that a material particle can stand by itself at the neutral zone and that therefore its motion is a geodesic. It is necessary to make definite assumptions as to the value of the material tensor in the neighbourhood of the particle. We have seen that discontinuities of $\rho$ and $\tau$ can be admitted in an infinitely small volume without modification of the field; we can therefore choose in the neighbourhood of the particle an energy tensor according to relation (9).

With this assumption, the calculation is extremely simple. Readers who would find this assumption too artificial, as it involves negative values of $\rho$, will find in the next section a solution of the problem, directly admissible from the physical point of view.

As $\lambda$ and $\nu$ do not depend on T in the neighbourhood of the particle, the equations of a geodesic are the same as for a statical field, and we have

$$\frac{dT}{ds} = ce^{\lambda},$$

where $c$ is a constant of integration. $e^{\lambda}$ is given by (8), and using this value in (1), we have for a radial geodesic

$$\left(\frac{dr}{ds}\right)^2 = -e^{-\lambda} + c^2,$$

or

$$\left(\frac{dr}{ds}\right)^2 = -1 + c^2 + \frac{\lambda}{3}r^2 + \frac{2m}{r} - \frac{\kappa}{r}\int pr^2 dr \quad . \quad . \quad (10)$$

For $p = 0$, $m$ does not vary with time, and writing

$$r = \sqrt{1 - c^2}\mathrm{R} \quad . \quad . \quad . \quad . \quad (11)$$

$$2m = a\left(\frac{r}{\mathrm{R}}\right)^3,$$

we have

$$\left(\frac{d\mathrm{R}}{ds}\right)^2 = -1 + \frac{\lambda}{3}\mathrm{R}^2 + \frac{a}{\mathrm{R}} \quad . \quad . \quad . \quad (12)$$

which is, for $ds = dt$, the equation of a constant mass universe of vanishing pressure.

When $p$ depends on T, $m$ is a function of T, but $\lambda$ depends only on $r$. We have therefore by derivation and suppression of the factor $dr/ds$

$$2\frac{d^2r}{ds^2} = \frac{2\lambda r}{3} - \frac{2m}{r^2} + \frac{\kappa}{r^2}\int pr^2 dr - \frac{\kappa}{r}pr^2,$$

and by elimination of $m$ and the integral

$$2r\frac{d^2r}{ds^2} + \left(\frac{dr}{ds}\right)^2 = -1 + c^2 + \lambda r^2 - \kappa p r^2 \quad . \quad . \quad (13)$$

or from (11),

$$\frac{2}{\mathrm{R}}\frac{d^2\mathrm{R}}{ds^2} + \frac{1}{\mathrm{R}^2}\left(\frac{d\mathrm{R}}{ds}\right)^2 + \frac{1}{\mathrm{R}^2} = \lambda - \kappa p \quad . \quad . \quad (14)$$

which is the correct expression of $p$ in a homogeneous universe of variable radius.

This result is completely independent of the degree or the variation of the condensations; it depends only on the radial pressure $p$ at the neutral zone.

### 4. *Expansion of the Universe deduced from the Motion of a Material Shell at the Neutral Zone.*

The foregoing investigation, although mathematically correct, may be thought rather artificial. I shall therefore investigate the motion of the neutral zone by supposing that it is materialised by a thin spherical shell of negligible mass and no interior stress. This shell separates altogether the matter inside the condensation from the matter outside. Matter crossing the shell from outside or from inside is forced to rebound on its boundary.

In order to put the problem in mathematical form, we have to find tensorial expressions of the properties of the shell. We define the motion of the shell, by a four-vector $u^\mu$ of unit length

$$g_{\mu\nu}u^\mu u^\nu = 1 \quad . \quad . \quad . \quad . \quad (15)$$

and the normal to the shell (in four dimensions) by a co-variant $\alpha^\mu$ such that

$$\alpha_\mu u^\mu = 0, \qquad g^{\mu\nu}\alpha_\mu\alpha_\nu = 1 \quad . \quad . \quad (16)$$

Using a local Galilean system of co-ordinates, we have for a particular point of the shell $\alpha_1 = 1$, $u^4 = 1$, the other components vanishing. Then we easily find expressions of the properties of the shell at this point and for this particular system of co-ordinates, and we transpose them in tensorial form by introducing $\alpha_1$ and $u^\mu$.

The shell is opaque, thus in the local system $T_4^1 = 0$ and in tensorial form

$$T_{\mu\nu}\alpha_\nu u^\mu = 0 \quad . \quad . \quad . \quad . \quad (17)$$

It is at rest in the local system, $\frac{d^2x_1}{ds^2} = 0$ or $\frac{du^1}{ds} = 0$, therefore in tensorial form

$$\alpha_\sigma\left[\frac{du^\sigma}{ds} + \Gamma_{\mu\nu}{}^\sigma u^\mu u^\nu\right] = 0 \; . \quad . \quad . \quad . \quad (18)$$

The normal pressure P is the same on both faces in the local system, and has in tensorial form the value

$$P = T^{\mu\nu}\alpha_\mu\alpha_\nu \quad . \quad . \quad . \quad . \quad (19)$$

The problem is first to eliminate $\alpha_\mu$, then to replace the Christoffel symbols and the material tensor by their expressions in terms of $\lambda$ and $\nu$, finally to eliminate $\lambda$ and $\nu$.

In spherical co-ordinates, we have

$$u^1 = \frac{dr}{ds} = u, \qquad u^4 = \frac{dT}{ds} = v \quad . \quad . \quad (20)$$

the other component vanishing as the movement is clearly radial. Then (16) gives

$$\frac{\alpha_1}{v} = \frac{\alpha_4}{-u} = e^{\frac{\lambda+\nu}{2}}, \qquad \alpha_2 = \alpha_3 = 0 \quad . \quad . \quad (21)$$

The equilibrium equation (18) becomes

$$v\left[2\frac{du}{ds} + \lambda_1 u^2 + e^{\nu-\lambda}\nu_1 v^2 + 2\lambda_4 uv\right] = u\left[2\frac{dv}{ds} + \nu_4 v^2 + e^{\lambda-\nu}\lambda_4 u^2 + 2\nu_1 uv\right] \quad (22)$$

and (15)

$$-e^\lambda u^2 + e^\nu v^2 = 1 \quad . \quad . \quad . \quad . \quad (23)$$

Differentiating (23) and eliminating $dv/ds$ with (22), we find

$$2\frac{du}{ds} + \lambda_1 u^2 + 2\lambda_4 uv + e^{\nu-\lambda}\nu_1 v^2 = 0 \quad . \quad . \quad (24)$$

The opacity equation (17) is

$$(p + \rho)uv + T_{14}[e^{-\nu}u^2 + e^{-\lambda}v^2] = 0,$$

or from the values (2), (3), (4) of the material tensor

$$e^{-\lambda}(\lambda_1 + \nu_1)uv + \lambda_4 e^{-\lambda-\nu}[1 + 2e^\lambda u^2] = 0.$$

Elimination of $\nu$ with (24) gives

$$2u\frac{du}{ds} + e^{-\lambda}(\lambda_1 u + \lambda_4 v) = 0.$$

Now

$$\lambda_1 u + \lambda_4 v = \frac{\partial\lambda}{\partial r}\frac{dr}{ds} + \frac{\partial\lambda}{\partial \mathrm{T}}\frac{d\mathrm{T}}{ds} = \frac{d\lambda}{ds};$$

therefore, $c$ being a constant of integration,

$$e^{-\lambda} = c - u^2 \quad . \quad . \quad . \quad . \quad (25)$$

The expression of the proper pressure P is, from (19),

$$\mathrm{P} = p + e^{\lambda}(p + \rho)u^2 + 2\mathrm{T}_{14}uv,$$

or

$$k\mathrm{P} - \lambda = \frac{e^{-\lambda} - 1}{r^2} + e^{-\lambda}\frac{\nu_1}{r} + \frac{\lambda_1 + \nu_1}{r}u^2 + \frac{2\lambda_4}{r}uv \quad . \quad (26)$$

Eliminating $\nu$ from (24) and $\lambda$ from (25) we have

$$k\mathrm{P} - \lambda = \frac{c - 1 - u^2}{r^2} - \frac{2}{r}\frac{du}{ds},$$

or writing

$$r = \sqrt{1 - c}\mathrm{R}$$

we have finally

$$\frac{2}{\mathrm{R}}\frac{d^2\mathrm{R}}{ds^2} + \frac{1}{\mathrm{R}^2}\left(\frac{d\mathrm{R}}{ds}\right)^2 + \frac{1}{\mathrm{R}^2} = \lambda - \kappa\mathrm{P} \quad . \quad . \quad (27)$$

which is equation (14) written with P in place of $p$.

It is clear that the expansion of the neutral zone depends only on P and not on any process of condensation which is altogether eliminated from the final result.

This method provides a very intuitional way of considering the equations of the universe, as the radius R of the universe is proportional to the radius of the neutral zone surrounding a condensation.

### 5. *Homogeneous Universe with Variable Mass.*

In the foregoing sections we have seen that a universe with condensations depends on equations essentially the same as those of a homogeneous universe, the only modification being that the density of energy $\rho$ and the density of matter $\delta$ have no more direct interpretation, although $p$ refers to a normal direction at the neutral zone between condensations. With this interpretation, we can deal with the universe as if it was strictly homogeneous.

For comparison with observation, it is convenient, following de Sitter, to measure the cosmical receding velocity by the de Sitter radius $\mathrm{R_S}$ according to

$$\frac{\mathrm{R}'}{\mathrm{R}} = \frac{v}{rc} = \frac{1}{\mathrm{R_S}} \quad . \quad . \quad . \quad . \quad (28)$$

and the proper density $\delta$ by the Einstein radius $R_E$, by

$$\kappa\delta = \frac{2}{R_E^2} \quad . \quad . \quad . \quad . \quad (29)$$

Using as a unit of distance $A = 10^{24}$ cm. $\simeq 10^6$ light years we have $R_S = 2000$ A and $R_E = 2000$ to 80,000 A.

We shall also represent the cosmological constant by a radius $R_C$, the cosmological radius, defined by

$$\lambda = \frac{3}{R_C^2} \quad . \quad . \quad . \quad . \quad (30)$$

The equation of the field in a homogeneous universe of variable radius may be put in a form very convenient for discussion by writing

$$x = \frac{R^2}{R_C^2}, \qquad \tau = \frac{t}{R_C}, \qquad y = \frac{\kappa\delta R^2}{3} = \frac{\kappa}{3\pi^2}\frac{M}{R} = \frac{2}{3}\frac{R^2}{R_E^2} \quad (31)$$

We find easily

$$\frac{d^2x}{d\tau^2} - 4x = 4y - 2 \quad . \quad . \quad . \quad . \quad (32)$$

and $p$ may be computed by

$$4\kappa p R^2 = \left(\frac{dx}{d\tau}\right)^2 - (2x-1)^2 + 1 - 4y \quad . \quad . \quad (33)$$

Let us consider first the particular case where $y = 0$—*i.e.* a universe empty of matter, but which may be full of radiation. We find

$$x = \tfrac{1}{2} + c_1 e^{2\tau} + c_2 e^{-2\tau},$$

which gives, for $c_1 = c_2 = \frac{1}{4}$ (de Sitter universe),

$$x = \cosh^2 \tau.*$$

In general we have

$$x = \tfrac{1}{2} + e^{2\tau}\left(c_1 + \int_0^\tau e^{-2\tau} y\, d\tau\right) + e^{-2\tau}\left(c_2 - \int_0^\tau e^{2\tau} y\, d\tau\right) \quad . \quad (34)$$

The equilibrium solution is found for $y$ to equal a constant $y_0$.

$$x = \tfrac{1}{2} - y_0.$$

If $y$ constant for $\tau < 0$ begins to vary from $\tau = 0$ we have

$$x = \tfrac{1}{2} - y_0 + e^{2\tau}\int_0^\tau e^{-2\tau}(y - y_0)d\tau - e^{-2\tau}\int_0^\tau e^{2\tau}(y - y_0)d\tau \quad . \quad (35)$$

or for $\tau$ small

$$x = \tfrac{1}{2} - y_0 + \tfrac{1}{2}y_0'(\sinh 2\tau - 2\tau) + \tfrac{1}{4}y_0''\left(\cosh 2\tau - 1 - \frac{(2\tau)^2}{2!}\right) + \ldots$$
$$+ \frac{1}{2^{2k-1}} y_0^{(2k-1)}\left(\sinh 2\tau - 2\tau - \ldots - \frac{(2\tau)^{2k-1}}{(2k-1)!}\right)$$
$$+ \frac{1}{2^{2k}} y_0^{2k}\left(\cosh 2\tau - 1 - \ldots - \frac{(2\tau)^{2k}}{(2k)!}\right) + \ldots . \quad (36)$$

* Prof. de Sitter found also the case $c_2 = 0$, *P.N.A.S.*, **16**, 485, 1930.

Therefore, if the Taylor development of $y$ begins by

$$y = y_0 + \frac{1}{k!} y_0^{(k)} \tau^k + \ldots,$$

we have for $x \sim R^2$

$$x = x_0 + \frac{4 y_0^{(k)}}{(k+2)!} \tau^{k+2} + \ldots,$$

and for $y\sqrt{x} \sim M$

$$y\sqrt{x} = y_0\sqrt{x_0} + \frac{1}{k!}\sqrt{x_0} y_0^{(k)} \tau^k + \ldots$$

If, in a universe in equilibrium, the proper mass begins to vary, the radius of the universe varies in the same sense.

From (33) we can also say: If, in a universe in equilibrium, the pressure begins to vary, the radius of the universe varies in the opposite sense.

Therefore stagnation processes induce expansion.

The above formulæ provide a method for studying in detail the expansion of the universe for any given law of $y$.

In the next section we shall work out the special case where the diminution of pressure responsible for the expansion arises suddenly.

### 6. *Expansion induced by a Sudden Stagnation.*

For the equilibrium before the stagnation arose, we have by (31), (32), (33),

$$\frac{6p_0}{\delta_0} = \frac{3x - 1}{1 - 2x} \quad . \quad . \quad . \quad . \quad (37)$$

with

$$x = \frac{R_1^2}{R_C^2} \quad . \quad . \quad . \quad . \quad . \quad (38)$$

$R_1$ is the equilibrium radius, $R_C$ the cosmological radius. For $x = \frac{1}{3}$ the pressure vanishes; for $x = \frac{1}{2}$ the density vanishes.

Let us suppose that for $t = 0$, the pressure $p_0$ suddenly drops to zero. From $t = 0$ the solution is a zero pressure, and thus a constant mass solution, from (12) and (30)

$$t = R_C \int_{R_1}^{R} dR \sqrt{\frac{R}{R^3 - R_C^2 R + \frac{\alpha}{3} R_C^2}} \quad . \quad . \quad (39)$$

where the constant $\alpha$ is related to the actual radius R of the universe by

$$\alpha = \kappa\delta R^3 = \frac{2R^2}{R_E^2};$$

for $t = 0$, $R = R_1$, $R' = 0$, and therefore $R_1$ is a root of the cubic

$$R_1^3 - R_C^2 R_1 + \frac{2}{3}\frac{R_C^2}{R_E^2} R^3 = 0,$$

and we have
$$\frac{R^3}{R_C R_E^2} = \frac{3}{2}(1-x)\sqrt{x} = \gamma^3 \quad . \quad . \quad . \quad (40)$$

for $x = \frac{1}{3}$, $\gamma^3$ has a maximum $\frac{1}{\sqrt{3}} = 0{\cdot}58$ and drops to $\frac{3}{4\sqrt{2}} = 0{\cdot}53$ for the extreme case $x = \frac{1}{2}$.

The value of the cosmological radius $R_C$ may be computed by
$$u = \left(\frac{R_E}{R_C}\right)^{\frac{2}{3}} \quad . \quad . \quad . \quad . \quad (41)$$

and
$$u^3 - \frac{1}{\gamma^2}u + \frac{2}{3} - \left(\frac{R_E}{R_S}\right)^2 = 0 \quad . \quad . \quad . \quad (42)$$

Some values are given in the following table (for $x = \frac{1}{3}$) :—

| $u$. | 1. | 2. | 3. | 4. | $\infty$. |
|---|---|---|---|---|---|
| $R_E/R_S$ | 0·47 | 2·41 | 4·83 | 7·67 | $\infty$ |
| $R_c/R_S$ | 0·47 | 0·85 | 0·93 | 0·96 | 1 |

It remains to compute $t$ by (39). This can be written
$$t = R_C \int_{R_1}^{R} \frac{dR}{\sqrt{(R-R_1)(R-R_2)}} \sqrt{\frac{R}{R+R_1+R_2}} \quad . \quad (43)$$

or writing
$$R = \frac{R_1 - R_2}{2}\cosh\phi + \frac{R_1 + R_2}{2}$$

we find
$$t = R_C \int_0^{\phi} d\phi \sqrt{\frac{R}{R+R_1+R_2}};$$

thus
$$\phi = \frac{\theta t}{R_C}$$

where $\theta$ is a function of $\phi$, the value of which lies between $\sqrt{3}$ and 1 (because $R > R_1 > R_2$).

The value of $R_2$ is easily computed in term of $R_C$ and $x$, we find
$$\frac{4R}{R_C} = [3\sqrt{x} - \sqrt{4-3x}]\cosh\frac{\theta t}{R_C} + \sqrt{x} + \sqrt{4-3x} \quad . \quad (44)$$

or for $x \sim \frac{1}{3}$ using (37) ; the approximative formula for $p_0$ small
$$\frac{4R}{R_C} = \frac{2}{3}\frac{p_0}{\delta_0}\cosh\frac{\theta t}{R_C} + 1 + \frac{1}{\sqrt{3}} \quad . \quad . \quad . \quad (45)$$

or for $t$ large
$$t = \frac{R_C}{\theta} \times 2{\cdot}303 \log_{10}\left[3\frac{\delta_0}{p_0}\left(4\frac{R}{R_C} - 1 - \frac{1}{\sqrt{3}}\right)\right] \quad . \quad . \quad (46)$$

The expression under the logarithmic sign is always positive as the minimum of $\frac{4R}{R_C}$ is $\frac{4}{\sqrt{3}}$.

The values of $R_C$ and R are practically independent of the importance of the initial stagnation. It is very curious to see how its influence on $t$ is slow. Computing $t$ for $\theta = 1$ and $R/R_C = 20$, we find

for $p_0/\delta_0 = \infty$, $t = 5R_C \cong 10^{10}$ years,
$p_0/\delta_0 = 10^{-8}$, $t = 24R_C \cong 5 \times 10^{10}$ years,
$p_0/\delta_0 = 10^{-14}$, $t = 38R_C \cong 7{\cdot}5 \times 10^{10}$ years.

The first case means that all the energy was in the form of electromagnetic radiation and suddenly condensed in matter; the second case supposes a radial free energy of 30 km./sec. suddenly bounded in condensations; the third case that one millionth of the mass was moving freely with this velocity and was captured by the rest of the matter.

Nevertheless, if $p_0$ tends to zero, $t$ tends to infinity, the limiting case being the solution emphasised in our 1927 paper. As was pointed out by Eddington, such logarithmic infinities have no real physical significance.

*Louvain, le 7 mars* 1931.

---

## *Some Further Remarks on the Rotation of the Stars.*

By E. A. Kreiken.

1. In a recent note * evidence was given that there exists a close correlation between the diameter of a star and its period of axial rotation. From the stars in Elvey's list † the following relation was obtained: ‡

$$\log P = 1{\cdot}49, \log D - 1{\cdot}25 \quad . \quad . \quad . \quad (1)$$

where P represents the period of axial rotation and D the hypothetical diameter of a star at the distance $\pi = 0''{\cdot}100$. The values of log P as derived from (1) still require a constant correction, which is due to the fact that only a fraction of the rotational velocity is observed. In the following we shall see how the numerical value of this constant may be determined. In the paper just mentioned we tentatively derived from (1) the values of log P for some spectroscopic binaries, some Cepheid variables, and some long-period M-type variables. The periods thus obtained were compared with the periods of revolution and the periods of light variation. The result was that with the spectroscopic binaries a strong correlation between the periods of axial rotation and of revolution was found. With the Cepheid and

* E. A. Kreiken, *M.N.*, **91**, 251 (1930 December).

† Elvey, *Astr. Journ.*, **71**, 221, 1930.

‡ A. Pannekoek drew my attention to the fact that the coefficient of log D is almost exactly what would be expected from Kepler's third law. This question will be considered in a future paper.

long-period variables the periods of light variation apparently were considerably shorter than the periods of rotation. As the numbers of stars were rather small, no very definite conclusions could be drawn; therefore these same problems are considered in this paper, but more extensive material has been used. Moreover, some additional groups of stars are considered.

2. *Numerical Amount of the Correction to be Applied to Formula* (1). —To the values of log P as derived from (1) a constant correction should be applied. Evidently the mean values of the rotational velocity as derived from the observed quantities will be too small. This is due to the fact that for each star only a part of the rotational velocity is observed, *i.e.* its component in the line of sight. For the present we may safely assume that the distribution of the poles of the axial rotation is a haphazard one. We now consider a group of stars for which the velocity of axial rotation in the outer layers is V. For a certain star let $\delta$ denote the angle between the line of sight and the axis of rotation. Then the observed velocity of rotation will be equal to $V_0 = V \sin \delta$.

It is evident that the frequency of the values $\delta$ will be proportional to $\sin \delta$. Consequently the mean observed value of the rotational velocity is

$$\frac{\int_0^{\pi/2} V \sin^2 \delta \, . \, d\delta}{\int_0^{\pi/2} \sin \delta \, . \, d\delta} \quad \text{or} \quad V\frac{\pi}{4}.$$

Therefore the correction to be applied to (1) is equal to $-0{\cdot}11$. In reality I applied a slightly larger correction, viz. $-0{\cdot}20$, because for very large values of $\delta$ the velocity of axial rotation may altogether escape observation. From the previous considerations we conclude that if the individual values of the periods are represented by

$$\log P = 1{\cdot}49, \log D - 1{\cdot}45 \quad . \quad . \quad . \quad (2)$$

large deviations will occur which are principally due to the scattering of the values $\delta$.

If this were the only cause of the spread of the observed quantities the frequency of the different deviations from (2) would be proportional to $\sin \delta$. An additional spread of the observed periods will, however, be caused by the probable error in the determination of the diameters, the probable error in the determination of the rotational velocities and by the actual spread of the individual periods of the stars with one and the same diameter. Owing to the large spread caused by the scattering of the values $\delta$, and owing to the small numbers of stars, we are not able to separate the different effects. In Table I. the observed distribution of the values $(\log P)_o - (\log P)_c$ is compared with the one derived from a haphazard spread of the values $\delta$ only. From this table it appears that the influence of probable error is by no means negligible.

Table I.

| $(\log P)_o-(\log P)_c$ | 0·0 | 0·2 | 0·4 | 0·6 | 0·8 |
|---|---|---|---|---|---|
| Obs. freq. | 39·6 | 18·7 | 14·6 | 27·1 | |
| Comp. freq. | 56 | 17 | 10 | 17 | |

3. *The Spectroscopic Binaries.*—In the first place I have compared the periods of revolution of the different spectroscopic binaries with the periods of axial rotation obtained from (2). I have not enumerated the different systems used here. It may be sufficient to state that all spectroscopic systems were used which are contained in Beer's general catalogue,* and for which the absolute magnitudes are given there. The hypothetical diameters (reduced to a distance $\pi = 0''{\cdot}100$) are computed from Hertzsprung's formula †

$$5 \log \sin \rho = -43{\cdot}44 + 2{\cdot}3\left(\frac{c_2}{T}\right)^{\cdot 93} - M_{vis} \quad . \quad . \quad . \quad (3)$$

where $\rho$ is the hypothetical semi-diameter. The quantities $\frac{c_2}{T}$ were obtained from the mean colour indices of the stars of different spectral types and absolute magnitudes given in *M.N.*, **91,** 242 (1930 December). As the values given there are based on the colour system introduced by Öpik,‡ the quantities $\frac{c_2}{T}$ are readily obtained if the relation between Öpik's colour system and the system $\frac{c_2}{T}$ of Hertzsprung (Wilsing) is known. From the stars common to Hertzsprung's and Öpik's catalogues the relation partly given in Table II. was derived. The values $\frac{c_2}{T}$ and C.I. of Table II. were plotted against each other, and through the points obtained in this way a smooth curve was drawn. The values $\frac{c_2}{T}$ used in (3) were read from this curve. With the reduced diameters the period of axial rotation is found from (2). When considering the results, binary systems with different values of the eccentricities were separately treated. The following groups were considered: binary systems with (*a*) $e \leqslant 0{\cdot}05$; (*b*) $0{\cdot}05 < e \leqslant 0{\cdot}15$; (*c*) $0{\cdot}15 < e \leqslant 0{\cdot}30$; (*d*) $0{\cdot}30 < e \leqslant 0{\cdot}60$; and finally (*f*) $e > 0{\cdot}60$. Within each group the stars were again combined into different sets according to the values of their reduced diameters, and within each set the mean value $\overline{\log P}$ (of orbital revolution) was computed. Table III. contains the results. Table III. also gives the period of axial rotation derived from (2), together with the differences O–C. The values of Table III. are graphically represented in fig. 1. In this figure the observed values $\overline{\log P}$ are plotted against the mean value log D. Black dots represent the values obtained from the binaries with $e \leqslant 0{\cdot}05$, while the other groups are represented by open circles ($0{\cdot}05 < e \leqslant 0{\cdot}15$); black squares

* A. Beer, *Veröff Berlin Babelsberg*, Band v., Heft 6, p. 68, 1927.
† E. Hertzsprung, *Annalen Sterrewacht Leiden*, deel. xiv., 1ste stuk, 1924.
‡ E. Öpik, *Publ. Tartu*, **27**, No. 1, 1929.

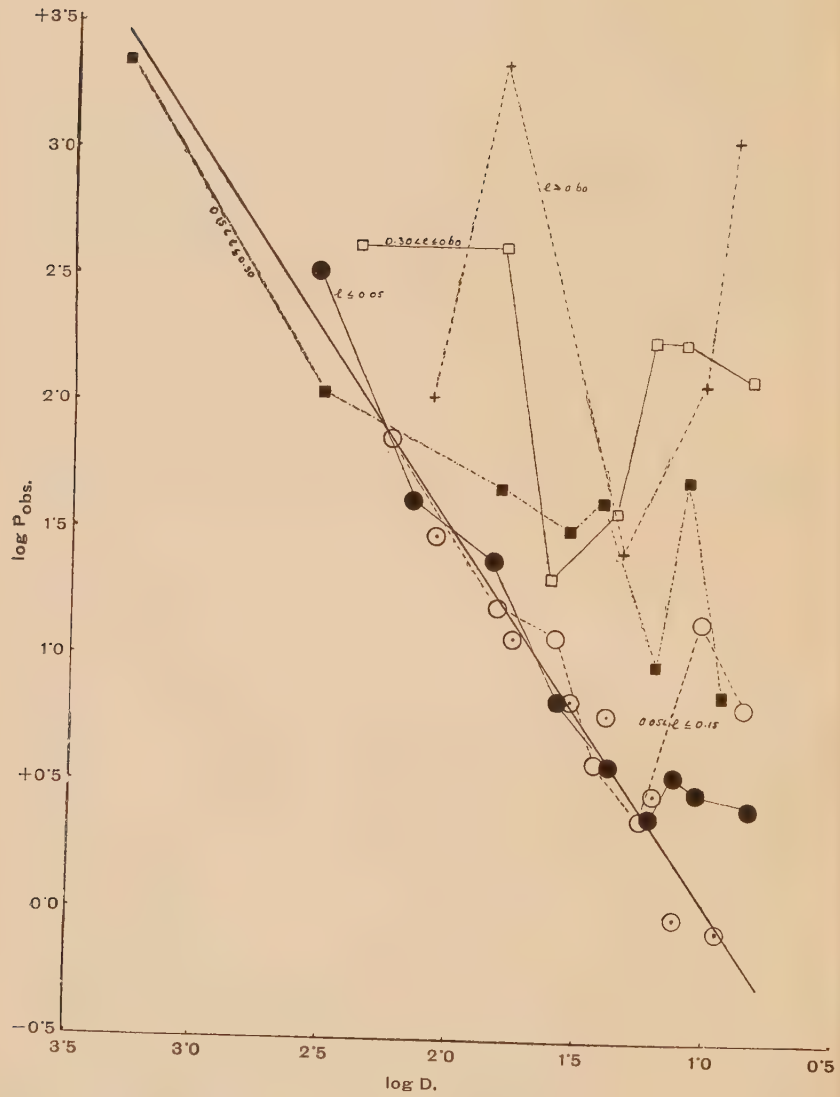


FIG. 1.—The mean periods of revolution of the spectroscopic binaries compared with the mean periods of rotation of the stars. The full drawn line and open circles with dots represent the mean periods of rotation for stars with different values of log D. Black dots represent binary stars with $e \leqslant 0{\cdot}05$; open circles those with $0{\cdot}05 < e \leqslant 0{\cdot}15$; black squares, those with $0{\cdot}15 < e \leqslant 0{\cdot}30$; open squares with $0{\cdot}30 < e \leqslant 0{\cdot}60$, and crosses the binaries for which $e > 0{\cdot}60$.

($0\cdot15 < e \leqslant 0\cdot30$); open squares ($0\cdot30 < e \leqslant 0\cdot60$); and crosses ($e > 0\cdot60$). Formula (2) is indicated by a full drawn line. Open circles with dots represent the mean values of the periods of axial rotation as derived from Elvey's list.*

TABLE II.

| C.I. | −·36 | +·40 | +·45 | +·86 | +1·25 | +1·65 | +1·94 |
|---|---|---|---|---|---|---|---|
| $c_2/T$ | 1·20 | 1·82 | 2·62 | 3·24 | 3·68 | 4·34 | 4·53 |

TABLE III.

*Logarithms of the Periods of Revolution and of the Periods of Rotation for Binary Systems with Different Eccentricities.*

| D. | $\overline{D}$. | log $\overline{D}$. | $\overline{\log P_{obs.}}$ | log $P_{comp.}$ | O–C. | *n.* |
|---|---|---|---|---|---|---|
| | | | $e \leqslant 0\cdot05$. | | | |
| >200 | 343 | 2·54 | 2·52 | 2·73 | − ·21 | 3 |
| 100–200 | 141 | 2·15 | 1·63 | 1·74 | − ·11 | 5 |
| 50–100 | 69 | 1·84 | 1·39 | 1·28 | + ·11 | 8 |
| 30–49 | 38 | 1·58 | 0·83 | 0·89 | − ·06 | 10 |
| 20–29 | 24·4 | 1·39 | 0·58 | 0·61 | − ·03 | 11 |
| 15–19 | 16·1 | 1·21 | 0·38 | 0·35 | + ·03 | 10 |
| 12–14 | 13·15 | 1·12 | 0·55 | 0·21 | + ·34 | 14 |
| 10–11 | 10·75 | 1·03 | 0·48 | 0·08 | + ·40 | 8 |
| <10 | 6·70 | 0·83 | 0·42 | − ·18 | + ·60 | 13 |
| | | | $0\cdot05 < e \leqslant 0\cdot15$. | | | |
| >100 | 175 | 2·24 | 1·86 | 1·88 | − ·02 | 4 |
| 50–100 | 64 | 1·81 | 1·20 | 1·25 | − ·05 | 6 |
| 30–50 | 39 | 1·59 | 1·09 | 0·90 | + ·19 | 1 |
| 20–29 | 26 | 1·41 | 0·58 | 0·65 | − ·07 | 7 |
| 15–19 | 17 | 1·23 | 0·37 | 0·38 | − ·01 | 5 |
| 10–14 | 11 | 1·04 | 1·16 | 0·09 | +1·25 | 7 |
| <10 | 7 | 0·85 | 0·82 | − ·15 | +1·07 | 11 |
| | | | $0\cdot15 < e \leqslant 0\cdot30$. | | | |
| >1000 | 2040 | 3·31 | 3·34 | 3·48 | − ·14 | 2 |
| 100–1000 | 324 | 2·51 | 2·04 | 2·29 | − ·25 | 3 |
| 50–100 | 65 | 1·81 | 1·67 | 1·24 | + ·43 | 5 |
| 30–49 | 35 | 1·54 | 1·50 | 0·84 | + ·66 | 4 |
| 20–29 | 25·5 | 1·41 | 1·61 | 0·65 | + ·96 | 8 |
| 15–19 | 16 | 1·20 | 0·97 | 0·33 | + ·64 | 3 |
| 10–14 | 12 | 1·08 | 1·70 | 0·15 | +1·55 | 7 |
| <10 | 9 | 0·95 | 0·86 | − ·01 | + ·87 | 2 |

* Elvey, *Astr. Journ.*, **71**, 221, 1930.

TABLE III.—*continued.*

| D. | $\overline{D}$. | log $\overline{D}$. | $\overline{\log P_{obs.}}$ | log $P_{comp.}$ | O–C. | *n*. |
|---|---|---|---|---|---|---|
| | | | $0{\cdot}30 < e \leqslant 0{\cdot}60$. | | | |
| >100 | 245 | 2·39 | 2·61 | 2·10 | + ·51 | 6 |
| 50–100 | 66 | 1·82 | 2·62 | 1·25 | +1·37 | 6 |
| 30–49 | 42 | 1·62 | 1·31 | 0·95 | + ·36 | 4 |
| 20–29 | 24 | 1·38 | 1·59 | 0·60 | + ·99 | 3 |
| 15–19 | 17 | 1·23 | 2·25 | 0·38 | +1·87 | 3 |
| 10–14 | 12·5 | 1·10 | 2·24 | 0·18 | +2·06 | 11 |
| <10 | 7 | 0·85 | 2·12 | − ·15 | +2·27 | 7 |
| | | | $e > 0{\cdot}60$. | | | |
| >100 | 122 | 2·09 | 2·04 | 1·65 | + ·39 | 2 |
| 50–100 | 64 | 1·81 | 3·34 | 1·24 | +2·10 | 2 |
| 30–49 | | | | | | |
| 20–29 | 22 | 1·34 | 1·42 | 0·54 | + ·88 | 3 |
| 15–19 | | | | | | |
| 10–15 | 11 | 1·04 | 2·09 | 0·09 | +2·00 | 2 |
| <10 | 8 | 0·90 | 3·04 | − ·08 | +3·12 | 4 |

From Table III. and from the figure it appears that with the binary systems of low eccentricity the correlation between the period of axial rotation and the period of orbital revolution is very marked. Both sets of values are nearly equal. With the larger eccentricities this correlation is less marked, and with those for which $e > 0{\cdot}60$ it completely disappears. It should be remarked that on the whole the correlation is best defined for the large diameters. With the small diameters large deviations already occur with the stars with $e \leqslant 0{\cdot}05$. For the larger eccentricities the deviations from (2) are nearly always positive, this being only another way of stating the well-known fact that the periods of the spectroscopic binaries with large eccentricity are generally longer than those of the systems with small eccentricity. In the different diagrams of fig. 2 the individual values of $(\log P)_o$ are plotted against the corresponding values of log D. The first five of these diagrams contain the stars with different eccentricities. In the last all systems are used. In each of the different diagrams the relation (2) has been indicated by a full drawn line. Nearly all deviations $(\log P)_o - (\log P)_c$ are positive, but there also are some negative values. For the different spectral types the distribution of the values O–C is given in Table IV. From this table we see that large negative excesses occur only with the very early spectral types. With the later types only a few negative excesses occur, whilst very large positive values are very frequent. This is due to the fact that with the dwarfs of later type the relative frequency of systems with large eccentricities

is great. For the occurrence of the large negative excesses the following explanations may be put forward:—

(*a*) They are due to the uncertainties in the determination of the colour. From the figures in *M.N.*, **91**, 242, it appears that for the very early types the relation between colour and spectral type is rather

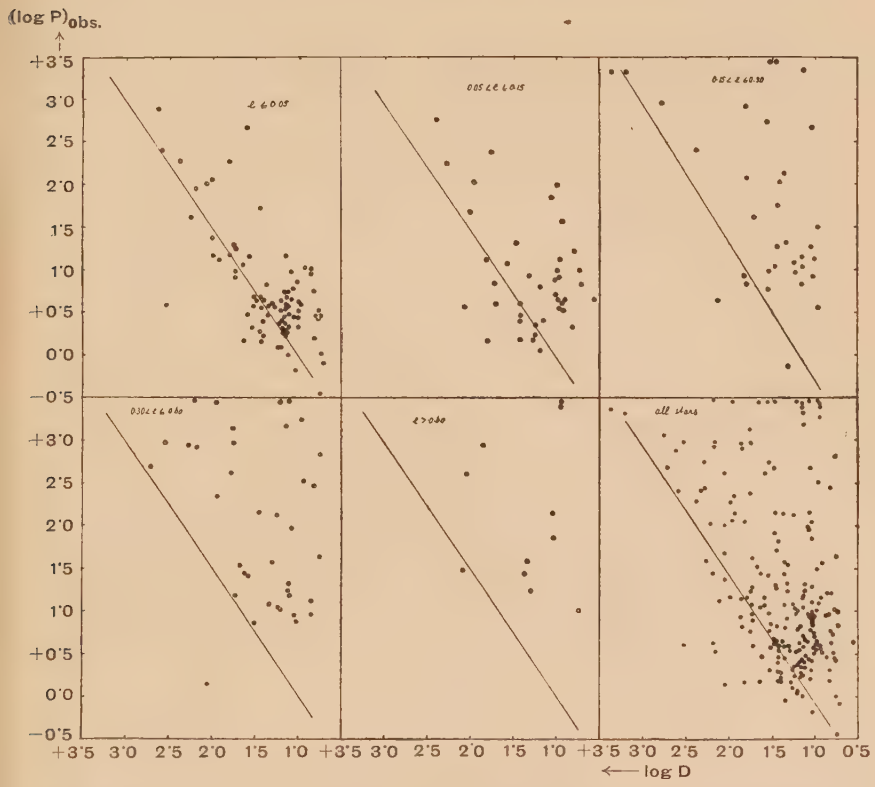


FIG. 2.—The individual values of log $P_{obs.}$ (P = period of revolution) plotted against the values of log D. The diagonal lines indicate the mean relation between the logarithm of the period of rotation and the logarithm of diameter.

uncertain. If the colour given there is too large, the diameter has been overestimated and the points indicating those early stars ought to be shifted to the right. The difference, however, is so large that an error of colour only is no sufficient explanation.

(*b*) The absolute magnitudes are too small. Evidently a larger absolute magnitude corresponds to a smaller diameter. A positive correction applied to the absolute magnitude would therefore imply an additional shift of our points to the right and a further decrease of our values O–C.

(*c*) The period of axial rotation of the stars of one and the same

diameter systematically depends on spectral type, the periods being smallest for the early stars. Owing to the scantiness of the observational data we are not able to control this point. With a view to the distribution of the values O–C in Table IV. the possibility of such an effect cannot be denied.

Table IV.

*Distribution of the Values* $\Delta=(log\ P)_o-(log\ P)_c$.

| Δ / Type. | $<-1\cdot00$. | $-1\cdot00$–$-\cdot50$. | $-\cdot25$. | $\cdot00$. | $+\cdot25$. | $+\cdot50$. | $+1\cdot00$. | $>+1\cdot00$. |
|---|---|---|---|---|---|---|---|---|
| O | 4 | 0 | 3 | 1 | 1 | 0 | 0 | 0 |
| Bo–B5 | 1 | 3 | 9 | 8 | 6 | 2 | 4 | 5 |
| B5–B9 | 0 | 2 | 1 | 4 | 3 | 0 | 5 | 4 |
| Ao–A9 | 0 | 0 | 3 | 3 | 7 | 10 | 11 | 12 |
| Fo–Go | 0 | 0 | 0 | 6 | 5 | 6 | 19 | 24 |
| Go–Ko | 0 | 0 | 1 | 0 | 4 | 2 | 7 | 14 |
| Ko–K8 | 0 | 0 | 0 | 1 | 3 | 2 | 7 | 5 |
| M | 0 | 0 | 0 | 1 | 1 | 2 | 0 | 0 |

(*d*) The relation between log P and log D slightly deviates from a straight curve.

(*e*) Stars with very large negative excesses ought to be classified as Pseudo-Cepheids or $\beta$ Canis-Majoris stars (see later on).

According to my opinion the small negative excesses are fully accounted for by the points mentioned under (*a*), (*b*), (*c*), and (*d*). For the very large negative excesses the explanation under (*e*) must perhaps be used. The systems with very large negative excesses have been enumerated in Table V.

Table V.

*Spectroscopic Systems for which* $\Delta<-0\cdot50$.

| No. Boss. | Type. | $M_{abs.}$ | $(log\ P)_o$. | $(log\ P)_c$. | $\Delta=O-C$. |
|---|---|---|---|---|---|
| 46* | O8 | $-6\cdot3$ | 0·55 | 2·29 | $-1\cdot64$ |
| 5565 | O6 | $-4\cdot0$ | 0·13 | 1·59 | $-1\cdot46$ |
| H.D. 19820* | O6 | $-4\cdot0$ | 0·53 | 1·77 | $-1\cdot24$ |
| 1899 | O7 | $-4\cdot6$ | 0·64 | 1·78 | $-1\cdot14$ |
| 2119 | B2 | $-3\cdot0$ | 0·16 | 1·24 | $-1\cdot08$ |
| 4277 | B3 | $-2\cdot4$ | 0·16 | 0·99 | $-0\cdot83$ |
| 3281 | B5 | $-0\cdot6$ | $-\cdot05$ | 0·58 | $-0\cdot63$ |
| 4776* | B5 | $-4\cdot7$ | 1·11 | 1·72 | $-0\cdot61$ |
| 4388 | B3 | $-1\cdot6$ | 0·31 | 0·83 | $-0\cdot52$ |
| 1349 | B3 | $-\cdot9$ | 0·17 | 0·68 | $-0\cdot51$ |

The stars marked with an asterisk are $\beta$ Lyræ variables.

Summarising, we have that with a few exceptions the periods of revolution are equal to or larger than the period of axial rotation obtained from (2). The positive excesses are small with the spectroscopic systems with small eccentricities. They do increase with increasing eccentricities. These results might have been anticipated. According to Jeans a spectroscopic binary may originate by fission, so that immediately after fission the periods of axial rotation and of revolution will be identical.* Consequently the period of revolution will be equal to the value derived from (2). Further, Jeans † suggests that the spectroscopic binaries as a class started with low values of the eccentricity $e$, which would be raised by interaction with other stars. Considering the effect of secular decrease of mass, Jeans concludes ‡ that as a binary system dissolves into radiation the linear dimensions of the orbit increase and the orbital period increases. So from Jeans's theory the following must be expected. With the younger spectroscopic systems, *i.e.* shortly after fission, the periods of revolution correspond to the periods of axial rotation and the eccentricities are small. With the older systems the eccentricities and the periods increase, and consequently the periods of revolution will be longer than the periods of axial rotation derived from the fundamental equation (2). Considering the different diagrams of figs. 1 and 2 we see that the agreement between theory and observation is very striking.

4. *The Cepheid Variables.*—In the present paper all Cepheids are taken into account for which reliable data as to colour and spectrum are available. All systems used here are included in the tables by A. Beer § and H. Ludendorff.‖ The absolute magnitude of the stars are derived from Shapley's period-luminosity relation. Then the colours and diameters are derived in the same way as for the spectroscopic binaries. For the stars for which the range in colour or in spectral type corresponding to the range in light has been observed, values of log D both at maximum and minimum light are derived. For all others mean values are computed. The results are graphically represented in the diagrams of fig. 3. In the first two of these diagrams the values of log P (period of light variation) are plotted against the maximum and minimum values of the diameter. Two points indicating one and the same star were connected. With the stars indicated by double points in the first diagram the range in spectral type has been observed, for those in the second the range in colour index. Less reliable data are represented by crosses. From the figure we see that with the Cepheids the period of light variation is considerably shorter than the period of axial rotation as derived from (2). This means either that the period of light variation is actually shorter than that of axial rotation, or that for the Cepheids

* *Cf.* G. Shajn and O. Struve, *M.N.*, **89**, 223, 1929.
† Jeans, *Astronomy and Cosmogony*, p. 298.
‡ Jeans, *ibid.*, p. 293. § A. Beer, *loc. cit.*, tables iii. and iv.
‖ H. Ludendorff, *Die Veränderl. Sterne.*, *Handbuch der Astroph.*, Band vi., Teil 2. p. 211.

the period of axial rotation widely deviates from that for the ordinary stars. Personally I think the first to be the case, but this opinion is

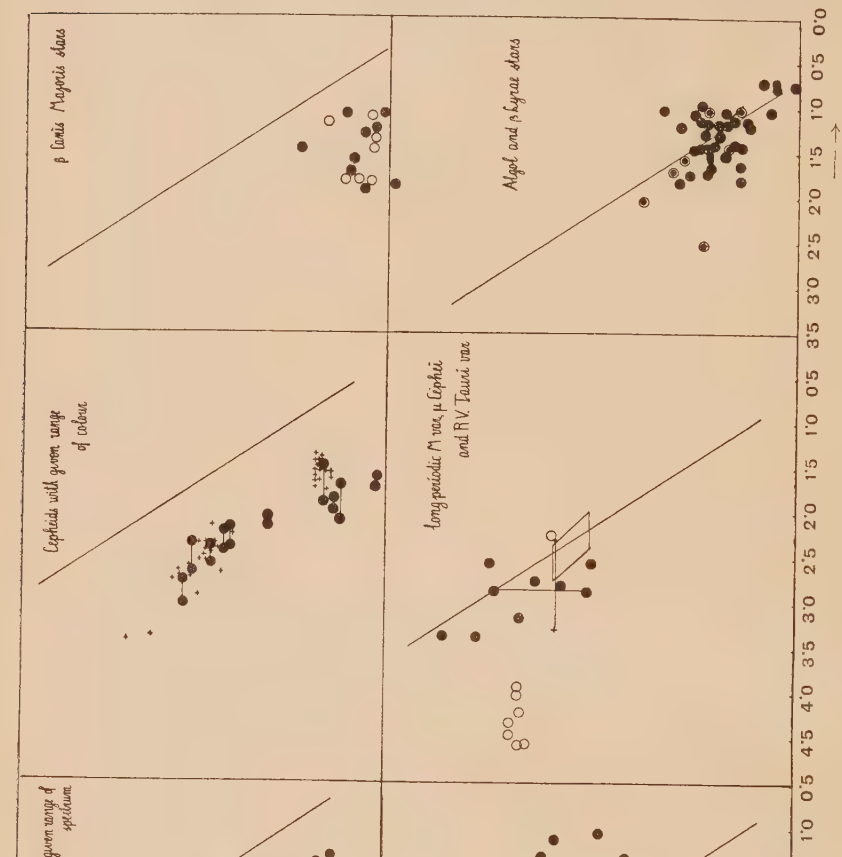


FIG. 3.—The period of light variation or of revolution of different groups of stars plotted against the log of diameter. The full drawn lines indicate in each diagram the fundamental equation (2) of stellar rotation.

entirely based on the fact that this agrees better with Jeans's theory. (It should be remarked that if a Cepheid is considered as a pulsating star the period of axial rotation cannot be quite a constant.) The

relation of the Cepheid variables with the other stars will be considered later on. There is a faint indication that the mean values O–C systematically depend on the period or the diameter, but it is doubtful whether this effect is real or is caused by a systematic error in the determination of the colour, so for the present it has been left out of consideration.

5. *The β Canis-Majoris Stars.*—From different observational data various authors * have concluded that the β Canis-Majoris stars as a class are closely correlated to the Cepheids. The amplitude of the light variation is very small. It was first observed by Guthnick † in β Cephei, where it was found to be $0^m.05$. The period of light variation corresponds to the spectroscopic period. In the present paper all β Canis-Majoris stars are used, which are enumerated in tables vi. and vii. of Beer's work ‡ on spectroscopic double stars. The absolute magnitudes of those stars were obtained from spectroscopic, trigonometric, or mean proper motion parallaxes. The colours corresponding to the different spectral types and absolute magnitudes were obtained in the same way as before. Then from the formulæ (2) and (3), log D and log P were computed. Just as with the Cepheids the differences O–C are always negative. The relation of the β Canis-Majoris stars with the Cepheid variables is very evident from the third diagram in fig. 3, where the values log P are plotted against log D. Black dots indicate the well-determined stars. Less reliable data are indicated by open circles. The distribution of the different dots and circles closely resembles the distribution obtained for the short-period Cepheid variables of RR Lyræ type. Summarising, we conclude from a comparison of their periods of axial rotation that the two groups of stars, the Cepheid variables and the β Canis-Majoris stars, are closely related.

6. *The Pseudo-Cepheids.*—The Cepheids generally are *c* stars with sharp narrow lines. There is a group of spectroscopic binaries, the spectra of which have also the *c* character, but for which so far no light variation has been detected. As the galactic concentration and absolute magnitudes of these stars closely resemble those of the Cepheids, they are generally denoted as Pseudo-Cepheids (Adams). For the Pseudo-Cepheids for which reliable data as to the spectroscopic periods are available, $(\log P)_c$ and log D are obtained in the same way as before. The observed values $(\log P)_o$ were plotted against the values log D. The results appear in the fourth diagram of fig. 3. From the diagram it appears that the name Pseudo-Cepheids is somewhat misleading. The distribution of the black dots indicating Pseudo-Cepheids is quite different from the distribution of dots representing the true Cepheids. On the other hand, the distribution of the Pseudo-Cepheids closely corresponds to the distribution of the ordinary spectroscopic binaries. We therefore conclude that, as a class, the Pseudo-Cepheids are not very distinct. The stars ought to be considered as ordinary spectroscopic doubles.

* See, for instance, Henroteau, *Publ. Dom. Obs.*, **9**, 22, 1924.
† Guthnick, *A.N.*, **196**, 357, 1913, and *A.N.*, **205**, 103, 1917.
‡ A. Beer, *loc. cit.*

7. *The Long-period Variables.*—In view of the heterogeneity of the observational material I first tried roughly to determine the region of the P.D. diagram where the long-period variables are to be expected. I selected from Prager's * catalogue the M-type variables with the shortest and longest periods. The limiting values of log P are 1·80 and 2·86. As a first approximation the diameters of these two variables were taken equal to the mean reduced diameter of all M*a*, M*b*, and M*c* stars, which are contained in Hertzsprung's catalogue and for which the value $m + 5 \log \mu \leqslant -2{\cdot}0$. In this way we find log D = 2·80. The two extreme values of log P were plotted against log D, and the two points obtained in that way were connected. The results appear in diagram 5 of fig. 3. As the two periods used here represent extreme values, the majority of the M variables will be distributed round this line.

We next consider the individual observational data available for the various stars. The following two groups were considered :—

(*a*) The Mira stars and $\mu$ Cephei variables, for which the hypothetical semi-diameters are given in Hertzsprung's catalogue; (*b*) the Mira stars, for which temperatures were determined by S. B. Nicholson and E. Pettit.†

The stars in the first group are given in Table VI., those of the second in Table VIa. The values $(\log P)_c$ in Table VI. were obtained by reducing Hertzsprung's diameters to a constant parallax $\pi = 0''{\cdot}100$ and using equation (2). The stars in Table VIa. were treated in a similar way. From the temperatures we obtain the values $\frac{c_2}{T}$, $c$ being equal to ‡ 14,600°. The absolute magnitudes are those of P. W. Merrill and G. Strömberg.§ Then from (3) and (2) the values log D and log P are obtained. The differences O C are negative for all but one star in each group. For the stars in the second group the numerical amount of the difference is considerably larger than for those in the first. The consequence is that the areas of the P.D. diagram covered by the two groups of stars are largely different. The difference in the computed value of log D is caused by the difference in the values $\frac{c_2}{T}$ as given by Hertzsprung and as derived from Nicholson and Pettit. Hertzsprung's values are chiefly based on colour-indices, while the latter authors obtained their values from measures with a vacuum thermocouple. At present I have not tried to decide which of the two sets of values is the correct one. It should, however, be remarked that owing to the strong absorption bands in the red, which occur with the M stars, the measured colour-index may turn out too small. The two different groups of stars are indicated in the diagram, those of Table VI. by black dots and those of Table VIa. by open circles. We conclude that with the long-period variables the period of light

* *Kleinerer Veröff. Berlin Babelsberg*, No. 5, 1928.
† S. B. Nicholson and Pettit, *Pop. Astr.*, **31**, 18, 1923.
‡ Wilsing, *Publ. Potsd.*, N. 74, Band xxiv., 1919.
§ P. W. Merrill and G. Strömberg, *Astroph. Journ.*, **59**, 97, 1924.

variation is shorter than the period of axial rotation or that the period of axial rotation is shorter than the one obtained from (2).

TABLE VI.

*Long-period Variables (Hertzsprung).*

| Star. | log D. | $(\log P)_o$. | $(\log P)_c$. | O–C. | Remarks. |
|---|---|---|---|---|---|
| $\mu$ Cep. | 3·39 | 3·00 | 3·59 | −·59 | J. Plasman, *Unters. über der Lichtw. v. $\mu$ Ceph. Münsteri. W.*, 1904. |
| $\alpha$ Ori.* | 3·36 | 3·34 | 3·53 | −·19 | Osthoff, *A.N.*, **216**, 187, 1922. |
| $\alpha$ Her. | 2·81 | 2·08 | 2·73 | −·65 | J. Stebbins, *Pop. Astr.*, **27**, 677, 1919. |
| $\beta$ Peg. | 2·56 | 1·72 | 2·35 | −·63 | Stebbins and Huffer, *Proc. Nat. Ac. Sc. Wash.*, **14**, 192. |
| $\eta$ Gem. | 2·77 | 2·37 | 2·67 | −·30 | |
| *o* Cet. | 3·17 | 2·52 | 3·26 | −·74 | |
| Boss 3827 | 2·52 | 2·88 | 2·30 | +·58 | Stebbins and Huffer, *Proc. Nat. Ac. Sc. Wash.*, **14**, 192. |

TABLE VIA.

*Long-period Variables of known Temperature.*

| Star. | T. | $c_2$/T. | log D. | $(\log P)_o$. | $(\log P)_c$. | O–C. |
|---|---|---|---|---|---|---|
| RT Cyg. | 3960° | 3·69 | 2·45 | 2·28 | 2·19 | + ·09 |
| $\chi$ Cyg. | 1690 | 8·64 | 4·47 | 2·61 | 5·20 | −2·59 |
| R Cnc. | 1910 | 7·64 | 4·01 | 2·55 | 4·52 | −1·97 |
| $\chi$ Oph. | 1940 | 7·53 | 3·99 | 2·53 | 4·48 | −1·95 |
| R Leo. | 1650 | 8·85 | 4·57 | 2·48 | 5·35 | −2·87 |
| R Hyd. | 1710 | 8·54 | 4·43 | 2·62 | 5·15 | −2·53 |
| R Aql. | 1810 | 8·06 | 4·23 | 2·50 | 4·85 | −2·35 |
| *o* Cet. | 1720 | 8·49 | 4·53 | 2·52 | 5·30 | −2·78 |

*Note.*—Without any doubt the most valuable contribution concerning the colours of long-period variables is the paper by B. P. Gerasimovic and H. Shapley.† For the present purpose, however, it is of little use. With these extreme colours the relation between the Harvard colour system and the system used by Öpik ‡ is uncertain. Moreover, for the colour-indices corresponding to the S, R, and N stars the relation between colour and effective temperature is undetermined; therefore the introduction of an additional number of points based on yet a third colour system would mean no real gain in accuracy and would only add to confusion. For these reasons these colour-indices have not been used here.

8. *The RV Tauri Stars.*—With the RV Tauri stars our knowledge

* J. Stebbins also finds a short periodic term of $250^d$ (*Pop. Astr.*, **21**. 5, 1913).
† B. P. Gerasimovič and H. Shapley, *Harvard Bulletin*, 872, 1930.
‡ E. Öpik, *Publ. Tartu*, **27**, No. 1, 1929.

concerning the data which we want for our computations is still more scanty than with the long-period variables. We must therefore content ourselves by roughly indicating the region of the P.D. diagram where these stars are to be expected. With the exclusion of a few M-type variables Table VII. contains the RV Tauri stars with both spectrum and period known.* We know that the RV Tauri stars are giants, and it has been assumed that their absolute magnitudes fall between the limits M = − 1 and − 3. Then log P and log D are found in the usual way. The values of log P of the star with the longest and shortest observed period were plotted against the maximum and minimum values of the diameter. The points obtained in this way were connected, and so we find the region indicated (see diagrams of fig. 3). For one RV Tauri variable, viz. R Scuti, the temperature has been determined by H. Vogt.† At maximum light its value is 4000°, at minimum 2500°. Adopting an absolute magnitude − 2 we obtain diameters log D = 2·30 and 3·31. These maximum and minimum diameters are also inserted in the figure. We conclude that with the RV Tauri stars also the period of light variation is shorter than the period of axial rotation (2). This is decidedly only a preliminary conclusion.

TABLE VII.

*RV Tauri Stars with known Period and Spectral Type.*

| Star. | Sp. | $(\log P)_o$. | $(\log P)_c$. M = −1·0. | $(\log P)_c$. M = −3·0. | O−C. M = −1·0. | O−C. M = −3·0. |
|---|---|---|---|---|---|---|
| TT Oph. | *c*F5*e* | 1·78 | 1·39 | 1·99 | +·39 | −·21 |
| R Sge. | *c*G1 | 1·85 | 1·77 | 2·36 | +·08 | −·51 |
| V Vul. | *c*G7*p* | 1·88 | 2·52 | 2·87 | −·44 | −·99 |
| A.C. Her. | F8 | 1·88 | 2·03 | 2·17 | +·31 | −·29 |
| U Mon. | *c*G0*p* | 1·96 | 2·11 | 2·29 | +·27 | −·33 |
| R Sct. | G5–K2*p* | 2·15 | 2·37 | 2·66 | +·08 | −·51 |

9. *The β Lyræ and Algol Stars.*—According to a remark by G. Shajn and O. Struve ‡ the periods of axial rotation and of orbital revolution are probably equal for the β Lyræ stars. According to these authors a difference between the two periods would result in marked changes in the light curve from one revolution to the next, this being caused by the elliptical shape of the components. No such changes have been detected. With some restrictions this same reasoning may also be applied to the short-period Algol variables or the eclipsing ones. Therefore the points indicating these stars should be distributed within a relatively narrow zone round the line indicating the relation (2). Diagram 6 of fig. 3 gives the results. The stars used in drawing up this diagram are those indicated by B.V. in Beer's general catalogue. §

* H. Ludendorff, *loc. cit.*, p. 171.
† H. Vogt, *A.N.*, **228**, 89, 1926.
‡ G. Shajn and O. Struve, *loc. cit.*
§ A. Beer, *loc. cit.*

Moreover, some additional variables were used for which reliable data as to colour, parallax, and period are available. In the figure dots surrounded by open circles indicate the $\beta$ Lyræ stars, while black dots represent the remaining eclipsing variables. It should be remarked that the majority of the stars used in the present diagram have already been included among the spectroscopic binaries. The few large negative deviations, for instance, correspond to the stars enumerated in Table V. The one large positive excess corresponds to the Pseudo-Cepheid $\epsilon$ Aurigæ. The period of this star is very long for an Algol variable. There is a slight indication that the periods of the $\beta$ Lyræ stars are shorter than those of the Algol stars. Owing to the small numbers the evidence as to this is by no means conclusive. From a comparison of figs. 2 and 3 we conclude that with the $\beta$ Lyræ and Algol stars the frequency of large positive excesses is considerably smaller than with the spectroscopic binaries in general. On the other hand, their distribution closely resembles that of the spectroscopic binaries of small eccentricity. This might have been anticipated.

10. *The Visual Double Stars.*—According to Jeans's theory * binary systems fall into two distinct classes :

(1) Systems formed by rotational fission whose periods are short but lengthening.
(2) Systems formed out of independent condensations in the parent nebulæ whose periods are long but decreasing.

The two classes correspond broadly to the two observational classes of spectroscopic and visual binaries. Jeans's point of view is confirmed by statistical investigation.† Consequently no relation can be expected to exist between the periods of axial rotation and the periods of revolution of the visual binaries.

11. *Some General Remarks and Conclusions.*—In fig. 4 all stars used previously are plotted in one and the same diagram. For indicating the various groups of stars different symbols are used, viz. :

Open circles with crosses for the long-period variables (Nicholson and Pettit).
Open circles for the long-period variables (Hertzsprung).
Black dots for the Cepheid variables. Mean diameters have been used throughout.
Open circles for the $\beta$ Canis-Majoris stars.
Double open circles for the eclipsing variables.
Black dots surrounded by circles for all remaining spectroscopic double stars.

The areas covered by the different groups of stars are indicated by faint drawn or dotted lines. These lines are drawn in such a way as to give no undue weight to a few exceptional stars which widely deviate from the mean.

Equation (2) has been indicated by a dotted line. From the figure

* Jeans, *loc. cit.*, pp. 239, 303.
† E. A. Kreiken, *Annals of Bosscha Obs.*, Misc. Papers, 4, 1930.

it appears that the line indicating the equation (2), *i.e.* the mean periods of axial rotation, roughly divides the P.D. diagram into two distinct

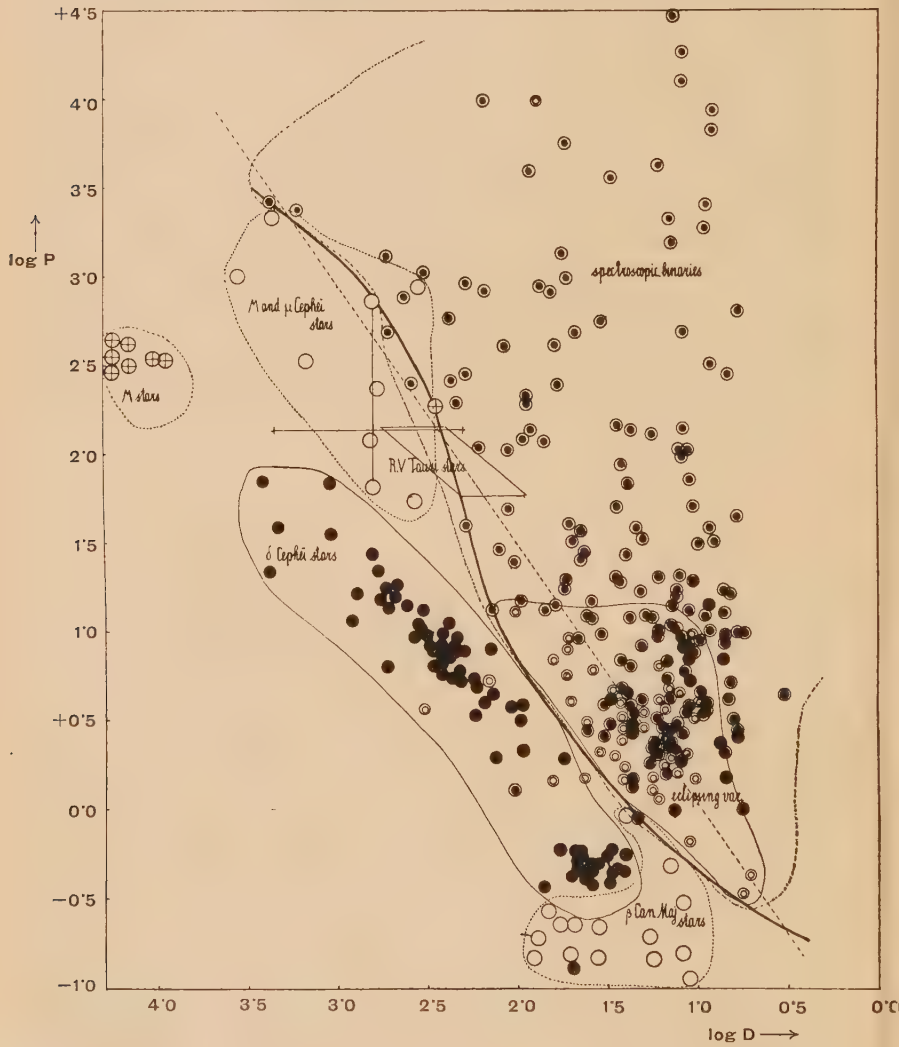


FIG. 4.—The observed periods of light variation and of revolution of the different groups of stars plotted against the logarithm of diameter. The mean period of axial rotation (form 2) has been indicated by a dotted straight line. A second solution for the period of axial rotation has been indicated by the curve.

parts. Of these the upper right part contains those stars which are recognised as doubles (the spectroscopic doubles and the eclipsing

variables), the lower left part contains those which have not been recognised or have not yet developed into doubles (the long-period variables, the Cepheids, and the $\beta$ Canis-Majoris stars). It should be remembered that equation (2) represents only an approximation to the relation between log. of period and log. of diameter. When deriving (2) a linear relation between the two quantities was adopted. Apparently the actual curve may deviate from a linear one. If instead of the straight line (2) we use the full drawn line indicated in the figure, the division of the correlation plane into two distinct parts is even more complete. With the exception of a few spectroscopic binaries of very early type (O and B1) no doubles occur on the left side of the curve. On the other hand, no variables such as are often believed to be in a state previous to that of the double stars are found on the right side of our curve. Therefore I think that the period of axial rotation (2) indicates a critical period in the process by which a variable develops into a spectroscopic binary. Presumably this critical stage is reached at the time when the period of light variation is connected in a definite way with the period of axial rotation. It is not necessary that this critical stage should be marked by the equality of the two periods, although our figure is rather suggestive of this. The period of axial rotation, however, as determined by us, is valid only for the outer layers of a star, the period of the core being shorter.

We now consider the relative positions of the different groups of stars in the P.D. diagram. When drawing conclusions from these relative positions we must remember that a certain number of $n$ parameters, $p_1$, $p_2$ . . . $p_n$, is wanted for completely representing the physical properties of a star. Therefore the distribution of our stars in the P.D. plane is the two-dimensional projection of an $n$-dimensional distribution. Consequently the different results must be checked by other observational data. Considering the areas to the left of the curve (2) we remark the close connection between the Cepheids and the $\beta$ Canis-Majoris stars. This agrees with the results obtained by other authors.* No new light is thrown on the relation between the long-period M variables, the $\mu$ Cephei stars, the RV Tauri variables, and the Cepheids. This is due to the lack of data concerning the RV Tauri stars and the uncertainties concerning the exact position of the M-type variables. If values based on Hertzsprung's catalogue are adopted (open circles), it is doubtful whether an M variable could develop into a Cepheid. If, on the other hand, the values derived from the measures by Nicholson and Pettit are adopted, then the continuous series of variables, M type, Cepheids, $\beta$ Canis-Majoris stars, might indicate the successive stages which are reached by an irregular M-type variable when developing into a spectroscopic double. According to Jeans's theory the period of axial rotation and of light variation (oscillation), which are different in the irregular M-type variables, become equal in the $\delta$ Cephei stars. Considering our diagram we see, however, that with the Cepheids the period of light variation is still considerably shorter than the period of axial rotation, unless it is assumed that the Cepheids represent a group of

* O. Struve, *Astr. Journ.*, **60**, 167, 1924, and *M.N.*, **86**, 63, 1925.

stars for which the velocity of axial rotation is unusually large when compared with that of the other stars of the same diameter. So there are two possibilities, viz. (*a*) the long-period variables (*i.e.* Mira, RV Tauri, and $\mu$ Cephei stars) and the Cepheids and $\beta$ Canis-Majoris stars represent two or more different groups of stars which separately may develop into spectroscopic doubles; (*b*) the M stars, Cepheids, and $\beta$ Canis-Majoris stars represent the different stages of development of one and the same group of variables which ultimately will split up into spectroscopic doubles. In the latter case the position of the RV Tauri stars remains dubious. Personally I think that (*a*) is the correct interpretation, but it is evident that whether view (*a*) or (*b*) is adopted axial rotation is of fundamental importance in this development.

We next consider the distribution of the stars on the right-hand side of the stellar rotation curve. As mentioned previously, small eccentricities probably denote the binary systems which have but recently originated by fission. Therefore with those stars the periods of revolution and of axial rotation should be equal. This has actually been found to be the case. Now it appears from our figure that such recent systems occur along the whole stellar rotation curve. Even with periods comparable to those of the Mira stars such systems are found. Consequently such binaries must have originated from variables with periods considerably larger than those of the Cepheids. A few might even have originated when the parent star was still in a stage previous to that indicated by the spectral type M. This was why I stated above that the Cepheid stage is not necessarily an intermediate stage in the evolution of the Mira stars into spectroscopic doubles. On the other hand, the position of the short-period binary systems relative to the Cepheids and $\beta$ Canis-Majoris stars suggests that these doubles really may have originated by fission from such short-period variables. It is, however, improbable that the point of transgression should be the same for all spectroscopic doubles. From the distribution of the different stars in the figure we should sooner conclude that this transgression may take place along a considerable interval of the stellar rotation curve. We now consider the spectroscopic doubles for which there is an appreciable difference between the period of axial rotation and the period of revolution. We find that the eccentricities of the orbits of these doubles are generally large, and they therefore represent the older systems, for which, according to Jeans, the periods have increased by a secular decrease of mass. We finally consider the $\beta$ Lyræ and Algol variables. From their distribution we conclude that these variables form a not very distinct part of the large group of spectroscopic doubles. They are most frequent with the shorter periods, which might have been anticipated.

*Bandoeng;*
1931 *February.*

## *The Theoretical Contours of Absorption Lines.* (Second Paper.)

By A. Pannekoek.

In our former paper under this title * we treated the case of an atmosphere of constant composition. Now in reality the different layers of an atmosphere cannot contain the same fraction of atoms of a certain kind, because the ionization changes with pressure and temperature. The most important factor is the change of electron pressure, from zero at the top steadily increasing downward. The change of ionization by the increase of temperature in the deeper layers plays a far less important rôle and will be neglected here.

The method of numerical integration described in the former paper (I., p. 144) can be applied to any case of a particular line in a certain star (with given temperature, gravity, abundance, ionization potential), as soon as the number of active atoms (neutral or ionized) in each layer by means of definite assumptions is computed. For the total contour of such a line this would involve the same labour as in the case, already treated, of an atmosphere of constant composition. If we wish to derive general results, it will be necessary, therefore, to keep the special parameters of each special case outside the process of numerical integration. The atmospheric layers which contribute the main part, say 80 to 90 per cent., to the formation of an absorption line, do not extend over a large range of pressure, not larger usually than between a certain P and 10P. Over such a range, part of the factors may be assumed to be constant, and the variation of the state of ionization can be expressed by a simplified formula.

The ionization formula

$$\frac{x_1}{x_0}\mathrm{P} \;=\; 10^{-5039\mathrm{V}_1/\mathrm{T}}\mathrm{T}^{2\cdot5}10^{-0\cdot48},$$

where $x_1$ and $x_0$ denote the ionized and the neutral fraction, and the electron pressure P is given in dynes/cm.$^2$, can be written, in Milne's notation,

$$x_1/x_0 \;=\; \mathrm{K}/\mathrm{P},$$

where K is a function of the temperature, containing only the ionization potential.

If $\mathrm{K}/\mathrm{P} > 10$, then $x_1/x_0 > 10$, and the fraction ionized is between ·90 and 1·00. Because the main part is ionized, for the neutral fraction we may use the simplified formula

$$x_0 \;=\; \mathrm{P}/\mathrm{K}.$$

The concentration of neutral atoms in the deeper layers increases regularly with the electron pressure. At the same time the concentration of the ionized atoms may be taken as constant.

* *M.N.*, **91**, 139, 1930 (which will be quoted as I.).

If, on the contrary, $K/P < 0{\cdot}10$ the fraction $x_0$ is between 0·9 and 1·0; now the concentration of neutral atoms may be taken the same for all depths, whereas for the ionized atoms we have

$$x_1 = K/P.$$

Here we have the case that the concentration of ionized atoms decreases with increasing depth. When by increasing temperature the atoms begin to ionize they behave in this way. After the first ionization is complete the second ionization begins to lower the number of singly ionized atoms. Since, however, the difference between two succeeding ionization potentials usually is rather large, the ratio of their values of K will amount to several powers of 10, and the range of pressures, over which the fraction of this state of ionization remains above 90 per cent., will be large.

Hence we have to distinguish the following three extreme cases :—

*A*. The concentration increases $\sim P$. This case is represented by the *Na* doublet in the sun, by the Balmer lines in the B stars, by the $Ca^+$ lines in the A stars, and more generally, where a line is already rapidly decreasing with increasing temperature.

*B*. The concentration is constant. This holds for lines of neutral atoms at low temperature (hydrogen in G and K stars, iron lines in K stars) and for resonance lines of ionized atoms at their maximum intensity ($Ca^+$ doublet in the sun).

*C*. The concentration decreases $\sim 1/P$. We meet this case with enhanced lines in their first appearance, such as $Fe^+$ lines in the sun and $He^+$ lines in the O stars.

Case B has been dealt with in our first paper; the others will be treated here.

2. *Case A*. The formula (8) for the monochromatic absorption coefficient (I., p. 150), expressing it in $\Delta\lambda$, and putting $b' = b\lambda_0^2/2\pi c$, may be written :

$$s_0 = \left\{\frac{2\pi\epsilon^4}{3m^2c^4m_H}\left(\frac{\lambda_0}{\Delta\lambda}\right)^2 + \frac{2\pi\sqrt{\pi}\epsilon^2}{mcbm_H}e^{-(\Delta\lambda/b)^2}\right\}\frac{n}{\mu}.$$

For the fractional abundance $n$ we substitute $n_0P/K$. We denote the result by $s_0 = \sigma P$, and substitute it into the equations (I., p. 143)

$$\frac{dy}{d\xi} = (k_0 + s_0)z\,; \qquad \frac{dz}{d\xi} = \left(k_0 + s_0\frac{P}{P+Q}\right)(y - 2E).$$

Putting

$$dx = k_0 d\xi = \kappa_0\frac{p'}{g}P\,dP\,; \qquad x = \tfrac{1}{2}\kappa_0\frac{p'}{g}P^2\,; \qquad q' = \tfrac{1}{2}\kappa_0\frac{p'}{g}Q^2,$$

we have for the optical depth which determines the temperature

$$\tau = \tfrac{1}{2}\bar{\kappa}\frac{p'}{g}P^2 = \frac{\bar{\kappa}}{\kappa_0}x,$$

and

$$\frac{dy}{dx} = \left(1 + \frac{\sigma}{\kappa_0}\right)z; \quad \frac{dz}{dx} = \left(1 + \frac{\sqrt{x}}{\sqrt{x} + \sqrt{q'}}\frac{\sigma}{\kappa_0}\right)\left(y - 2E_0\left(1 + c\frac{\bar{\kappa}}{\kappa_0}x\right)\right) \quad (1)$$

In the wings of an absorption line, where the collision part of the monochromatic coefficient may be neglected compared with the continuous absorption, these formulæ reduce to the simpler form

$$\frac{dy}{dx} = \left(1 + \frac{\sigma}{\kappa_0}\right)z; \quad \frac{dz}{dx} = y - 2E_0\left(1 + c\frac{\bar{\kappa}}{\kappa_0}x\right) \quad . \quad (2)$$

The coefficients are constant, because the monochromatic and the continuous absorption both increase proportionately to the electron pressure. The equations can be integrated now in a finite form. Putting $1 + \sigma/\kappa_0 = n^2$ we find

$$y_0 = z_0 = 2E_0\frac{1 + c\frac{\bar{\kappa}}{\kappa_0}/n}{1 + n}.$$

The continuous background has the intensity $E_0\left(1 + c\frac{\bar{\kappa}}{\kappa}\right)$, so that the residual intensity is

$$r = \frac{2}{1 + n}\frac{1 + c\frac{\bar{\kappa}}{\kappa_0}/n}{1 + c\frac{\bar{\kappa}}{\kappa_0}} \quad . \quad . \quad . \quad . \quad (3)$$

For $r = \frac{1}{2}$ this formula gives the value of $n$ corresponding to the half-width of a line. It depends on the value of $c\frac{\bar{\kappa}}{\kappa_0}$ assumed. For

| $c\frac{\bar{\kappa}}{\kappa_0}$ = | 0·8 | 1·0 | 1·2 | 1·5 | 2·0 | 3·0 |
|---|---|---|---|---|---|---|
| $n$ = | 2·078 | 2·0 | 1·942 | 1·878 | 1·808 | 1·732 |
| $\frac{\sigma}{\kappa_0}$ = | 3·32 | 3·0 | 2·77 | 2·53 | 2·27 | 2·00. |

Substituting in the formula for $s_0$ the values of the physical constants, we find (I., p. 154)

$$s_0 = [-1{\cdot}00]\frac{n}{\mu}\left(\frac{\lambda_0}{\Delta\lambda}\right)^2$$

and

$$\sigma = [-1{\cdot}00]\frac{1}{K}\frac{n_0}{\mu}\left(\frac{\lambda_0}{\Delta\lambda}\right)^2.$$

Taking, as in our former computations, $c\frac{\bar{\kappa}}{\kappa_0} = 1{\cdot}5$, hence $\frac{\sigma}{\kappa_0} = 2{\cdot}53$,

and assuming $\kappa_0 = [-2{\cdot}1]$, the largest possible theoretical value (I., p. 166), the expression for the half-width for $r = \frac{1}{2}$ becomes

$$\left(\frac{\Delta\lambda}{\lambda_0}\right)^2 = [0{\cdot}70]\frac{1}{K}\frac{n_0}{\mu} \quad . \quad . \quad . \quad (4)$$

We apply this formula to the $D_1D_2$ doublet of *Na* in the solar spectrum. With $T = 6000°$, $V_1 = 5{\cdot}12$ we find $K = [4{\cdot}70]$. For $\Sigma(\Delta\lambda)^2 = 0{\cdot}116$ (I., p. 154) we find $\frac{n_0}{\mu} = [-4{\cdot}48]$, $n_0 = [-3{\cdot}12]$. This is the abundance of all the sodium atoms, neutral or ionized, which, therefore, constitute 0·076 per cent. in mass, $\frac{1}{3}\frac{1}{0}\frac{1}{0}$ per cent. in number of the total atmosphere. In our former treatment, where a constant abundance of neutral atoms throughout the atmosphere was assumed, a total abundance $[-2{\cdot}6]$ was found. The present result is, of course, more reliable.

3. For the darkest centre of a line we may assume just the reverse: the continuous absorption is negligible compared with the collision part of the monochromatic absorption. Then the same method may be used as in I., § 6; the general solution of the differential equation is a definite integral. We now put

$$x = \tfrac{1}{2}\sigma\frac{p'}{g}P^2; \qquad q = \tfrac{1}{2}\sigma\frac{p'}{g}Q^2.$$

(This $q$ is for $\sigma Q = s_0$ identical with $q$ in I.) Then the solution of

$$\frac{d^2y}{dx^2} = \frac{\sqrt{x}}{\sqrt{q}}(y - 2E_0)$$

is given by

$$y - 2E_0 = B\int_1^\infty e^{-tp}(p^2-1)^{-\frac{9}{10}}dp$$

$$z = -B(\tfrac{4}{5})^{-\frac{1}{5}}\int_t^\infty e^{-u}(u^2-t^2)^{-\frac{9}{10}}u\,du,$$

where $t = \frac{4}{5}q^{-\frac{1}{4}}x^{\frac{5}{4}}$ and $pt = u$.

For the boundary $x = 0$, $t = 0$ these integrals are

$$y_0 - 2E_0 = B\int_1^\infty (p^2-1)^{-\frac{9}{10}}dp = BI_1$$

$$z_0 = -B(\tfrac{4}{5}q)^{-\frac{1}{5}}\Gamma(\tfrac{1}{5}) = -Bq^{-\frac{1}{5}}I_2,$$

from which, by the condition $y_0 = z_0$, we find

$$y_0 = z_0 = 2E_0\frac{I_2}{I_2 + I_1\sqrt[5]{q}}.$$

For the integrals in this formula we find

$$I_1 = \int_0^{\frac{1}{2}\pi}\frac{d\phi}{\sqrt[5]{\sin^4\phi\cos\phi}} = 6{\cdot}018 \quad \text{and} \quad I_2 = 4{\cdot}389,$$

hence

$$y_0 = z_0 = \frac{2E_0}{1 + 1{\cdot}37\sqrt[5]{q}} \quad . \quad . \quad . \quad (5)$$

4. *Case C.* In this case we have for the concentration of active atoms :

$$n = n_0 K/P.$$

Indicating by $s_0{}^0$ the coefficient of monochromatic absorption in the case of a concentration $n_0$, we have $s_0 = s_0{}^0 K/P$. Introducing it into the equations of § 2, where again we put

$$d\xi = \frac{p'}{g}dP\,; \qquad k_0 = \kappa_0 P\,; \qquad \tfrac{1}{2}\kappa_0\frac{p'}{g}P^2 = x\,;$$

we find

$$\frac{dy}{dx} = \left(1 + \frac{s_0{}^0 K}{\kappa_0 P^2}\right)z\,; \qquad \frac{dz}{dx} = \left(1 + \frac{s_0{}^0 K}{\kappa_0 P(P+Q)}\right)(y - 2E).$$

Now a difficulty arises for the topmost layers of the atmosphere, in consequence of $P^2 = 0$ appearing in the denominator and producing a logarithmic infinity. It is, however, not essential, and is solely due to the numerical approximation introduced ; the quantity $n = n_0 K/P$, which for $P = 0$ would become infinite, is practically restricted to the cases $K << P$. The difficulty can be removed by making use of the exact expression

$$\frac{n}{n_0 - n} = \frac{K}{P}\,; \qquad n = n_0\frac{K}{P + K}.$$

Then the equations become

$$\frac{dy}{dx} = \left(1 + \frac{s_0{}^0 K}{\kappa_0 P(P+K)}\right)z\,; \qquad \frac{dz}{dx} = \left(1 + \frac{s_0{}^0 K}{\kappa_0 (P+K)(P+Q)}\right)(y - 2E).$$

Putting now

$$\tfrac{1}{2}\kappa_0\frac{p'}{g}Q^2 = q'\,; \qquad \tfrac{1}{2}\kappa_0\frac{p'}{g}K^2 = k\,; \qquad \frac{1}{2}\frac{p'}{g}K s_0{}^0 = \sigma'$$

they take the form

$$\frac{dy}{dx} = \left(1 + \frac{\sigma'}{x + \sqrt{kx}}\right)z\,;$$

$$\frac{dz}{dx} = \left[1 + \frac{\sigma'}{(\sqrt{x} + \sqrt{k})(\sqrt{x} + \sqrt{q'})}\right]\left[y - 2E_0\left(1 + c\frac{\bar{\kappa}}{\kappa_0}x\right)\right] . \quad . \quad (6)$$

The numerical difficulty of the integrand in the first interval from $x = 0$ coming down from infinity can be overcome by starting the integration not at $x = 0$ but at some low value of $x$. This procedure of omitting the lowest interval even corresponds to the physical reality, because in the uppermost layers, at the lowest pressure, the number

of active atoms, after reaching a maximum, must go down by second ionization.

The equations in this form do not hold solely for Case C, but so far are quite general. We want them, however, only for the case that $K < P$, *i.e.* $k < x$. At the same time $x << q'$, because the P in the layers most contributing to the absorption are far smaller than Q. Then the fraction $\frac{\sqrt{x}}{\sqrt{x}+\sqrt{q'}}$ of the monochromatic absorption, which is removed by collisions, is small and may be neglected compared with the continuous absorption, especially in the wings of the line. In this case, where only one parameter has to be assumed in the computations, the formulæ are simplified to

$$\frac{dy}{dx} = \left(1 + \frac{\sigma'}{x+\sqrt{kx}}\right)z\,; \qquad \frac{dz}{dx} = y - 2E_0\left(1 + c\frac{\bar{\kappa}}{\kappa_0}x\right). \qquad (7)$$

It may be remarked that the coefficient $k$, though necessary at the lower limit of $x$, has only a small influence upon the result; this means that the radiated intensity $y_0$ depends only on $\sigma'$, which does not contain the continuous absorption coefficient. We can understand this by the consideration that in this case chiefly the uppermost layers absorb the continuous light coming chiefly from deeper layers; thus $\kappa_0$ appears only in the scale of the integration steps and not in the result.

The numerical integrations have been performed with $k = 10^{-2}$ (corresponding for solar conditions to $K = 10^2$) for three different values of $\sigma'$. The results are

| | | | |
|---|---|---|---|
| $\sigma' = 0{\cdot}1$ | $y_0 = z_0 = 2E_0\left(0{\cdot}432 + 0{\cdot}404c\frac{\kappa}{\kappa_0}\right)$; | | $r = 0{\cdot}830$ |
| 1 | 0·198 | 0·129 | ·313 |
| 10 | 0·0403 | 0·00522 | ·038. |

The residual intensity was computed with $c\frac{\bar{\kappa}}{\kappa_0} = 1{\cdot}5$. This residual intensity is 0·5 for $\log\sigma' = -0{\cdot}35$; hence for the half-width we have

$$\frac{1}{2}\frac{p'}{g}Ks_0^0 = [-0{\cdot}35], \qquad s_0^0 = [-1{\cdot}00]\frac{n_0}{\mu}\left(\frac{\lambda_0}{\Delta\lambda}\right)^2,$$

or

$$\left(\frac{\Delta\lambda}{\lambda_0}\right)^2 = [-0{\cdot}95]\frac{p'}{g}K\frac{n_0}{\mu} \quad . \quad . \quad . \quad (8)$$

5. It may be interesting to compare the contours of absorption lines obtained in the three Cases A, B, C. For this purpose the residual intensity was computed for a number of values of $\sigma$, $s_0$, or $\sigma'$, increasing in the ratio $\sqrt{10}$ (corresponding to a number of values $\Delta\lambda$ on an arbitrary scale decreasing in the ratio $\sqrt{10}$), chosen in such a way that the residual intensity 0·5 is included in the series.

TABLE I.

*Comparison of Contours.*

| Case A. | | | | Case B. | | Case C. | |
|---|---|---|---|---|---|---|---|
| $\Delta\lambda$. | $\log\frac{\sigma}{\kappa^0}$. | $n$. | $r$. | $\log a$. | $r$. | $\log\sigma'$. | $r$. |
| 3·16 | 9·403 | 1·119 | 0·883 | +1·65 | 0·926 | | |
| 1·78 | ·903 | 1·342 | 723 | +0·65 | 762 | −0·85 | 0·768 |
| 1·00 | 0·403 | 1·879 | 500 | −0·35 | 500 | −0·35 | ·500 |
| 0·56 | ·903 | 3·0 | 300 | −1·35 | 258 | +0·15 | ·244 |
| 0·32 | 1·403 | 5·128 | 169 | −2·35 | 110 | +0·65 | ·089 |
| 0·18 | ·903 | 9·0 | 093 | −3·35 | 048 | | |
| 0·10 | 2·403 | 15·90 | 052 | −4·35 | 022 | | |

Thus in Case A the contour lines at medium residual intensity are less steep, in Case B they are steeper, and in Case C still somewhat more so. The cause of this difference is easily understood ; the active atoms are in Case A more strongly concentrated in the deepest layers, where the outer parts of the wings are formed, so that in the outer wings the line is darker in Case A than in Case B. In Case C, on the contrary, the atoms are more concentrated in the superficial layers and deepen there the inner parts of the absorption line, whereas its outermost parts, produced in the deep layers, are less blackened here. This difference in shape can be expressed in the form of a difference in half-width for various residual intensities. So we find this half-width

| | | | |
|---|---|---|---|
| for $r$ = | 0·25 | A. 0·47 | B. 0·55 | C. 0·57 |
| | 0·50 | 1· | 1· | 1· |
| | 0·75 | 1·92 | 1·72 | 1·68 |

The difference is not pronounced, and it is questionable whether in the present state of the photometry of absorption lines in stellar spectra it can be discerned with certainty.

6. The results obtained for the half-width in each of these cases may be used to derive the change of intensity of a line over the series of spectral classes, *i.e.* for a continuous change of temperature. Then we have first to consider the variation with temperature of the different coefficients in our formulæ. The variation of the continuous absorption coefficient $\kappa_0$ is not considerable ; according to the formulæ, I., § 13, it changes proportionally to $T^{-\frac{3}{2}}$. Much more important, however, is the variation of $p'$, the ratio of the total pressure to the electron pressure.

At lower temperatures only a small fraction of the atoms are ionized ; the number of free electrons is small compared with the total number of atoms. Then the continuous absorption coefficient $k_0 = \kappa_0 P$ is also small, the gas is rather transparent, we can see down to a deep level with high total pressure, and the absorption exerted by the great number of atoms is strong. In our formulæ this is expressed by a large value of $p' = p/P$. Because this ratio always presents itself

in the combination $g/p'$, it appears that low temperature works just as a small gravitation in increasing the intensity of the lines.

To compute the relative number of electrons in a stellar atmosphere it would be necessary to know the elementary composition of the atmosphere, *i.e.* the fractional abundance of each kind of atoms. Though a precise knowledge on this point is lacking at present, we may assume, probably, the following qualitative statements: 1. Hydrogen forms by far the most important part of the atmosphere, perhaps 95 to 98 per cent. in mass, and in the first case helium contributes a considerable part to the rest. 2. The metal atoms constitute only some small percentage of the total mass. Then we may deduce the following consequences of this state of things, also qualitatively expressed. (1) As long as the ionization of hydrogen is insignificant (below 8000°) the number of electrons, all of them produced by the metal atoms, remains small. (2) The ionization of hydrogen, between 8000° and 11,000°, raises the number of electrons so much that it equals the number of atoms, and $p'$ is lowered to 2. (3) For higher temperatures this number is not materially increased by multiple ionization of the metal atoms; perhaps the helium atoms may give some increase.

The relative number of electrons is not the same in each layer; in the atmospheric layers it will decrease with the depth. We will neglect here these differences and introduce its mean value for the mean of the layers which contribute chiefly to the absorption. These layers are characterised by a certain value of the optical depth $\int k_0 dx$, which in I., p. 143, is denoted by $\alpha x^2$. From the numerical integration we find the value of $\alpha x^2$ for these layers to be nearly 0·4 (log $= -0{\cdot}4$). The relation

$$s_0 \frac{p'}{g} \mathrm{P} = x, \quad \text{hence} \quad \mathrm{P}^2 = \alpha x^2 \frac{g}{p' \kappa_0} \quad \text{or} \quad p' = \frac{0{\cdot}4 g}{\kappa_0 \mathrm{P}^2}$$

connects the coefficient $p'$ with the electron pressure P in that most contributing layer. If we denote the fraction ionized of each constituent of the atmosphere by $x_1$ and its abundance by A, then the number of electrons, produced by all the constituents, relative to the number of atoms, is given by

$$\frac{\mathrm{P}}{p - \mathrm{P}} = \frac{1}{p' - 1} = \Sigma \mathrm{A} x_1.$$

The ionization $x_1$ itself depends on the unknown electron pressure P. Expressing it by means of $\frac{x_1}{1 - x_1} \mathrm{P} = \mathrm{K}$, and eliminating $p'$ by the preceding formula, we find an indirect formula for P:

$$\Sigma \mathrm{A} \frac{\mathrm{K}}{\mathrm{K} + \mathrm{P}} = \frac{\mathrm{P}^2}{0{\cdot}4 g/\kappa_0 - \mathrm{P}^2} \quad . \quad . \quad . \quad (9)$$

For a given temperature the function K can be computed for each element. The term $0{\cdot}4 g/\kappa_0$, with $\kappa_0 = [-2{\cdot}1]$ and with $g = [4{\cdot}4]$

(sun) and $g = [2{\cdot}4]$ (giant star) takes the values [6·1] and [4·1]. For the composition of the atmosphere a simplified model is, tentatively, assumed, consisting of a small number of elements with different ionization potentials, which may be considered as representative. In this model the atmosphere consists, in number of atoms, of 0·005 per cent. with ionization potential $V_1 = 4{\cdot}3$ (for *K*), 0·01 per cent. with $V_1 = 5{\cdot}1$ (for *Na*), 0·01 per cent. with $V_1 = 6{\cdot}1$ (for *Ca, Al*), 0·02 per cent. with $V_1 = 7{\cdot}7$ (for *Fe, Mg, Si*), 100 per cent. with $V_1 = 13{\cdot}54$ (for *H*). This corresponds roughly to a mass fraction 0·2 per cent. for *K*, 0·2 per cent. for *Na*, 0·4 per cent. for *Ca, Al*, 1 per cent. for *Fe, Mg, Si*. Perhaps the abundance of atoms with lowest ionization potential is still overestimated here; an error from this reason may be compensated if there is some diffusion of electrons from the deeper and hotter layers into the atmosphere. With these values of A and $V_1$, and K computed from $V_1$ and T, the equation (9) was solved by trial and error; the results for P and $p'$ are contained in Table II. (where also the difference in $\log \kappa_0$ with the constant value $-2{\cdot}1$ computed for $T = 6000°$ is given in the second column).

TABLE II.

*Electron Abundance.*

| T. | $\Delta \log \kappa_0$. | $\log g = 4{\cdot}4$. | | | $\log g = 2{\cdot}4$. | | |
|---|---|---|---|---|---|---|---|
| | | log P. | log $\Sigma A x_1$. | log $p'$. | log P. | log $\Sigma A x_1$. | log $p'$. |
| ° | | | | | | | |
| 2,000 | +·72 | −0·47 | −7·04 | 7·04 | −1·14 | −6·36 | 6·36 |
| 2,500 | +·57 | +0·31 | −5·49 | 5·49 | −0·38 | −4·87 | 4·87 |
| 3,000 | +·45 | 0·77 | −4·57 | 4·57 | −0·07 | −4·22 | 4·22 |
| 3,500 | +·35 | 1·02 | −4·07 | 4·07 | +0·12 | −3·84 | 3·84 |
| 4,000 | +·27 | 1·15 | −3·81 | 3·81 | 0·22 | −3·66 | 3·66 |
| 5,000 | +·12 | 1·28 | −3·54 | 3·54 | 0·35 | −3·40 | 3·40 |
| 6,000 | 00 | 1·43 | −3·25 | 3·25 | 0·62 | −2·86 | 2·86 |
| 7,000 | −·10 | 1·84 | −2·41 | 2·41 | 1·16 | −1·78 | 1·79 |
| 8,000 | −·18 | 2·29 | −1·53 | 1·54 | 1·58 | −0·89 | 0·94 |
| 9,000 | −·26 | 2·60 | −0·84 | 0·90 | 1·81 | −0·29 | 0·47 |
| 10,000 | −·33 | 2·80 | −0·35 | 0·52 | 1·88 | −0·07 | 0·34 |
| 11,000 | −·39 | 2·87 | −0·11 | 0·36 | 1·89 | −0·01 | 0·30 |
| 12,000 | −·45 | 2·89 | −0·03 | 0·32 | 1·90 | 0·00 | 0·30 |
| 13,000 | −·50 | 2·90 | 0·00 | 0·30 | 1·90 | 0·00 | 0·30 |

The influence of two distinct sources of free electrons, the easily ionizable metal atoms and afterwards the more resistant hydrogen atoms, is clearly recognized in these figures. Till 6000° (or 5000°) the decrease of $p'$ is slowing down as if a limit will be reached, but then it becomes large again, till the limit 2 is gradually approached.

It must be remarked that the basis of this computation is the assumption that the continuous absorption depends on collisions with electrons only. If collisions of atoms with atoms play a perceptible part in

this absorption in gases with a small number of free electrons, the value for $p'$ for low temperatures should be lowered.

7. The varying behaviour of a line through the series of spectral classes is, in this treatment, separated into three (or two) distinct parts, each represented by a nearly straight line, one ascending (C), one horizontal (B), one descending (A). Between them there are regions of transition where the assumptions underlying each of these cases begin to break down. They must be considered separately.

In Case B the percentage of active atoms in all the layers is assumed to be the same. This does not mean that it is 100 per cent. everywhere. Also when by partial ionization it is lower, the differences between the different layers are not necessarily so large, that the formulæ of Case B are not good approximations. But in this case $n$, occurring in the formulæ, is lower than $n_0$ and must be computed by means of the electron pressure in a mean or most contributing layer. In the case that B represents the maximum of ionized atoms, the formulæ for the increasing and the decreasing side are

$$n = n_0 \frac{K_1}{K_1 + P} \qquad \text{and} \qquad n = n_0 \frac{P}{K_2 + P},$$

whereas for a neutral atom there is only a decreasing branch with

$$n = n_0 \frac{P}{K_1 + P}.$$

In the Cases A and C the formulæ contain $n_0$. But here also a correction outside their proper regions is necessary. In Case A we have used a fractional factor P/K, where the real value should have been P/(K + P). If for the change of this factor with depth a wrong value was assumed, still the result will be nearly right if for its mean amount the right value was taken. Hence in the result the denominator should be replaced by K + P, where for P the electron pressure of the most contributing layer is taken. This will make a difference only in the transition regions. In the same way, in Case C the factor K/P is used instead of K/(K + P); here the result has to be multiplied by P/(K + P) in the transition regions. We see that in these regions the correction factors for B and for the adjacent (C or A) case are complementary.

8. We first apply our results to the behaviour of the $Ca^+$ lines H and K. The formulæ to be used for the ascending, the maximum, and the descending branches, with their corrections, are

$$\left.\begin{array}{lll} \text{C.} & \left(\frac{\Delta\lambda}{\lambda_0}\right)^2 = [-\cdot 95]\frac{p'}{g} K_1 \frac{n_0}{\mu}; & \text{Corr. } \frac{P}{K_1 + P} \\ \text{B.} & \left(\frac{\Delta\lambda}{\lambda_0}\right)^2 = [-1\cdot 17]\sqrt{\frac{p'}{g\kappa_0}} \frac{n}{\mu}; & n = n_0 \frac{K_1}{K_1 + P} \quad \text{or} \quad n = n_0 \frac{P}{K_2 + P} \\ \text{A.} & \left(\frac{\Delta\lambda}{\lambda_0}\right)^2 = [-1\cdot 40]\frac{1}{\kappa_0 K_2} \frac{n_0}{\mu}; & \text{Corr. } \frac{K_2}{K_2 + P} \end{array}\right\} \quad (10)$$

In Table III. the necessary data and the results are put down. The temperature functions $K_1$ and $K_2$ are computed with $V_1 = 6{\cdot}09$ and $V_2 = 11{\cdot}82$; for $\kappa_0$ the value $[-2{\cdot}1]$ for $T = 6000°$ is used; for the other temperatures the correction $\Delta\kappa_0$ from Table II. has been applied. As results, the values of the coefficients of $\frac{n_0}{\mu}$ or $\frac{n}{\mu}$ are given, with the corrections or the factors $n/n_0$ already applied. The computations are made for the sun ($\log g = 4{\cdot}4$) as well as for a giant star with $g$ one hundred times smaller. In the last columns $\Delta\lambda$ itself is given in an arbitrary unit; in the case of H and K, where the contours of the lines are almost entirely determined by the resonance wings, the total absorption of the line and its effective width will be proportional to these values.

TABLE III.

*Lines of Ionized Calcium.*

| T. | $K_1$. | $K_2$. | Dwarf. (C). (A). | Dwarf. (B). | Giant. (C). (A). | Giant. (B). | $\Delta\lambda$. Dwarf. | $\Delta\lambda$. Giant. |
|---|---|---|---|---|---|---|---|---|
| 2,500° | −4·25 | | −4·11 | | −2·73 | | ·88 | 4·3 |
| 3,000 | −2·02 | | −2·80 | | −1·15 | | 4·0 | 27 |
| 3,500 | −0·39 | | −1·69 | −1·88 | −0·02 | −0·20 | 14·2 | 98 |
| 4,000 | +0·86 | | −0·86 | −1·02 | +0·44 | +0·29 | 37 | 140 |
| 5,000 | +2·63 | −3·14 | −0·55 | −0·63 | | +0·32 | 48 | 145 |
| 6,000 | +3·82 | −0·96 | | −0·70 | | +0·10 | 45 | 112 |
| 7,000 | +4·75 | +0·62 | | −1·10 | | −0·48 | 28 | 58 |
| 8,000 | | +1·83 | −1·54 | −1·59 | −1·14 | −1·20 | 16 | 27 |
| 9,000 | | +2·79 | −2·05 | −2·15 | −1·87 | −1·97 | 9·4 | 11·6 |
| 10,000 | | +3·56 | −2·60 | | −2·53 | | 5·0 | 5·4 |
| 12,000 | | +4·76 | −3·62 | | −3·61 | | 1·55 | 1·55 |
| 14,000 | | +5·63 | −4·38 | | −4·38 | | ·49 | ·49 |

The dotted lines separate the regions where the correction is less than $[-0{\cdot}30]$.

The table and the curves show a rather rapid increase to a flat maximum, at 5300° for $g = [4{\cdot}4]$, at 4400° for $g = [2{\cdot}4]$, and a slower decline for higher temperatures. For giant stars the intensity is stronger than for dwarfs, especially at lower temperature; for high-temperature stars the difference disappears. The result for 6000°, viz. $[-0{\cdot}70]\frac{n_0}{\mu}$, corresponds for the sun to a value $\left(\frac{\Delta\lambda}{\lambda_0}\right)^2 = 60/16 \,.\, 10^6$ for the H and K lines taken together (I., p. 154); hence we find $\log \frac{n_0}{\mu} = -4{\cdot}73$ and $\log n_0 = -3{\cdot}13$ or $n_0 = 1/1350$. This is much

smaller than was found in my former paper, chiefly because $p'$, which was then assumed to be 2, turns out now to be a thousand times larger. That this large value of $p'$, *i.e.* the extremely small percentage of free electrons and the small continuous absorption of the solar atmosphere, is probably real, may be seen from the curve of the $Ca^+$ line intensities. With a small value of $p'$ the intensity for the lower temperatures would be strongly diminished and the maximum would be displaced to a temperature of nearly 7000°, certainly not in accordance with observation. The observed low temperature of the maximum of the $Ca^+$ lines (viz. in the K-type stars) may, in the same way, support an argument that atomic collisions cannot give an important contribution to the continuous absorption when free electrons are scarce.

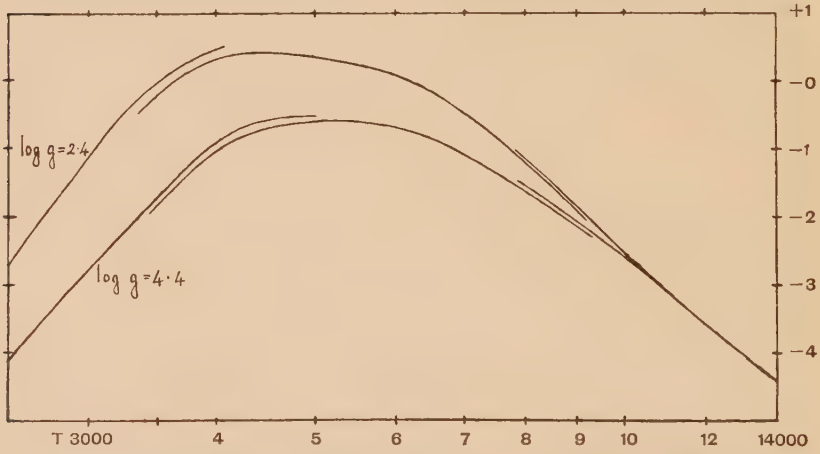


9. In the spectrum of hydrogen we have to deal with Cases B and A only. For the Balmer lines the number of neutral hydrogen atoms has to be multiplied by the Boltzmann factor. By the increase of this factor the number of atoms in the second state increases with temperature ; afterwards it decreases by the ionization of these atoms. Denoting the Boltzmann factor by $\beta$,

$$\beta = e^{-V_1/V_T}; \qquad \log \beta = -\frac{5039 V_1}{T},$$

we have for the half-width of a line

$$\left.\begin{aligned} \text{B.} \quad & \left(\frac{\Delta\lambda}{\lambda}\right)^2 = [-1{\cdot}17]\beta\sqrt{\frac{p'}{g\kappa_0}}\frac{n}{\mu}; \qquad n = n_0\frac{P}{K+P} \\ \text{A.} \quad & \left(\frac{\Delta\lambda}{\lambda}\right)^2 = [-1{\cdot}40]\frac{\beta}{\kappa_0 K}\frac{n}{\mu}; \qquad \text{Corr.}\ \frac{K}{K+P} \end{aligned}\right\} \quad . \quad (11)$$

The data for the computation and the results are found in Table IV. The functions K are computed with $V_1 = 13{\cdot}56$ ; for gravitation again two values $\log g = 4{\cdot}4$ and $2{\cdot}4$ are used.

Table IV.

*Balmer Lines of Hydrogen.*

| T. | log K. | log β. | Dwarf. (B). | Dwarf. (A). | Giant. (B). | Giant. (A). | Δλ. Dwarf. | Δλ. Giant. |
|---|---|---|---|---|---|---|---|---|
| 4,000° | −8·53 | −12·80 | −13·35 | | −12·42 | | ·021 | ·062 |
| 5,000 | −4·87 | −10·23 | −10·84 | | − 9·91 | | ·48 | 1·11 |
| 6,000 | −2·40 | − 8·53 | − 9·23 | | − 8·42 | | 2·4 | 6·2 |
| 7,000 | −0·62 | − 7·31 | − 8·38 | | − 7·70 | | 6·5 | 14·1 |
| 8,000 | +0·75 | − 6·40 | − 7·87 | | − 7·22 | −7·16 | 11·6 | 24·5 |
| 9,000 | +1·83 | − 5·68 | − 7·49 | −7·39 | − 6·95 | −6·84 | 18 | 35·5 |
| 10,000 | +2·70 | − 5·12 | − 7·25 | −7·14 | − 6·99 | −6·85 | 25 | 37 |
| 11,000 | +3·42 | − 4·65 | − 7·26 | −7·09 | | −6·99 | 28 | 32 |
| 12,000 | +4·03 | − 4·27 | | −7·18 | | −7·15 | 26 | 26·5 |
| 14,000 | +5·02 | − 3·65 | | −7·42 | | −7·42 | 19·5 | 19·5 |
| 16,000 | +5·77 | − 3·20 | | −7·63 | | −7·63 | 15·3 | 15·3 |
| 20,000 | +6·86 | − 2·56 | | −7·94 | | −7·94 | 10·7 | 10·7 |

For the dwarf stars with large gravity the maximum is found to occur at 10,500°, for the giant stars at 9500°. At low temperature the giant stars have stronger absorption lines than the dwarfs; a gravity 100 times smaller works as if the concentration were 9 times more, and the lines, in normal circumstances, would be 3 times as wide. The broadening by the Stark effect, however, spoils these simple relations. If we take account of the increase of the Boltzmann factor by the radiation from the hotter layers at great depth,* which is larger for low than for high temperatures, the theoretical maxima are displaced to a somewhat lower temperature.

---

*Wave-lengths of Oxygen and Nitrogen Lines in the Stellar Region.*
By C. S. Beals, D.I.C., Ph.D.

*Introduction.*—This paper contains the results of an investigation conducted for the purpose of obtaining precise laboratory values of the wave-lengths of oxygen and nitrogen lines which occur in the ordinary stellar region of observation. Originally suggested by Professor A. Fowler, the work was begun at the Imperial College, London, and finished some years later at the Dominion Astrophysical Observatory, Victoria, B.C. A previous investigation by J. S. Clark,† undertaken after Sebastian

* *Cf.* A. Unsöld, *Zeitschr. f. Astrophysik*, **1**, 1, 1930.
† *Ap. J.*, **11**, 332, 1914.

Albrecht * had called attention to the need for accurate measurements of oxygen and nitrogen lines for stellar radial velocity work, covered the same region, though somewhat different experimental methods were employed. It is hoped that the greater weight which naturally attaches to measures derived independently by more than one observer will justify the labour of redetermining these wave-lengths, which are of considerable importance in studies of the velocities of early-type stars.

*Observational Details.*—The sources of light were ordinary capillary discharge tubes filled with oxygen or nitrogen at low pressure. The tubes were used in the end-on position, and the spectra were excited by condensed discharges of as low voltage as would suffice to produce lines of the required intensity. The iron arc was used as a comparison source and was so arranged that the exposure of the comparison spectrum could be made simultaneously with that of the spectrum to be measured. This was done, according to a suggestion by Professor Fowler, by placing a microscope cover-glass in the path of the direct beam from the discharge tube to the slit, and inclined at an angle of 45° to the direction of the beam. The iron arc was placed some distance away in a direction at right angles to the primary beam, and its light was reflected on to the slit by the cover-glass, which acted as a mirror. The recommendations of the International Astronomical Union were strictly adhered to in the use of the iron arc, and care was taken to have the collimation as nearly perfect as possible so that the grating was evenly illuminated by both the primary and the comparison sources. About twelve exposures of the iron arc at equal intervals of time were made during the time the plate was being exposed to the light from the discharge tube. For some of the photographs in the region $\lambda$ 4590–4700, when exposures of the discharge tube of 15 to 30 minutes were required while the iron arc would have had to be exposed nearly twice as long, the cover-glass was dispensed with and direct exposures of the comparison spectrum were made before and after that of the spectrum to be measured.

The spectrograph at the Imperial College is a 10-feet concave grating instrument. The grating was ruled by Rowland and was used in the original mounting designed by Eagle. The Victoria instrument was of Littrow form, with a plane grating ruled by Anderson and a quartz lens of approximately 9 feet 7 inches focal length made by Hilger. The mounting was similar in its general features to the Imperial College instrument, and was made by Mr. S. S. Girling of Victoria according to designs by the writer. It has proved very satisfactory in use, being very stable and having convenient arrangements for making the necessary adjustments when focussing or when changing to a different region. Both instruments were used in the third order and gave nearly the same dispersion, approximately 1·7 A. and 1·8 A. per mm. respectively. The average time of exposure for the plates taken at the Imperial

* The wave-lengths of lines in B and O spectra have recently been discussed by Albrecht in some detail (*Ap. J.*, **67**, 305, 1928).

College was about 2 hours. The exposures at Victoria were on the whole shorter, ranging from 15 to 150 minutes; the average was about 40 minutes.

The plates were measured in the usual way with red to right and left in succession. When reducing the measures it was found possible to use a linear formula, $\lambda = \lambda_0 + ax$, for the plates taken with the concave grating, though the corrections were rather large where long ranges were covered. The linear formula was found to be impracticable for plates taken with the Littrow instrument, and a quadratic formula, $\lambda = \lambda_0 + ax + bx^2$, was found to give satisfactorily small corrections even when a length of 8 inches of the plate was covered at one time. For the construction of the correction curves, only those iron lines were used which have been adopted as secondary or tertiary standards by the International Astronomical Union.

*Results.*—The measures are recorded in Tables I. and II. Values obtained at the Imperial College (designated I.C.) may be found in the first column. In the second column is given opposite each line the number of spectrograms on which it has been measured. Similar information concerning Victoria measures is given in columns three and four, while the mean wave-lengths, weighted according to the number of spectra, are in column five. The probable errors, in the sixth column, have been computed from residuals given by successive spectra, since the actual errors of setting are generally small compared with the variations from plate to plate. Some lines which show large variations are almost certainly unstable, while others are suspected of instability. The nitrogen line $\lambda$ 4227·394 is one of a considerable number of lines which have been investigated by Pretty * and found to show large shifts of wave-length with changes of pressure in the tube. Notes concerning other lines suspected of being unstable will be found in the "Remarks" column. The estimates of intensity in column seven are mainly due to Fowler for oxygen, and Fowler and Freeman for nitrogen, though some estimates by the present writer have been substituted. In the eighth column is given what is considered to be the best previous measure of each line. Measures given to ·001 A., unless otherwise indicated, are due to Clark, while others (to ·01 A.) are by Fowler,† or Fowler and Freeman.‡

The lines in Table I. are all due to the singly ionised atom of oxygen (*O*II). Those in Table II. are due mainly to *N*II, though some lines of the doubly ionised atom of nitrogen (*N*III) are included. The *N*III lines are indicated in the "Remarks" column.

* *Proc. Phy. Soc. London*, **41**, 442, 1929.
† *Proc. Roy. Soc.*, A, **110**, 476, 1926.
‡ *Ibid.*, A, **114**, 662, 1927.

[Table

TABLE I.

*Oxygen Wave-lengths.*

| Beals. | | | | | | | Previous Measures: Clark, Fowler. | Remarks. |
|---|---|---|---|---|---|---|---|---|
| I.C. | | Victoria. | | Weighted Mean λ. | Probable Error. | Int. | | |
| λ. | No. | λ. | No. | | | | | |
| 3882·197 | 2 | | | 3882·197 | ·003 | 7 | 3882·194 | |
| 3911·960 | 4 | | | 3911·960 | ·001 | 10 | 3911·951 | |
| 3919·287 | 2 | | | 3919·287 | ·001 | 6 | 3919·279 | Measure by Fowler. |
| 3945·048 | 2 | | | 3945·048 | ·002 | 5 | 3945·033 | |
| 3954·375 | 3 | 3954·365 | 1 | 3954·372 | ·002 | 7 | 3954·368 | |
| | | 3967·441 | 1 | 3967·441 | | 1 | 3967·44 | |
| 3973·264 | 3 | 3973·260 | 1 | 3973·263 | ·002 | 10 | 3973·266 | |
| 3982·718 | 2 | 3982·721 | 1 | 3982·719 | ·002 | 5 | 3982·725 | |
| 4069·635 | 4 | 4069·637 | 3 | 4069·636 | ·001 | 4 | 4069·635 | |
| 4069·898 | 3 | 4069·897 | 2 | 4069·897 | ·003 | 6 | 4069·903 | |
| 4072·160 | 4 | 4072·169 | 4 | 4072·164 | ·002 | 8 | 4072·156 | |
| 4075·869 | 3 | 4075·868 | 4 | 4075·868 | ·002 | 10 | 4075·869 | |
| | | 4078·862 | 1 | 4078·862 | | 4 | 4078·86 | |
| | | 4083·907 | 1 | 4083·907 | | 2n | 4083·90 | |
| | | 4085·124 | 4 | 4085·124 | ·002 | 3 | 4085·12 | |
| | | 4089·295 | 4 | 4089·295 | ·003 | 4n | 4089·28 | |
| | | 4092·940 | 4 | 4092·940 | ·002 | 5 | 4092·94 | |
| | | 4096·543 | 2 | 4096·543 | ·003 | 3 | 4096·54 | |
| | | 4097·260 | 3 | 4097·260 | ·003 | 4n | 4097·25 | |
| | | 4103·017 | 1 | 4103·017 | | 5 | 4103·01 | |
| | | 4104·743 | 4 | 4104·743 | ·003 | 5 | 4104·74 | |
| 4105·004 | 2 | 4104·998 | 4 | 4105·000 | ·002 | 7 | 4105·001 | |
| | | 4110·795 | 3 | 4110·795 | ·002 | 3 | 4110·80 | |
| | | 4112·029 | 4 | 4112·029 | ·003 | 4 | 4112·04 | |
| 4119·222 | 3 | 4119·221 | 4 | 4119·221 | ·001 | 8 | 4119·222 | |
| 4120·268 | 2 | 4120·284 | 4 | 4120·279 | ·003 | 3 | 4120·267 | Possibly unstable. |
| | | 4120·554 | 1 | 4120·554 | | 2 | 4120·55 | |
| 4132·804 | 2 | 4132·808 | 3 | 4132·806 | ·001 | 6 | 4132·82 | Possibly unstable. |
| 4153·301 | 3 | 4153·303 | 4 | 4153·302 | ·002 | 7 | 4153·310 | |
| | | 4169·230 | 2 | 4169·230 | ·001 | 4 | 4169·23 | |
| 4185·460 | 2 | 4185·453 | 4 | 4185·456 | ·002 | 8 | 4185·453 | |
| 4189·787 | 3 | 4189·789 | 4 | 4189·788 | ·002 | 10 | 4189·793 | |
| 4317·140 | 4 | 4317·139 | 7 | 4317·139 | ·001 | 8 | 4317·160 | |
| 4319·632 | 4 | 4319·630 | 7 | 4319·631 | ·001 | 8 | 4319·647 | |
| | | 4336·865 | 4 | 4336·865 | ·003 | 6 | 4336·86 | |
| 4345·569 | 3 | 4345·558 | 7 | 4345·562 | ·002 | 7 | 4345·570 | Possibly unstable. |

TABLE I.—*continued.*

| Beals. I.C. λ. | Beals. I.C. No. | Beals. Victoria. λ. | Beals. Victoria. No. | Weighted Mean λ. | Probable Error. | Int. | Previous Measures: Clark, Fowler. | Remarks. |
|---|---|---|---|---|---|---|---|---|
| 4347·427 | 3 | 4347·424 | 7 | 4347·425 | ·001 | 5 | 4347·429 | |
| 4349·432 | 3 | 4349·422 | 7 | 4349·426 | ·002 | 8 | 4349·435 | Possibly unstable. |
| 4351·269 | 3 | 4351·269 | 7 | 4351·269 | ·001 | 6 | 4351·275 | |
| 4366·897 | 3 | 4366·896 | 6 | 4366·896 | ·001 | 7 | 4366·906 | |
| 4414·911 | 4 | 4414·907 | 4 | 4414·909 | ·002 | 10 | 4414·888 | |
| 4416·974 | 4 | 4416·976 | 4 | 4416·975 | ·002 | 8 | 4416·974 | |
| | | 4452·377 | 2 | 4452·377 | ·004 | 6 | 4452·38 | |
| 4590·976 | 3 | 4590·970 | 8 | 4590·971 | ·001 | 9 | 4590·983 | |
| 4596·178 | 3 | 4596·173 | 8 | 4596·174 | ·002 | 8 | 4596·189 | |
| 4638·865 | 3 | 4638·853 | 8 | 4638·854 | ·002 | 6 | 4638·865 | |
| 4641·818 | 3 | 4641·810 | 8 | 4641·811 | ·001 | 9 | 4641·827 | |
| 4649·146 | 3 | 4649·137 | 8 | 4649·139 | ·001 | 10 | 4649·148 | |
| 4650·847 | 3 | 4650·840 | 8 | 4650·841 | ·002 | 6 | 4650·853 | |
| 4661·644 | 3 | 4661·633 | 7 | 4661·635 | ·001 | 9 | 4661·650 | |
| 4676·235 | 1 | 4676·234 | 8 | 4676·234 | ·002 | 8 | 4676·246 | |
| 4705·344 | 2 | 4705·356 | 8 | 4705·355 | ·002 | 8 | 4705·36 | |

TABLE II.

*Nitrogen Wave-lengths.*

| Beals. I.C. λ. | Beals. I.C. No. | Beals. Victoria. λ. | Beals. Victoria. No. | Weighted Mean λ. | Probable Error. | Int. | Previous Measures:* Clark, Fowler, and Freeman. | Remarks. |
|---|---|---|---|---|---|---|---|---|
| 3919·005 | 2 | | | 3919·005 | ·002 | 6 | 3919·003 | |
| 3955·853 | 2 | 3955·850 | 4 | 3955·851 | ·001 | 6 | 3955·851 | |
| 3994·996 | 2 | 3994·996 | 4 | 3994·996 | ·0003 | 10 | 3994·995 | |
| 4026·081 | 2 | 4026·079 | 4 | 4026·080 | ·001 | 3n | 4026·087 | |
| 4035·084 | 2 | 4035·089 | 4 | 4035·087 | ·001 | 4n | 4035·090 | |
| 4041·320 | 2 | 4041·322 | 4 | 4041·321 | ·001 | 5n | 4041·325 | |
| | | 4043·537 | 4 | 4043·537 | ·003 | 3n | 4043·54 | |
| | | 4073·055 | 4 | 4073·055 | ·001 | 2n | 4073·04 | |
| | | 4082·280 | 2 | 4082·280 | ·001 | 2n | 4082·28 | |
| 4097·324 | 2 | 4097·335 | 4 | 4097·331 | ·002 | 10 | 4097·327 *N*III | Probably |
| 4103·387 | 2 | 4103·398 | 4 | 4103·394 | ·002 | 9 | 4103·393 *N*III | unstable. |
| | | 4124·081 | 2 | 4124·081 | ·001 | 1 | 4124·10 | |
| 4133·668 | 2 | 4133·669 | 3 | 4133·669 | ·002 | 2 | 4133·654 | |

* Unless otherwise indicated, measures to 0·001 A. are due to Clark. Others are by Fowler and Freeman.

TABLE II.—*continued.*

| Beals. | | | | | | Previous Measures: * | | |
|---|---|---|---|---|---|---|---|---|
| I.C. | | Victoria. | | Weighted Mean λ. | Probable Error. | Int. | Clark, Fowler, and Freeman. | Remarks. |
| λ. | No. | λ. | No. | | | | | |
| 4145·763 | 2 | 4145·765 | 4 | 4145·764 | ·001 | 3 | 4145·759 | |
| | | 4171·608 | 2 | 4171·608 | ·003 | 2n | 4171·63 | |
| 4176·157 | 2 | 4176·168 | 3 | 4176·164 | ·002 | 3n | 4176·163 | Possibly unstable. |
| | | 4179·667 | 2 | 4179·667 | ·002 | 1n | 4179·68 | |
| 4227·739 | 2 | 4227·754 | 4 | 4227·749 | ·002 | 3n | 4227·738 | Unstable. |
| 4236·929 | 2 | 4236·930 | 3 | 4236·930 | ·002 | 5 | 4236·99 | Measure by Clark. |
| 4237·045 | 2 | 4237·051 | 3 | 4237·049 | ·001 | 4 | | |
| 4241·784 | 2 | 4241·789 | 3 | 4241·787 | ·001 | 8n | 4241·787 | |
| | | 4379·103 | 2 | 4379·103 | ·004 | 10n | 4379·09 | |
| | | 4432·739 | 5 | 4432·739 | ·002 | 6n | 4432·71 | |
| 4447·028 | 3 | 4447·036 | 5 | 4447·033 | ·001 | 10 | 4447·035 | |
| 4507·550 | 2 | 4507·564 | 4 | 4507·559 | ·003 | 3 | 4507·58 | Possibly unstable. |
| 4510·896 | 3 | 4510·903 | 9 | 4510·901 | ·002 | 6 | 4510·92 | *N*III † Possibly |
| 4514·856 | 3 | 4514·861 | 9 | 4514·860 | ·002 | 7 | 4514·865 | *N*III unstable. |
| 4530·407 | 3 | 4530·401 | 8 | 4530·403 | ·003 | 5 | 4530·421 | |
| 4552·506 | 1 | 4552·544 | 4 | 4552·536 | ·005 | 4 | 4552·50 | Possibly unstable. |
| 4601·474 | 4 | 4601·479 | 11 | 4601·478 | ·001 | 8 | 4601·490 | |
| 4607·150 | 4 | 4507·154 | 10 | 4607·153 | ·001 | 7 | 4607·167 | |
| 4613·869 | 4 | 4613·868 | 8 | 4613·868 | ·001 | 6 | 4613·884 | |
| 4621·392 | 4 | 4621·392 | 10 | 4621·392 | ·001 | 7 | 4621·405 | |
| 4630·542 | 4 | 4630·536 | 10 | 4630·537 | ·001 | 10 | 4630·551 | |
| 4634·152 | 2 | 4634·136 | 6 | 4634·138 | ·003 | 8 | 4634·165 | *N*III Probably |
| 4640·637 | 3 | 4640·624 | 6 | 4640·627 | ·003 | 10 | 4640·649 | unstable. |
| 4641·875 | 1 | 4641·863 | 5 | 4641·864 | ·004 | 3 | 4641·90 | |
| 4643·091 | 3 | 4643·085 | 10 | 4643·086 | ·001 | 8 | 4643·106 | |

An examination of Tables I. and II. will immediately reveal the existence of a systematic difference of considerable amount between the results of the present work and the previous measures of Clark in the region λ 4500–4700. This systematic difference was first observed when the measurement of the Imperial College plates was completed, and the desirability of securing an independent check on their accuracy led to the second determination being undertaken at Victoria. Disregarding three lines due to *N*III which are believed to be unstable, the average values of the systematic difference, Clark *minus* Beals, for the I.C. plates in this region are 0·007 A. for oxygen and 0·014 A. for nitrogen. For the Victoria plates they are 0·014 A. for oxygen and 0·015 A.

* Unless otherwise indicated, measures to 0·001 A. are due to Clark. Others are by Fowler and Freeman.

† Measures of *N*III lines to 0·01 A. are due to Freeman.

for nitrogen. These values make it apparent that the systematic difference is confirmed by the second investigation, though there is an average difference of 0·007 A. between the I.C. and Victoria plates for the oxygen lines. Owing to the uncertainty in these wave-lengths, a larger number of spectra in this region was secured in the Victoria investigation than would otherwise have been considered necessary. Measures of eight plates for oxygen and ten for nitrogen gave probable errors of less than 0·001 for nearly all lines, and it seems improbable, in so far as the iron standards in this region can be trusted, that any of the Victoria values are in error by as much as 0·005 A.

Owing to the weakness of the iron spectrum in the region λ 4590–4700, fourth order lines, of wave-length λ 3370–3530 approximately, were used as standards for the I.C. plates, which were secured, as has already been mentioned, with a concave grating instrument. Unfortunately, corrections to reduce the wave-lengths to standard conditions of temperature and pressure, necessary where methods involving the coincidence of different orders are used, were not applied, and it may be that this is the cause of the systematic difference between the I.C. and Victoria plates in this region. In computing mean wave-lengths, these I.C. values have accordingly been given low weight. Use of fourth order lines was confined to this region, so that there appears no reason to suspect systematic displacements in other Imperial College wave-lengths.

On the whole, the agreement between the two sets of measures is reasonably good. As has already been pointed out, the two investigations were made with different spectrographs, different measuring instruments, and different methods of plate reduction. There seems some reason, therefore, to suppose that the mean wave-lengths of Tables I. and II. are not far from the true values.

In conclusion, the writer wishes to thank Professor Fowler, who suggested the investigation, for his kindly help and advice on experimental details. My thanks are also due to Dr. J. S. Plaskett, Director of the Dominion Astrophysical Observatory, whose encouragement and assistance in securing a high dispersion instrument made the Victoria investigation possible.

*Dominion Astrophysical Observatory,*
*Victoria, B.C., Canada:*
1931 *January* 13.

---

*Luminosity Curve of Early B Stars.* By B. P. Gerasimovič.

Luminosity curves of later type stars are so far comparatively well investigated. Different lines of attack (trigonometric and spectroscopic parallaxes, distribution of the apparent magnitudes in the clusters, proper motions, etc.) lead to very satisfactory and concordant results. Unfortunately things are quite different in the case of early stars. Individual parallaxes, both trigonometric and spectroscopic, are not of great

value here. Individual proper motions are too small to be of any use. Even the study of apparent magnitudes in the clusters or local groups of early stars can afford no more than rather meagre indirect information with regard to the shape of the luminosity curve. A great dispersion of colours and an unknown percentage of yellowish stars make the separation of B stars in clusters a rather dubious enterprise. Extended groups of brighter B stars with well-classified spectra could be used for this purpose with greater advantage, but unfortunately we meet here in an overwhelming majority of cases some difficulties of special kinds. We never are certain as to whether the observed distribution of apparent magnitudes is complete to the absolutely fainter stars. On the other hand local groups of B stars usually have no clear boundaries and are apparently immersed in a large mass of background stars, to say nothing about the foreground objects.

Our present information on the luminosity curve of early B stars can be summarised as follows. The first steps, or rather preparatory steps, in this direction consisted in establishing some characteristics associated with the absolute magnitude and also in determining the dispersion of a preliminary Gaussian curve. As early as in 1916 the present writer showed * that for the same Harvard subtype, B stars belonging to the descending branch of Lockyer's classification were absolutely fainter than those belonging to the ascending branch. In more modern and much more practical form the same phenomenon has been established by Adams and Joy and used as a basis of their well-known classification of B stars according to the character of spectrum lines. Of course this division by itself does not prove that the luminosity curve of early B stars has two maxima, but still it may give some ground for such a hypothesis.

The size of the dispersion of a preliminary Gaussian distribution curve as based on proper motion and radial velocity data has afforded another indirect indication. Charlier † and the present writer ‡ showed that this dispersion is by no means so small as was supposed before. These results were more than compatible with Wilson's deductions with regard to the dispersion of absolute magnitudes of O-type stars.

More determined data were derived from the study of the apparent magnitudes in clusters and local groups. Separating early stars by means of their colour indices, Malmquist § has shown that their luminosity curves in three open clusters and in the North Galactic Pole region have two distinct maxima. Though this result chiefly pertains to A-type stars, it has nevertheless some significance for the B stars too. Otto Struve,‖ I believe, was the first who found this two-topped luminosity curve for the earliest B stars (O–B3) based on the data of H.D.C. and H.D.E. for Cygnus group. This study has been much extended by Pannekoek.¶ Though, as was indicated above, local

* Sur les deux groupes des étoiles d'helium, *Bulletin de l'Académie Petrograd*, 1419, 1916.

† *Lund Medd.*, II, 34, 1926.

‡ *V.J.S.*, **61**, 219, 1926.

§ *Lund Medd.*, II, 46, 39, 1927.

‖ *Astr. Nachr.*, **231**, 19, 1927.

¶ *Public. Astr. Inst. Amsterdam*, **2**, 49, 1929.

groups of B stars are not quite suitable for the determination of a luminosity curve, Pannekoek reached some very interesting results. In the groups (Orion, P Cygni, etc.) which seem to be statistically complete, well separable, and apparently free from background stars, he found the luminosity curve to have three distinct maxima. This short summary shows how meagre is our information on the luminosity curve of the early B stars.

Under these circumstances it seems quite natural to ask whether accumulated proper motion and radial velocity data cannot give us this information which we lack. G. Strömberg * has devised recently a simple and seemingly practical method of deriving the luminosity curve from the frequency curves of $\tau$-components and peculiar radial velocities. This method has been applied to K and M type stars and has brought to light some very interesting though not unexpected characteristics of their luminosity curves. Referring to the details of Strömberg's original paper, I shall describe briefly the general principle of this new method. It consists in the comparison of two frequency curves, those of $\tau$ components taken without the signs (a variable $x = \log \tau + 0{\cdot}2m$ is used) and peculiar radial velocities (a variable $y = \log V' - 1{\cdot}676$). The calculated distributions of $x$ and $y$ are to be corrected for errors of observation and smoothed on the side of smallest value. Since $x = M' + y$, where $M' = 0{\cdot}2M$, the distribution $F_1(x)dx$ can be computed from the distribution $F_2(y)dy$, and an unknown distribution curve of absolute magnitudes $F_3(M')dM'$ obtained by solving the following integral equation

$$F_1(x) = \frac{N_1}{N_2 N_3}\int_{-\infty}^{+\infty} F_2(x - M')F_3(M')dM'$$

where $N_1, N_2, N_3$ are the total numbers of stars in the three distributions. The solution for $F_3(M')$ is attained by successive approximations. We assume some distribution curve for $M'$, *i.e.* $F_3(M')$, calculate $F_1(x)$ and compare the result with the observed $F_1(x)$. This comparison gives a set of values $\Delta F_1(x)$ which are used for the improvement of the assumed $M'$ distribution for a number of $M'$-values. The integral equation is to be transformed into an equation in finite differences containing the unknown corrections for $F_3(M')$, and solved by least squares. We proceed in this way until such an approximation to $F_3(M')$ is reached as gives $F_1(x)$ in substantial agreement with the observed $x$-distribution.

B-type stars are not so favourable for the application of Strömberg's method as K and M stars. There are the following difficulties here :—

(1) Clustering tendency and group motions of the B stars can gravely affect the deduced M-distribution, producing spurious maxima and minima. This difficulty, however, is not so big as it seems to be at first glance. Except for such groups as Scorpio-Centaurus and Perseus, these local motions are merely a matter of conjecture. On the other hand, since these groups are numerous and the material

* *Mount Wilson Contr.*, 395 and 396, 1930.

includes a good many dispersed stars, the possible irregularities in the final $x$- and $y$-distributions as produced by this cause seem to be largely eliminated.

(2) It is well known that the mean absolute magnitude increases rapidly from B5 to Bo. It appears therefore necessary to derive M-distributions for various subtypes separately. But since the early B stars are not abundant in general, proper motion and radial velocity data, if subdivided into three or more groups, will not be numerous enough for statistical discussion.

(3) Unexcluded orbital motions in the radial velocities. This difficulty arises whenever we use radial velocities of B stars for statistical purposes. It simply increases the respective mean probable errors.

(4) Since B stars are dispersed along the galactic belt and belong to most distant objects, cosmic absorption as deduced by Trumpler and van d. Kamp can affect the reduced $\tau$-components. It is my opinion that the recent data on cosmic absorption permit another interpretation. Until stronger arguments based on the study of galactic clouds are presented, it seems hardly necessary to take the alleged cosmic absorption into account.

Notwithstanding all these difficulties, which cannot be entirely eliminated, the application of Strömberg's method in the study of early B stars can give us some valuable results and at least is worth trying.

## *The Material.*

1. *$\tau$-Components.*—Four years ago in a general study of the early B stars * I calculated $\tau$-components from all the existing proper motion data. Campbell's apex (A = 269°, D = + 27°) was assumed in the course of these computations and the following weights assigned to the proper motions, compiled from the best catalogues.

| Catalogue. | Weight. |
|---|---|
| P.G.C. | 1·00 |
| Groombridge | 0·40 |
| Cape (−40° to −52°) | 0·44 |
| Greenwich 1910 | 0·16 |
| Cambr. Mass. Zone | 0·16 |
| Yale (+50° to +55°) | 0·20 |
| Kopenhagen (*A.N.*, 5349–50) | 0·32 |

All proper motions were carefully reduced to the Boss system and corrected for $\mu_\delta$ error (according to van Rhijn and van d. Kamp) and for the error of Newcomb's precession as suggested in the Introduction to the P.G.C. I considered it unnecessary to recalculate $\tau$-components, using Raymond's modern corrections to the $\mu_\delta$ in Boss's system.

Only Bo–B5 stars brighter than 7·5 vis. mag. are made use of in the

* *V.J.S.*, **61**, 219, 1926.

following as material for $x$-distribution curves. Since the weights of deduced $\tau$-components are not equal, it seemed reasonable to use as a dependent variable not the number of stars in the given $x$-interval, but the sum of corresponding weights. The mean error of Boss $\tau$-components was assumed to be $\pm 0''\cdot005$. The interval in $x$ is made uniform and equal to 0·1. All the values of $x$ less than $-1\cdot7$ were combined in one group and then distributed according to the logarithmic scale as suggested by Strömberg. The resulting distributions were computed separately for Bo–B2, B3 and B5 groups. The totals of the weights ($\Sigma p$) and the numbers of stars used are as follows :—

| Group. | $\tau$-Components. | |
|---|---|---|
| | $\Sigma p$. | Stars. |
| Bo–B2 | 141 | 168 |
| B3 | 289 | 341 |
| B5 | 169 | 226 |

The stars known as members of the Pleiades, Perseus and Scorpio-Centaurus clusters were not taken into account when calculating $x$- and $y$-distributions. The resulting frequency curves were not corrected for errors of observation, since a preliminary investigation proved the errors to be small and too uncertain to be taken into account.

2. *Radial Velocities.*—It has been shown in my previous study* that the solar velocity is substantially the same for brighter and fainter Bo–B5 stars. On the other hand the K term is entirely negligible for stars fainter than $5^m\cdot5$. The following data have been assumed for the calculation of peculiar radial velocities :—

$$V_0 = -20\cdot5 \text{ km./sec.}$$
$$K = +4\cdot3 \ (0^m\cdot-5^m\cdot5).$$
$$K = 0 \ (5^m\cdot5-7^m\cdot5).$$

The number of stars used are as follows :—

| | |
|---|---|
| Bo–B2 | 162 |
| B3 | 241 |
| B5 | 150 |

The mean error of one peculiar velocity V′ was assumed to be $\pm 3\cdot5$ km./sec., the frequencies for $y < -1\cdot13$, that is for V′ less than 3·5 km., being grouped together and distributed according to logarithmic scale.

## *The Results.*

The $y$-distributions are shown in Table I., $x$-distributions in Table II. (columns two, three, four). By successive (four or five) approximations final $x$-distribution curves were computed together with resulting M-distributions. O–C for these $x$-distributions are shown in

* *Loc. cit.*

Table II. (columns five, six, seven). They seem to be satisfactory, not showing any marked systematic run, and are reasonably small, remembering that *no smoothings of* x- *and* y-*distributions have been performed except those mentioned above.* Simple Gaussian curves

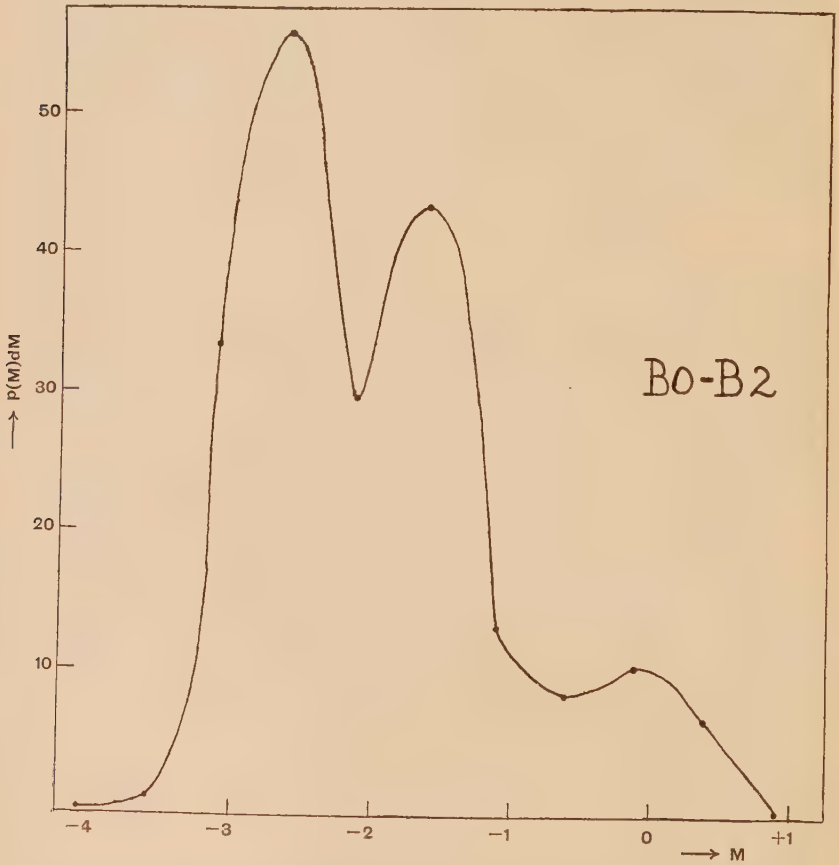


FIG. 1.—Distribution of absolute magnitudes for B0–B2 stars. The points are computed from the distribution of reduced $\tau$-components and peculiar radial velocities.

were assumed for a first approximation to $F_3(M')$, the values of the parameters being taken from my previous work.

Resulting M-distribution curves are given in Table III. and graphically in figs. 1–4, where the computed values are indicated by dots and the total numbers adjusted to 200 without any smoothing. The curve for B0–B5 is a composite curve computed in order to make our results comparable with those based on the study of local groups. As M-distribution curves differ greatly for various subtypes, the composite

curve for Bo–B5 stars taken together will depend on the assumed relative frequency of these stars. This curve (shown in fig. 1) was computed for a "normal" local group—*i.e.* for a group which contains various subtypes of the early B stars in the same proportion as our local system and brighter field stars in general. Star-counts in H.D.C. up to $9^{m}\cdot0$ show that in such a "normal" group the numbers of Bo–B2, B3, and B5 stars are as 0·28 : 0·22 : 0·50. The absolute magnitudes of Bo–B2 and B5 groups were reduced to B3 by applying the corrections + $1^{m}\cdot5$ and − $1^{m}\cdot0$ as based on the data for mean absolute magnitudes derived from parallactic motions.

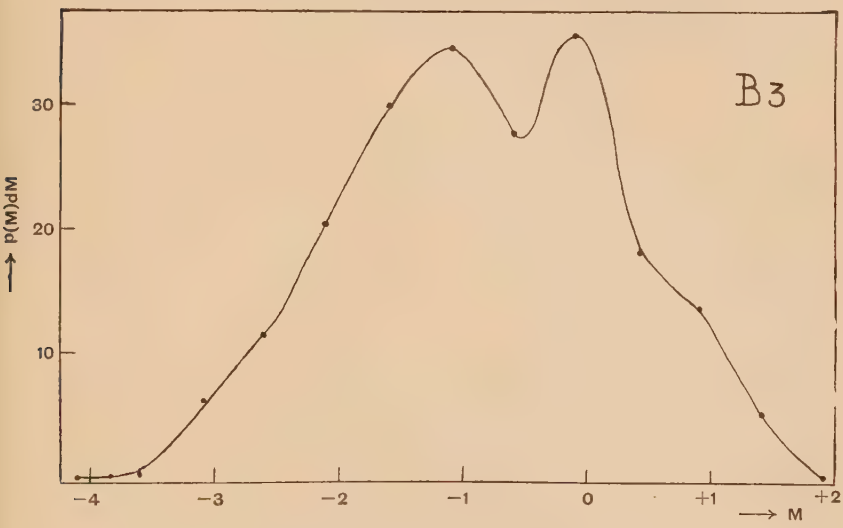


Fig. 2.—Distribution of absolute magnitudes for B3 stars.

Before examining the computed M-curves it seems necessary to point out that no great weight can be attached to the absolute values of the resulting mean M's. The application of Russell's criterion shows that for the stars under consideration, mean absolute magnitudes as deduced from $\tau$-components cannot be so accurate as those derived from parallactic motion. Thus M-distribution curves, as computed above, are of relative value; they give us some information as to the shape of the luminosity curve—nothing else.

These curves exhibit some very interesting features. It is evident that the luminosity curve of the early B stars is by no means so simple as it was supposed to be a few years ago. We find the following statistical characteristics of the first order with their mean errors :—

| | Bo–B2. | B3. | B5. |
|---|---|---|---|
| | m m | m m | m m |
| Mean | −1·89±0·006 | −0·87±0·09 | −0·72±0·13 |
| Dispersion | 0·85±0·04 | 1·20±0·07 | 1·89±0·09 |

Thus the dispersion is rather large and increases from Bo to B5. The curves for Bo–B2 and B3 have much in common. The first is decidedly three-topped—the flattest top being on the side of faintest magnitudes. This subsidiary maximum persists in the B3 curve as a noticeable hump. The data for the highest luminosity (Bo–B2) stars are not trustworthy. These stars have the smallest $\tau$-components, of the order of the assumed probable errors, and their distribution is artificially smoothed out in a final $x$-curve. Thus we can say nothing on the distribution of Bo–B2 stars of say $-4^{m}\cdot0$ or $-3^{m}\cdot5$. A slight inflection in the B3 curve at $-2^{m}\cdot6$ may be considered as an additional low maximum.

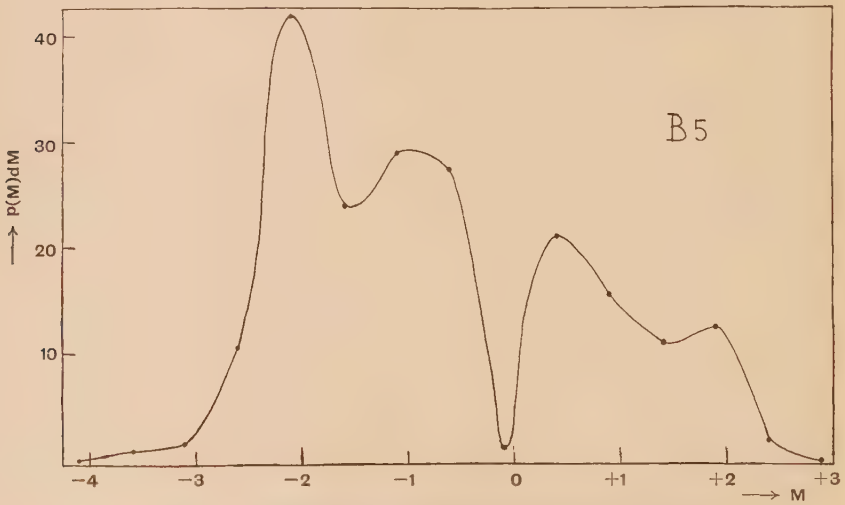


FIG. 3.—Distribution of absolute magnitudes for B5 stars.

Bo–B2 and B3 curves can be dissected into three distributions; their apparent maxima are at

| Bo–B2. | B3. |
|---|---|
| m | m |
| −2·6 | −1·1 |
| −1·6 | −0·1 |
| −0·1 | (+1·0) |

Successive maxima of the B3 curve correspond closely to those of the Bo–B2 curve shifted to the right by $1^{m}\cdot5$, in agreement with the difference of mean absolute magnitudes for these groups calculated from parallactic motion.

Passing from B3 to B5 we notice striking changes in the M-distribution curve. The B5 curve exhibits remarkably large dispersion and four well-expressed maxima of frequency. We can follow this change only in a hypothetical way. The minimum of the B3 curve at $-0^{m}\cdot5$

deepens and become very low in the B5 curve at $0^{m}\cdot0$. The left component of the B3 curve is resolved into two subcomponents with a marked minimum at $-1^{m}\cdot5$. The relative number of super-giants rapidly increases. The right-hand (double) component of B3 flattens and extends far towards fainter magnitudes.

In trying to understand these changes we should not forget some possible errors of the spectrum classification in H.D.C. It has been pointed out on an earlier occasion that amongst fainter Bo–B2 stars of H.D.C. there is present not a negligible number of O stars. A contrary

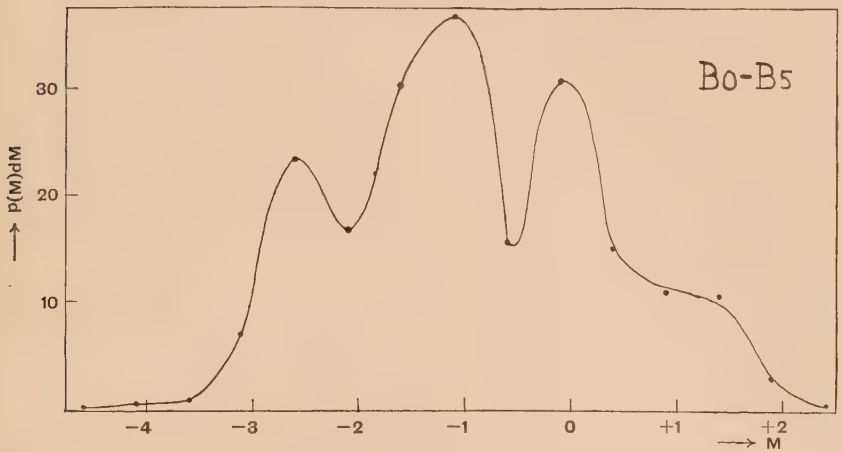


Fig. 4.—Composite M-distribution curve for a "normal" group of Bo–B5 stars.

error is to be expected in the case of B5 stars. Fainter stars classified as B5 very likely contain several B8–B9 stars more affiliated with the A than with the B group. This admixture can affect the computed M-distribution for B5 stars for fainter absolute magnitudes. This remark of course does not explain the striking shape of the B5 curve, which can hardly be attributed to any kind of observational errors.

An interesting check can be provided by our composite Bo–B5 curve. It shows the same three tops as Pannekoek's curves for the groups most favourable in this respect (*e.g.* Orion). The distances between the tops of the computed curve amount to $1^{m}\cdot5$ and $1^{m}\cdot0$. Corresponding distances for Pannekoek's two best curves are $1^{m}\cdot2$ and $1^{m}\cdot6$. The difference can be easily attributed to insufficient resolving power of the method used above, "non-normality" of local groups, etc.

[Table

TABLE I.

*F*(*y*)*dy*.

| *y*. | Bo-B2. | B3. | B5. |
|---|---|---|---|
| .. | .. | .. | .. |
| −1·88 | 7 | 11 | 13 |
| −1·78 | 9 | 14 | 15 |
| −1·68 | 11 | 18 | 19 |
| −1·58 | 14 | 23 | 25 |
| −1·48 | 17 | 28 | 31 |
| −1·38 | 22 | 35 | 39 |
| −1·28 | 27 | 45 | 49 |
| −1·18 | 35 | 56 | 61 |
| −1·08 | 81 | 73 | 73 |
| −0·98 | 99 | 73 | 73 |
| −0·88 | 81 | 110 | 107 |
| −0·78 | 50 | 114 | 87 |
| −0·68 | 87 | 69 | 146 |
| −0·58 | 74 | 98 | 60 |
| −0·48 | 81 | 81 | 60 |
| −0·38 | 93 | 53 | 40 |
| −0·28 | 68 | 12 | 33 |
| −0·18 | 19 | 28 | 0 |
| −0·08 | 43 | 4 | 20 |
| +0·02 | 31 | 4 | 0 |
| +0·12 | 31 | 4 | 6 |
| +0·22 | 0 | 8 | 0 |
| +0·32 | 0 | 0 | 0 |

TABLE II.

*F*(*x*)*dx*.

| *x*. | Observed Distribution. | | | Observed minus Computed Distribution. | | |
|---|---|---|---|---|---|---|
| | Bo-B2. | B3. | B5. | Bo-B2. | B3. | B5. |
| −2·5 | 2 | 2 | 2 | + 1 | + 2 | + 2 |
| −2·4 | 2 | 4 | 3 | − 2 | + 3 | + 2 |
| −2·3 | 5 | 5 | 6 | 0 | + 2 | + 2 |
| −2·2 | 5 | 5 | 6 | − 3 | 0 | 0 |
| −2·1 | 9 | 9 | 12 | − 2 | + 1 | + 2 |
| −2·0 | 9 | 9 | 12 | − 4 | − 3 | − 2 |
| −1·9 | 14 | 14 | 19 | − 4 | − 4 | 0 |
| −1·8 | 19 | 19 | 25 | − 3 | − 4 | 0 |
| −1·7 | 39 | 33 | 25 | + 4 | + 3 | − 7 |
| −1·6 | 55 | 47 | 21 | + 2 | +10 | −19 |
| −1·5 | 70 | 31 | 42 | + 6 | −16 | − 7 |

TABLE II.—*continued.*

| $x$. | Observed Distribution. | | | Observed minus Computed Distribution. | | |
|---|---|---|---|---|---|---|
| | Bo–B2. | B3. | B5. | Bo–B2. | B3. | B5. |
| −1·4 | 35 | 39 | 55 | −34 | −18 | − 3 |
| −1·3 | 120 | 94 | 68 | +47 | +27 | − 2 |
| −1·2 | 66 | 91 | 85 | − 9 | +13 | + 8 |
| −1·1 | 84 | 87 | 99 | + 9 | 0 | + 8 |
| −1·0 | 127 | 79 | 115 | +43 | −10 | +31 |
| −0·9 | 46 | 98 | 55 | −36 | + 8 | −26 |
| −0·8 | 57 | 53 | 48 | −11 | −32 | −29 |
| −0·7 | 49 | 87 | 48 | −11 | +15 | −12 |
| −0·6 | 67 | 80 | 51 | +14 | +21 | − 6 |
| −0·5 | 28 | 43 | 79 | −13 | − 3 | +32 |
| −0·4 | 17 | 31 | 28 | −18 | − 3 | − 7 |
| −0·3 | 30 | 13 | 40 | + 7 | − 9 | +12 |
| −0·2 | 24 | 6 | 18 | +10 | − 8 | − 2 |
| −0·1 | 7 | 14 | 3 | 0 | + 6 | − 7 |
| 0·0 | 4 | 6 | 13 | − 1 | + 1 | + 5 |
| +0·1 | 0 | 2 | 11 | 0 | − 1 | + 7 |
| +0·2 | 0 | 1 | 3 | 0 | − 1 | + 1 |
| +0·3 | 0 | 4 | 6 | 0 | + 3 | + 5 |
| +0·4 | 2 | 0 | 0 | + 2 | − 1 | − 1 |
| +0·5 | 0 | 0 | 0 | 0 | 0 | 0 |

TABLE III.

$F(M)dM$.

| M. | Bo–B2. | B3. | B5. | Composite Curve reduced to B3 (0·28 : 0·22 : 0·50) |
|---|---|---|---|---|
| −4·1 | 0·0 | 0·0 | 0·0 | 0·4 |
| −3·6 | 0·2 | 0·2 | 0·8 | 0·7 |
| −3·1 | 33·3 | 6·1 | 1·4 | 6·9 |
| −2·6 | 55·6 | 11·5 | 11·2 | 23·4 |
| −2·1 | 29·4 | 20·3 | 41·8 | 16·6 |
| −1·6 | 43·4 | 29·9 | 24·1 | 30·4 |
| −1·1 | 13·0 | 34·4 | 28·9 | 36·8 |
| −0·6 | 8·3 | 27·8 | 27·3 | 15·4 |
| −0·1 | 10·2 | 35·6 | 2·2 | 30·7 |
| +0·4 | 6·6 | 15·5 | 21·0 | 14·8 |
| +0·9 | 0·0 | 13·6 | 15·7 | 10·8 |
| +1·4 | 0·0 | 5·1 | 11·0 | 10·4 |
| +1·9 | 0·0 | 0·0 | 12·8 | 2·7 |
| +2·4 | 0·0 | 0·0 | 1·8 | 0·0 |
| +2·9 | 0·0 | 0·0 | 0·0 | 0·0 |

We have assumed in the course of the present investigation that the observed apparent magnitudes of B stars are true magnitudes, *i.e.* not affected by cosmic absorption. If there exists in interstellar space any appreciable continuous absorption, the reduced $\tau$-components as calculated with apparent magnitudes would be too large, thus producing some distortion in the resulting $x$-distribution. It seems of interest to estimate this distortion, assuming for a moment Trumpler's value of the coefficient of cosmic absorption. Obviously the largest effect is to be expected for the absolutely brightest stars of fainter apparent magnitudes. Owing to the system of weights used in this investigation only the fainter stars of P.G.C. are to be taken into account, *i.e.* stars between $5^{m}\cdot5$ and $6^{m}\cdot5$. The most luminous star ($M = -3$) of this apparent brightness would correspond to a distance of about 1000 parsecs; the distortion of M-distribution would be about $0^{m}\cdot7$ for the brightest stars. This is only an upper limit, as luminous stars are recruited from all distances. We can therefore estimate provisionally $0^{m}\cdot3 - 0^{m}\cdot4$ as a possible distortion of M-distribution on the side of the most luminous stars, which can hardly change our final deductions as to the shape of the luminosity curve.

As could be anticipated on statistical grounds, the distances between the two main tops of the computed M curves are larger than those between two divisions of the Mount Wilson classification. In an earlier work * I have shown that considerable dispersion in colour of the early B stars is an absolute magnitude phenomenon, whitish B stars being $1^{m}\cdot5$ fainter absolutely than those showing yellowish colours. It seems attractive to correlate the main components of the M-distributions with such a colour effect, but unfortunately we have not so far any direct indication in this respect. Careful investigation of the colour indices in such easily separable groups as Orion or P Cygni are necessary in order to settle this question. Such investigations are much needed in all respects.

It seems premature to correlate the main minima in M-distributions of early B stars with such a phenomenon as dwarf-giant division for later types. Early B stars are also closely associated with O-type stars, which are known to show relatively large dispersion in absolute magnitudes. These stars are, moreover, subdivided into two groups (O absorption and Wolf-Rayet stars) showing some difference in mean absolute magnitudes. Taken as a whole the question seems to be too complicated to be definitely settled without collecting additional data of various kinds.

* *H.C.*, **339**, 15, 1929; substantiated by Öhman (*Medd. Upsala*, 47, 1930).

*Astronomical Observatory,*
*Kharkov, U.S.S.R.,*
1931 *February.*

## *Effect of Atmospheric Absorption in Stellar Spectrophotometry.*

By J. Dufay.

(*Communicated by Professor Chapman.*)

1. Atmospheric absorption is perhaps the most important source of error in stellar spectrophotometry. In their recent works, Professor Sampson,* Messrs. Greaves, Davidson, and Martin,† and Dr. Gerasimovič ‡ attempted to correct the observations for the effect of differential absorption, but the adopted treatment must be regarded as a rough and empirical first approximation.§ I will show, in the present note, in what way the treatment should be modified in order to lead to more correct results.

2. In modern investigations the spectrophotometric temperature of a star is determined by means of the *gradient* relative to a standard comparison star at given temperature. The *relative gradient* G, first introduced by Professor Sampson, is defined as

$$G = -0{\cdot}922\frac{d\Delta m_\lambda}{d(1/\lambda)} \quad . \quad . \quad . \quad . \quad (1)$$

$\lambda$ being the wave-length and $\Delta m_\lambda$ the difference in magnitude between the two stars at wave-length $\lambda$. The magnitude differences $\Delta m_\lambda$ are plotted against the reciprocal wave-lengths $1/\lambda$. If the stars radiate as black bodies, according to Planck's law, the representative diagram is, with a good approximation, a straight line. The slope of the line gives the relative gradient G.

We have implicitly assumed that the two stars are at the same altitude, but this is not generally true. All the investigators have recognised that the observed gradients vary with the zenith distances of the stars, and they have applied to the *observed gradient* G′ a correction in order to find the *true gradient* G that should be observed when the two stars are at the same altitude.

The correcting term now usually added has the form :

$$G - G' = A(\sec \zeta_1 - \sec \zeta_2) \quad . \quad . \quad . \quad (2)$$

where $\zeta_1$ is the zenith distance of the observed star, $\zeta_2$ the zenith distance of the comparison star (the Pole Star in the work of Professor Sampson), and A a constant.

According to formula (2), the values of G′ being plotted against $(\sec \zeta_1 - \sec \zeta_2)$, we should obtain a straight line. This is not really the case for the Greenwich observations (see fig. 1, the graph drawn from the Greenwich data). Professor Sampson's diagrams show large

* *M.N.*, **83**, 174, 1923 ; **85**, 212, 1925 ; **90**, 636, 1930.

† *M.N.*, **86**, 33, 1925 ; **87**, 352, 1927 ; **90**, 104, 1929.

‡ *H.C.O.*, Circ. 339, 1929.

§ Professor Sampson writes in his recent paper : "The treatment of atmospheric absorption resulting in a zenith distance correction, as given below, must be regarded still as preliminary" (*M.N.*, **90**, 637, 1930).

dispersion. Only Gerasimovič obtains, by chance, a straight line. He has also computed the value of A corresponding to the solar observations of Abbot and Fowle at Washington, and he remarks that "the deviation from the straight line is rather great." That is indeed not surprising, for the relation (2), in fact, is incorrect.

Let $\Delta m_\lambda'$ be the apparent magnitude difference at wave-length $\lambda$;

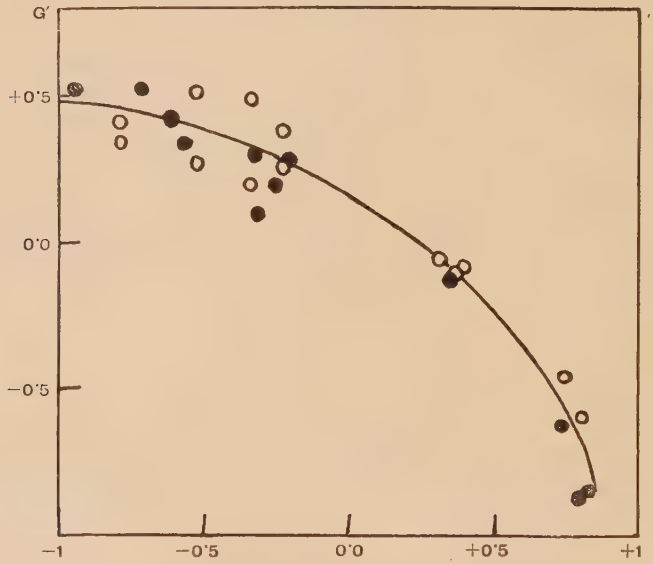


Fig. 1.

Abscissæ = sec $\zeta_1$ − sec $\zeta_2$. Ordinate = observed gradients.

Black dots represent comparisons between $\alpha$ Lyr. and $\varepsilon$ UMa, circles comparisons between $\alpha$ Lyr. and $\zeta^1$ UMa (see *M.N.*, **87**, 356, Table II.).

$\Delta m_\lambda$ the true difference as observed at the same altitude. We may write:

$$\frac{d(\Delta m_\lambda' - \Delta m_\lambda)}{d(1/\lambda)} = \frac{A}{0{\cdot}922}(\sec \zeta_1 - \sec \zeta_2),$$

hence, by integration,

$$\Delta m_\lambda' - \Delta m_\lambda = \frac{1{\cdot}086A}{\lambda}(\sec \zeta_1 - \sec \zeta_2) + \text{Const.}$$

*Relation* (2) *assumes therefore that atmospheric absorption, expressed in magnitude, is a linear function of reciprocal wave-length* $1/\lambda$. This hypothesis has, however, neither observational nor theoretical support.

3. Since the absorption coefficient is not a linear function of $1/\lambda$, *differential absorption does not simply change the slope of the theoretical straight line represented by equation* (1), *but distorts it*, so that the representative diagram should exhibit more or less marked curvature.

Abbot's and Fowle's observations at stations of high altitude have

shown that, with a pure blue sky, atmospheric absorption in the largest part of the visible and ultra-violet spectrum results only from molecular scattering.* The absorption coefficient of the atmosphere may be generally expressed by :

$$K_\lambda = a + b/\lambda^4.$$

The constant $b$ has nearly the exact value predicted by the theory of molecular scattering, and the constant $a$ is always small or zero.† At stations of low altitude, the effect of dust and smoke is more apparent : the constant $b$ increases, and the absorption coefficient will not be an exact linear function of $1/\lambda^4$.

We suppose, for instance, that a star of spectral type $A_0$, observed at the zenith distance $\zeta_1$, is compared with the Pole Star, at 45° from the zenith. The atmosphere is assumed perfectly pure, free from dust and smoke, though the observations are made at sea-level. Computing the absorption coefficients by the practical formula given previously by Cabannes and the writer,‡

$$K_\lambda = \frac{1{\cdot}048}{\lambda^4} 10^{-24} cm^{-1} \quad . \quad . \quad . \quad (3)$$

we find,

$$\Delta m_\lambda' - \Delta m_\lambda = \frac{9{\cdot}103}{\lambda^4} \cdot 10^{-19}(\sec \zeta_1 - \sec 45°).$$

Numerical results, relative to some wave-lengths, for $\zeta_1 = 55°$, 60°, and 65° are summarised below :

| $\lambda(\mu)$ | | 0·7 | 0·6 | 0·5 | 0·45 | 0·4 | 0·38 |
|---|---|---|---|---|---|---|---|
| $1/\lambda$ | | 1·429 | 1·667 | 2·000 | 2·222 | 2·500 | 2·632 |
| $\zeta_1$ | 55° | 0·012 | 0·023 | 0·048 | 0·073 | 0·117 | 0·144 |
| | 60° | 0·022 | 0·041 | 0·085 | 0·130 | 0·208 | 0·256 |
| | 65° | 0·036 | 0·067 | 0·139 | 0·211 | 0·339 | 0·416 |

If the $A_0$ star were observed at the same zenith distance as the Pole Star, we should obtain the theoretical straight line of fig. 2. According to Sampson, the slope of this line (1·247) corresponds to the gradient 1·15. The curvature of the lines corresponding to zenith distances 55° and 60° is, in the figure, very conspicuous, but in practical work it has possibly escaped notice on account of the scattering of the observational dots. With decreasing wave-lengths, the slopes of the three curves vary from 1·18 to 1·06, from 1·14 to 0·92, and from 1·07 to 0·73, involving errors in the observed gradients of perhaps more than 10 per cent.

4. Evidently the most accurate method is to compare the stars at nearly the same altitude, so as to avoid introducing large corrections for differential absorption, but this is not always possible. Then the appro-

* This conclusion has been recently confirmed by Link and Hugon's terrestrial experiments at Pic du Midi (*C.R.*, **190**, 810, 1930).

† See Cabannes and Dufay, *Journ. Phys.*, **7**, 257, 1926. In the yellow part of the spectrum only, selective absorption by ozone slightly increases the optical density of the atmosphere.

‡ *Journ. Phys.*, **8**, 125, 1927. $K_\lambda$ is defined as $I/I_0 = e^{-K_\lambda x}$; in the formula (3) $\lambda$ is expressed in *cm.*

priate method in order to correct the observational data for atmospheric absorption is not to add a correcting term to the observed gradient, but *to correct separately each observed value of the magnitude difference* $\Delta m_\lambda'$ *before computing the gradient.* The true magnitude difference, as observed at the same zenith distance, is

$$\Delta m_\lambda = \Delta m_\lambda' + B_\lambda(\sec \zeta_1 - \sec \zeta_2).$$

Without any assumption as to the law of variation of $B_\lambda$ with wave-

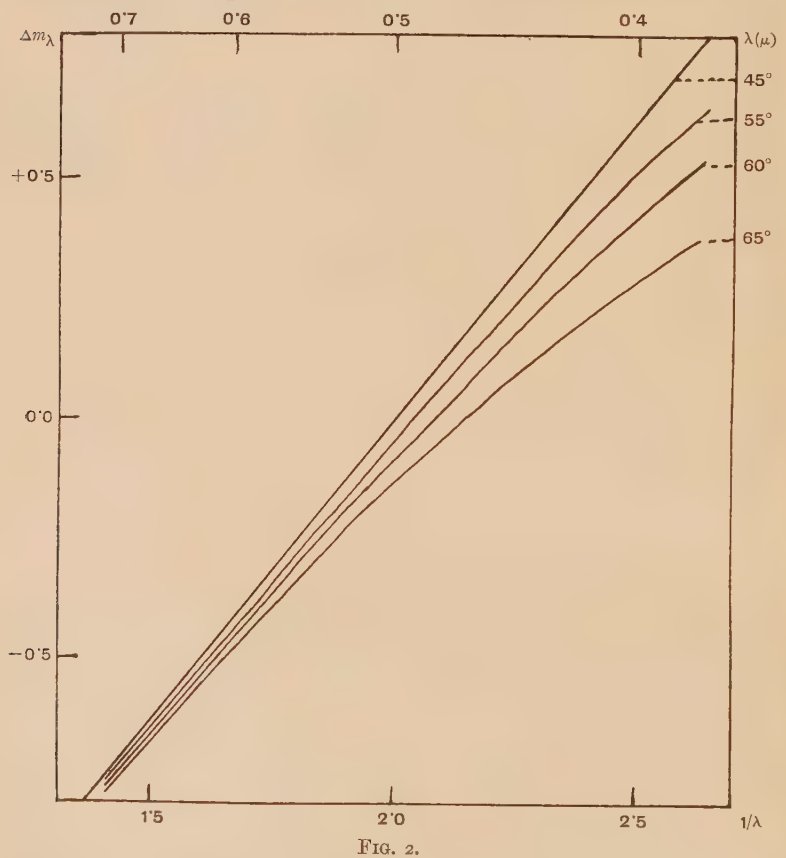


Fig. 2.

length, the mean value of this quantity may be determined, for each wave-length, by plotting the observed magnitude differences $\Delta m_\lambda'$ against (sec $\zeta_1$ − sec $\zeta_2$).

The correct method is indeed longer and much more laborious than the empirical and theoretically incorrect method used at present, but the difficult and important researches undertaken during recent years by English astronomers certainly merit the most accurate reduction.

*Observatoire de Lyon.*

*Expansion of the Disturbing Function in Terms of the True Longitude of the Disturbed Planet.* By C. A. Shook.

(*Communicated by Professor E. W. Brown.*)

1. The purpose of this paper is to give a method of performing the expansion indicated in the title, and to write out this expansion to the second order. It is planned to extend the expansion to a higher order in the near future. In the usual notation, the disturbing function R is

$$\mathrm{R} = m'\left(\frac{1}{\Delta} - \frac{r\cos \mathrm{S}}{r'^2}\right),$$

$$\Delta^2 = r^2 + r'^2 - 2rr'\cos \mathrm{S},$$

$$\cos \mathrm{S} = \cos(v-\theta)\cos(v'-\theta) + \cos \mathrm{I}\sin(v-\theta)\sin(v'-\theta),$$

the plane of the disturbing body being taken as reference plane. The first part of the work consists of substituting for $r$ and $r'$ their values in terms of $v$ and $v'$ respectively. For this various methods are available. The method adopted here is that recently given by E. W. Brown (*Astron. Journal*, No. 935, 1930). The resulting expression is next arranged as a series of cosines of multiples of $v$ and $v'$. Finally, there is substituted for $v'$ its value in terms of $v$. This is the chief part of the labour. We begin with $1/\Delta$. The second term of R is easily obtained from this (see § 10).

2. The value of $r$ in the usual notation is

$$r = \frac{a(1-e^2)}{1+e\cos f}, \qquad f = v - \varpi.$$

In order to make use of known expansions it is convenient to put $e = 2\eta/(1+\eta^2)$, so that

$$r = \frac{a}{1+\eta^2}\frac{(1-\eta^2)^2}{1+\eta^2+2\eta\cos f} = \frac{a}{1+\eta^2}\mathrm{P} = r_0\mathrm{P}, \text{ say.}$$

Similar equations hold with all letters accented. Finally, let

$$\alpha = \frac{r_0}{r_0'} = \frac{a}{a'}\frac{1+\eta'^2}{1+\eta^2}.$$

Use is now made of the theorem (*loc. cit.*, § 3),

$$f(p\alpha) = p^{\mathrm{D}}f(\alpha), \qquad \mathrm{D} = \alpha\frac{d}{d\alpha}.$$

Applying this theorem, we have

$$\frac{1}{\Delta} = \frac{1}{r'}f\left(\frac{r}{r'}\right) = \frac{1}{r_0'\mathrm{P}'}f\left(\alpha\frac{\mathrm{P}}{\mathrm{P}'}\right) = \frac{1}{r_0'\mathrm{P}'}\left(\frac{\mathrm{P}}{\mathrm{P}'}\right)^{\mathrm{D}}f(\alpha),$$

or

$$\frac{1}{\Delta} = \frac{1}{r_0'}\mathrm{P}^{\mathrm{D}}\mathrm{P}'^{-\mathrm{D}-1}\frac{1}{\Delta_0}. \qquad . \qquad . \qquad . \qquad (\mathrm{A})$$

where

$$\Delta_0^2 = 1 + \alpha^2 - 2\alpha\cos \mathrm{S}.$$

For the expansion of $P^D$ we have *

$$\left[\frac{(1-\eta^2)^2}{1+\eta^2+2\eta\cos f}\right]^D = (1-\eta^2)\sum_i \eta_i \cos if, \qquad i = 0, \pm 1 \ldots \quad \text{(B)}$$

$$\eta_i = \frac{D(D+1)\ldots(D+i-1)}{1\cdot 2\ldots i}(-\eta)^i\left[1+\frac{1-D}{1}\frac{1-D+i}{i+1}\eta^2 + \frac{(1-D)(2-D)}{1\cdot 2}\frac{(1-D+i)(2-D+i)}{(i+1)(i+2)}\eta^4+\ldots\right]$$

The value of $P'^{-D-1}$ is obtained by replacing $\eta$, $\eta_i$, $f$ by the same letters with accents and putting $-D-1$ for D. These values are to be substituted in (A).

3. It is now necessary to expand $1/\Delta_0$ in powers of the inclination and to express each term of this expansion as a series of cosines of multiples of $v$ and $v'$. Putting $\kappa = \cos^2 \frac{1}{2}I$, the expression for cos S may be written

$$\cos S = \kappa \cos(v - v') + \sin^2 \tfrac{1}{2}I \cos(v + v' - 2\theta) \quad . \quad (3.1)$$

Substituting this value of cos S in $1/\Delta_0$ and expanding in powers of the last term by the binomial theorem, we get, if $T = \tan \frac{1}{2}I$ (E. W. Brown, *loc. cit.*, § 5),

$$\frac{1}{\Delta_0} = R_0 + R_1 T^2 2\cos(v + v' - 2\theta) + R_2 T^4 \frac{2^2}{2!}\cos^2(v + v' - 2\theta) + \ldots \quad \text{(C)}$$

where

$$R_{s-\frac{1}{2}} = \frac{\frac{1}{2}\cdot\frac{3}{2}\ldots(s-1)(a\kappa)^{s-\frac{1}{2}}}{[1+a^2-2a\kappa\cos(v-v')]^s}, \qquad s = 1/2,\ 3/2\ \ldots, \quad (3.2)$$

the numerator being unity when $s = 1/2$.

Finally, $R_{s-\frac{1}{2}}$ is obviously expansible in a Fourier cosine series. The equation

$$R_{s-1/2} = \Sigma\, \beta_s^{(i)} \cos i(v - v'), \qquad i = 0, \pm 1 \ldots \quad \text{(D)}$$

serves to define the coefficients $\beta_s^{(i)}$. It is supposed that $\beta^{(i)} = \beta^{(-i)}$.

4. Equations (A) to (D) furnish the material necessary for the expansion of $1/\Delta$ in a series of cosines of multiples of $v$ and $v'$, with coefficients depending on $\beta_s^{(i)}$ and their derivatives, and on $\eta$, $\eta'$, and T. In substituting (D) in (C), the powers of $\cos(v + v' - 2\theta)$ are to be expressed as cosines of multiples of $(v + v' - 2\theta)$ and these in turn combined with $\cos i(v - v')$. Let us put $\beta_s^{(i)} = a_i, b_i, c_i \ldots$ for $s = 1/2,\ 3/2 \ldots$ When we neglect terms of the eighth order in T, (C) becomes

$$\frac{1}{\Delta_0} = \sum_i \{(a_i + c_i T^4)\cos i(v - v') + (2b_i T^2 + d_i T^6)\cos[(i+1)v - (i-1)v' - 2\theta] + c_i T^4 \cos[(i+2)v - (i-2)v' - 4\theta]\} \quad . \quad . \quad . \quad (4.1)$$

* Tisserand, *Méc. Cél.*, **1**, 280 (L'), and 271 (A).

This value of $1/\Delta_0$ and the expanded values of $P^D$ and $P'^{-D-1}$ are to be substituted in (A), after which products of cosines are to be expressed as sums of cosines. The result to the second order is

$$\begin{aligned}\frac{a'}{\Delta} = \sum_i \{&[1 + \eta^2(D^2 - 2D) + \eta'^2(D + 2)^2]a_i \cos is \\ &- 2\eta D a_i \cos(is + f) + 2\eta'(D + 1)a_i \cos(is + f') \\ &+ (D^2 + D)a_i[\eta^2 \cos(is + 2f) - 2\eta\eta' \cos(is + f \pm f') + \eta'^2 \cos(is + 2f')] \\ &+ 2 \tan^2\tfrac{1}{2}I b_i \cos[(i + 1)s + 2v' - 2\theta]\} \quad . \quad . \quad . \quad . \quad . \quad (4.2)\end{aligned}$$

where $s = v - v'$.

5. The final step consists of substituting for $v'$ in terms of $v$. The relation between these is given by the two equations,

$$\begin{aligned} v' &= g' + \varpi' + \Sigma b_j \sin jg', \\ nt + \epsilon &= v + \Sigma a_i \sin if, \end{aligned}$$

where $a_i$ and $b_j$ are functions of $\eta$ and $\eta'$ respectively. We have to eliminate $t$ from these equations, remembering that

$$g' = n't + \epsilon' - \varpi'.$$

Let us put

$$m = n'/n, \qquad \epsilon_1 = \epsilon' - m\epsilon, \qquad v_1 = mv + \epsilon_1, \qquad f_1 = v_1 - \varpi'.$$

Multiplying the first by $m$ and adding $\epsilon_1$ to both sides, we get

$$g' + \varpi' = v_1 + \Sigma m a_i \sin if$$

or

$$g' = f_1 + \Sigma m a_i \sin if.$$

Substituting this in the second equation, we find

$$v' = v_1 + y,$$

$$y = \sum_i m a_i \sin if + \sum_j b_j \sin j\left[f_1 + \sum_i m a_i \sin if\right] \quad . \quad (5.1)$$

If we put

$$z = \Sigma j m a_i \sin if$$

for the moment, the last term after expansion becomes

$$\sum_j b_j \left\{ \sin jf_1 \left(1 - \frac{z^2}{2!} + \frac{z^4}{4!} - \ldots\right) + \cos jf_1 \left(-\frac{z^3}{3!} + \frac{z^5}{5!} - \ldots\right)\right\}.$$

It is obvious that $y$ is of the form

$$y = \Sigma c_{j,j_1} \sin(jf + j_1 f_1) \quad . \quad . \quad . \quad (5.2)$$

where we may suppose that $j, j_1 = 0, \pm 1, \pm 2. \ldots$ It is convenient to write $y$ in the equivalent form,

$$y\sqrt{-1} = \Sigma c_{j,j_1} \exp (jf + j_1 f_1)\sqrt{-1}.$$

Any power of $y$ will evidently have the same form. We put

$$\frac{(y\sqrt{-1})^\kappa}{\kappa!} = \Sigma c_{\kappa,j,j_1} \exp (jf + j_1 f_1)\sqrt{-1}.$$

6. When the coefficients $c_{\kappa,j,j_1}$ have been found for $\kappa = 1$, their values for other values of $\kappa$ can be found from a recurrence formula. We have

$$\frac{(y\sqrt{-1})^{\kappa+1}}{(\kappa+1)!} = \frac{1}{\kappa+1}(y\sqrt{-1})\frac{(y\sqrt{-1})^\kappa}{\kappa!}$$

$$= \frac{1}{\kappa+1}\Sigma c_{1,g,g_1} c_{\kappa,h,h_1} \exp [(g+h)f + (g_1+h_1)f_1]\sqrt{-1},$$

where $g, g_1, h, h_1 = 0, \pm 1. \ldots$ Putting $h = j - g$, $h_1 = j_1 - g_1$, we find

$$c_{\kappa+1,j,j_1} = \frac{1}{\kappa+1}\Sigma c_{1,g,g_1} c_{\kappa,j-g,j_1-g_1}, \quad . \quad . \quad (6.1)$$

where $g, g_1 = 0, \pm 1. \ldots$

The following relations are of importance:—

$$\left.\begin{aligned} c_{\kappa,-j,j_1}(m) &= c_{\kappa,j,j_1}(-m) \\ c_{\kappa,j,-j_1}(m) &= (-1)^\kappa c_{\kappa,j,j_1}(-m) \\ c_{\kappa,-j,-j_1}(m) &= (-1)^\kappa c_{\kappa,j,j_1}(+m) \end{aligned}\right\} \quad . \quad . \quad (6.2)$$

The truth of these relations for $\kappa = 1$ follows immediately from (5.1). The first relation, for example, results from the fact that if we change the sign of $f$ and $m$ in (5.1), $y$ is not altered. Applying this to (5.2) we have

$$y = \Sigma c_{j,j_1}(-m) \exp (-jf + j_1 f_1)\sqrt{-1}, \qquad j, j_1 = 0, \pm 1. \ldots$$

If in this sum we change the sign of $j$, we find

$$c_{-j,j_1}(-m) = c_{j,j_1}(m).$$

The proof of (6.2) for all values of $\kappa$ is now easily made by mathematical induction, using the relation (6.1). The importance of the relations (6.2) lies in the fact that they enable us to confine our attention to values of $j, j_1, \geqq 0$.

7. The following table gives the values of $c_{\kappa,j,j_1}$ to the fourth order. The factor $\eta^j \eta'^{j_2}$ has been suppressed for convenience. It may be noted that $c_{0,j,j_1}$ is zero unless $j$ and $j_1$ are both zero, in which case it is unity.

$$c_{0,0,0} = 1, \qquad c_{1,0,0} = 0 = c_{3,0,0}.$$

$$c_{2,0,0} = -(4m^2\eta^2 + 4\eta'^2 + 16m^2\eta^2\eta'^2 - \tfrac{23}{4}m^2\eta^4 - \tfrac{23}{4}\eta'^2).$$

$$c_{4,0,0} = 4m^4\eta^4 + 4\eta'^4 + 16m^2\eta^2\eta'^2.$$

| $j$ | $j_1$ | $\kappa=1$. | $\kappa=2$. |
|---|---|---|---|
| 1 | 0 | $-2m(1-\eta^2)$ | $3m^2\eta^2$ |
| 0 | 1 | $2-8m^2\eta^2-3\eta'^2$ | $-(16m^2\eta^2+5\eta'^2)$ |
| 2 | 0 | $\frac{3}{2}m-2m\eta^2$ | $2m^2-\frac{20}{3}m^2\eta^2$ |
| 1 | 1 | $\begin{cases}-4m+6m\eta'^2\\ +2\eta^2(4m+3m^2+4m^3)\end{cases}$ | $\begin{cases}-4m+14m\eta'^2\\ +4\eta^2(m+3m^2+2m^3)\end{cases}$ |
| 0 | 2 | $\frac{5}{2}-40m^2\eta^2-\frac{20}{3}\eta'^2$ | $2-56m^2\eta^2-\frac{28}{3}\eta'^2$ |

| $j$ | $j_1$ | $\kappa=3$. | $\kappa=4$. |
|---|---|---|---|
| 1 | 0 | $4m^3\eta^2+8m\eta'^2$ | .. |
| 0 | 1 | $-(8m\eta^2+4\eta'^2)$ | .. |
| 2 | 0 | $-(6m^3\eta^2+6m\eta'^2)$ | $-(\frac{9}{8}m^4\eta^2+8m^2\eta'^2)$ |
| 1 | 1 | $6\eta^2(m^2+3m^3)-\frac{34}{3}m\eta'^2$ | $8m^3\eta^2+8m\eta'^2$ |
| 0 | 2 | $-(\frac{110}{3}m^2\eta^2-10\eta'^3)$ | $-(8m^2\eta^2+\frac{8}{3}\eta'^2)$ |

| | | $\kappa=1$. | $\kappa=2$. | $\kappa=3$. | $\kappa=4$. |
|---|---|---|---|---|---|
| 3 | 0 | $-\frac{4}{3}m$ | $-3m^2$ | $-\frac{4}{3}m^3$ | .. |
| 2 | 1 | $3m+4m^2$ | $3m+8m^2$ | $4m^2$ | .. |
| 1 | 2 | $-10m$ | $-13m$ | $-4m$ | .. |
| 0 | 3 | $\frac{13}{3}$ | 5 | $\frac{4}{3}$ | .. |
| 4 | 0 | $\frac{5}{4}m$ | $\frac{21}{24}m^2$ | $3m^3$ | $\frac{9}{8}m^4$ |
| 3 | 1 | $-(\frac{5}{3}m+6m^2+\frac{8}{3}m^3)$ | $-(\frac{8}{3}m+12m^2+8m^3)$ | $-(8m^2+6m^3)$ | $-\frac{8}{3}m^3$ |
| 2 | 2 | $\frac{15}{2}m+20m^2$ | $\frac{30}{4}m+36m^2$ | $3m+\frac{11}{3}m^2$ | $4m^2$ |
| 1 | 3 | $-26m$ | $-\frac{116}{3}m^3$ | $-18m$ | $-\frac{8}{3}m$ |
| 0 | 4 | $\frac{103}{12}$ | $\frac{283}{24}$ | 5 | $\frac{2}{3}$ |

8. After (B), (C), (D) have been substituted in (A), its form is like that of (4.2). Hence we have to put $v' = v_1 + y$ in an expression of the form $\cos(hv' + p)$, where $h$ is an integer and $p$ depends on $v$, $\varpi$, $\varpi'$, $\theta$. Let R.P. denote "the real part of." Then

$$\cos(hv' + p) = \text{R.P.} \exp(hv' + p)\sqrt{-1}$$
$$= \text{R.P.}[\exp hy\sqrt{-1}][\exp(hv_1 + p)\sqrt{-1}].$$

Now

$$\exp hy\sqrt{-1} = \Sigma h^\kappa \frac{(y\sqrt{-1})^\kappa}{\kappa!}, \qquad \kappa = 0, 1, 2 \ldots$$
$$= \Sigma h^\kappa c_{\kappa, j, j_1} \exp(jf + j_1 f_1)\sqrt{-1}, \quad j, j_1 = 0, \pm 1, \ldots$$

Substituting this value,

$$\cos(hv' + p) = \text{R.P.}\Sigma h^\kappa c_{\kappa, j, j_1} \exp(hv_1 + p + jf + j_1 f_1)\sqrt{-1}$$
$$= \Sigma h^\kappa c_{\kappa, j, j_1} \cos(hv_1 + p + jf + j_1 f_1) \quad . \quad . \quad . \quad \text{(E}$$

This formula is applied in turn to each term of (4.2). The result obtained from each term will be a series of terms similar to those of (4.2), except that $f'$ and $v'$ are replaced by $f_1$ and $v_1$.

9. The value of $1/\Delta$ to the second order is

$$\begin{aligned}\frac{a'}{\Delta} = \sum_i \{&[1 + \eta^2(D^2 - 2D - 4m^2i^2) + \eta'^2(D^2 - 4i^2)]a_i \cos is_1 \\ &- 2\eta(D - 2mi)a_i \cos(is_1 + f) + 2\eta'(D + 1 - 2i)a_i \cos(is_1 + f_1) \\ &+ \eta^2[D^2 + D(1 - 4mi) - 3mi + 4m^2i^2]a_i \cos(is_1 + 2f) \\ &- 2\eta\eta'[D^2 + D(1 \mp 2i - 2mi \pm 2m) \pm 2m - 6mi \pm 4mi^2]a_i \cos(is_1 + f \pm f_1) \\ &+ \eta'^2[D^2 + D(5 - 4i) + 4i^2 - 9i + 4]a_i \cos(is_1 + 2f_1) \\ &+ 2\tan^2 \tfrac{1}{2}\mathrm{I} b_i \cos[(i + 1)s_1 + 2v_1 - 2\theta]\} \quad . \quad . \quad . \quad . \quad (\mathrm{F})\end{aligned}$$

in which

$$\eta = \frac{e}{2} \text{ (to the second order), since } e = \frac{2\eta}{1 + \eta^2},$$

$a_i$, $b_i$ are defined in § 4, and

$$D = \alpha\frac{d}{d\alpha}, \qquad \alpha = \frac{a}{a'}\frac{1 + \eta'^2}{1 + \eta^2},$$

$$m = n'/n, \quad \epsilon_1 = \epsilon' - m\epsilon, \quad v_1 = mv + \epsilon_1 = f_1 + \varpi, \quad s_1 = v - v_1.$$

10. The second term of R is easily obtained from the value of $1/\Delta$. If in (4.1) we put $a_{+1} = a_{-1} = b_0 = -\alpha\kappa/2$ and put $\beta^{(i)}_{j+\frac{1}{2}} = 0$ for all other values of $j$ and $i$, the value of $1/\Delta_0$ becomes

$$-\alpha\kappa \cos(v - v') - \alpha\kappa\mathrm{T}^2 \cos(v + v' - 2\theta).$$

If this value is substituted in (A), and D taken equal to unity, $1/\Delta$ becomes

$$-\frac{\alpha}{r_0'}\frac{\mathrm{P}}{\mathrm{P}'^2}[\kappa \cos(v - v') + \sin^2 \tfrac{1}{2}\mathrm{I} \cos(v + v' - 2\theta)].$$

Putting $\alpha = r_0/r_0'$, $r_0\mathrm{P} = r$, $r_0'\mathrm{P}' = r'$, we see by (3.1) that this is nothing but $-r \cos \mathrm{S}/r'^2$. Hence we have the following rule for finding the second term of R :—

$$-\frac{r \cos \mathrm{S}}{r'^2} \text{ is what } \frac{1}{\Delta} \text{ becomes when we put}$$

$$a_1 = a_{-1} = b_0 = -\frac{\alpha\kappa}{2}; \quad \text{all other } \beta^{(i)}_{j+\frac{1}{2}} = 0; \qquad D = 1.$$

If we apply this rule to the expansion of $1/\Delta$ in § 9, and then put $\kappa = \cos^2 \frac{1}{2}\mathrm{I} = 1 - \mathrm{T}^2$, to the second order, we get

$$\begin{aligned}-\frac{r \cos \mathrm{S}}{r'^2} = -\frac{a}{a'^2}\{&[1 - \eta^2(1 + 4m^2) - 3\eta'^2 - \tan^2 \tfrac{1}{2}\mathrm{I}] \cos is_1 \\ &- \eta(1 \pm 2m) \cos(s_1 \mp f) + 4\eta' \cos(s_1 - f_1) \\ &+ \tfrac{1}{2}\eta^2[(-2 - 3m + 4m^2) \cos(s_1 + 2f) + (6 + 3m + 4m^2) \cos(s_1 - 2f)] \\ &- 4\eta\eta'(1 \pm 4m) \cos(s_1 \mp f - f_1) \\ &+ \tfrac{1}{2}\eta'^2[\cos(s_1 + 2f_1) + 27 \cos(s_1 - 2f_1)] \\ &+ \tan^2 \tfrac{1}{2}\mathrm{I} \cos(s_1 + 2v_1 - 2\theta)\}.\end{aligned}$$

*Bethlehem, Pa.:*
1930 *November* 29.

## *Note on Astronomical Refraction.*

By Alan Fletcher, M.A.

(*Communicated by W. M. Smart.*)

1. The usual equation giving refraction R at apparent zenith distance $\zeta$, on the assumption that the surfaces of equal refractivity are concentric spheres, is

$$\mathrm{R} = -\sin\zeta\int\frac{d\mu/\mu}{\sqrt{\dfrac{r^2\mu^2}{r_0^2\mu_0^2}-\sin^2\zeta}} \quad . \quad . \quad . \quad (1)$$

where $\mu$ is the refractive index at distance $r$ from the centre, and, as elsewhere in this note, (*a*) the suffix o indicates values at the place of observation, (*b*) the integration is to be performed outwards (so that $r$ increases from $r_0$ to $\infty$ and $\mu$ decreases from $\mu_0$ to 1).

This equation may be written

$$\left.\begin{aligned} \mathrm{R} &= -\sin\zeta\int\frac{d\nu'}{\sqrt{2u+\cos^2\zeta}} \\ 2u &= \frac{r^2\mu^2}{r_0^2\mu_0^2}-1, \qquad \nu' = \log_e\mu \end{aligned}\right\} \quad . \quad . \quad (2)$$

in which

$u$ is zero when $r = r_0$, and increases with $r$ (except where temperature is increasing with height at more than about 1° C. per 9 metres). If we write $\nu$ for the refractivity $\mu - 1$, $\nu'$ equals $\nu - \frac{1}{2}\nu^2$ . . . and differs little from $\nu$.

2. If we make the nearly Laplacian hypothesis that

$$\nu' = \mathrm{C}\left(1+\frac{fu}{l}\right)e^{-u/l} \quad . \quad . \quad . \quad . \quad (3)$$

where C, $l$, $f$ are independent of $u$, we find by integration of (2) that

$$\left.\begin{aligned} \mathrm{R} &= \frac{\mathrm{C}}{\sqrt{2l}}\sin\zeta[f\mathrm{T}+2(1-\tfrac{1}{2}f-f\mathrm{T}^2)\psi(\mathrm{T})] \\ \mathrm{T} &= \frac{\cos\zeta}{\sqrt{2l}}, \qquad \psi(\mathrm{T}) = e^{\mathrm{T}^2}\int_{\mathrm{T}}^{\infty}e^{-t^2}dt \end{aligned}\right\} \quad . \quad (4)$$

where

Extensive tables of the function $\psi$ were constructed by Radau.*

3. It is well known that the refraction at a given moderate zenith distance depends for all practical purposes on the two independent variables $\nu_0$ and $\mathrm{H}_0$, the latter being the ratio $l_0/r_0$ of the height $l_0$ of the homogeneous atmosphere to $r_0$. For example, Rayleigh † found

$$\mathrm{R} = \nu_0(1-\mathrm{H}_0)\tan\zeta - \nu_0(\mathrm{H}_0-\tfrac{1}{2}\nu_0)\tan^3\zeta \quad . \quad . \quad (5)$$

which is the common element of all expressions for refraction and the fundamental formula of refraction for practical purposes; equivalent though frequently less direct expressions are a commonplace of

* *Annales de l'Observatoire de Paris, Mémoires*, **18**, 1885.

† *Phil. Mag.*, **36**, 141, 1893.

refraction theory, inasmuch as (5) must be obtained from any expression for the refraction containing two or more adjustable constants when expanded in powers of $\nu_0$, $H_0$ as far as $\nu_0^2$, $\nu_0 H_0$ (to which order (5) is correct, the term in $\nu_0^2 \tan \zeta$ vanishing); no reasonable theory differs from (5) by more than a few thousandths, hundredths, tenths of a second at $\zeta = 60°$, $70°$, $75°$ respectively. At rather larger zenith distances the refraction still depends to a considerable degree of accuracy simply on $\nu_0$ and $H_0$, though (5) ceases to sum up this dependence as accurately as it exists. At large zenith distances the refraction depends to an appreciable extent, and beyond $\zeta =$ about $85°$ to an undue extent for practical purposes, on the particular function $\nu'(u)$ used in integrating (2), and no introduction of a third independent variable suffices to the same extent; nevertheless, the refraction depends mainly on $\nu_0$, $H_0$ and the value of $d\mu/dr$ in the first few kilometres above the ground, and we shall write $r_0(-d\mu/dr)_0/\nu_0 = G_0$.

It remains to relate the quantities C, $l$, $f$ occurring in the formula (4) with the quantities $\nu_0$, $H_0$, $G_0$, which at a given place of observation are determined mainly by the atmospheric density, temperature, and vertical temperature gradient respectively; alternatively, with $\nu_0$, $H_0$, and the horizontal refraction.

4. The identification

$$C = \nu_0' \quad . \quad . \quad . \quad . \quad . \quad (6)$$

is implicit in (3), while putting $\zeta = 90°$ in (4) gives

$$\frac{\sqrt{\pi}(1 - \frac{1}{2}f)C}{\sqrt{2l}} = \text{horizontal refraction} \quad . \quad . \quad (7)$$

From (3) and the definition of $\nu'$ in (2) we have

$$\frac{1-f}{l} = \frac{1}{C}\left(-\frac{d\nu'}{du}\right)_0 = \frac{1}{C\mu_0}\left(-\frac{d\mu}{du}\right)_0,$$

while from the definition of $u$ in (2)

$$(du)_0 = \frac{(dr)_0}{r_0} + \frac{(d\mu)_0}{\mu_0},$$

so that, using (6),

$$\frac{1-f}{l} = \frac{\nu_0 G_0}{\nu_0'(\mu_0 - \nu_0 G_0)} \quad . \quad . \quad . \quad (8)$$

which is approximately $\dfrac{G_0}{1 - \nu_0 G_0}$.

5. The usual equation

$$H_0 = -\int \frac{\rho}{\rho_0} d\left(\frac{r_0}{r}\right),$$

where $\rho$, $\rho_0$ are the densities at distances $r$, $r_0$ from the centre, becomes, from the definition of $u$ in (2),

$$H_0 = -\int \frac{\rho}{\rho_0} d\left(\frac{\mu}{\mu_0\sqrt{1+2u}}\right) \quad . \quad . \quad . \quad (9)$$

Let us for the moment consider only terms of order $\nu_0$, $l$, and $l^2$ on the right. We may to this order put $\rho/\rho_0 = \nu/\nu_0 = \nu'/\nu_0'$, $\mu_0 = 1$, so that

$$\begin{aligned} H_0 &= -\int \frac{\rho}{\rho_0} d(1+\nu)(1-u+\tfrac{3}{2}u^2) \\ &= \int \frac{\rho}{\rho_0}(du - d\nu - 3udu) \\ &= \int_{u=0}^{\infty} \frac{\nu'}{\nu_0'} du - \int_{\nu=\nu_0}^{0} \frac{\nu}{\nu_0} d\nu - 3\int_{u=0}^{\infty} \frac{\nu'}{\nu_0'} udu, \end{aligned}$$

which, using (3) and (6), gives

$$H_0 = (1+f)l + \tfrac{1}{2}\nu_0 - 3(1+2f)l^2,$$

or

$$(1+f)l = H_0 - \tfrac{1}{2}\nu_0 + 3(1+2f)l^2 \quad . \quad . \quad . \quad (10)$$

To carry the approximation to a higher power in $\nu_0$ it is necessary to assume $\rho$ proportional not to $\nu$ but to $\nu + k\nu^2$, where $k$ is a constant of which, for example, the value would be $\frac{1}{2}$ or 0 if $\rho$ were proportional to $\mu^2 - 1$ or $\mu - 1$ respectively. By expanding (9) in powers of $\nu'$ and $u$, the value of $H_0$ has been found as far as terms of order $\nu_0^2$, $\nu_0 l$, $\nu_0 l^2$, $l^3$; but the only correction to the right-hand side of (10) which might conceivably be sensible is found to be

$$+ \{(1+\tfrac{1}{2}k)(1+f) - \tfrac{1}{4}(1+k)f^2\}\nu_0 l \quad . \quad . \quad (10a)$$

In the presence of water-vapour the value of $H_0$ determined by (9) with $\rho$ a function of $\nu$ is not quite that determined by consideration of surface temperature; the slight difference has been investigated by Radau.*

6. In *Mécanique Céleste*, vol. iv., bk. x., ch. i., Laplace showed that the formula (4) corresponds, subject to certain approximations, to the relation between $\mu$ and $r$:

$$\left.\begin{aligned} \frac{\mu^2 - 1}{\mu_0^2 - 1} &= \left(1 + \frac{fu'}{l}\right)e^{-u'/l} \\ u' &= 1 - \frac{r_0}{r} - \frac{\mu_0^2 - \mu^2}{2\mu_0^2} \end{aligned}\right\} \quad . \quad . \quad . \quad (11)$$

and with the following identifications of C, $l, f$:

$$C = \frac{\mu_0^2 - 1}{\mu_0^2 + 1} \quad . \quad . \quad . \quad . \quad (12)$$

$$(1+f)l = H_0 - \frac{\mu_0^2 - 1}{4\mu_0^2} \quad . \quad . \quad . \quad (13)$$

together with (7).

(12) gives $C = \nu_0 - \frac{1}{2}\nu_0^2$ . . ., which agrees with the exact form (6) except for terms of order $\nu_0^3$, which are quite insensible for all practical purposes; while (7) is an exact deduction from (4).

* *Annales de l'Observatoire de Paris, Mémoires*, **19**, 17, 1889.

(13) gives $(1+f)l = H_0 - \frac{1}{2}\nu_0$ . . . The correction (10*a*) is minute, but the term $3(1+2f)l^2$ in (10), though small, is not always negligible.

7. If (4) is a possible refraction formula, it must correspond with a definite hypothetical relation between $\mu$ and $r$, and therefore with definite expressions for $\mu_0$, $H_0$, $G_0$ in terms of $C$, $l$, $f$, provided in the case of $H_0$ that we know the connection between refractivity and density. The procedure here employed determines them exactly except in the case of $H_0$, which is found to an improved degree of approximation. Laplace's formula thus becomes available for the purpose of integrating (2), which is linear in $\nu'$, so that the refractions corresponding with different relations $\nu'(u)$ can be superposed. At the same time, for $\zeta < 85°$ the small differences (fractions of a second) which exist between the results of the formula and the tables based on Radau's more elaborate theory are reduced by about 40 per cent. by using (10) in place of (13), the comparison being made for the same values of $\nu_0$, $H_0$, and either $G_0$ or horizontal refraction. For $\zeta > 85°$ it becomes of decreasing importance that our fictitious atmosphere shall have the right $H_0$, and of increasing importance that it shall have the right $\mu$ in the first few kilometres; the formula agrees reasonably with the tables whichever equation is used for $(1+f)l$, and there is little point in using (10) rather than (13); beyond $\zeta = 85°$ or even less the ability of any theory to predict the amount of the refraction rapidly dwindles.

8. When $f = 0$ the formulæ (4) may be written

$$\left.\begin{aligned} R &= C \tan\zeta \,.\, L(T) \\ T &= \frac{\cos\zeta}{\sqrt{2l}}, \qquad L(T) = 2Te^{T^2}\int_T^\infty e^{-t^2}dt \end{aligned}\right\} . \qquad (14)$$

L(T) is Laplace's continued fraction, of which the asymptotic expansion for large T is

$$1 - \frac{1}{2T^2} + \frac{1\cdot 3}{(2T^2)^2} - \frac{1\cdot 3\cdot 5}{(2T^2)^3} + \ldots;$$

$\log_{10} L(T)$ varies only from 0 to $\bar{1}\cdot 98$ for the range (approximately $T > 3$) normally correspo ding with $\zeta < 80°$. (6) still holds, and from (10) we see that $l$ is now to be determined by

$$= H_0 - \tfrac{1}{2}\nu_0 + 3l^2 \qquad . \quad . \quad . \quad (15)$$

At $\zeta = 80°$ these formul give results differing by about $0''\cdot 05$ from Radau's tables for mean temperature gradient at all temperatures and pressures; by the omission of $3l^2$ from (15) the difference is approximately doubled. Probably at this point the deviations of the refraction from the mean, due to fluctuations of temperature gradient in the lower atmosphere, are usually less than $0''\cdot 2$, so that the formulæ express fairly accurately the practical dependence of the refraction on $\nu_0$, $H_0$ which exists up to about $\zeta = 80°$ (always on the assumption that the surfaces of equal refractivity are concentric spheres).

*Star-streaming in Galactic Zones.* By R. D. H. Jones, B.A.

1. *Summary.*—(*a*) I have examined the proper motions of stars contained in Boss's Preliminary General Catalogue, which formed the data used by Sir A. S. Eddington in certain of his investigations into star-streaming.

(*b*) The celestial sphere has been divided up into four zones parallel to the galactic equator, and each zone has been subdivided into two or more regions by meridians of galactic longitude.

(*c*) In order to discover whether there are any variations in the nature of the star-streams as we move away from the galactic equator, separate solutions have been made for three of the zones. The chief feature of the results is a decrease in the velocity of Drift I. from 1·727 at the galactic equator to 1·415 in galactic latitude 69°.

(*d*) The combination of the four zones gives the following values for the constants of the star-streams :—

| | | | |
|---|---|---|---|
| $kV_1$ | 1·536 ± ·036 | $kV_2$ | 0·851 ± ·039 |
| $\alpha_1$ | 88°·9 ± 1°·9 | $\alpha_2$ | 279°·4 ± 4°·2 |
| $\delta_1$ | − 18°·3 ± 1°·4 | $\delta_2$ | − 54°·1 ± 2°·6 |

which may be compared with Eddington's values :

| | | | |
|---|---|---|---|
| $kV_1$ | 1·516 | $kV_2$ | 0·855 |
| $\alpha_1$ | 90°·8 | $\alpha_2$ | 287°·8 |
| $\delta_1$ | − 14°·6 | $\delta_2$ | − 64°·1 |

(*e*) The co-ordinates of the vertex of star-streaming are found to be :

R.A. 91°·7 ± 1°·4 ; Dec. + 6°·1 ± 1°·6.

(*f*) The co-ordinates of the solar apex are :

R.A. 266°·5 ; Dec. + 37°·4.

I am indebted to Mr. J. B. Langford of Clare College for performing much of the preliminary work.

2. The data used are the proper motions of stars contained in Boss's Preliminary General Catalogue, certain classes of stars being excluded for various reasons : viz. fainter components of multiple systems, stars of the Orion type, and members of the Taurus stream and other moving clusters.

The proper motions in Boss's Catalogue were used by Sir A. S. Eddington in his examinations of the phenomenon of star-streaming, but whereas his regions were demarcated by meridians and parallels of declination, we have employed regions separated by parallels of galactic latitude in order to examine whether any variation may be detected in the elements of the star-streams with changes in the galactic latitude.

3. The celestial sphere has been divided up into four zones bounded by parallels of galactic latitude, and each zone has been subdivided into four or more areas by meridians of galactic longitude. Each area is

taken with its antipodal area, the two together constituting a "region." By so doing we double the number of stars without allowing the region to become unduly extended, the circumstances of projection of the drift velocities being the same in antipodal areas. The boundaries of the regions and zones are shown in the following table :—

Table I.

*Division of Celestial Sphere.*

Zone I.
(Galactic Latitude +10° to −10°.)

| Region. | Limits of Gal. Longitude. | Centre of Region. λ. | Centre of Region. β. |
|---|---|---|---|
| H | 90°–135° | 112½° | 0° |
| I | 135°–180° | 157½° | 0° |
| J | 180°–225° | 202½° | 0° |
| K | 225°–270° | 247½° | 0° |

Zone II.
(Galactic Latitude +10° to +30° and −10° to −30°.)

| Region. | Limits of Gal. Longitude. | Centre of Region. λ. | Centre of Region. β. |
|---|---|---|---|
| E | 90°–150° | 120° | +20° |
| F | 150°–210° | 180° | +20° |
| G | 210°–270° | 240° | +20° |
| L | 90°–150° | 120° | −20° |
| M | 150°–210° | 180° | −20° |
| N | 210°–270° | 240° | −20° |

Zone III.
(Galactic Latitude +30° to +60° and −30° to −60°.)

| Region. | Limits of Gal. Longitude. | Centre of Region. λ. | Centre of Region. β. |
|---|---|---|---|
| B | 90°–150° | 120° | +43° |
| C | 150°–210° | 180° | +43° |
| D | 210°–270° | 240° | +43° |
| P | 90°–150° | 120° | −43° |
| Q | 150°–210° | 180° | −43° |
| R | 210°–270° | 240° | −43° |

Zone IV.
(Galactic Latitude +60° to +90° and −60° to −90°.)

| Region. | Limits of Gal. Longitude. | Centre of Region λ. | Centre of Region β. |
|---|---|---|---|
| A | 90°–270° | 180° | +69° |
| S | 90°–270° | 180° | −69° |

4. *Analysis of the Drift Curves.*—The analysis of the drift curves was effected by the method of Eddington. In most regions Drift I. is quite prominent, while Drift II. gives a flatter curve owing to the smaller value of $hV_2$. It was impossible to find a reliable value for the position angle of Drift I. in region M, or for that of Drift II. in regions E, F, and L. The solution for Zone II. was therefore made from the data derived from regions E, F, G, L, and N for Drift I., and from G, M, and N for Drift II.

5. *Determination of Drift Constants.*—The method employed for finding the drift constants is as follows : if X, Y, Z are the components of the linear velocity in space of a drift—referred to rectangular equatorial axes—and if $\alpha$, $\delta$ are the co-ordinates of the centre of the region, then

$$\left.\begin{aligned} -X\sin\alpha \quad &+ Y\cos\alpha \quad &= hV\,.\sin\theta \\ X\cos\alpha\,\sin\delta &+ Y\sin\alpha\,\sin\delta - Z\cos\delta &= -hV\,.\cos\theta \end{aligned}\right\},$$

where $hV$ is the projected drift velocity and $\theta$ is the position angle.

There is then one pair of equations of the above form for each region of the sky: from these, X, Y, Z are found by a least-squares solution, the weights assigned to the region being proportional to the number of stars and to the ease or otherwise with which the two drifts can be separated. For Zones I., II., and III. solutions were made in both equatorial and galactic co-ordinates in order to provide a check upon the numerical work. The results are:

Zone I.
$$\begin{cases} X_1 = \phantom{-}0{\cdot}070 \pm {\cdot}060 & X_2 = \phantom{-}0{\cdot}308 \pm {\cdot}081 \\ Y_1 = \phantom{-}1{\cdot}595 \pm {\cdot}070 & Y_2 = -0{\cdot}534 \pm {\cdot}091 \\ Z_1 = -0{\cdot}660 \pm {\cdot}074 & Z_2 = -0{\cdot}616 \pm {\cdot}083 \end{cases}$$

Zone II.
$$\begin{cases} X_1 = -0{\cdot}060 \pm {\cdot}078 & X_2 = -\phantom{0}{\cdot}087 \pm {\cdot}087 \\ Y_1 = \phantom{-}1{\cdot}543 \pm {\cdot}084 & Y_2 = -\phantom{0}{\cdot}242 \pm {\cdot}119 \\ Z_1 = -0{\cdot}674 \pm {\cdot}096 & Z_2 = -\phantom{0}{\cdot}914 \pm {\cdot}113 \end{cases}$$

Zone III.
$$\begin{cases} X_1 = -0{\cdot}187 \pm {\cdot}087 & X_2 = \phantom{-}0{\cdot}057 \pm {\cdot}034 \\ Y_1 = \phantom{-}1{\cdot}366 \pm {\cdot}075 & Y_2 = -0{\cdot}516 \pm {\cdot}031 \\ Z_1 = -\phantom{0}{\cdot}318 \pm {\cdot}079 & Z_2 = -0{\cdot}627 \pm {\cdot}030 \end{cases}$$

The results for the whole sky, *i.e.* those determined from 17 regions for Drift I. and 15 regions for Drift II., are:

$$\begin{array}{ll} X_1 = \phantom{-}{\cdot}023 \pm {\cdot}032 & X_2 = \phantom{-}{\cdot}082 \pm {\cdot}037 \\ Y_1 = \phantom{-}1{\cdot}458 \pm {\cdot}036 & Y_2 = -{\cdot}492 \pm {\cdot}039 \\ Z_1 = -{\cdot}481 \pm {\cdot}038 & Z_2 = -{\cdot}690 \pm {\cdot}038 \end{array}$$

From these results we deduce the following co-ordinates of the apices and values for the space velocities of the drifts, relative to the Sun and in terms of the theoretical unit $\frac{1}{h}$:

| | | Zone I. | Zone II. | Zone III. | Zones I., II., III., and IV. |
|---|---|---|---|---|---|
| Drift I. | $hV_1$ | 1·727±·070 | 1·684±·086 | 1·415±·076 | 1·536±·036 |
| | $\alpha_1$ | 87·5°±2·1° | 92·2°±2·8° | 97·8°±3·6° | 88·9°±1·9° |
| | $\delta_1$ | −22·5°±2·5° | −23·6°±3·2° | −13°±3·2° | −18·3°±1·4° |
| Drift II. | $hV_2$ | 0·871±·085 | 0·949±·113 | 0·814±·031 | 0·851±·039 |
| | $\alpha_2$ | 300°±7·7° | 252·2°±19·3° | 276·3°±3·8° | 279·4°±4·2° |
| | $\delta_2$ | −45°±7·5° | −74·6°±10·2° | −50·4°±2·1° | −54·1°±2·6° |

The larger values for the probable errors in the co-ordinates of the apex of Drift II., as determined from the region of Zone II., are due not only to the fact that the regions from which the co-ordinates are found are only three in number, but also to the high value of the declination found for the apex which increases the probable error in R.A. On account of the presence of these large probable errors, I have also calculated the constants of Drift II. for the whole sky, omitting this zone. The results are:

Zones I., III., and IV.
$$\begin{cases} X_2 = \phantom{-}{\cdot}124 \pm {\cdot}030 \\ Y_2 = -{\cdot}520 \pm {\cdot}030 \\ Z_2 = -{\cdot}664 \pm {\cdot}030 \end{cases}$$

From this we deduce the following co-ordinates of the apex and value for the space velocity of the drift :—

$$\text{Zones I., III., and IV.} \begin{cases} hV_2 = \cdot 853 \pm \cdot 029 \\ \alpha_2 = 283^\circ\cdot 4 \pm 3^\circ\cdot 1 \\ \delta_2 = -51^\circ\cdot 2 \pm 2^\circ\cdot 2 \end{cases}$$

With these values for the elements of the star-streams derived from the whole sky, and from Zones I., III., and IV., we may compare the values found by Sir A. S. Eddington for the whole sky from a study of the same material,* *i.e.* the proper motions contained in Boss's Catalogue :

| | | | |
|---|---|---|---|
| $hV_1$ | 1·516 | $hV_2$ | 0·855 |
| $\alpha_1$ | 90°·8 | $\alpha_2$ | 287°·8 |
| $\delta_1$ | −14°·6 | $\delta_2$ | −64°·1 |

Table II. below shows the comparison between the calculated and observed values of the position angles of the drifts for Zones I., II., and III., the positions of the apices used in these calculations being those appropriate for each zone as found above.

Table II.

*Calculated and Observed Values of the Position Angles of the Drifts.*

| | Drift I. | | | | Drift. II. | | | |
|---|---|---|---|---|---|---|---|---|
| | Region. | θ cal. | θ obs. | θ cal.−θ obs. | Region. | θ cal. | θ obs. | θ cal.−θ obs. |
| | | ° | ° | ° | | ° | ° | ° |
| Zone I. | H | 146 | 140 | + 6 | H | 238 | 260 | −22 |
| | I | 184 | 170 | +14 | I | 218 | 235 | −17 |
| | J | 257 | 275 | −22 | J | 187 | 170 | +17 |
| | K | 280 | 280 | 0 | K | 159 | 170 | −11 |
| Zone II. | E | 180 | 175 | + 5 | | | | |
| | F | 217 | 200 | +17 | | | | |
| | G | 277 | 270 | + 7 | G | 162 | 150 | +12 |
| | L | 135 | 140 | − 5 | | | | |
| | | | | | M | 180 | 170 | +10 |
| | N | 334 | 325 | + 9 | N | 166 | 180 | −14 |
| Zone III. | B | 221 | 220 | + 1 | B | 94 | 70 | +24 |
| | C | 236 | 240 | − 4 | C | 143 | 160 | −17 |
| | D | 261 | 265 | − 4 | D | 143 | 145 | − 2 |
| | P | 109 | 115 | − 6 | P | 220 | 220 | 0 |
| | Q | 86 | 90 | − 4 | Q | 203 | 200 | + 3 |
| | R | 46 | 40 | + 6 | R | 205 | 200 | + 5 |

* *M.N.*, **71**, 40, 1910.

Table III. shows the comparison between the observed and calculated drift velocities. As in the calculation of the quantities in the previous table, we take for the positions of the apices for each zone the positions determined by our solutions for that zone.

TABLE III.

*Calculated and Observed Values of the Projected Drift Velocities.*

| Drift I. | | | Drift II. | | |
|---|---|---|---|---|---|
| Region. | Drift Vel. Cal. | Drift Vel. Obs. | Region. | Drift Vel. Cal. | Drift Vel. Obs. |
| H | 1·72 | 1·6 | H | 0·68 | 0·5 |
| I | 1·15 | 1·3 | I | 0·52 | 0·4 |
| J | 0·65 | 0·7 | J | 0·79 | 1·0 |
| K | 1·42 | 1·3 | K | 0·85 | 0·8 |
| E | 1·68 | 1·5 | | | |
| F | 1·12 | 1·0 | | | |
| G | 1·38 | 1·6 | G | 0·82 | 0·8 |
| L | 1·61 | 1·7 | | | |
| | | | M | 0·94 | 1·0 |
| N | 1·08 | 1·2 | N | 0·63 | 0·65 |
| B | 1·40 | 1·2 | B | 0·36 | 0·5 |
| C | 1·12 | 1·2 | C | 0·59 | 0·6 |
| D | 1·31 | 1·4 | D | 0·81 | 0·8 |
| P | 1·33 | 1·4 | P | 0·73 | 0·7 |
| Q | ·85 | 0·9 | Q | 0·79 | 0·8 |
| R | 1·17 | 1·1 | R | 0·73 | 0·75 |

6. *The Vertex of Star-streaming.*—The co-ordinates of the vertices of star-streaming may now be derived. We have:

Zone I. $\begin{cases} X_1-X_2 = -\cdot238\pm\cdot101 \\ Y_1-Y_2 = \ 2\cdot029\pm\cdot115 \\ Z_1-Z_2 = -\cdot044\pm\cdot111 \end{cases}$

Zone II. $\begin{cases} X_1-X_2 = -\cdot027\pm\cdot117 \\ Y_1-Y_2 = \ 1\cdot785\pm\cdot146 \\ Z_1-Z_2 = \ \cdot240\pm\cdot148 \end{cases}$

Zone III. $\begin{cases} X_1-X_2 = -\cdot244\pm\cdot094 \\ Y_1-Y_2 = \ 1\cdot882\pm\cdot081 \\ Z_1-Z_2 = \ \cdot309\pm\cdot084 \end{cases}$

Zones I., II., III., and IV. $\begin{cases} X_1-X_2 = -\cdot059\pm\cdot049 \\ Y_1-Y_2 = \ 1\cdot950\pm\cdot053 \\ Z_1-Z_2 = \ \cdot209\pm\cdot054 \end{cases}$

From these are deduced the following positions for the vertices:—

| | Zone I. | Zone II. | Zone III. | Zones I., II., III., and IV. |
|---|---|---|---|---|
| R.A. of vertex | $96°\cdot7\pm2°\cdot8$ | $89°\cdot1\pm4°\cdot0$ | $97°\cdot4\pm2°\cdot8$ | $91°\cdot7\pm1°\cdot4$ |
| Dec. „ | $-1°\cdot2\pm3°\cdot1$ | $7°\cdot6\pm4°\cdot7$ | $9°\cdot3\pm2°\cdot5$ | $6°\cdot1\pm1°\cdot6$ |

or, expressed in galactic co-ordinates :

| | Zone I. | Zone II. | Zone III. | Zones I., II., III., and IV. |
|---|---|---|---|---|
| Long. of vertex | 179°·1 | 167°·7 | 170°·1 | 170°·3 |
| Lat. ,, | −4°·4 | −7°·0 | +1°·0 | −5°·5 |

For the whole sky Eddington derived the following position for the vertex :—

R.A. of vertex 94°·2 ; Dec. of vertex +11°·9

The velocities of one stream relatively to the other are found to have the following values in terms of the theoretical unit :—

| Zone I. | Zone II. | Zone III. | Zones I., II., III., and IV. |
|---|---|---|---|
| 2·045±·117 | 1·803±·146 | 1·923±·082 | 1·962±·053 |

Eddington found that the relative velocity of the two drifts was 1·87 units.

7. *The Apex of the Solar Motion.*—The position of the apex of the solar motion can also be derived from the constants of the star-streams : if $N_1$, $N_2$ are the numbers of stars in a zone forming the two drifts whose linear velocity components are $X_1Y_1Z_1$ and $X_2Y_2Z_2$, then the solar motion has components :

$$-\frac{1}{N_1+N_2}\{N_1X_1+N_2X_2\}, \quad -\frac{1}{N_1+N_2}\cdot\{N_1Y_1+N_2Y_2\},$$

$$-\frac{1}{N_1+N_2}\cdot\{N_1Z_1+N_2Z_2\}.$$

Hence we deduce the following results :—

| | Zone I. | Zone II. | Zone III. | Zones I., II., III., and IV. |
|---|---|---|---|---|
| R.A. of apex | 260°·5 | 274°·7 | 278°·3 | 266°·5 |
| Dec. ,, | +35°·5 | 41°·6 | 33°·3 | 37°·4 |
| Speed of solar motion in terms of unit $\frac{1}{h}$ | 1·110 | 1·152 | ·7921 | 1·061 |

The position of the solar apex found by Eddington is

R.A. of apex 267°·3 ; Dec. of apex 36°·4

and the velocity of the solar motion was found to be 0·908.

8. *Conclusion.*—The chief feature of the results obtained is a decrease in the velocity of Drift I. from 1·727 at the galactic equator to 1·415 at the poles. Owing to the uncertainties connected with the determination of the elements of Drift II., the relative velocity of the two streams shows no marked tendency to vary with galactic latitude.

The speed of the solar motion is somewhat higher than that found by Sir A. S. Eddington.

## *The Precise Measurement of Time.* By Alfred L. Loomis. (Plates 9 and 10.)

In August 1928 an investigation was started at this laboratory on the precise measurement of time. Among others, it had the following objects in view :—

(1) A study of the most accurate types of pendulum clocks now in existence.

(2) A study of other time-keeping devices.

(3) The development of methods for the automatic and continuous intercomparison of a group of time-keepers.

(4) The development, if possible, of improved time-keepers after a comprehensive study of the limitations of existing instruments.

This preliminary paper deals only with certain aspects of the first three of these objects.

In my opinion, the Shortt clock * is, at the present time, the most accurate time-keeper for all periods longer than a day. This opinion is based upon the published papers of Professor R. A. Sampson dealing with Shortt Clocks No. 0 and No. 4 at the Royal Observatory at Edinburgh,† the papers of Dr. J. Jackson and Mr. W. Bowyer dealing with the Shortt Clocks No. 3 and No. 11 at the Royal Observatory at Greenwich,‡ my own studies and those of Professor E. W. Brown and Dr. Brouwer § of Shortt Clocks Nos. 20, 21, 22 at Tuxedo, and the publications of the B.I.H. dealing with the performance of a large number of Riefler and Leroy clocks at the Paris Observatory. I have also personally inspected the clock installations at a considerable number of places.

For periods of one day or less, I believe the most precise method of measuring intervals of time is with the crystal oscillators developed at the Bell Telephone Laboratories in New York under the direction of Mr. W. A. Marrison.|| Since 1929 May these crystal oscillators have been continuously compared with the Shortt clocks at Tuxedo by means of a private wire between New York and Tuxedo and the chronograph to be described in the next section. I know of no published results that indicate that there is any other type of crystal oscillator or tuning-fork controlled oscillator that can compare with the Bell Telephone Laboratories oscillators.

These oscillators can be read more precisely than the Shortt clocks over periods of a day or less solely because of their greater "velocity." They oscillate 100,000 times a second, and two of them can be compared with each other (as described by Mr. Marrison in his paper) with such precision that a change of 1 part in $10^{10}$ can be detected over a period of 10 seconds. In this period they have completed $10^6$ oscillations.

* Designed by Mr. Shortt and manufactured by The Synchronome Company, London.

† *Proc. Roy. Soc. of Edinburgh*, **48**, pt. ii., No. 13, 1928.

‡ *M.N.*, **88**, 469, 1928; *M.N.*, **89**, 242, 1929; *M.N.*, **90**, 268, 1930.

§ *M.N.*, **91**, 575, 1931.

|| W. A. Marrison, *Bell Telephone Laboratories Journal*, **8**, 493, 1929.

In the same period the pendulum of a Shortt clock has moved only 350 mm. The paper by Professor Brown and Dr Brouwer shows the limits of accuracy to which the clocks can be read over periods of one hour. This question is also discussed in the next section.

### *The Loomis Chronograph.*

No comprehensive study of a group of time-keepers can be made without a continuously recording chronograph. Chronograph No. 1 was designed and built in this laboratory in 1928 August and was in constant operation until 1930 March when it was superseded by Chronograph No. 2, identical in principle but containing several refinements. This chronograph (see figs. 1 and 2) gives a continuous record permitting the direct intercomparison between the clocks and the crystals and between the clocks themselves. It gives the same resolution as would be obtained by a tape moving past a pen at the rate of 10 feet per second and on which was recorded a signal from each clock every 30 seconds. This result is obtained as follows : The motor of the chronograph has a toothed iron disc mounted on a vertical shaft which is caused to rotate ten times a second and whose exact speed is controlled by the master crystal oscillator in New York. This oscillator has a frequency of 100,000 cycles per second, and by the use of a submultiple generator controls the frequency of a 1000-cycle oscillator. This 1000-cycle frequency is led over the private wire from the Bell Telephone Laboratories in New York to Tuxedo and is fed, through an amplifier, to three small magnets round the iron disc of the chronograph. This disc has 100 teeth, and when spinning in approximate synchronism with the 1000-cycle impulses makes 10 revolutions per second (advancing one tooth per cycle). As a result, it is "locked" to the master oscillator in New York and must follow all variations in frequency of the master.

At the top of the vertical shaft carrying the rotor is a short horizontal arm of bakelite revolving inside a bakelite ring. This ring carries 100 steel phonograph needles, equally spaced around a horizontal circle, and pointing inward towards the revolving arm. Above this circle of needles is a circle of brass, and on the end of the insulated revolving arm there is mounted a short piece of tungsten, its upper end approaching to within a millimetre of the brass circle and its lower end sweeping past the needle-points.

An insulated wire leads from each of the 100 needles in the ring to 100 needles mounted in a horizontal strip of bakelite, called the "comb." The needles in the comb are in a straight line and spaced $\frac{1}{10}$ of an inch apart, the comb being 10 inches in length.

The rest of the chronograph consists of a large roll of coarse paper, slightly more than 10 inches in width, which is fed slowly through brass rollers which print 100 parallel lines spaced $\frac{1}{10}$ of an inch apart. The paper then passes under the needles in the "comb," each of the 100 needle-points being directly over one of the 100 lines. Directly under the paper is a brass plate which is kept at ground potential. When a high potential is suddenly applied to the brass circle in the

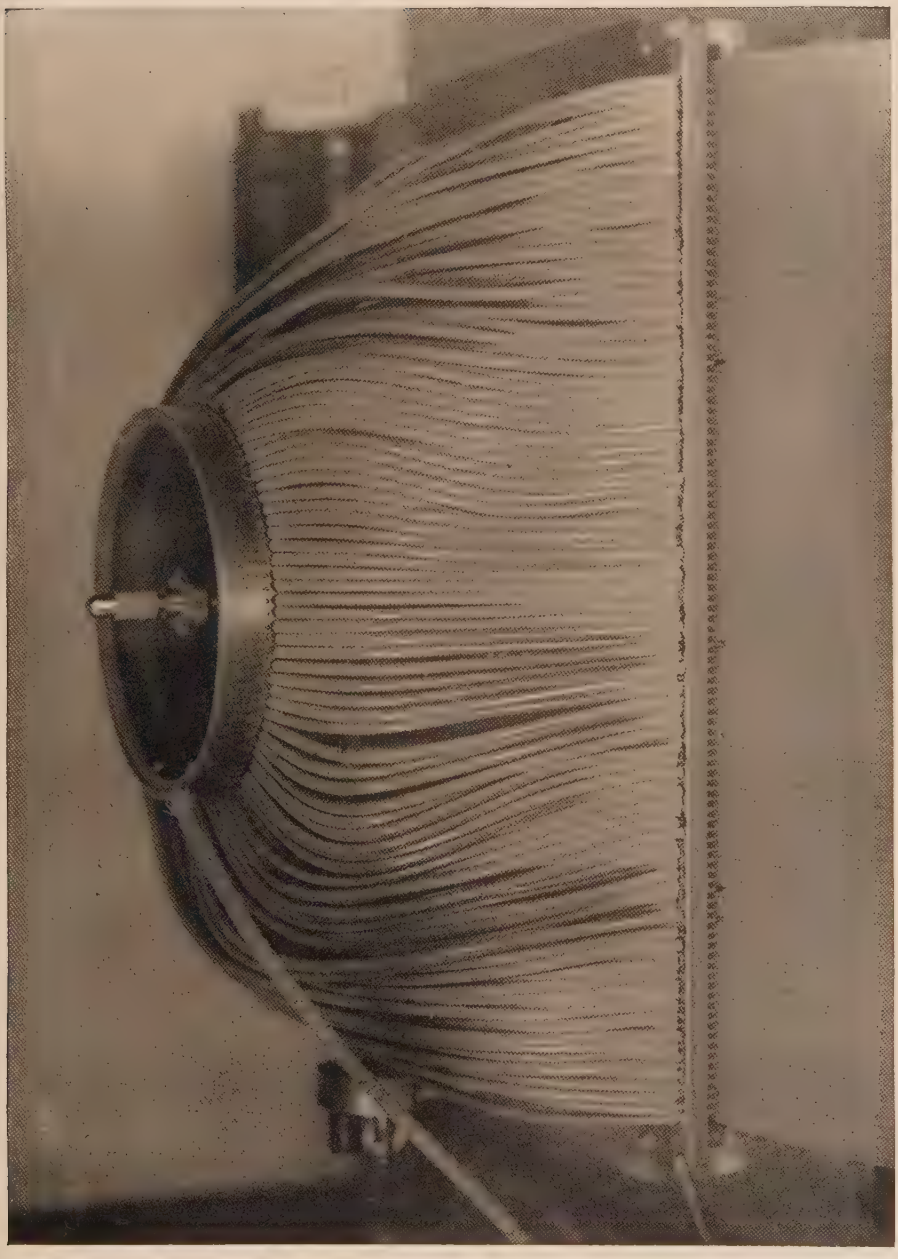

bakelite ring a spark jumps from this circle to the upper end of the piece of tungsten on the rotating arm, then from its lower end to the nearest needle in the bakelite ring. From here the impulse travels down the wire to the corresponding needle in the "comb," and from this needle a spark jumps through the paper to the brass plate below.

The paper is caused to pass at a uniform rate under the needle-points by brass rollers connected through reduction gears directly with the revolving shaft of the chronograph. The paper is fed at the rate of approximately a foot an hour. At this rate it takes about six weeks for a roll of the paper to be fed through the chronograph.

The operation of the instrument is as follows :—

The rotating "spark point" on the bakelite arm sweeps past 1000 needle-points per second. The points in the comb are $\frac{1}{10}$ of an inch apart, and this distance on the paper therefore corresponds to 1 milli-second (·001$^s$). Each master clock sends out a signal every 30 seconds. This signal operates a special relay which causes a spark to pass as described above (the details of the spark circuit are described later). If a clock and the crystal oscillator are keeping exactly the same time, each successive spark will jump from the same needle-point and, as the paper is continuously moving, a straight line of spark-marks will be formed parallel to the edge of the paper. The scale of this chronograph is so enormous that a change of one part in a million is immediately apparent by the mere inspection of a few hours' record. Thus if two clocks are maintaining the same rate and are, for example, 10 milli-seconds different in phase, they will trace two parallel lines of sparks 1 inch (10 milli-seconds) apart. If one clock changed its rate by one part in a million, it would then gain (or lose as the case might be) on the other clock 10 milli-seconds in ten million milli-seconds, or approximately 3 hours. As the paper would have travelled 3 feet in this time, the two lines would have then come together or separated to a distance of 2 inches—a change easily visible by inspection.

The shift of a line in respect to the paper gives the relative rates of the clock making such line and the master crystal. The relative shift of two lines with respect to each other gives the relative rates of two clocks irrespective of the rate of the master crystal.

Fig. 2 is a photograph of the record as it comes from the chronograph. Lines 1, 2, and 3 were made by the three clocks. They are parallel to within a few milli-seconds per day. Line 4, which has a pronounced slope, was made by another crystal oscillator. It was losing on the clocks at the rate of $\frac{2}{10}$ of a second per day.

The chronograph records for a 240-day period beginning 1929 September 7 have been most carefully analysed by Professor E. W. Brown and Dr. Brouwer. Their results are contained in their paper which appears on p. 575. They show that the mean hourly rates, each determined from 120 sparks (one every 30 seconds) will have a probable error of less than ·0001 second.

This remarkable result is accomplished through the possibility of averaging a large number of observations. A single impulse from a master Shortt clock has an uncertainty of 1 or 2 milli-seconds. The

master pendulum carries a small wheel. The impulse arm rests on this wheel, and as the pendulum swings out the pallet on this arm travels down the edge of the wheel, finally falling clear. It then trips an arm which falls, making the electric contact. If the small wheel is not exactly circular the arm will fall at slightly different times as the wheel is given a small turn with each fall. These variations are entirely smoothed out when a series of sparks are averaged.

In the three clocks at Tuxedo the small wheels have slightly different irregularities, and as a result the line of sparks from each of the clocks has its own characteristic irregularities. These irregularities have persisted over the entire two years of observation and are of great convenience in permitting the ready identification of different lines of sparks. Calculation shows that a variation of 1 milli-second in the record would be made by a difference of radii of ·005 millimetre in two parts of one of these small wheels.

We know that this variation between successive sparks of 1 or 2 milli-seconds is not caused by variations in any other part of the recording system because such variations are entirely absent when we use another crystal oscillator instead of a Shortt clock to send 30-second impulses to the chronograph.

An essential part of the chronograph concerns the method of producing "the sparks." As is well known, the use of ordinary sparks for recording phenomena is almost obsolete. Unless specially prepared paper is used, the spark holes are almost impossible to detect. But with the method here used each spark causes a small "explosion" in the coarse wrapping-paper, which leaves a "crater" easily visible across the room when viewed under oblique illumination. This result is obtained by using a special circuit. A 30 m.f. condenser is slowly charged up to 240 volts, through a high resistance. The voltage is supplied from six "B" batteries. The current drain is so small that a set of such batteries lasts for about a year. When a relay is closed the impedance in the circuit is so small that a momentary current of the order of 50 amperes is rapidly built up in the primary of a small induction coil. This is sufficient to charge a Leyden jar to 20,000 volts, at which voltage a control gap breaks down, and the spark jumps at the needle-point. Some care was required in adjusting the voltage, resistance, capacity, and size of the control gap, but when once adjusted it has operated without attention since 1928 August. This type of circuit produces a high voltage surge of short duration and small energy. This produces the explosive effect in the paper without burning it in the slightest.

As previously stated, the chronograph prints 100 parallel lines on the paper and the sparks fall on these lines. The printing rollers are so arranged that a short gap occurs in each 10th line at 20-minute intervals. Thus the exact time of the occurrence of each spark can be readily obtained. The 100 lines are thus also broken up into groups of 10. The 1st, 5th, and 9th lines in each group of 10 are suppressed. It is thus possible, by mere inspection, and without the use of any scale, to give the exact milli-second in which any spark occurred. The reading of the record is therefore not so laborious as would at first

seem, and the record is always visible, right up to the point at which the sparks are occurring, and there is no delay such as would be caused by having to develop or otherwise treat the paper. An hourly average can be quickly obtained by merely counting the number of sparks in each column. From these numbers the mean can be quickly found by calculation. For example, if the 120 sparks are distributed as follows : 40 in column 10, 60 in column 11, and 20 in column 12,—the mean for the hour is 10·83 milli-seconds [(400 + 660 + 240) ÷ 120].

*The Installation at Tuxedo.*—The three clocks at Tuxedo are mounted on independent massive masonry piers. The piers are arranged in a triangle so that the planes of the three pendulums form an equilateral triangle. The piers are built directly on the solid rock which makes up the mountain on which the laboratory is situated. The neighbourhood is remarkably free from vibration, as the nearest railway is more than two miles distant and there is no heavy road traffic within a mile. The vault in which the piers are located is kept at a constant temperature of 21°·00 ± ·02 centigrade.

Clock No. 20 was installed in 1928 July, and clocks No. 21 and No. 22 in 1928 December, and all have been functioning remarkably well ever since.

*Comments on the Shortt Clocks.*—After two years of observation of the Shortt clocks the following considerations occur to me :—

(*a*) The pressure in the clock case should be adjusted to be within the range 15 to 25 mm. of mercury. As the pressure in the clock case is reduced from 760 mm. to 25 mm. the rate of the clock increases about 9 seconds per day. In the range 15 to 25 mm. the change of rate is very small, but when the pressure is further reduced from 15 mm. to less than 1 mm. the rate decreases over a second per day. This was first observed at Tuxedo when the clocks were installed in 1928. Air was admitted 1 mm. at a time and the rate observed on the chronograph. The fact that the maximum rate is found with a pressure of about 15 mm. has also been observed by Dr. Jackson.* This maximum results from the fact that the curve " Rate *v.* Pressure " is the resultant of two curves, one being " Pressure *v.* Effective Mass of Bob." As the pressure is reduced, less air is carried along with the pendulum and less air is displaced by the pendulum. The resultant of these two effects is to cause the effective centre of gravity to rise and the rate to increase. We have studied this effect with a " constant amplitude " clock (referred to later). The other curve is " Pressure *v.* Amplitude." As the pressure is reduced the amplitude increases, because a larger amplitude is needed to dissipate the constant increments of energy fed in every 30 seconds. This effect is most marked at the lower pressures. Owing to the " circular error," this causes a reduction in rate as the pressure is decreased. We have also studied this effect with the " constant amplitude " clock by keeping the pressure constant and changing the amplitude.

* *M.N.*, **90**, 276, 1930.

The best way to adjust the pressure in a Shortt clock is to pump it down as far as possible, then admit nitrogen from a tank, and then pump the nitrogen down to the desired pressure. When air is used, the sparks occurring at the contact of the resetting device gradually "clean up" the oxygen, thus reducing the pressure. Several observers have reported the reduction of pressure with time in a sealed clock case.

It seems extraordinary to physicists who are used to the usual "vacuum technique" that such large waxed joints as are found in all precision clocks can hold tight for years; yet the experience at Greenwich, Tuxedo, and elsewhere indicates that these waxed joints in the Shortt clocks do in fact hold. Nevertheless, when a clock changes its rate there is always a suspicion that there may be a small leak. For example, a variation of over $\frac{1}{2}$ second in a year would be caused at a pressure of 24 mm. if the pressure changed $\frac{1}{30}$ of a mm. Therefore, at Tuxedo we are experimenting, in connection with another kind of clock, to see if we cannot have an "all glass" case sealed off in the flame.

The clocks contain a mercury and an oil gauge. N-Butyl-phthalate should be used in the oil gauge. This compound has the lowest vapour pressure of any suitable organic compound and is extremely stable at room temperature. The mercury in the other gauge should also be covered with a small quantity of this compound to prevent the mercury from distilling on to the pendulum.

(*b*) The variation of arc of the pendulum is by far the most serious factor to be contended with. This applies to all conventional types of clocks, and in the Shortt "free pendulum" type it is probably less serious than in the usual type which has an "escapement" drive. This factor comes into play because of the "circular error." A variation of over $\frac{1}{2}$ second a year would be caused by a variation of arc of $\frac{1}{100}$ of a millimetre.

From this point of view and because of the "circular error" a conventional type clock is an ungoverned motor. Energy is fed in at as constant a rate as possible, and the velocity of the pendulum increases until it dissipates energy at the same rate. A new position of equilibrium is required for each change in energy input. It is essential, therefore, that on existing clocks the "amplitude" be regularly read and recorded. Dr. Jackson (*M.N.*, **90**, 272, 1930) shows how most of the large variations in Greenwich clock No. 3 can be explained and corrected by applying corrections for variation of arc.

We have attacked this problem at Tuxedo from a different angle. A clock is now operating there whose arc is kept constant at a figure slightly less than that which it would take if unregulated. Whenever the arc exceeds this predetermined amount by more than a micron the energy input is momentarily cut off. In principle it is essentially a motor with a governor. It is too early to report as to whether or not this principle is superior to the principle of an automatic device to record changes in arc.

(*c*) The Shortt clocks have invar pendulums and "type-metal" bobs. Invar is known to be a rather unstable alloy. It was selected because

of its small temperature coefficient. Many Shortt clocks have shown a progressive slowing down, as if the pendulums were slowly lengthening or as if the bobs were settling. On one of the clocks at Greenwich an invar bob was substituted in 1929.

Fused quartz has been suggested by a number of people for the pendulum rod. I know of no installation where this material has been used and tested for a sufficient length of time to show whether or not it is superior to invar. We are making experiments at this laboratory along this line.

(*d*) If a master Shortt clock is accidentally stopped by failure of the "slave" clock, broken wire, or battery failure, etc., it can easily be started again without breaking the vacuum seals. All that is necessary is to open for a second the valve which is located in the side of the case opposite the bob. The rush of air causes the bob to move slightly. If the valve is then opened slightly and closed at regular 2-second intervals in phase with the pendulum, the full amplitude can be built up in a minute or two. Then the pressure can be pumped down to the original amount.

(*e*) The brass case of the Shortt clock contains four bolt-holes for fastening the clock to the wall. Only the upper two holes should be used. The lower part of the clock should merely press against a layer of plaster of Paris placed on the wall. When four bolts are used any shifting in the masonry necessarily puts a strain on the case, causing a slow leak. In each of the clocks at Tuxedo a slow leak developed in about six months after installation, and in each case it was instantly cured when the lower nuts were loosened. I also understand that several other installations have had the same trouble.

While the installation at Tuxedo was made chiefly for experimental purposes, the recording, with some interruptions, has been continuous, and is being continued under somewhat better conditions. It has, however, been remembered that it is possible to carry out experiments which are denied to an observatory, where the clocks are needed for the time service and for astronomical observations, and it is hoped that these opportunities can be further utilised.

*Tuxedo Park, N.Y.:*
1931 *February* 16.

---

*Analysis of Records made on the Loomis Chronograph by Three Shortt Clocks and a Crystal Oscillator.* By Ernest W. Brown and Dirk Brouwer.

The chronograph, clocks, and oscillator have been described by Mr. A. L. Loomis in the previous paper. In this paper we give the results of a somewhat extensive analysis of records furnished by Mr. Loomis, extending over several months.

*Frequency of Reading.*—Let us denote the time shown by the quartz crystal system by Q and those by the three Shortt clocks

by $C_1$, $C_2$, $C_3$. Then if $0^s{\cdot}001$ be named a milli-second (ms.), the record consists of readings every $30^s$ of the differences

$$C_1 - Q, \qquad C_2 - Q, \qquad C_3 - Q,$$

to the nearest ms. The three clocks thus give 360 records per hour or 8640 per day.

Several problems were presented. The first was to discover the degree of constancy of the rates of the crystal and clock and chronograph systems over intervals of the order of a minute, an hour, a day, a month. . . . In this connection it has to be remembered that between the pendulum of each clock and the Loomis chronograph there is a chain of mechanical and electrical links, and that each of these links could cause small random errors additional to the errors peculiar to the crystal and the pendulums. The nature of these recording mechanisms and of their connections was, however, such that they should not have been able to produce accumulated errors at any time greater than a few ms. at most.

Examination of the records showed that changes greater than 1 ms. during any $30^s$ interval were rarely present. Thus the perforations which gave the record for any one clock deviated from a straight line drawn to follow their mean direction by amounts rarely greater than 1 ms. over intervals of 20 minutes or so. In fact, the irregular changes in the hourly rates as obtained from reading and averaging the results from all the perforations were generally considerably less than 1 ms. Fig. 1 gives a sample of these hourly rates, covering 8 days.

Economy of effort requires that the frequency of reading of the records shall not be greater than that demanded by the problem under consideration. It was therefore necessary to find out what was the loss of accuracy caused by taking readings at longer intervals than the $30^s$ given on the record. For this purpose, for the days 0–54 (1929 September 7, $0^h$, to October 31), every record on the sheets was read and averaged into hourly means. This material is denoted below by the symbol M. As stated above, it was evident that oscillations greater than 1 ms. during any hour were rarely present, so that these hourly means should have a probable error not greatly in excess of 1/11 that of a single reading.

*Dispersion of the Hourly Means.*—Three samples of two and one-half days each were taken, and smooth curves were drawn through the points representing the hourly rates for clocks minus crystal and for the differences between the clocks. If $\mu_0$, $\mu_1$, $\mu_2$, $\mu_3$ be the mean errors of the readings of the four mechanisms against an ideal clock with no dispersion and assumed to be represented by the smooth curves, we obtain six equations giving the sums of values of the $\mu^2$ in pairs. The deduced values were consistent to less than 5 per cent. and gave $\mu_0 = \pm 0^s{\cdot}00013, \mu_1 = \pm 0^s{\cdot}00014, \mu_2 = \pm 0^s{\cdot}00023, \mu_3 = \pm 0^s{\cdot}00024$. The probable errors of the hourly means for the material M are therefore in the neighbourhood of $\pm 0^s{\cdot}0002$. Only a portion of each error is due to the fact that the individual reading is made to the

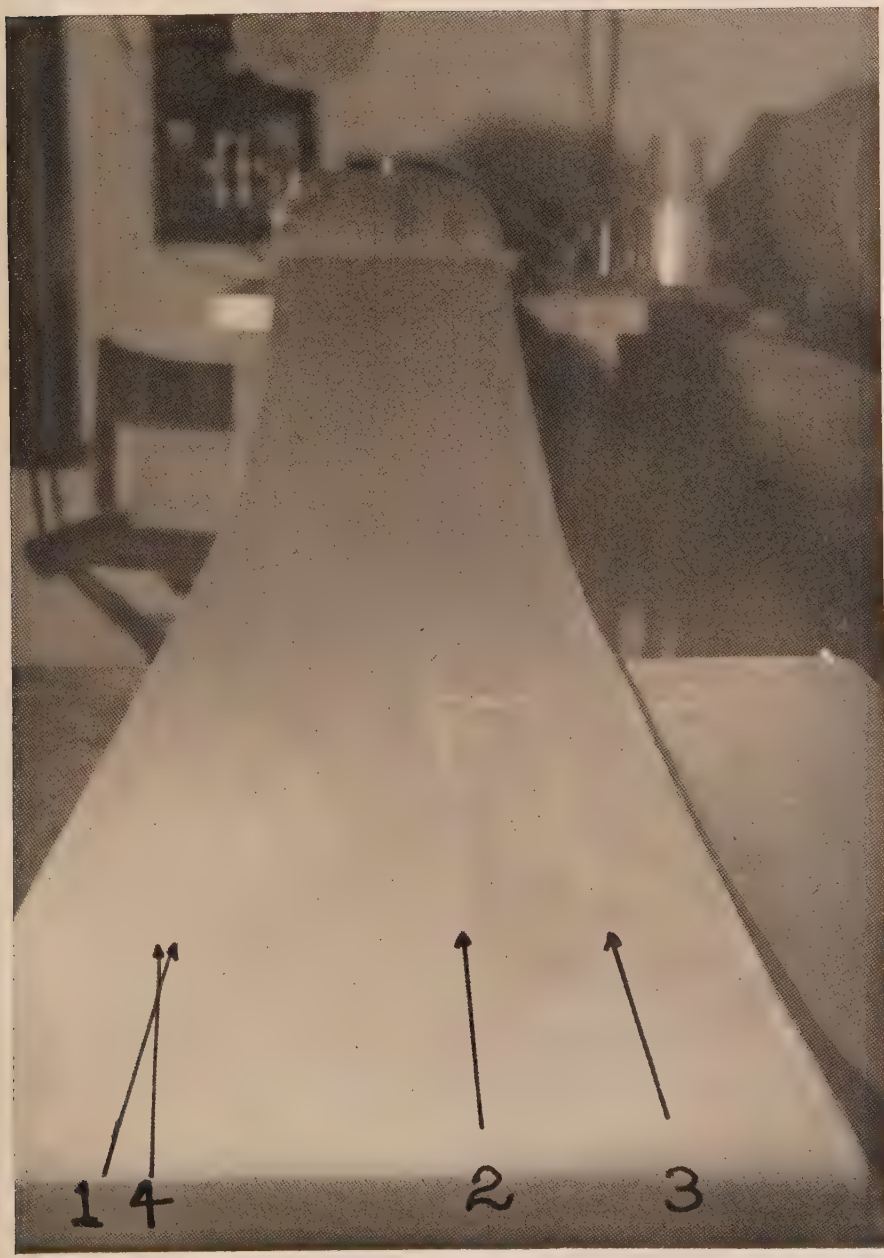


Fig. 2.

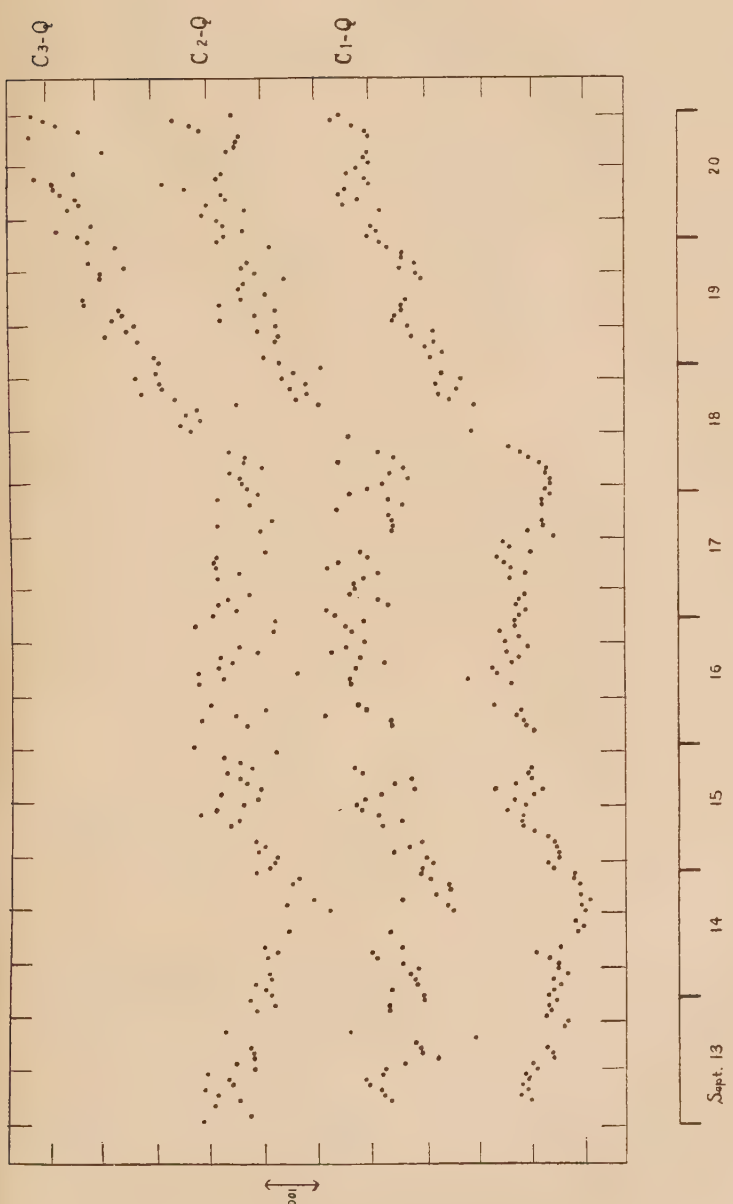
C3-Q
C2-Q
C1-Q
.001
Sept. 13
14
15
16
17
18
19
20
Hourly rates: Clocks minus Crystal.

FIG. 1.

nearest ms., since the probable error due to this cause should be less than $\pm 0^s{\cdot}0001$.

Owing to the method adopted, the irregularities considered here should diminish in taking means according to the Gaussian law. The comparisons of the results obtained below for the lunar term indicate that this is the actual fact.

In the sample of the record shown in fig. 1 it is noticeable that the dispersion for Clock 1 is considerably less than that for either of the other clocks, and this is the case throughout the whole interval of 55 days used to find the material M. These dispersions are probably due mainly to variations in the signalling systems between the pendulums and the chronograph. Thus the smaller dispersion of hourly rates shown by Clock 1 indicates only that its signalling system is more regular than those of the other clocks and not that it is a better time-keeper. In fact, the indications given below show it was more subject to sudden changes of rate, which were maintained over intervals of many days.

Next, the material for days 0–146 (1929 September 7 to 1930 January 31) was read at hourly intervals only by noting the position of the intersection of the line of perforations with that giving the hour. As the angle of intersection of these two lines was greater than 70°, the "hour" line was needed only to an accuracy of a minute or so; actually it is obtained to within 5 or 10 seconds. The probable error of such a reading, denoted by H, should be less than 1 ms., and a comparison of readings with the results of the material M showed that this was the case.

*General Treatment of the Records.*—As stated above, the material M consists of the hourly means of the readings taken every $30^s$ for days 0–54, and the material H consists of the readings at $0^h$, $1^h$, . . . for days 0–146. The times are E.S.T. = G.C.T. $- 5^h$.

Constant rates were subtracted from the readings of $C_2 - Q$, $C_3 - Q$, so as to make the average rates of these as near $C_1 - Q$ as possible.* These were determined from the material M but served sufficiently for the period of 147 days. The object was merely to diminish the magnitudes of the numbers. The amounts applied were, per day,

$0^s{\cdot}048$ to Cl. 2, $0^s{\cdot}216$ to Cl. 3.

The hourly differences were then formed for both M and H. At this stage the gaps in the record were bridged by the method given below, for the convenience of having a continuous record. From this material the differences $C_1 - C_2$, $C_1 - C_3$ (and $C_2 - C_3$ as a check) were formed, and thereafter the results for $C_1 - Q$, $C_1 - C_2$, $C_1 - C_3$ were used. The procedure of using the hourly differences, giving small numbers, can be used for all operations which involve only additions and subtractions. At any stage the actual values of the readings can always be found. The final stage before a harmonic analysis was the recovery of these readings.

* The notations $C_1 - C_2$, etc., have the opposite signs to those given by the clock readings. They were used for convenience in the analysis.

*Gaps in the Record.*—Owing to interruptions in the telephone line connecting the oscillating crystal (in New York) and the chronograph (in Tuxedo), the latter stopped on a number of occasions and remained at rest until the stoppage was discovered and the chronograph started again. These stoppages in no way affected the running of the clocks or the oscillations of the crystal, nor did they affect the determination of the rates between clocks and crystal while the chronograph was running. The readings were only lost during the stoppages.

To avoid the inconvenience of analysis with discontinuous series, the gaps were bridged by making use of the fact that the rates of the clocks and crystal were nearly constant over periods of several hours. By finding the rates just before and just after the break, and assuming that they changed uniformly in the interval, the gaps could be filled without errors greater than 1 or 2 ms. in the clock readings. The readings of the clock differences $C_1 - C_2$, $C_1 - C_3$, $C_2 - C_3$ are not affected, since for them only multiples of 120 ms.* had to be found and there was never any doubt as to these. For clock-crystal only one number, which is equivalent to the change of the zero of the record, has to be found, and as it could be found separately from each of the clocks, there was little doubt as to its amount. In the interval, September 7 to October 31, there are seven gaps of between 15 and 24 hours, and a few additional ones of shorter interval. The bridging of the gaps by constant rates diminished the probable error of any systematic change, but the total extent of the gaps was not great enough to do so materially.

*Analysis for Oscillations with Periods of the Order of Half a Day to a Day.*—As soon as the hourly rates obtained from the material M were plotted, it was seen at once that there was a daily oscillation in these rates with a half amplitude of ·2 or ·3 ms., and that this oscillation was substantially the same for all three clocks. It was noticed, however, that these daily curves showed considerable differences in shape, amplitude, and phase from day to day. In over 50 per cent. of the cases where a minimum could be detected graphically, this minimum occurred near $17^h$ or at 5 p.m. An analysis for a daily period was made in the following manner.

The mean values of the rates for each hour of the day were obtained for $C_1 - Q$, $C_1 - C_2$, $C_1 - C_3$ with the material M, $0^d$–$54^d$; H, $0^d$–$54^d$; H, $0^d$–$146^d$. These rates have progressive increases or decreases due to the secular and long-period changes. Constant changes of rates were first applied to each series in order to free them from these changes. The accumulated errors at each hour of the day were then obtained, and these showed the average errors of the clocks at each hour of the day. The results showing these errors in the readings of $C_1 - Q$, $C_1 - C_2$, $C_1 - C_3$, $C_2 - C_3$ are plotted in the twelve curves of fig. 2.

It is evident that there is little, if any, trace of the effect in the clock differences. Clocks 1, 2 appear to be free from it; there is a slight trace in Clock 3. As the temperature controls of the three free pendulums and of the crystal are very close, the source of the effect is probably to

* The chronograph used during that time was one with 120 teeth instead of the 100 teeth in the later type described by Mr. Loomis.

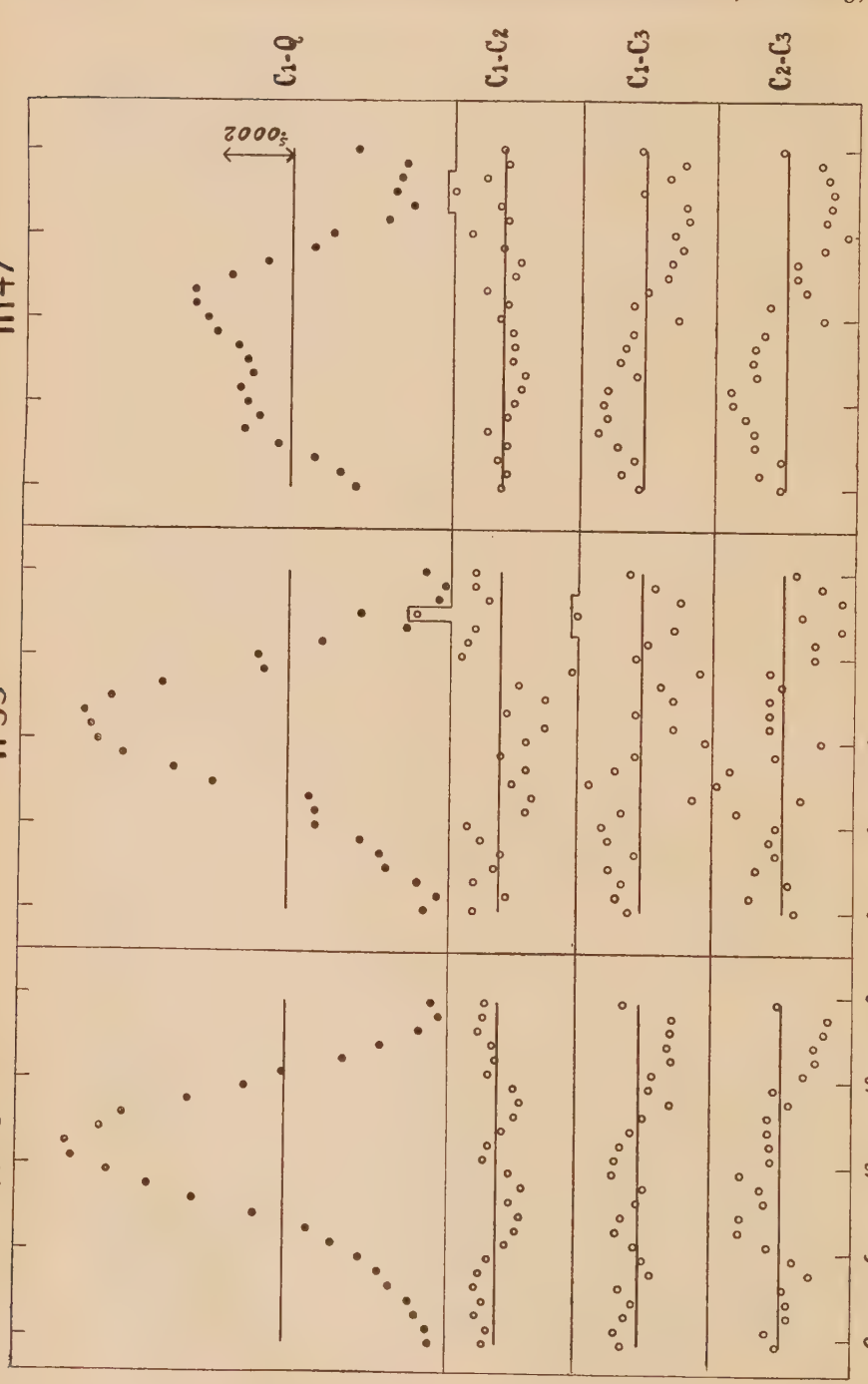
M 55
M 55
H 147
C1-Q
C1-C2
C1-C3
C2-C3
.0002
0
6
12
18
0
Mean Solar hours
Solar term

be found in temperature changes in the signalling system, including the forty-mile telephone line from New York. The average hours of change of rate, namely, 10 a.m. and 5 p.m., are significant. The irregular character of this diurnal oscillation is also indicated by the fact that its average amplitude over a period of 147 days is considerably less than that over a period of 55 days.

Another point which is evident from the figure is the evidence that the material M gives smoother curves than the material H. This might be expected in view of the relation of the amplitude to the accuracy of measurement.

*The Influence of the Moon.*—If the daily oscillation just discussed was due to some portion of the recording mechanisms, as seems probable, and was not present in the oscillations of the crystal or of the free pendulums, some other test of the accuracy of the latter over periods of the order of a day or half a day is needed. For this purpose the lunar day, the interval between successive transits of the moon—which on the average is $24^h\ 50^m$—was selected. If averages over intervals of multiples of 29 days be taken, any effects due to influences with periods of a solar day or of its submultiples should be eliminated. A preliminary calculation showed that the direct attraction of the moon on the pendulum should give an oscillation with a half amplitude of $0^s{\cdot}00015$ for the period of half a lunar day.

It was of interest to see whether so small an effect could be detected.

*Analysis for the Lunar Semi-diurnal Term.*—The material used for the analysis of the term with the period of a solar day was adapted to the lunar day in the manner devised by G. H. Darwin for tidal analysis,* with the particular form given to it by one of us.† In this form, the portions due to secular and long-period changes, which had to be subtracted in the case of the solar day, automatically disappear. If averages over multiples of 29 days be used, there should be little or no sensible effect of the somewhat irregular solar day term. In this method the analysis is made by finding the nearest solar hour at which each lunar day begins, and putting under that hour the corresponding values of the function. If for any particular solar day the value chosen is that at $h$ hour, the remaining twenty-three values at intervals of a solar hour are taken to be the values at $h+1, h+2, \ldots 23, 0, 1, \ldots h-1$ hours. This is done for each solar day, and twenty-four averages are then obtained. These are the averages at $0^h, 1^h \ldots 23^h$ from the beginning of the lunar period, but it is sufficiently accurate to consider them as proceeding at intervals of 1/25 of the lunar period, with the last missing. For the degree of accuracy needed here, each can be taken in the Fourier analysis as separated by 1/24 of the period.

The analysis was made

(*a*) with the material M for days 0–54,
(*b*) with the material H for days 0–54,
(*c*) with the material H for days 0–146,

and each was carried out for $C_1 - Q$, $C_2 - C_1$, $C_3 - C_1$.

* *Coll. Works*, vol. i. p. 216. † E. W. Brown, *Amer. Jn. Sci.*, Series 4, **39**, 386, 1915.

The results are shown in the twelve curves of fig. 3. As might be expected, the differences between the clocks show no traces of the term, for the effect, being a change in the value of $g$, should be the same on all three clocks, and the oscillation of the crystal should be independent of small changes in $g$. The smooth curve under M55 for $C_1 - Q$, obtained with the material M, may be compared with that under H55 for the material H, and with that under H147 for the material H over an interval three times as long. There is evidently a lunar daily as well as a lunar half-daily term present: this is smaller in H147 than in M55 or H55.

The Fourier analysis for a term with the period of half the lunar day gives

| | d d | s | h m |
|---|---|---|---|
| (M), $C_1 - Q$, | 0–54 | + 0·000128 | sin $2(\phi -$ 0 0) |
| (M), $C_2 - Q$, | ,, | 147 | + 0 13 |
| (M), $C_3 - Q$, | ,, | 106 | − 0 36 |
| (H), $C_1 - Q$, | 0–146 | 150 | − 0 24 |
| (H), $C_2 - Q$, | ,, | 135 | − 0 25 |
| (H), $C_3 - Q$, | ,, | 127 | − 1 0 |
| Theory, direct attraction of moon, | | 153 | sin $2\phi$ |

As the probable errors of the coefficients deduced from (H) lie between $\pm$ 0s·00001 and $\pm$ 0s·00002, the agreement between them is satisfactory. The method of procedure has diminished the coefficients by perhaps 5 per cent.

The same effect would be produced if the clocks were given a vertical oscillation with a semi-amplitude of 2·5 inches and with the same period. An amplitude of 1 inch could be detected in a month's observations. This fact is remarkable testimony not only to the sensitiveness of the Shortt clocks, but also to that of the crystal oscillator and of the Loomis chronograph.

*Theory of the Lunar Effect.*—The calculation of the direct attraction of the moon on the pendulum is obtained from the tidal potential V. The change $g_M$ in $g$, due to this potential, is given by

$$-\frac{g_M}{g} = \frac{2M}{E}\sin^3\pi\left(\tfrac{3}{2}\cos^2 z - \tfrac{1}{2}\right),$$

where M, E are the masses of the earth and moon, $\pi$ is the parallax of the moon, and $z$ its zenith distance at any time.

The coefficients of the various periodic terms in the expansion of $\cos^2 z$ can be obtained from the development by G. H. Darwin.* For the principal semi-diurnal lunar tide he gives a coefficient ·454, so that with E = 81·5M, $\sin^3\pi = 1/219000$, we obtain

$$-\frac{g_M}{g} = 2\frac{\cdot 454}{1\cdot 19 \times 10^7}\cos^2\lambda\cos 2\phi,$$

* *Coll. Works,* vol. i. p. 6.

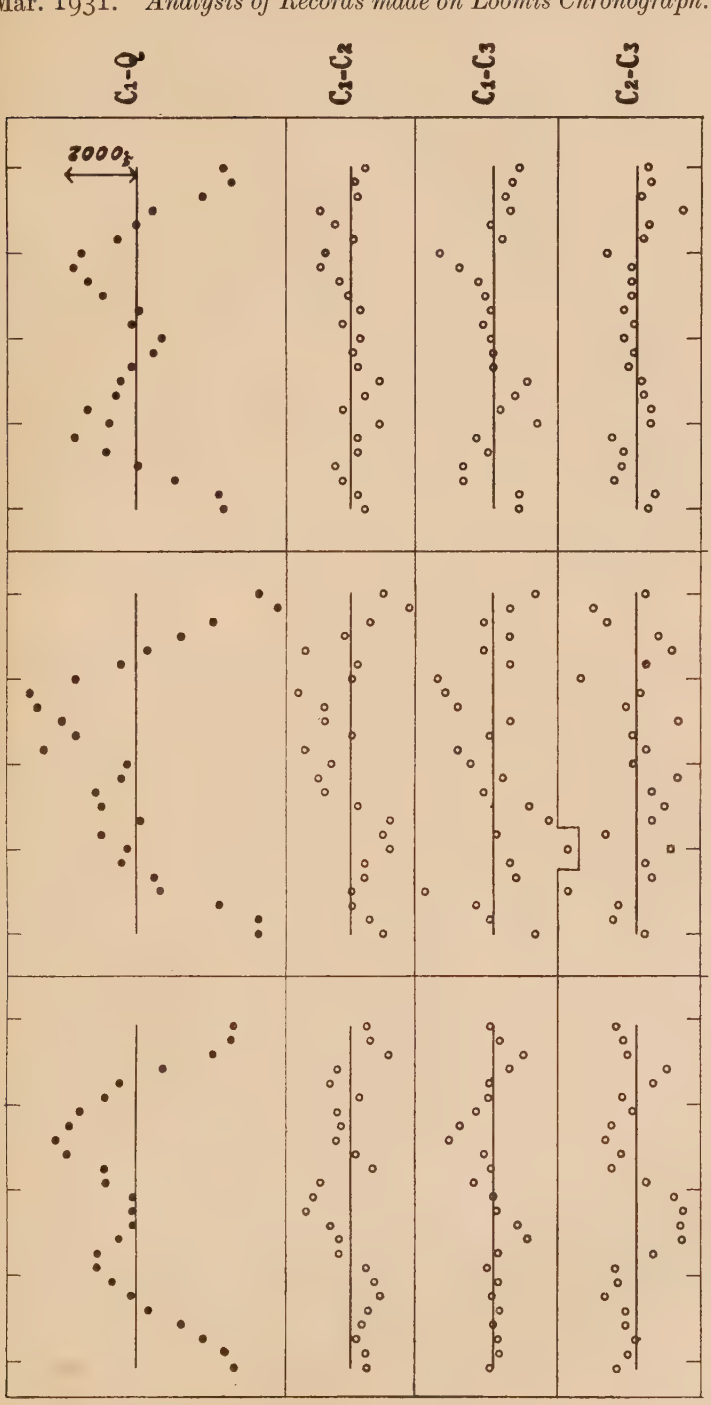
C1-Q
C1-C2
C1-C3
C2-C3
M 55
M 55
H 147
2000
0
6
12
18
0
Lunar hours
Lunar tidal term

FIG. 3.

where $\lambda$ is the latitude of the place of observation, and $2\phi$ is the argument of the tide having a period of $12^h\ 25^m$. With $\lambda = 41°$ (the latitude of Tuxedo Park) we obtain

$$\frac{g_M}{g} = -4{\cdot}3 \times 10^{-8} \cos 2\phi.$$

Hence, if P be the half-period of the pendulum ($1^s$) and $\delta$P the change in P due to $g_M$, we have for the error of the clock at any time,

$$-\int \delta P dt = \tfrac{1}{2}\int \frac{g_M}{g} dt = -2{\cdot}15 \times 10^{-8} \times \frac{44714^s}{2\pi} \sin 2\phi = -0^s{\cdot}000153 \sin 2\phi,$$

where $\phi$ is zero when the moon is on the meridian.

This direct attraction is, however, only a portion of the change of $g$ caused by the moon. First, there is the change of height caused by the bodily earth tide due to the attraction of the moon: denote the ratio of the effect of this to that of the direct attraction by $h$. Secondly, there is the effect due to the redistribution of mass caused by this bodily tide, giving a ratio $k$. These have the same periods and phases as the terms due to the direct attraction, and both of them are positive. According to Jeffreys *

$$h = {\cdot}60, \qquad k = {\cdot}27,$$

so that these two alone would increase the coefficient by nearly 90 per cent.

There are, in addition, two "local" effects. One is the depression of the ocean-bed and near-by coast caused by the accumulation of water at high tide. Darwin estimates † this at $-(h+k)/7$ for the Atlantic coast. Another local effect is that produced by the change of attraction of the ocean tide. If this were uniform all over the earth, it would have the same sign as $k$—that is, the component of the attraction in quadrature would be greater than that when the moon is on the meridian. In the northern hemisphere the portion of the quadrature component contributed by the Atlantic is small; that by the North Pacific Ocean will be larger. The chief effect will be contributed by the portion in the southern hemisphere where the motion of the tide is not much disturbed by the presence of land masses, so that the net effect is to give a negative coefficient. If we accept the results from the Shortt clocks as showing the total effect, it would appear that these local effects balance $h + k$. An attempt to calculate them is therefore desirable. The discussion of these points is pertinent to the subject of this paper, however, only in so far as it has a bearing on the degree of accuracy which is obtainable from the clocks and chronograph.

The tidal theory also gives terms which have nearly, but not quite, twice the period of the semi-diurnal tide discussed above. Darwin gives coefficients ·19 sin $1\lambda$, ·18 sin $2\lambda$, ·08 sin $3\lambda$ for three of them as compared with ·454 $\cos^2\lambda$ for the principal semi-diurnal tide. The

* *The Earth*, 2nd edition, p. 237.
† *Coll. Works*, vol. i. p. 457.

first two of these give coefficients in $g$ nearly double that of the principal tide, but owing to the differences of period they will tend to disappear in averages over a long interval of analysis for the latter. There is evidently a lunar-diurnal effect in the first group of curves of fig. 3, which is probably a residual from these tides. It is noticeable that the effect is smaller for the interval of 147 days than for that of 55 days, a result which might be expected as due to the better elimination in the longer interval.

*Irregular and Secular Changes.*—Next in order should come the discussion of oscillatory changes taking place in periods of a week or more, but the existence and explanation of a marked oscillation with a period of 10·5 days and with a considerable amplitude required a knowledge of the secular and irregular changes of rate, so that these will be considered next.

The actual changes of rate under discussion are very much larger than those previously considered, and it was consequently possible to neglect the small oscillatory changes of rate taking place during a single day. The values of the accumulated errors at $0^h$ (midnight) of each day were taken from the material H, and from these were formed the daily rates, 147 values of the latter being thus available. Later, material carrying the daily rates up to $237^d$ was added. In this latter portion there were considerable gaps of some days at a time, so that it was only possible to obtain the differences between the clock rates. For these the gaps could be bridged in the same manner as before. We have therefore the daily rates for Cl − Q to $147^d$ and Cl − Cl to $237^d$.

For the investigation of these, the following device was adopted. Let any value at $t$ days be represented by $f(t)$ and put

$$f(t) = a_0 + a_1 t + a_2 t^2 + \ldots + \Sigma A \sin(nt + a) + \psi(t) \ . \qquad (1)$$

Here the coefficients $a_2$, $a_3$ . . . represent changes of rate which in general can be confined to the coefficient $a_2$. The function $\psi(t)$ represents irregular changes. If we form the functions

$$f_1(t) = f(t+k) - f(t), \quad f_2(t) = f(t+2k) - 2f(t+k) + f(t) = f_1(t+k) - f_1(t),$$

and plot the curves with $t$ as abscissa and $f_1$ or $f_2$ as ordinates, the average rate $a_1 k$ becomes the average ordinate in $f_1$ and disappears from $f_2$. The secular change $2a_2 k$ becomes the slope of $f_1$ and the ordinate of $f_2$. The periods of the harmonic terms are unchanged, but their amplitudes and phases are respectively altered to

$$2A \sin \tfrac{1}{2}nk, \qquad a + \tfrac{1}{2}nk + \frac{\pi}{2}; \qquad 4A \sin^2 \tfrac{1}{2}nk, \qquad a + nk + \pi.$$

Some care is needed in the interpretation of $\psi_1$, $\psi_2$. A sudden permanent change of rate, for example, gives a change of the ordinate of $f_2$ with a single oscillation of period $2\pi/k$ at the change. An irregular oscillatory change will give one or two oscillations with a period depending on $k$ and on the interval of the oscillation.

If we put $k = 2\pi/n$, the corresponding harmonic term will disappear from $f_1$, $f_2$. If, however, the phase and/or amplitude A is not quite constant, the term may still be present with a small amplitude, and, as just stated, an oscillation with this period may from time to time appear from $\psi$. If, then, we give $k$ a value nearly equal to $2\pi/n$, and if the irregularities are not large, we can eliminate the periodic term without losing the secular changes of rate.

If $k = \pi/n$, the amplitude of the term with period $2\pi/n$ will be multiplied by four and the amplitudes of other periodic terms will be relatively diminished. The secular change $a_2$ has only half the effect in $f_1$ and one-quarter that in $f_2$, while $\psi_2$ may give an occasional oscillation of period $2\pi/n$ and thus alter the apparent phase and amplitude of the harmonic term with this period. These occasional changes, however, will have little or no effect on a harmonic analysis to find A over an interval many times that of the period.

To obtain the secular and irregular changes free from the marked 10·5-day oscillation, the value $k = 11^{d}$, near enough to the actual period to eliminate the term from the diagram, was taken for $k$. This requires simply the formation of the differences of the readings 11 days apart. For the reason stated earlier and because the irregular changes of rate of the crystal were considerable, the discussion is mainly confined to the differences between the clocks. The lower three curves in fig. 4 give the three plots for $f_1$; the lowest curve is, of course, the difference between the other two. The ordinates show the daily rates.

By a comparison of these curves, it is possible to detect the sudden changes of rate of each clock, on the assumption that two clocks will not have the same change at the same time. Such an inspection gives five considerable changes to Clock 1, three to Clock 3, and one doubtful one to Clock 2, in the interval of $237^{d}$.

The curves show at once the extent to which the clocks may be trusted over any given interval. The maximum change of rate per day is $0^{s}\cdot003 \times \frac{1}{2}$, but the maximum accumulated error of a clock reading in a week is $0^{s}\cdot05$. The main point is, however, that the continued comparison of three clocks by means of the Loomis chronograph gives a standard of time measurement over long periods because of the possibility of detecting the changes of rate of each individual clock from the differences. Four such clocks, under proper conditions of temperature and pressure control, could possibly furnish a control on the annual changes in the rate of rotation of the earth.

*The 10·5-Day Oscillation.*—Quite early in his comparison Mr. Loomis had noticed an oscillation with this period and with an amplitude of one or two hundredths of a second, and had connected it with the "beat" period of Clocks 2 and 3. It was difficult to see how the two free pendulums could sensibly influence one another, and it therefore seemed worth while to analyse the records in some detail with reference to such an effect.

In order to bring out the oscillation freed from the greater part of the secular changes, the value $k = 5^{d}$ was used in the formula

and the resulting curves for $f_2$ were plotted. Those for the three clock differences as far as $227^d$ are shown in the upper three curves of fig. 4, and those for clock − crystal in fig. 5.

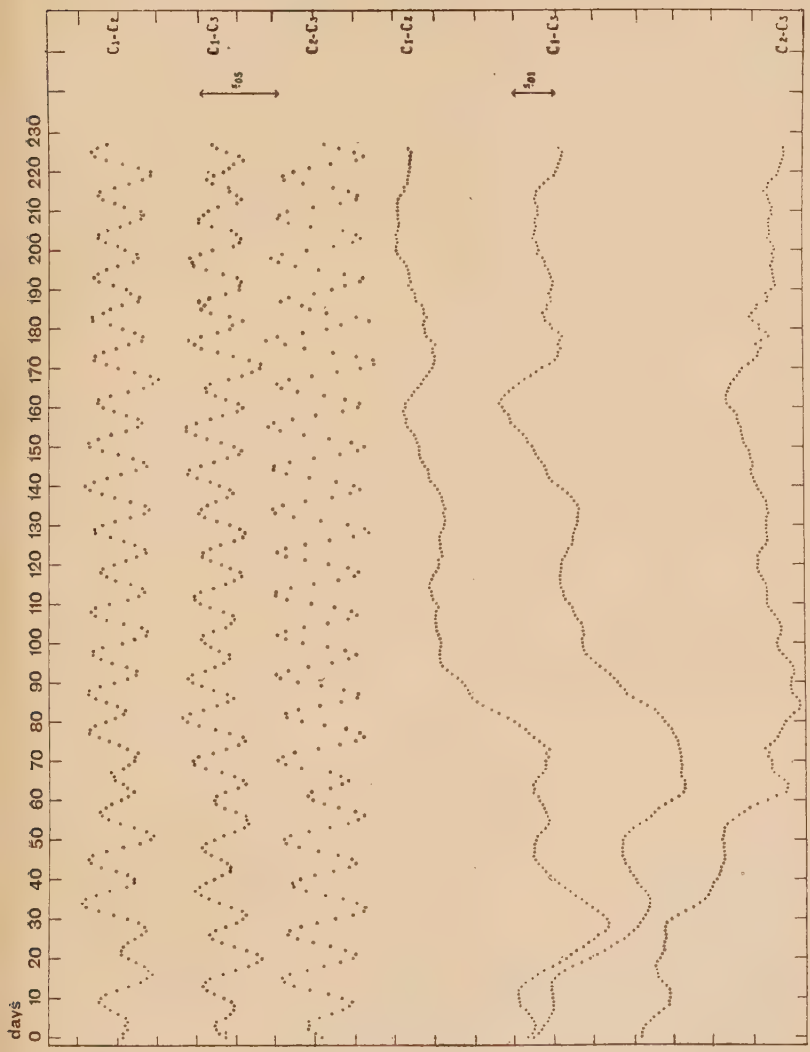


Fig. 4.—Upper Curves: The 10·6-day term in the clock *readings*. Lower Curves: Mean *daily rates*, after elimination of the 10·6-day term.

The remarkable regularity of these curves in fig. 4 can leave no doubt as to the real existence of the effect. The comparison gives a period of $10^d{\cdot}5 \pm {\cdot}1$ and a phase difference between Cl 1 − Cl 2, Cl 1 − Cl 3 of 3 or 4 days. The differences Cl − Q are much larger and show the effect only in a partial way.

The first question to settle is whether the period does, in fact, correspond to the "beat" period of Clocks 2, 3. To examine this point, we refer to the lowest curve in fig. 4, which gives the relative rates of the two clocks freed from the term. Between $0^d$ and $80^d$ this rate changes from $-0^s.160$ to $-0^s.196$, giving a beat period ranging from $12^d.5$ to $10^d.2$. Between $90^d$ and $227^d$ it changes much less and has an average value of about $10^d.5$. In the third curve of fig. 4 it is evident

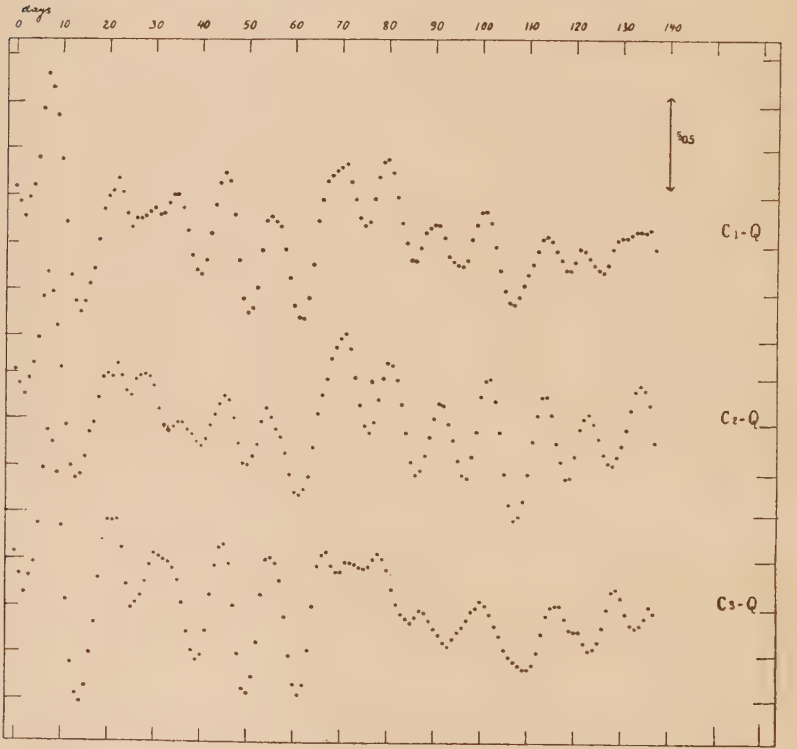


FIG. 5.—The 10·5-day term in the clock readings; Clocks minus Crystal.

that the first five oscillations have a mean period of about 11·5 days, while after $90^d$ it is 10·5 days with very little variation. The irregularity at $60^d$ corresponds to the sudden change of rate at that time. To secure more detailed information, numerical analysis must be used. This analysis has been confined to the interval between $90^d$ and $227^d$ when the relative rates were nearly constant.*

We wished to find the average amplitude and phase, particularly

* Mr. Loomis informs us that in November 1930, after the completion of this analysis, the rate of Clock 3 was purposely changed in connection with a new series of experiments, and that with the change the 10·5-day period disappeared, as might have been expected.

the latter, on account of its bearing on hypotheses as to the source of the effect. The ordinary Fourier analysis was modified in the following manner, in order to avoid the influence of variations in the length of the period. The beginning of each period was chosen at the moment when the difference of the readings of Clocks 2, 3 was an integral multiple of $2^s$, the period of oscillation of the pendulums. The daily readings during each such period were to be interpolated, so that each entry corresponded to 1/12 of the interval: thus there were twelve entries for each period corresponding to phase differences of 30°. Actually, instead of the interpolated values, those nearest to the given times were chosen, as in tidal analysis. Twelve complete periods were available, and the means for each 30° of phase were formed and analysed for a constant and a periodic term in the usual manner.

The results on the clock readings are as follows :—

$$\text{Cl } 2 - \text{Cl } 3, + 0^s{\cdot}0271 \sin\phi ;$$
$$\text{Cl } 1 - \text{Cl } 3, - 0^s{\cdot}0150 \sin\phi + 0^s{\cdot}0059 \cos\phi ;$$
$$\text{Cl } 1 - \text{Cl } 2, + 0^s{\cdot}0121 \sin\phi + 0^s{\cdot}0059 \cos\phi ;$$

where $\phi$ has the period of the " beat " and is evidently taken to be zero when the term in Cl 2 − Cl 3 is zero. The probable errors of these coefficients, as deduced from the daily rates, are less than $0^s{\cdot}002$.

According to almost any hypothesis as to the interaction of the clocks, it is difficult to see how (1) can be affected by the beat period of (2), (3). The average beat period of (1), (3) is $9^d{\cdot}6$, and that between (1), (2) is of the order of $100^d$. The latter cannot be detected owing to the irregular changes of rate, and we have been unable to find any reliable evidence of the former—if there is such a term, its coefficient is not much greater than $0^s{\cdot}001$. If, then, (1) is free from the term, the second of the results gives the effect of (2) on (3), and the third the effect of (3) on (2).

The amplitudes of the two terms are not very different, but there is a marked phase difference of about 130° which is noticeable as existing throughout the interval in the plots. Further, when the times at which the two pendulums are in the same phase are compared with the times of maxima and minima of the term in Cl 2 − Cl 3, it is at once seen that the two do not correspond, but differ throughout by 1 or 2 days. Thus the beat effect is not at a maximum when the pendulums are in the same or opposite phases.

Let us return to the possible existence of the effect in Cl 1 − Q. The first of the curves of fig. 5 appears to give evidence of its existence. When it is examined more closely, however, it is seen that between $35^d$ and $65^d$ there are three such oscillations and then a sudden reversal of phase. This is followed by four more oscillations, a change of phase, and a fading out. Now it has been pointed out that in the process of forming $f_2$ a single oscillation with a period of $10^d$ will be produced by a sudden change of rate, but it is difficult to account for four successive oscillations as due to irregular changes of rate. Nevertheless, we know that the term exists in (2) and (3), and the regularity has disappeared

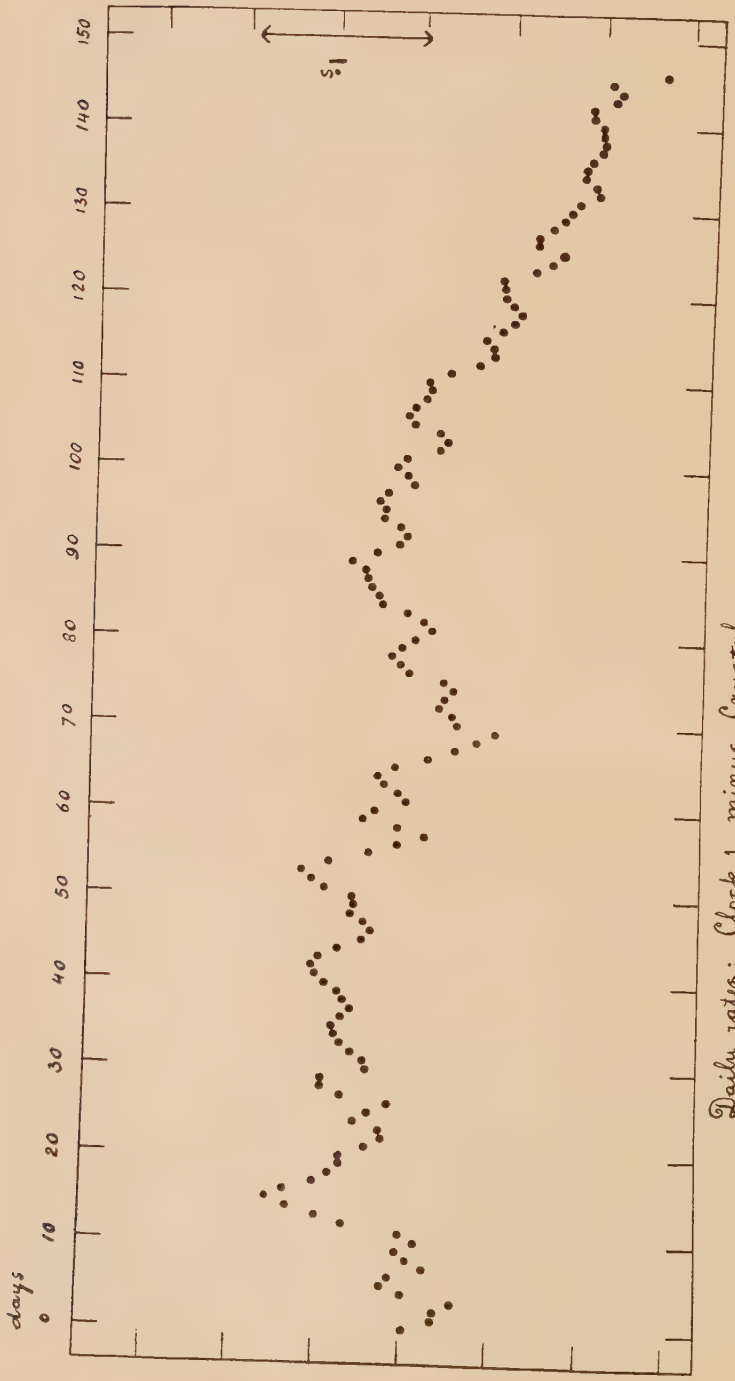
days
0
10
20
30
40
50
60
70
80
90
100
110
120
130
140
150
1s
Daily rates; Clock 1 minus Crystal.

FIG. 6.

from the curve for Cl 3 − Q, showing that the term in (3) is combined with an irregularity in Q of the same order of magnitude. We can only conclude that the irregularities in the crystal system are such that no reliable evidence as to the 10·5-day term can be deduced from the curves of fig. 5, and that we must rely on those of fig. 4.

In order to get rid of the introduction of spurious $10\frac{1}{2}$-day periods by the process of forming $f_2$, the daily rates of Cl 1 − Q are plotted in fig. 6. There is little, if any, trace of the 10·5-day period in this curve, and it is less difficult to see how the successive four periods in the first curve may have been produced by accident. No Fourier analysis has been made of the curves Cl − Q, because whatever might be obtained, the interpretation of the result would be doubtful on account of the changing period. It is only when we have a long succession of periods with comparatively small changes of period that the process used in the previous analysis can be usefully adopted.

The most obvious explanation of the term is an oscillation of the pier to which each clock is bolted, which may be communicated from one pier to the other in some manner. If this explanation be adopted, it is necessary to account for the difference of phase. Since the planes of motion of the pendulums of the two clocks intersect in a line which is equally distant from the two clocks, it is necessary to suppose that the piers do not oscillate with the same freedom in all directions.* The magnitudes appear to require amplitudes of oscillation of the order of one or two wave-lengths of light at the points of suspension of the pendulums. Mr. Loomis points out, however, that while these piers have not been directly tested for such motions, other clocks less rigidly mounted have shown movements less than a small fraction of a fringe. A vertical compressional wave would seem to have too small an amplitude to give the effect; it again would require lack of symmetry in the yielding material to explain the phase difference. Calculation shows that the direct attraction of the pendulums on one another is far too small and that it would require the phase difference to be 0° or 180°. The observed phase difference appears to cut out any attempted explanation based on the interference of the electrical connections of the clocks.

The various processes followed in the analysis, a summary of which is contained in this paper, involved a large amount of calculation, much of which was performed by Mrs. D. Brouwer. We felt, however, that a full examination of the records might be useful, since it is the first time that a continuous record has been made of the performance of a clock to a degree of accuracy beyond that of the clock. The expense of the computations was met by the Loomis Institute.

* The horizontal section of the pier of Clock 2 is a square, that of Clock 3 is a right-angled isosceles triangle.

*Yale University:*
1930 *December.*

## *A New Test for Cassegrainian and Gregorian Secondary Mirrors.*

By J. H. Hindle. (Plate 11.)

1. The figuring of the secondary mirrors for compound reflectors has always been considered a difficult problem. The comparatively recent revival of the Cassegrain is undoubtedly due to the "parallel ray" system of testing adopted by Professor Ritchey, and illustrated and described on p. 39 of his work, *The Modern Reflecting Telescope*. It may be noted that the concave secondary mirror for a Gregorian can equally well be tested by the same method (see fig. 1).

2. That test leaves much to be desired. No matter how carefully the mirrors are collimated, the convex does not appear a perfect surface of revolution when examined under the knife-edge, probably because the illuminated pin-hole and the eye cannot simultaneously be on the optical axis. There is a large blind spot in the centre of the convex, due to its interposition in the parallel rays returning from the plane mirror. The area visible is that due to point illumination only. The supports for the convex obstruct the view to some extent, in addition to which there are diffraction effects around all obstructions. The plane mirror used must be at least as large as the paraboloid, and requires first a spherical mirror from which it is derived with diminished accuracy. The five reflections are objectionable; to a certain extent they drown that figure of the secondary mirror which we wish to see.

3. By the remarkably simple device of substituting a slightly larger *spherical* mirror in place of the *paraboloid*, with a radius of curvature approximately equal to the focal length of the latter (fig. 2), we immediately *dispense with the parallel rays*, and *reduce the number of reflections to three*. The secondary mirror is then seen under the shadow test in no uncertain manner. It can be correctly figured over a larger diameter. The blind spot in the centre is much smaller, and the supports for the secondary mirror do not obstruct the view. Diffraction effects are therefore negligible.

The circles to the left of figs. 1 and 2 show respectively the appearance of the small mirrors from the secondary focus in each system.

4. The mirrors are set up at approximately the required distance apart and squarely facing each other by reflection. The exact value of the radius of curvature of the spherical mirror is not of any importance; it is only necessary that its centre of curvature and the shorter conjugate focus of the secondary mirror should coincide when testing.

5. If the image of the pin-hole is examined with an eyepiece before the secondary mirror is corrected, there is such a considerable difference of focus that two distinct images may be found along the line of aberration, with much dispersion of light. When the secondary is correctly figured to look perfectly flat, all the light is concentrated within the image of the pin-hole, the details of which are plainly visible. The expansion of the image is the same on both sides of focus; in fact, the test is precisely similar to that of a spherical mirror at its centre of

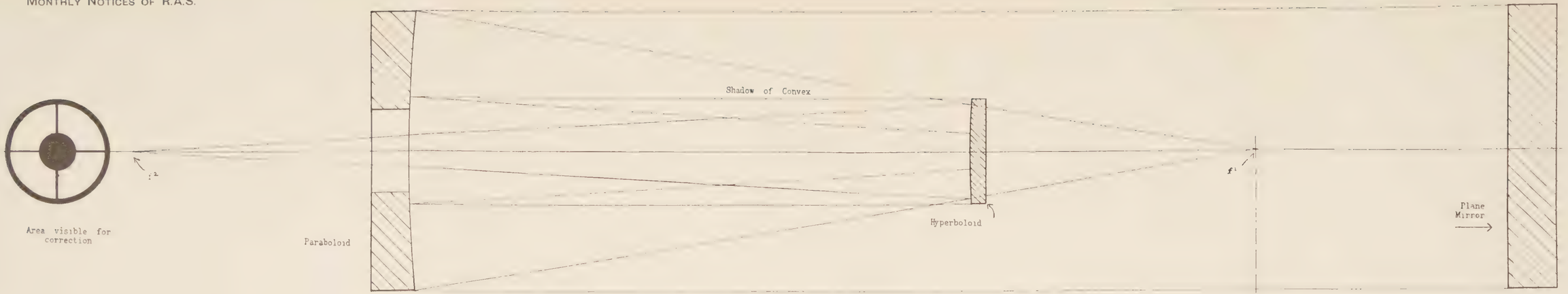


Fig. I. RITCHEY PARALLEL RAY TEST.

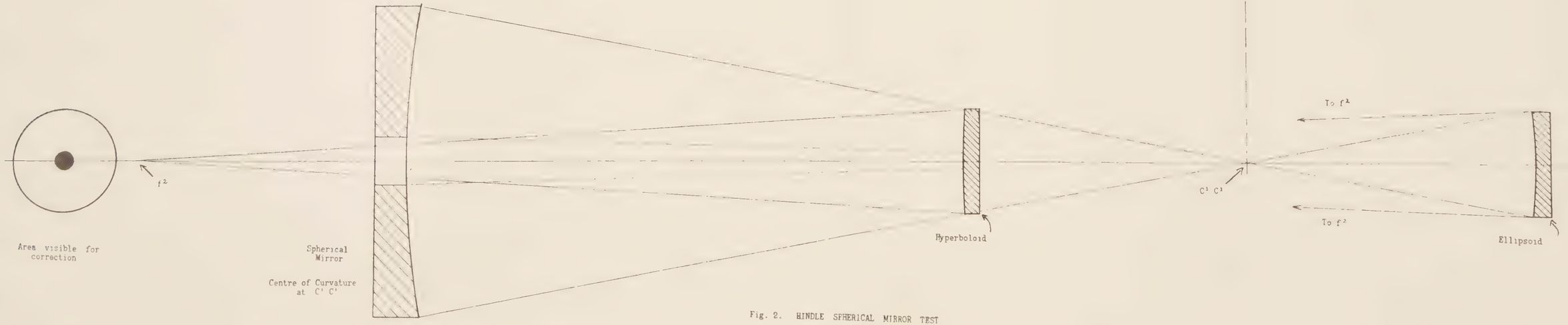


Fig. 2. HINDLE SPHERICAL MIRROR TEST

curvature. It therefore follows that the surface of the secondary mirror *must* be accurate to within a very small fraction of a wave-length.

It is obviously better to refer secondary mirrors to a spherical mirror, whose accuracy can be tested at any time by visual inspection, rather than to a combination of mirrors derived from the same source, with diminishing accuracy. It is likewise of the utmost importance to be able to produce secondary mirrors without reference to the paraboloidal mirrors with which they have to work.

6. The uncorrected secondary mirrors for Cassegrain and Gregorian telescopes show diametrically opposite appearances under the knife-edge test. The former has a protuberant, the latter a depressed intermediate zone, at the average focus. The hyperboloid is therefore more difficult to produce, having a depression in the convex spherical surface, reaching a maximum depth at the intermediate zone, and diminishing to nothing at the edges and centre. A corrected convex, if resting inside a concave spherical surface of suitable curvature, would make contact on the edge and centre only. Such a figure cannot be produced haphazard, and if the depressed zone is unsymmetrical, an astigmatic image results.

7. The Gregorian concave, like the paraboloid, is corrected by excavating the centre more deeply, the excavation diminishing to nothing at the edge. It can therefore, more easily than the Cassegrain, be corrected by star tests if workshop tests are unavailable, gradually making the ellipsoid deeper until full correction is attained. This probably explains the predominance of the Gregorian before workshop tests were devised.

1931 *January* 27.

---

## *Observations of Solar Flocculi made with the Spectrohelioscope at the Royal Observatory, Greenwich, during the Year* 1930.

(*Communicated by the Astronomer Royal.*)

This note gives an advance summary of observations made with the spectrohelioscope during the year 1930 of bright and dark solar flocculi seen in $H\alpha$ light. In particular, the observations relate to measures of radial velocity shown by flocculi in the central zone of the sun's disc. Further details of the measures will be published in the *Greenwich Photoheliographic Results.*

The spectrohelioscope lent by the Mount Wilson Observatory in the autumn of 1929 was set up in the south attic of the New Building. A description of the instrument is given by Dr. Hale in the *Astrophysical Journal*, **70**, 265–311, 1929. The spectrum is formed by a Rowland grating ruled with 14,438 lines to the inch, the observations being made in the light of $H\alpha$. The second order spectrum was used until April 29, and the first order spectrum from April 30 to the end of the year. The

scale of the first order is approximately 1 mm. = 4 A. The width of the second slit was usually 0·1 mm., *i.e.* about one-third of the width of the *Hα* line in the first order spectrum. The diameter of the monochromatic image of the sun's disc at the second slit is about 50 mm., of which a strip 6 mm. wide and 28 mm. long is rendered visible by the rotating rectangular prisms. The eyepiece used magnifies twice.

Measures of radial velocity are taken with the "line-shifter," whose scale is 10 divisions (0–10) = 0·37 A. = 17 km./sec. at *Hα*. The zero of the *Hα* line is determined from measures of the darkest part of the line in an undisturbed portion of the sun near the centre of the disc. The purpose of the observations being chiefly to locate large radial velocities, measured displacements are interpreted as being due to Doppler effects.

The probable error of a single measure of radial velocity, as determined from a number of successive readings, is about 3 km./sec., including the probable error of the zero determination. Three or four measures being usually made on each flocculus, the probable errors of the tabulated values in Tables I., II., and III. are about 2 km./sec.

*Observations.*—Observations were made on 135 days during the year 1930; on about half of these occasions the conditions were such as to allow of a detailed survey of the whole disc. Although the observations were made for the purpose of locating large eruptions, measures of radial velocities of flocculi * were made regularly, and summaries of these are given for the central zone of the disc, a zone of diameter half that of the disc. The observations have been classified as follows :—

(*a*) Areas of bright *Hα* flocculi.
(*b*) Dark *Hα* flocculi not associated with sunspots or bright flocculi.
(*c*) Dark *Hα* flocculi associated with sunspots or bright flocculi.
(*d*) Summary of observations of specially bright *Hα* flocculi.

(*a*) Measures were made of 122 areas of bright *Hα* flocculi in the central zone of the sun's disc. The average measured displacement of the wave-length of their maximum intensity from the centre of *Hα* is equivalent to a radial velocity of − 2·2 km./sec. Table I. gives the frequency of the measured values ranging from − 11 to + 7 km./sec., a minus sign indicating an outward motion from the sun and a plus sign inwards. For purposes of comparison, measures of 103 bright flocculi outside the central zone are also tabulated.

This table shows that the bright *Hα* flocculi are not associated with large vertical movements, in the sense usually applicable to chromospheric phenomena.

A few measures of stable prominences gave − 3·6 km./sec. for the east limb and + 0·8 km./sec. for the west limb. This would imply a systematic error of − 1 or − 2 km./sec. As the mean negative result of − 2·2 km./sec. is shared by the flocculi near the centre of the disc and those at a distance averaging, say, 50° from the central meridian, the

* Following Hale's definition, the term "flocculi" is applied to all bright or dark clouds of vapour observed in projection on the sun's disc in monochromatic light (*Ap. J.*, **70**, 291–292, 1929).

conclusion to be drawn from Table I. is that the bright flocculi are stationary in radial velocity within the limits of measurement of this instrument.

TABLE I.

*Measures of Radial Velocity of Bright Hα Flocculi.*

| Velocity. | Number. | | Velocity. | Number. | |
|---|---|---|---|---|---|
| km./sec. | Central. | Non-central. | km./sec. | Central. | Non-central. |
| −11 | 2 | 0 | −1 | 15 | 5 |
| 10 | 2 | 1 | 0 | 15 | 19 |
| 9 | 2 | 2 | +1 | 10 | 8 |
| 8 | 4 | 0 | 2 | 7 | 4 |
| 7 | 0 | 9 | 3 | 6 | 5 |
| 6 | 7 | 10 | 4 | 2 | 3 |
| 5 | 13 | 10 | 5 | 0 | 0 |
| 4 | 12 | 8 | 6 | 1 | 0 |
| 3 | 11 | 6 | +7 | 0 | 1 |
| −2 | 13 | 12 | | | |

(*b*) Measures were made of 167 dark flocculi not associated with sunspots or bright *Hα* flocculi. These flocculi were usually conspicuous dark markings of average length about 3′. It was characteristic of them that, as the line-shifter was turned, they appeared or disappeared as a whole, thus exhibiting no appreciable differences of radial velocity along their length. Another characteristic was their longevity, which was comparable with the duration of sunspots.

The mean of the measured radial velocities of these 167 dark flocculi was − 1·6 km./sec. Table II. summarises the measures. Measures were also made of 308 similar flocculi outside the central zone, giving as their mean radial velocity − 1·3 km./sec.

It may be concluded from Table II. that the dark flocculi not associated with sunspots or bright flocculi have, in general, scarcely measurable radial motions. The few largest velocities are, however, probably real. It is possible that, whilst Table II. represents the almost stationary conditions of the stable phase of these flocculi, high radial velocities may accompany the dissipation of a number of them—a phase that would occupy a very small part of their existence. An observation bearing on this is given in Table III. with a footnote.

(*c*) Table III. contains a summary of the measures of radial velocity of 89 dark flocculi that were observed in the immediate vicinity of sunspots or within the confines of bright *Hα* flocculi. Generally, these dark flocculi were short-lived and appeared as narrower and shorter markings than those of class (*b*), the average length being a little over 1 . Differences of radial velocity along the length of the markings were frequently observed. On the average the larger velocities were associated with the smaller markings, some of which appeared as well-defined

black dots about 20″ in diameter. The large radial velocities often shown by these dark flocculi are in striking contrast to the doubtful radial velocities measured for dark flocculi outside the disturbed regions of the solar surface marked by sunspots and bright flocculi.

TABLE II.

*Measures of Radial Velocity of Dark Hα Flocculi not associated with Sunspots or Bright Flocculi.*

| Velocity. | Number. | | Velocity. | Number. | |
|---|---|---|---|---|---|
| km./sec. | Central. | Non-central. | km./sec. | Central. | Non-central. |
| −30 | 0 | 1 | − 2 | 14 | 32 |
| 28 | 0 | 1 | − 1 | 18 | 20 |
| 27 | 0 | 1 | 0 | 22 | 49 |
| .. | .. | .. | + 1 | 16 | 25 |
| 18 | 0 | 1 | 2 | 10 | 24 |
| 17 | 0 | 0 | 3 | 10 | 16 |
| 16 | 0 | 1 | 4 | 7 | 12 |
| 15 | 0 | 3 | 5 | 1 | 8 |
| 14 | 1 | 0 | 6 | 2 | 4 |
| 13 | 0 | 2 | 7 | 2 | 3 |
| 12 | 1 | 1 | 8 | 0 | 3 |
| 11 | 2 | 1 | 9 | 0 | 2 |
| 10 | 0 | 2 | 10 | 0 | 2 |
| 9 | 1 | 5 | .. | .. | .. |
| 8 | 4 | 8 | 15 | 0 | 1 |
| 7 | 8 | 10 | .. | .. | .. |
| 6 | 14 | 12 | 18 | 0 | 1 |
| 5 | 7 | 24 | 19 | 0 | 1 |
| 4 | 11 | 12 | 20 | 1 | 0 |
| − 3 | 15 | 19 | +21 | 0 | 1 |

The first column of Table III. gives the date of observation. In the second column is tabulated the measured radial velocity in km./sec.; where two values are given connected by an arrow it is to be understood that differential velocities were observed along the length of the flocculus and that the tabulated values are the extreme velocities measured, which in most cases correspond to the two ends of the flocculus. In those cases in which one end of a flocculus closely approached or appeared projected on a sunspot, the addition of an asterisk denotes the radial velocity observed at that extremity of the flocculus. The third and fourth columns give the time of the central meridian passage and latitude of the associated sunspot. A dash in these columns indicates that no spot was visible in the area of bright flocculi.

TABLE III.

*Measures of Radial Velocity of Dark Flocculi associated with Sunspots or Bright Flocculi.*

| Date. 1930. | Velocity, km./sec. + | | Velocity, km./sec. − | Sunspot. C.M.P. | Sunspot. Latitude. |
|---|---|---|---|---|---|
| | | | | | ° |
| Apr. 27 | | | 2 | | |
| 29 | | 0 | | Apr. 28·6 | 6 S. |
| 30 | | | 1 | | |
| 30 | 37 | | | | |
| 30 | | | 5 | Apr. 29·2 | 13 N. |
| May 5 | 20 | | | — | — |
| 28 | 37 | | | May 29·7 | 12 N. |
| 29 | 5 | | | | |
| 29 | 1 | | | May 28·5 | 10 N. |
| 29 | | | 3 | | |
| June 5 | 18 | | | June 6·0 | 1 N. |
| 5 | 32 | → | 21 | | |
| 6 | 35 | | | June 11·1 | 6 S. |
| 6 | 11 | | | — | — |
| 6 | 20 | → | 28 | — | — |
| 12 | | | 11 | June 12·3 | 13 N. |
| 14 | | | 3 | | |
| 24 | | | 4 | — | — |
| 24 | 29 | → | 28 | — | — |
| 24 | | | 7 | — | — |
| 25 | | | 7 | June 26·1 | 14 N. |
| 30 | | | 8 | | |
| 30 | 24 | | | July 1·5 | 13 N. |
| July 2 | 6 | → | 24 | | |
| 3 | | | 2 | | |
| 6 | 22 | → | 19 | July 8·3 | 8 N. |
| 6 | 1 | | | July 7·0 | 7 S. |
| 7 | | | 9 | | |
| 7 | 5 | | | July 6·4 | 4 N. |
| 14 | 11 | | | — | — |
| 14 | 1 | | | — | — |
| 14 | 38 | → | 19 | July 16·2 | 7 S. |
| 17 | 13 | | | | |
| 18 | 45 | | | July 18·7 | 5 N. |
| Aug. 1 | 19* | → | 7 | July 30·7 | 2 N. |

TABLE III.—*continued.*

| Date. 1930. | Velocity, km./sec. + | Velocity, km./sec. − | Sunspot. C.M.P. | Sunspot. Latitude. |
|---|---|---|---|---|
| | | | | ° |
| Aug. 11 | 3* → | 10 | | |
| 11 | | 17 | | |
| 12 | | 33 | | |
| 12 | 33 → 116 | | | |
| 12 | 20 → | 5 | Aug. 12·3 | 7 S. |
| 14 | 4 | | | |
| 14 | | 19 → 32 | | |
| 14 | | 25 | | |
| 14 | 6 → 35* | | | |
| 26 | 0 | | — | — |
| 29 | | 2 | Aug. 29·9 | 10 S. |
| 30 | | 2 | | |
| Sept. 2 | 44 → | 42 | Sept. 2·6 | 13 S. |
| 3 | | 1 | | |
| 3 | 5 | | | |
| 3 | | 37 | Sept. 4·2 | 5 N. |
| 3 | 19 → 40 | | | |
| 4 | 20* → | 17 | | |
| 4 | 0 | | Sept. 2·8 | 10 N. |
| 5 | 17 → 49* | | Sept. 4·2 | 5 N. |
| 8 | | 7 | Sept. 8·2 | 8 S. |
| 8 | 2 | | Sept. 9·7 | 19 S. |
| 11 | 0 | | — | — |
| 11 | 36 | | Sept. 11·3 | 17 N. |
| 18 | | 1 | Sept. 19·5 | 20 S. |
| Oct. 3 | 6 | | Oct. 2·4 | 3 S. |
| 3 | | 3 | | |
| 3 | | 2 | — | — |
| 9 | | 2 | | |
| 9 | | 33 | | |
| 9 | | 27 | | |
| 9 | | 37 | | |
| 9 | 0 | | Oct. 10·8 | 7 N. |
| 9 | 23 → | 18 | | |
| 10 | 11 | | | |
| 10 | | 7 | | |
| 10 | 28 | | | |

TABLE III.—*continued.*

| Date. 1930. | Velocity, km./sec. + | | − | Sunspot. C.M.P. | Latitude. |
|---|---|---|---|---|---|
| | | | | | ° |
| Oct. 10 | | 0 | | | |
| 10 | 32* | → | 25 | | |
| 11 | 34 | | | Oct. 10·8 | 7 N. |
| 11 | 28 | | | | |
| 11 | 2 | | | | |
| 25 | 17* | → | 24 | Oct. 23·7 | 5 N. |
| 28 | 32 | → | 10 | Oct. 30·1 | 7 S. |
| 29 | 36* | → | 46 | Oct. 28·5 | 6 S. |
| 29 | 1 | | | | |
| Nov. 6 | | | 2 | — | — |
| 6 | | | 2 | — | — |
| 7 | 1 | | | — | — |
| 10 | 40 | | | Nov. 9·2 | 13 N. |
| 25 | 110 | → | 450 | Nov. 24·7 | 6 S. |
| 26 | 7 | | | | |
| 26 | | | 2 | — | — |
| Dec. 13 | 3 → 46 | | | Dec. 15·4 | 6 N. |

The flocculi observed on August 12 are described in *M.N.*, **90**, 820, 1930.

An account of the eruption on November 25 is given in *M.N.*, **91**, 239, 1930. There is doubt as to whether these measures should be in Table II. or Table III. When first observed at $9^h\ 51^m$, the flocculus approximated to those of Table II.; its association later with bright flocculi after $10^h\ 34^m$ places it in Table III.

(*d*) *Eruptions of Bright Hα Flocculi.*—During 1930 the appearance of very bright or brilliant patches of *Hα* flocculi were occasionally observed as tabulated in Table IV. The eruptions of August 12 and November 25 were considerable, the former being closely associated with a sunspot and the latter being about 9° of longitude behind a sunspot and its accompanying bright flocculi. The other eruptions took place in the vicinity of sunspots but were of much smaller extent. The duration of the phenomenon appears not to exceed a few hours and has been observed for so short a duration as $\frac{1}{4}$ hour. The increased brightness of the flocculi was not accompanied by a measurable increase in radial velocity.

Table IV. gives (1) the date of the eruption, (2) the approximate time of central meridian passage, latitude, and area (in millionths of the sun's hemisphere) of the associated sunspot, (3) the time of commencement of a magnetic disturbance of "storm" range ($D \geq 30'$, or H or $V \geq 150\gamma$) that began at Greenwich (Abinger) within 4·0 days of the central meridian passage of the sunspot.

TABLE IV.

*Eruptions of Bright Hα Flocculi.*

| Date of Eruption. | Sunspot. C.M.P. | Latitude. | Area. | Magnetic Storm Commenced. |
|---|---|---|---|---|
| 1930 | | | | |
| Feb. 9·5 | Feb. 8·8 | 19° S. | 250 | None. |
| Mar. 3·7, 8·5 | Mar. 7·1 | 16 S. | 600 | None. |
| Mar. 4·5, 8·5 | Mar. 8·0 | 19 S. | 350 | Mar. 11·6 |
| Mar. 31·4 | Apr. 1·8 | 5 S. | 500 | None. |
| Apr. 10·4 | Apr. 7·6 | 12 N. | 600 | Apr. 6·7 |
| May 5·4 | May 7·3 | 16 N. | 600 | May 5·0 |
| July 2·4 | July 1·5 | 13 N. | 80 | None. |
| July 4·4, 5·4 | July 8·3 | 8 N. | 40 | July 9·6 |
| July 7·4 | July 7·1 | 7 S. | 20 | July 9·6 |
| Aug. 12·5 | Aug. 12·3 | 7 S. | 300 | Aug. 14·8 |
| Sept. 3·4, 4·3, 5·4 | Sept. 4·2 | 5 N. | 250 | Sept. 3·5 |
| Sept. 11·4 | Sept. 6·5 | 0 | 40 | Sept. 3·5 |
| Oct. 6·4, 9·5, 11·4, 13·4 | Oct. 10·8 | 7 N. | 500 | None.* |
| Oct. 28·5, 29·5, 31·5 | Oct. 28·5 | 6 S. | 450 | Oct. 25·7, Oct. 28·7 |
| Nov. 25·4 | Nov. 24·7 | 7 S. | 200 | Nov. 23·8 |

Although a causal connection is not evident between the bright eruptions themselves and the magnetic storms tabulated, it may be remarked that in ten out of fifteen cases the central meridian passage of the accompanying sunspot was associated with the occurrence of a small magnetic storm. Furthermore, during 1930 there were twenty such magnetic storms: eight of these commenced within 4·0 days of the central meridian passage of a sunspot of mean area 200 or greater (there were twenty-three such spots during the year), and all of these eight storms appear in the above table.

* A magnetic disturbance began with a marked "sudden commencement" at October 14·2, but the ranges (D = 29′ : H = 145γ) were just less than those defined at Greenwich for a small storm.

*Royal Observatory, Greenwich :*
1931 *February* 19.

## *Preliminary Values of the Variation of Latitude at Greenwich in* 1930.

(*Communicated by the Astronomer Royal.*)

This paper contains the preliminary values of the latitude variation derived from observations made with the Cookson Floating Telescope.

The star places used were those derived from the final discussion of the observations for the period 1919–1926. The number of plates obtained was about the average, but owing to cloudy weather there was a comparatively small number of plates in May, September, and November.

The increase in the variation which took place towards the end of 1929, after a period of four years of very small variation, was maintained during 1930.

The following table gives the value of the variation in the sense: mean latitude minus observed latitude :—

| Date. | Variation. | Number of Trails. |
|---|---|---|
| | ″ | |
| 1930·047 | +·207 | 107 |
| ·172 | +·196 | 72 |
| ·268 | +·087 | 102 |
| ·365 | +·089 | 53 |
| ·437 | −·025 | 87 |
| ·499 | −·051 | 96 |
| ·590 | −·164 | 47 |
| ·652 | −·152 | 165 |
| ·781 | −·094 | 83 |
| ·850 | +·024 | 41 |
| ·940 | +·099 | 64 |
| 1931·044 | +·196 | 103 |

From a curve drawn to represent the observed results as closely as possible, the following corrections, applicable to observed north polar distances, were derived :—

| | ″ | | ″ |
|---|---|---|---|
| 1930·0 | + ·20 | 1930·6 | − ·16 |
| 30·1 | + ·20 | 30·7 | − ·14 |
| 30·2 | + ·17 | 30·8 | − ·06 |
| 30·3 | + ·10 | 30·9 | + ·06 |
| 30·4 | + ·02 | 1931·0 | + ·16 |
| 30·5 | − ·07 | | |

To correct a slight error in the reductions, the variation for 1929·659 should be taken as − ″·073 instead of − ″·063, and for 1929·926, + ″·163 instead of + ″·180. (See *M.N.*, **90**, 561, 1930.)

*Royal Observatory, Greenwich:*
1931 *February* 21.

*Variability of B.D. + 72°733.* By F. Sargent.

Since the year 1921 the variable star R Ursæ Minoris has been under regular observation at the Durham Observatory.

During 1923 July a change of method introduced the star B.D. +72°733 to the list of "comparison stars."

A departure from the H.C.O. reputed magnitude of this star of 9·74 was at once noted, and since 1923 August 9, when easy comparisons established its magnitude as 9·4, this star has been under regular observation, and variability over a range of about one magnitude has been established.

The variation must be classed as "irregular," and is characterised by rapid changes of considerable range in magnitude, yet through the series of observations may be traced a periodicity approximating to about 360 days.

The "comparison stars" usually relied upon were Nos. 15, 21, and 26 of Hagen's Charts, with H.C.O. reputed magnitudes of 9·26, 9·62, and 10·21 respectively, although occasionally seven other stars from the same charts have been used.

Appended are the observations taken from 1923 August 9 to 1930 December 31.

| Date. | Mag. | Date. | Mag. | Date. | Mag. |
|---|---|---|---|---|---|
| 1923 Aug. 9 | 9·4 | 1924 Sept. 24 | 9·5 | 1925 Oct. 17 | 9·3 |
| 15 | 9·2 | Oct. 1 | 9·4 | 25 | 9·4 |
| 21 | 9·2 | 23 | 9·7 | Nov. 11 | 9·3 |
| 22 | 9·3 | Nov. 3 | 9·5 | 18 | 9·4 |
| 26 | 9·4 | 24 | 9·4 | Dec. 1 | 9·4 |
| 28 | 9·4 | 28 | 9·9 | 16 | 9·2 |
| Sept. 1 | 9·2 | Dec. 16 | 9·4 | 1926 Jan. 4 | 9·6 |
| 4 | 9·3 | 27 | 9·8 | Feb. 15 | 9·4 |
| 7 | 9·2 | 1925 Jan. 14 | 9·4 | Mar. 6 | 9·8 |
| 18 | 9·3 | 31 | 9·9 | 12 | 9·8 |
| Oct. 2 | 9·3 | Feb. 18 | 9·7 | Apr. 9 | 9·6 |
| 4 | 9·3 | Mar. 7 | 9·7 | 16 | 9·6 |
| Nov. 7 | 9·3 | 24 | 9·8 | May 5 | 10·1 |
| Dec. 3 | 9·4 | Apr. 3 | 9·8 | 16 | 9·7 |
| 23 | 9·6 | 13 | 9·5 | June 11 | 9·3 |
| 1924 Jan. 20 | 9·7 | May 8 | 9·8 | July 16 | 9·4 |
| Mar. 10 | 9·8 | 16 | 9·3 | 26 | 9·3 |
| 27 | 9·7 | 30 | 9·1 | Aug. 3 | 9·3 |
| Apr. 14 | 9·8 | June 6 | 9·2 | 20 | 9·5 |
| May 5 | 9·6 | 17 | 9·5 | 28 | 9·4 |
| 16 | 9·2 | July 7 | 9·3 | Sept. 7 | 9·3 |
| June 13 | 9·5 | 18 | 9·4 | 15 | 9·5 |
| 27 | 9·3 | Aug. 6 | 9·4 | 24 | 9·2 |
| Aug. 15 | 9·4 | 15 | 9·2 | Oct. 10 | 9·3 |
| 27 | 9·4 | Sept. 21 | 9·2 | 18 | 9·4 |
| Sept. 3 | 9·3 | 30 | 9·4 | Nov. 3 | 9·4 |
| 17 | 9·1 | Oct. 8 | 9·4 | Dec. 3 | 9·2 |

| Date. | Mag. |
|---|---|
| 1926 Dec. 14 | 9·3 |
| 1927 Jan. 16 | 9·6 |
| 25 | 9·5 |
| 29 | 9·5 |
| 31 | 9·4 |
| Feb. 4 | 9·5 |
| 24 | 9·6 |
| Mar. 1 | 9·7 |
| 6 | 9·8 |
| 24 | 9·8 |
| 30 | 9·8 |
| Apr. 5 | 9·8 |
| 14 | 9·7 |
| 25 | 9·7 |
| 30 | 9·8 |
| May 25 | 9·6 |
| June 8 | 9·6 |
| 24 | 9·7 |
| July 5 | 9·3 |
| 8 | 9·5 |
| 18 | 9·2 |
| 24 | 9·5 |
| Aug. 3 | 9·3 |
| 17 | 9·3 |
| 25 | 9·4 |
| Sept. 9 | 9·3 |
| 27 | 9·4 |
| Oct. 3 | 9·4 |
| 19 | 9·3 |
| 26 | 9·4 |
| 31 | 9·4 |
| Nov. 3 | 9·4 |
| 8 | 9·4 |
| 24 | 9·5 |
| Dec. 27 | 9·6 |
| 1928 Jan. 2 | 9·5 |
| 9 | 9·3 |
| 18 | 9·2 |
| Feb. 21 | 9·7 |
| Mar. 28 | 9·6 |
| Apr. 4 | 9·6 |

| Date. | Mag. |
|---|---|
| 1928 Apr. 21 | 9·7 |
| May 5 | 9·4 |
| June 1 | 9·5 |
| 11 | 9·6 |
| 20 | 9·2 |
| 29 | 9·5 |
| July 14 | 9·5 |
| Aug. 9 | 9·2 |
| 23 | 9·2 |
| Sept. 6 | 9·4 |
| 12 | 9·4 |
| 19 | 9·1 |
| 29 | 9·3 |
| Oct. 4 | 9·4 |
| 13 | 9·5 |
| 18 | 9·4 |
| 25 | 9·3 |
| Nov. 5 | 10·1 |
| 25 | 9·5 |
| 30 | 9·5 |
| Dec. 1 | 9·4 |
| 6 | 9·3 |
| 17 | 9·4 |
| 1929 Feb. 13 | 9·6 |
| Mar. 6 | 9·5 |
| 13 | 9·9 |
| 22 | 10·1 |
| 29 | 9·8 |
| Apr. 6 | 9·7 |
| 21 | 10·1 |
| 30 | 10·1 |
| May 8 | 9·6 |
| 25 | 9·3 |
| June 6 | 9·9 |
| 20 | 9·4 |
| July 7 | 9·5 |
| 13 | 9·5 |
| 19 | 9·4 |
| Aug. 11 | 9·4 |
| 24 | 9·2 |
| Sept. 5 | 9·3 |

| Date. | Mag. |
|---|---|
| 1929 Sept. 11 | 9·2 |
| 23 | 9·2 |
| 29 | 9·2 |
| Oct. 9 | 9·2 |
| 18 | 9·6 |
| 25 | 9·3 |
| Nov. 6 | 9·4 |
| 12 | 9·3 |
| 24 | 9·5 |
| Dec. 2 | 8·9 |
| 12 | 9·4 |
| 19 | 9·5 |
| 1930 Jan. 8 | 9·4 |
| 20 | 9·6 |
| Feb. 20 | 9·6 |
| Mar. 19 | 9·7 |
| 29 | 9·5 |
| Apr. 22 | 9·8 |
| May 1 | 9·6 |
| 9 | 9·7 |
| 13 | 9·7 |
| 28 | 9·3 |
| June 7 | 9·5 |
| 11 | 9·5 |
| 14 | 9·6 |
| 27 | 9·4 |
| July 6 | 9·2 |
| 12 | 9·6 |
| Aug. 15 | 9·2 |
| Sept. 1 | 9·2 |
| 8 | 9·4 |
| 18 | 9·2 |
| 24 | 9·2 |
| Oct. 6 | 9·3 |
| Nov. 4 | 9·5 |
| 11 | 9·4 |
| 25 | 9·3 |
| 30 | 9·6 |
| Dec. 8 | 9·5 |
| 20 | 9·5 |
| 31 | 9·5 |

*University Observatory,*
*Durham:*
1931 *March* 12.

*Occultations of Stars by the Moon, observed at the University of Birmingham during the Year* 1930. By James Young.

| No. | Star. | Mag. | Phase. | Date. | G.M.T. h m s | Corr. s |
|---|---|---|---|---|---|---|
| 1 | W.Z.C. 103 | 6·7 | D | Jan. 8 | 19 6 4·0 | −0·3 |
| 2 | *o* Piscium | 4·5 | D | Jan. 8 | 21 46 41·8 | 0·5 |
| 3 | *ω* Cancri | 6·1 | D | Mar. 10 | 21 54 59·9 | 0·4 |
| 4 | B.D.+23° 648 | 7·0 | D | Apr. 30 | 19 57 30·0 | 0·4 |
| 5 | W.Z.C. 435 | 6·7 | D | May 2 | 19 43 32·7 | 1·0 |
| 6 | *ψ'* Aquarii | 4·5 | D | Nov. 1 | 17 51 48·0 | 0·3 |
| 7 | *δ* Arietis | 4·5 | D | Nov. 6 | 21 53 48·2 | 0·3 |
| 8 | *δ* Arietis | 4·5 | R | Nov. 6 | 23 0 52·0 | 0·5 |
| 9 | 47 Geminorum | 5·6 | R | Nov. 10 | 23 4 17·2 | 0·7 |

The G.M.T. shown are corrected values. The average correction applied to disappearances is about $-0^s.4$; and to reappearances, $-0^s.6$. The actual values of the corrections applied in individual cases to allow for lag, personal error, etc., are shown in the last column.

The co-ordinates of the observatory are given in the *Nautical Almanac* for 1932.

---

*Occultations of Stars by the Moon, observed at Tomsk University Observatory during the Year* 1930. By N. Goryatscheff.

(*Communicated by the Secretaries.*)

($\phi = 56° 28' 07''$ N.; $l = 5^h 39^m 47^s.4$ East of Greenwich.)

| Date (U.T.). 1930. | Local Sidereal Time. h m s | Star. | Mag. | Phase. | ΔT. s |
|---|---|---|---|---|---|
| II. 6·518305 | 3 09 48·2 | B.D.+15°397 | 8·3 | D | +11·5 |
| IV. 3·640059 | 9 46 23·5 | B.D.+23°672 | 7·2 | D | +10·5 |
| IV. 3·644802 | 9 53 14·5 | B.D.+23°668 | 8·1 | D | + 8·3 |
| IV. 3·650570 | 10 01 34·2 | B.D.+23°675 | 7·7 | D | + 3·9 |
| IV. 6·683187 | 11 00 29·7 | B.D.+26°1564 | 7·3 | D | +11·9 |
| IV. 6·766256 | 13 00 26·5 | B.D.+26°1588 | 7·8 | D | +10·3 |
| V. 3·737296 | 14 05 04·5 | 134 B Geminorum | 6·5 | D | +11·2 |
| V. 3·741234 | 14 10 45·7 | B.D.+26°1510 | 7·4 | D | +12·4 |
| V. 3·750901 | 14 24 43·3 | B.D.+26°1512 | 7·9 | D | +14·5 |
| V. 4·730581 | 13 59 19·3 | B.D.+24°1903 | 7·0 | D | +13·0 |
| V. 4·754033 | 14 33 11·0 | *λ* Cancri | 6·2 | D | +13·3 |
| V. 31·678211 | 14 30 09·2 | B.D.+25°1805 | 8·7 | D | +11·9 |

| Date (U.T.). | Local Sidereal Time. | Star. | Mag. | Phase. | ΔT. |
|---|---|---|---|---|---|
| 1930. | h m s | | | | s |
| V. 31·692634 | 14 50 58·7 | B.D.+25°1810 | 8·0 | D | + 9·5 |
| V. 31·718360 | 15 28 07·5 | B.D.+25°1819 | 8·5 | D | + 8·1 |
| VII. 2·663682 | 16 15 20·3 | 13 Virginis | 5·9 | D | +11·6 |
| VII. 2·675699 | 16 32 41·4 | $\eta$ Virginis | 4·0 | D | + 9·4 |
| VII. 17·828087 | 21 11 52·1 | B.D.+ 1°142 | 8·7 | R | +11·5 |
| VII. 20·821867 | 21 14 42·9 | B.D.+18°424 | 7·8 | R | +11·8 |
| IX. 14·747455 | 23 08 03·4 | 62 Tauri | 6·1 | R | +10·5 |
| IX. 14·904151 | 2 54 18·8 | B.D.+24°662 | 8·2 | R | + 3·8 |
| IX. 14·930012 | 3 31 39·4 | B.D.+24°663 | 7·3 | R | + 9·5 |
| X. 10·921341 | 5 01 38·6 | 63 Arietis | 5·2 | R | +13·1 |

*Apparent Places of Occulted Stars of Magnitude > 6·5.*

| Star. | $\alpha$. | $\delta$. | Authority. |
|---|---|---|---|
| | h m s | ° ′ ″ | |
| B.D.+15°397 | 2 47 58·36 | +16 12 42·8 | Bord. ph. +17°244 rep. |
| B.D.+23°672 | 4 15 32·84 | +23 34 18·2 | Abbadia 1998 |
| B.D.+23°668 | 4 14 50·70 | +23 51 38·6 | Abbadia 1989 |
| B D.+23°675 | 4 15 50·50 | +23 25 59·4 | Abbadia Suppl. |
| B.D.+26°1564 | 7 23 43·27 | +26 22 21·1 | $Gr_{1910}$ 3787 |
| B.D.+26°1588 | 7 28 55·56 | +26 16 02·4 | $Gr_{1910}$ 3840 |
| B.D.+26°1510 | 7 12 56·52 | +26 29 30·4 | $Gr_{1910}$ 3687 |
| B.D.+26°1512 | 7 13 35·54 | +26 27 44·1 | $Gr_{1910}$ 3695 |
| B.D.+24°1903 | 8 14 59·60 | +24 23 46·1 | $Gr_{1910}$ 4220 |
| B.D.+25°1805 | 7 55 14·08 | +25 06 33·0 | $Gr_{1910}$ 4065 |
| B.D.+25°1810 | 7 56 12·88 | +25 13 45·2 | $Gr_{1910}$ 4071 |
| B.D.+25°1819 | 7 57 52·33 | +25 10 25·7 | $Gr_{1910}$ 4082 |
| B.D.+ 1°142 | 0 44 38·90 | + 2 21 03·3 | Alg. ph.+2°·040·57 ; +3°·044·115 |
| B.D.+18°424 | 3 06 45·39 | +18 28 53·5 | Abbadia 1387 |
| B.D.+24°662 | 4 27 03·82 | +24 53 05·0 | Abbadia 2086 ; $Gr_{1910}$ 1949 |
| B.D.+24°663 | 4 28 08·44 | +25 02 25·8 | Abbadia 2095 ; $Gr_{1910}$ 1954 |

The proper motions are computed from Schorr, *Eigenbewegungslexikon*.

*Observer.*—N. Goryatscheff.

*Instruments.*—Zeiss telescope, 90-mm. aperture ; magnifying power 90. Observations made with eye and ear.

The time-corrections of the chronometer were found from the Bordeaux, Rugby, and Nauen wireless signals.

*Tomsk, Siberia, U.S.S.R.,*
*University Astronomical Observatory :*
1931 *January* 25.

*Errata.*

P. 238, *for* Hartmann *read* Hopmann.
P. 376, third line from bottom, *for* 1930 Comet II. *read* 1930 Comet I.
P. 422 *et seq.*, *for* Gröningen *read* Groningen.
P. 433, line 21 from bottom, *for* thus *read* also.